Role of Formyl Peptide Receptor in Transformed Cells

A THESIS SUBMITTED TO

SAVITRIBAI PHULE PUNE UNIVERSITY

FOR AWARD OF DEGREE OF

DOCTOR OF PHILOSOPHY (Ph.D.)

IN FACULTY OF CHEMISTRY

BY

Harshit Kumar Soni

UNDER THE GUIDANCE OF

Dr. Vaijayanti A. Kumar

Dr. Nishigandha Naik

DIVISION OF ORGANIC CHEMISTRY

CSIR-NATIONAL CHEMICAL LABORATORY

PUNE-411008

INDIA

May-2016

CERTIFICATE OF THE GUIDE

CERTIFIED that the work incorporated in the thesis "**Role of Formyl Peptide Receptor in Transformed Cells"** Submitted by **Mr. Harshit Kumar Soni** was carried out by the candidate under my supervision/ guidance. Such materials has been obtained from other sources has been duly acknowledged in the thesis.

Date: **Research Guide**

Research Co-Guide

DECLARATION BY THE CANDIDATE

I declare that the thesis entitled "**Role of Formyl Peptide Receptor in Transformed Cells"** submitted by me for the degree of Doctor of Philosophy is the record of work carried out by me during the period from 26.05.2009 to 20.12.2015 under the guidance of **Dr. Vaijayanti A. Kumar** and **Dr. Nishigandha Naik** and has not formed the basis for the award of any degree, diploma, associateship, fellowship, titles in this or any other University of other institution of Higher learning.

I further declare that the material obtained from other sources has been duly acknowledged in the thesis.

Date: **Signature of the Candidate**

Acknowledgement

Obtaining a PhD is a group effort. While the work presented in this thesis is my own, it would never have been possible without the help of numerous people who have given me immense support in many ways during my long and arduous five years of study. I am deeply indebted to my guide, Dr. Vaijayanti A. Kumar and co-guide Dr. Nishigandha Naik. They provided me with many gifts, the greatest being a completely different mindset from the one I had at the beginning of my doctoral studies. The ability to think critically, to ask the right questions, and to resolve the problems through experiments are the traits that I didn't possess before meeting them. I thank them for allowing me freedom and resources to pursue different lines of research.

I owe a huge debt of gratitude to Director NCL, Director Piramal Lifesciences Ltd., Director Haffkine Institute for Training Research and Testing and HOD, organic chemistry division for allowing me to work at their respective institutes. As no one person contains complete wisdom, I have been blessed to be a part of NCL and Piramal scientific community for which a high level of excellence and commitment to research has been established far and beyond most other institutions.

I would also like to thank Dr. Anjali Shiras and her lab where I learned real time PCR. My Sincere gratitude to my doctoral committee members Dr. Padma Shastry, Dr. Mahesh J. Kulkarni and Dr. Ashok Giri for their invaluable comments and unconditional support. I would also like to thank Dr. Dr. Dibyendu Bhattacharyya and his co-worker Mrs. Vaishali Kailaje for helping me during my confocal microscopy experiments. I also like to thank Dr. Nafisa H. Balasinor for allowing me to work in her laboratory.

I would like to convey my sincere thanks to Dr. Moneesha Fernandes, Dr. Vandana Pore, Dr. Anita Gunjal, Mrs. Meenal Mane their helping and caring nature.

Special thanks goes to my lab members Khirud, Sachin, Madhuri, Seema, Namrata, Venu, Kiran, Manoj, Anjan, Tanaya, Amit, Govind, Manisha, Ragini, Harsha, Madhura, Leena, Ankita, Kavita, Soma, and Prem for unreserved support I have received countless time from them. They were always helped me during my difficult times and were incredibly supportive.

I would like to thank University Grant Commission, New Delhi, for the financial support. Finally none of this would have been possible were it not for the lifelong love and encouragement of my parents and family. What I am today I owe to them.

Harshit Kumar Soni

Table of Contents

Symposia attended / Poster / Oral Presentations

1. 31st Annual Convention **of Indian Association of Cancer Research (IACR) and International Symposium on "Cancer Genomics and its impact on the Clinics"** from the 26th to 29th January, 2012 organized by Advance centre for treatment, research and education in cancer, Navi Mumbai. Poster presented: **FPR and bcr-abl: Old players with new interactions;** Authors: Soni Harshit Kumar and Dr. Naik Nishigandha R.
2. 27th Annual convention of **Indian Association for Cancer Research and International Symposium on Frontiers in functional Genomics**" in February 2008 organized by Gujrat Cancer and Research Institute, Ahmedabad Gujrat, India. Oral Presentation: **Role of formyl peptide receptors in breast cancer cell lines;** Authors: Joglekar Aditi T., Soni Harshit Kumar, Naik Nishigandha R.

Abbreviations

AP	Accelerated phase
ABD	Actin-binding domain
APS	Ammonium persulphate
BM	Bone marrow
BSA	Bovine serum albumin
BCR	Breakpoint cluster region
CD	Cluster of differentiation
CMAC	Cell-matrix adhesion complex
CML	Chronic myeloid leukemia
CML-BC	Chronic myeloid leukemia- Blast crisis
CML-CP	Chronic myeloid leukemia- chronic phase
CP	Chronic phase
CC	Coiled coil domain
CCyR	Complete cytogenetic response
CHR	Complete hematological response
DMSO	Dimethyl sulfoxide
ERK	Extracellular regulated MAP kinase
FBS	Fetal bovine serum
FACS	Fluorescence-activated cell sorting
FPR	Formyl peptide receptor
GAM	Goat anti-mouse antibody
GAR	Goat anti-rabbit antibody
G-CSF	Granulocyte - colony stimulating factor
GAPs	GTPase activating protein
GEF	Guanine nucleotide exchange factor
GTP	Guanosine 5' triphosphates
GDP	Guanosine 5' diphosphate
GTPases	Guanosine triphosphatases
HSCs	Hematopoietic stem cells
ICAM	Intercellular adhesion molecule
JNK	JUN- terminal kinase

LCM	Laser scanning confocal microscope
LSCs	Leukemic stem cells
LT	Long term
MMR	Major molecular response
mTOR	Mammalian target of rapamycin
MMP9	Matrix metalloproteinases 9
MAPK	Mitogen activated kinase-like protein
MAPKAPK2	Mitogen-activated protein kinase-activated protein kinase 2
MDR	Multidrug resistance
MPPs	Multipotent progenitors
GMPs	Granulocyte – macrophage progenitors
TEMED	N', N, N', N' tetramethylethylenediamine
fMLP	n-formyl- Methionyl- Leucyl- Phenylalanine
NADPH	Nicotinamide adenine dinucleotide phosphate
NFM	Non fat milk
NOD/SCID	Non-diabetic dynamic / Severe combined immunodeficiency
NF-kb	nuclear factor-kappa-b
NLS	Nuclear localization signal
NMR	Nuclear magnetic resonance
Ph^1	Philadelphia chromosome
PI3K	Phosphoinositide 3 kinase
PTEN	Phosphatase and tensin homolog
PBS	Phosphate buffered saline
PECAM	platelet endothelial cell adhesion molecule
PH	Pleckstrin homology domain
PMNL	Polymorphonuclear leukocytes
PP2A	Protein phosphatase 2A
QPCR	Quantitative real time polymerase chain reaction
RT	Room temperature
S/T Kinase	Serine/ threonine kinase
ST	Short term
STAT	Signal transducers and activators of transcription
SDS	Sodium dodecyl sulphate
SDS PAGE	Sodium dodecyl sulphate Polyacrylamide gel

	electrophoresis
FYN	Src-like kinase
SEM	Standard error of mean
SAPK	Stress-activated protein kinase
SOCS2	Suppressor of cytokine signaling 2
TK	Tyrosine kinase
TKI	Tyrosine kinase inhibitor
LYN	v-yes-1 Yamaguchi sarcoma viral related oncogene homolog
WHO	World health organization

Abstract

Formyl peptide receptor (FPR) are chemoattractant receptors that belong to the G protein coupled receptor (GPCR) family and are present on professional phagocytes like PMNL, macrophages, etc. The FPR are activated by n-formyl peptides, released from bacteria and mitochondria leading to trafficking of phagocytes to the sites of bacterial invasion or tissue damage. Over the past five years, data from several groups have indicated that these receptors might act in a more complex manner. Other than phagocytic leukocytes, FPR were also detected in mesenchymal stem cells (MSCs), dendritic cells, astrocytes, hepatocytes, but their biological significance in these cells is not well understood. FPR are involved in chemotaxis, cytoskeletal reorganization, Ca^{++} mobilization and inflammation. All these parameters are altered in transformed cells leading to rounded cell morphology, reduced adherence, increased growth rate, loss of contact inhibition, etc. Furthermore, expression of functional FPR on solid tumors and alteration of FPR expression and FPR related functions in PMNL form chronic myeloid leukemia (CML) patients collectively suggest that FPR have an important role in cellular transformation.

This Ph.D. project entitled “Role of Formyl Peptide Receptor in Transformed Cells” was aimed to study the possible role of FPR in oncogenic transformation with specific reference to CML and breast cancer. In addition, role of FPR in drug resistance and cellular pluripotency of these cancers was also explored.

CML is a myeloproliferative disorder, characterized by the presence of the Ph^{1} chromosome. It is one of the most extensively studied human malignancy. PMNL from CML exhibit defects in various events which are activated by the FPR. FPR

on normal PMNL activated PMNL for host defense after binding to fMLP. PMNL from CML were reported to be defective in adhesion, transmigration, motility, chemotaxis, actin polymerization, phagocytosis and respiratory burst activities. The results demonstrated that interphase cells from CML patients showed decreased expression of FPR1, FPR2 and FPR3 than that in normal interphase cells while CML PMNL showed lesser FPR1 expression than that in CML PMNL. All CML cell lines showed FPR gene and protein expression. Similar to clinical samples FPR1 and FPR2 gene and FPR1, FPR2 and FPR3 protein expressions were less in bcr-abl positive cell lines than that in bcr-abl negative cell lines. All the receptors in the cell lines were functional as they all showed ligand binding which was higher than that in bcr-abl negative cell line. This ligand binding resulted in increase in cytoplasmic Ca^{2+} and F-actin polymerization. Increase in calcium in CML cell lines was at par with bcr-abl negative cell line, while F-actin polymerization in response to 10^{-6} M fMLP was higher in CML cell lines than that in bcr-abl negative cell line. CML cell lines were more pluripotent as they expressed higher CD34 and CD117. Changes in the expression of FPR1, FPR2, FPR3 genes & protein, bcr-abl protein, CD34, CD117 and CD38 in imatinib resistant (SR) cell lines in comparison to the imatinib sensitive cell lines vary depending on the type of bcr-abl fusion transcript expressed by these cell lines. SR cell lines showed higher ligand binding than their respective sensitive cell lines and therefore were more sensitive to the FPR ligands. Imatinib treatment increased expression of all the three FPR homologues in bcr-abl positive cell lines while bcr-abl negative cell line was unaffected. Role of FPR as therapeutic target in CML especially in imatinib resistant cell lines was established by the results that the FPR antagonist doubled the cytotoxic effect of imatinib in all the SR cell

lines. The results suggested that FPR might play role in imatinib resistance of stem like CML cells.

Another model system chosen for the study was human breast cancer, because more than 80% cancers are of epithelial origin. Breast carcinoma is the most common malignancy among women worldwide and is second only to lung cancer as the cause of death in women. Earlier, unpublished data from our lab showed expression of FPR in breast cancer cell lines. In view of these results, role of FPR in breast cancer was explored. The results from present study showed expression of all the three functional FPR homologues, in breast cancer and normal breast epithelial cell lines. Decreased FPR1 expression and increased FPR2 and FPR3 expressions was found in human breast cancer cell lines (HBCC) than that in the normal breast epithelial cell line. Expression of FPR1 and FPR2 was found to be associated with the aggressive and invasive nature of cell line as the highest aggressive and invasive cell line MDA-MB-231 showed the highest FPR1 and FPR2 gene and protein expression. FPR1 association was also found to be associated with the Cox-2 expression while FPR2 and FPR3 expressions were found to be linked with cellular pluripotency markers –oct-3/4, nanog, and klf4. FPR stimulation led to change in F-actin content in HBCC and induced epithelial-mesenchymal transition like process. FPR stimulation also led to increase in the level of cellular pluripotency markers in MCF-7. FPR1 and FPR2 stimulation by fMLP and WKYMVm, respectively led to activation of PI3K-Akt and Ras-Raf-MEK-Erk pathways in HBCC. Both of these pathways are responsible for oncogenic transformation and drug resistance in breast cancer. FPR1 and FPR2 transactivated EGFR and each other. Moreover, they showed cross talk with JAK-STAT pathway. These results indicated that FPR played important role in

oncogenic transformation of breast cells. Furthermore, inhibition of FPR signalling resulted in inhibition of MCF-7 and MDA-MB-231 cell proliferation suggesting that FPR could be a molecular target for drug development in breast cancer too. Their utility as biomarkers in prognosis of the breast cancer needs to be explored using clinical samples.

Introduction

Phagocytic leukocytes accumulate at the site of inflammation and microbial infection in response to a variety of chemoattractants. The first structurally defined such chemoattractant was the N-formyl peptide[1]. As prokaryotes and eukaryotic mitochondria initiate protein synthesis with *N*-formyl methionine, the N-formyl peptide could originate from either an endogenous source or exogenous source[1]. This N-formyl peptide was recognized by the formyl peptide receptors (FPR) present on the cell surface of phagocytic leukocytes[1]. Although the FPR was identified and cloned many years ago, its biological significance in cells other than hematopoietic origin remained poorly understood.

Formyl Peptide Receptor (FPR)

FPR is a family of chemoattractant receptors that belong to the G-protein coupled receptors (GPCR) super family and is present on professional phagocytes like PMNL, macrophages, etc.[2] (Table-IN 1). FPR family consists of three FPR members – FPR1, FPR2 and FPR3 (Table-IN 1 and Fig IN 1 & 2). The three members of the human FPR gene family are clustered on chromosome 19q13.3–19q13.4[3, 4]. FPR1 was the first discovered member of the FPR family[2]. It is a high affinity fMLP receptor, with Kd in the nanomolar range (Table IN 2). It binds to the variety of ligands, which are listed in the Table IN 2. FPR2, also known as FPRL1, FPR2/ALX, is a low affinity fMLP receptor[2]. Other than fMLP, FPR2 also binds to lipoxin A4 (LXA4), aspirin-triggered lipoxins (Table IN3). FPR2 shares 69% of its amino acids with FPR1 (Table-IN 1). FPR2 showed more affinity to mitochondria-derived formyl peptide than fMLP[5]. Agonists for FPR2 are

Table IN 1: FPR Family

FPR isotype	Other Names Used	Gene Location	Homology with FPR1
FPR1	FPR, NFPR, FMLP, FMLPR	19q13.41	NA
FPR2	FPR2/ALX, FPRL1, FPRH1, RFP, LXA4R, ALXR, HM63, FMLPX, FPR2A	19q13.3-q13.4	69%
FPR3	FPRL2, FPRH2, FMLPY	19q13.3-q13.4	56%

NA: Not Applicable
Source: *Trends Immunol*. 23(11):541-548, 2002

Table IN 2: Agonists of FPR1

Ligand	Origin	Kd/EC50/IC50
fMLP and analogues	Gram negative bacteria	0.1–1 nM
T20 (DP178)	HIV-1LAVgp41 (aa 643–678)	0.5 mM
T21 (DP 107)	HIV-1LAVgp41 (aa 558–595)	0.1 mM
gG-2p20	HSV type 2	0.6 mM
WKYMVm	Random peptide library	1 nM
WKYMVM	Random peptide library	30 nM
Annexin 1	Endogenous (ubiquitary)	N.A.
Ac2-12	Annexin 1 (aa 1–12)	N.A.
Ac2-26	Annexin 1 (aa 1–26)	5 mM
Ac9-25	Annexin 1 (aa 9–25)	10 mM
Cathepsin G	Endogenous (neutrophils)	85 nM
Formylated peptides	Mitochondrial proteins	0.1–1 nM

NA: Not Applicable
Source: *Cytokine Growth Factor Rev. 17(6):501-519, 2006.*

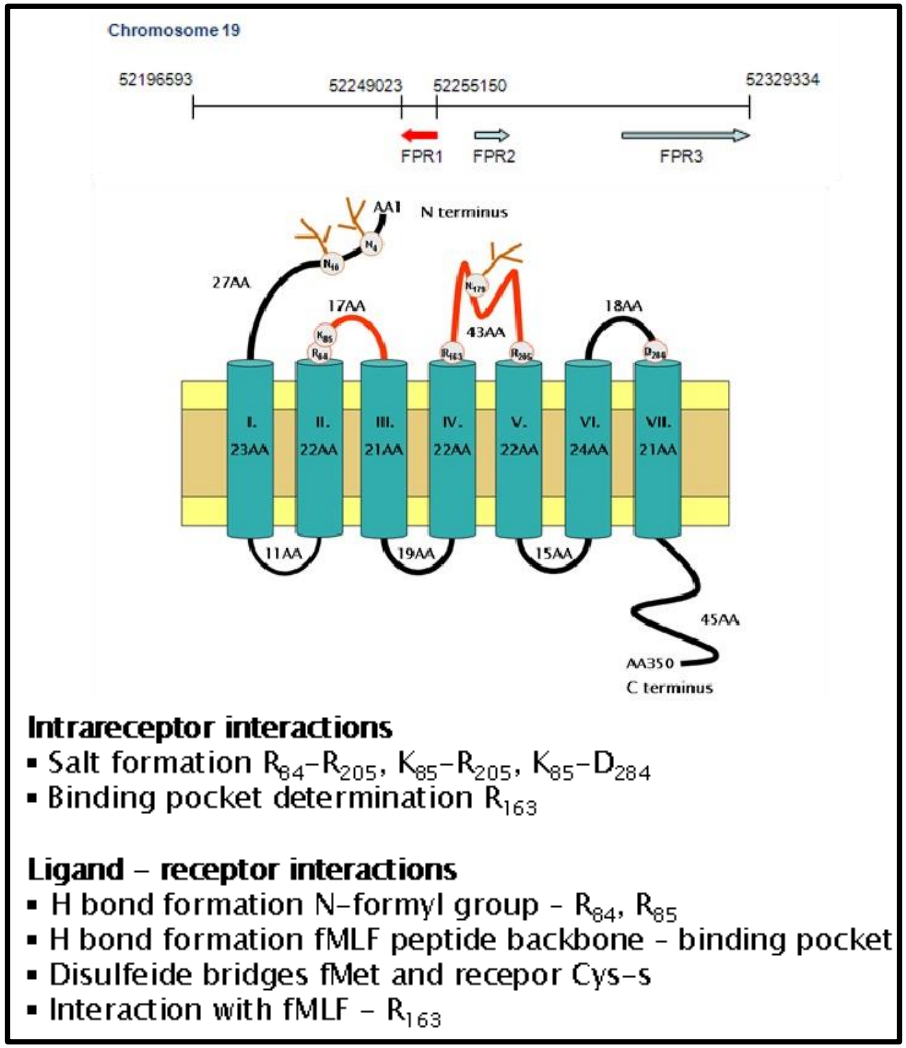

Fig IN 1: Chromosome location and structure of FPR: Mapping of FPR1, FPR2 and FPR3 on human chromosome 19. Seven transmembrane structure of FPR1. Transmembrane domains are predicted based on hydrophobicity of amino acid.

Source: Kohidai L 2008 https://commons.wikimedia.org/wiki/File:FPR.png

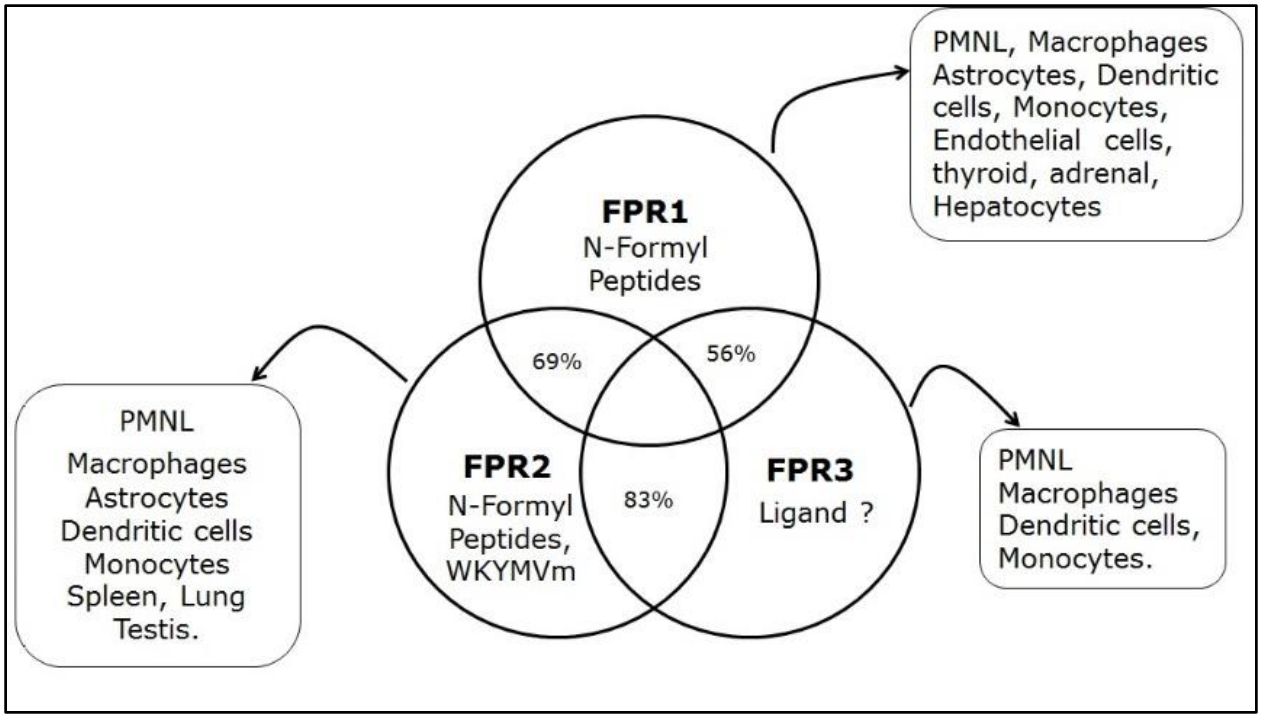

Fig IN 2: Members of FPR family: Percent homology among the human FPR family proteins -FPR1, FPR2 and FPR3; their expression in various tissues and main ligands are shown schematically.

Source: Pharmacol Rev 61: 119-161, 2009

listed in Table IN 3. The third member of this family is FPR3, also known as FPRL2. It does not show any binding to fMLP[6] though; it has shown activity in calcium flux assays when stimulated with fMMYALF, a peptide derived from a mitochondrial protein, which could be an agonist for FPR3[5]. FPR3 shares 56% sequence homology with FPR1 at the protein level. Its agonists are listed in Table IN 4. After binding with the ligand these receptors activate a cascade of signalling, which results in chemotaxis and activation of leukocytes[2] (Fig IN 3). In depth studies using recombinant FPR, showed that these receptors mediate fMLP induced calcium mobilization[7], actin polymerization[8], production of superoxide[9], NADPH oxidase activation[10] and chemotaxis in pertussis toxin sensitive manner[2]. When cells are treated with antagonists for FPR (Table IN 5), the above mentioned events are inhibited. These observations indicate that these receptors play an important role in host defence and inflammation.

Cellular and Tissue Distribution of FPR

The three receptors of the FPR gene family are primarily found in myeloid cells, but the distribution varies within myeloid cell subsets (Fig IN 2). FPR2 and FPR3 can be detected together with FPR1 in monocytes, although the expression pattern changes with the differentiation of monocyte into dendritic cells (DCs) and macrophages. In particular, in the process of monocyte differentiation into immature DCs, the cellular expression of FPR2 progressively declines[11], whereas FPR2 expression remains unchanged during monocyte differentiation into macrophages. There is a progressive loss of FPR1 during differentiation of immature DC to mature DC, making FPR3 as the predominant human FPR in mature DC[6, 12]. Biological significance of differential expression of FPR in

monocytes, macrophages and DCs has not yet been clearly delineated. Becker et al. (1998) found immunoreactivity for FPR at the histological level in multiple

Table IN 3: Agonists of FPR2

Ligand	Origin	Kd/EC50/IC50
fMLP and analogues	Gram negative bacteria	1 mM
Hp2-20	Helicobacter pylori	0.3 mM
N36	HIV-1LAVgp41 (aa 546–581)	12.5 mM
F peptide	HIV-1Bru gp120 (aa 414–434)	10 mM
V3 peptide	HIV-1MNgp120 (V3loop)	2 mM
T21 (DP 107)	HIV-1LAVgp41 (aa 558–595)	50 nM
WKYMVm	Random peptide library	1pM
WKYMVM	Random peptide library	2 nM
Other hexapeptides	Random peptide library	
MMK1	Random peptide library	0.5 nM
Quin-C1	Synthetic	1.9 mM
NADH dehydrogenase subunit I-derived peptide	Mitochondria	0.5 nM
Lipoxin A4	Endogenous	1 nM
Annexin 1	Endogenous	0.9 mM
Ac2-26	Annexin 1	0.9 mM
Ac2-12	Annexin 1	20 mM
LL37	hCAP18 (aa 1–37)	1 mM
Temporin	Rana temporaria	250 nM
sCKb8-1	Human CCL23	1 nM
D2D388–274	Human uPAR (aa 88–274)	0.1 nM/83 nM
uPAR84–95	Human uPAR (aa 84–95)	Not determined
SAA	Human acute phase protein	50 nM
Ab42	Human APP (aa 1–42)	0.2–1 mM
PrP106-126	Human prion protein (aa 106–126)	25 mM
Humanin	Endogenous	3.5 nM
Formylated humanin	Humanin	0.12 nM
Formylated peptides	Mitochondrial proteins	0.1–1 nM
PACAP27	Endogenous	1 mM

Source: *Cytokine Growth Factor Rev. 17(6):501-519, 2006.*

Table IN 4: Agonists of FPR3

Ligand	Origin	Kd/EC50/IC50
Hp(2–20)	Helicobacter pylori	10 mM
WKYMVm	Random peptide library	3 mM
WKYMVM	Random peptide library	3 mM
Annexin 1	Endogenous	>10 mM
Ac2-26	Annexin 1	>10 mM
Humanin	Endogenous	2.6 nM
Formylated peptides	Mitochondrial proteins	>1 mM
F2L	Heme-binding protein	10 nM

Source: *Cytokine Growth Factor Rev. 17(6):501-519, 2006.*

Table IN 5: Antagonists for FPR Family

Ligand	Assay	Potency	Selectivity
Chemotaxis inhibitory protein of S. aureus (CHIPS)	Binding	pKd=7.46	FPR1
FPRL1-inhibitor protein (FLIPr)	Binding, Ca2flux	N.D.	FPR2/ALX>>FPR1
Trp-Arg-Trp-Trp-Trp-Trp (WRW4)	Ca2 flux	pIC50=6.64	FPR2/ALX>>FPR1≈FPR3
CsH	Binding	pKi=7.00	FPR1
CsA	Enzyme release	pKi=6.22	FPR1
i-Boc-Met-Leu-Phe	$O2^-$ generation	pIC50=6.60	FPR1
t-Boc-Met-Leu-Phe	Enzyme release	pIC50=6.19	FPR1
t-Boc-Phe-Leu-Phe-Leu-Phe	Enzyme release	pIC50=6.59	FPR1>>FPR2/ALX
Quin-C7	Binding	pKi=5.19	FPR2/ALX
CDCA	Binding	pKi=4.76–4.52	FPR1>FPR2/ALX
DCA	Binding	pKi=4.00	FPR1
Spinorphin	$O2^-$ generation	pIC50=4.30	FPR1

Source: *Pharmacol Rev*. 61(2):119-161, 2009

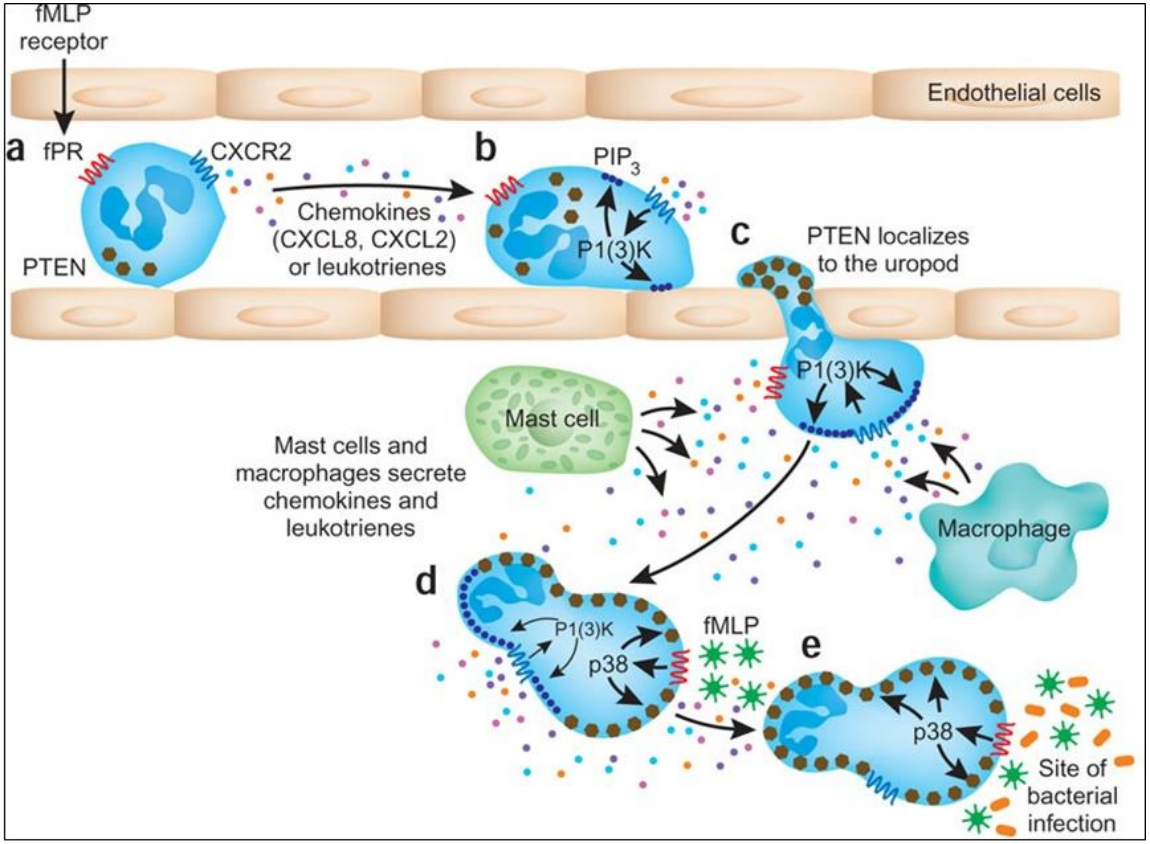

Fig IN 3: Acitvation of PMNL: Microbicidal action of PMNL is stimulated by binding of FPR1 to its ligand (a). This triggers a series of events in a cell such as cell margination (b), rolloing along the wall of blood capillaries, transmigration (c), activation by cytokines (d) ultimately reaching the cell to the site of infection (e).

Source: Nature Immunology 9: 716-718, 2008

organs and tissues that include epithelial cells in organs with secretory functions, endocrine cells (including follicular cells of the thyroid and cortical cells of the adrenal gland), hepatocytes, Kupffer cells, smooth muscle cells, endothelial cells, brain, spinal cord and both, motor and sensory neurons[13]. In most cases, this has not yet been verified at the RNA level or by functional studies. Human FPR2 has a tissue distribution pattern similar to that of FPR1 (Table IN 6). Another study showed endothelial cells expressing formyl peptide binding sites[14]. Functional FPR1 has also been found in brain[15], hepatocytes, dendritic cells, and astrocytes[16, 17], lung epithelial cells[18], fibroblasts[19], bone marrow-derived MSCs[20], hepatocytes, glial cells, astrocytes, and platelets[16, 21, 22]. Since chemotaxis and degranulation are not the primary functions of these cells, the role of the FPR in these cells is not clear and remains to be defined.

Table IN 6: Cell Type and Tissue Expression of FPR Family

FPR	Cells and tissues	Methods of detection
FPR1	Neutrophils; monocytes/macrophages; differentiated U937, HL-60 and NB4	Ligand binding
	Immature dendritic cells; astrocytes (HSC2), microglia, neuroblastoma; glioblastoma; hepatocytes; Kupffer cells; endothelial cells; lung carcinoma cells; epithelial enzyme-secreting cells, smooth muscle cells of muscularis propria and of mucosa of ileum, arterioles, retina, some neurons	Flow cytometry, immunofluorescence, RT-PCR, and immunohistochemistry
FPR2	Neutrophils; monocytes/macrophages; differentiated HL-60 cells	Ligand binding and calcium mobilization
	Colonic epithelial cells (T84, HT29, Caco-2, CL. 19A); medial tissue of coronary arteries; astrocytoma cell lines	Immunohistochemistry ligand binding and RTPCR
FPR3	Monocytes; immature and mature dendritic cells; lung; medial tissue of coronary arteries	Immunohistochemistry and Northern blot

Source: *Biochimie*. 89(9):1089-1106, 2007

Signal Transduction and Cellular Function of FPR

FPR1, FPR2 and FPR3 are all coupled to the Gi family of the G-proteins, which is sensitive to pertussis toxin[2]. Upon agonist binding, FPR undergoes rapid phosphorylation and internalization. FPR phosphorylation is catalysed by G protein-coupled receptor kinases (GRK) and does not require G protein activation[2]. After binding to its agonists, the receptor activates the heterotrimeric G protein, which dissociates into α and $\beta\gamma$ subunits[2]. These subunits then activate complex signalling events (Fig IN 4), which could be classified as follows:

- Activation of Calcium signalling
- Activation of NFκB pathway
- Activation of PI3K-Akt pathway
- Activation of mitogen-activated protein kinase (MAPK) pathway
- Activation of Rho-GTPase pathway
- Transactivation by FPR

Activation of Calcium signalling

Ligand binding to FPR activates PLCβ. Activation of PLCβ results in hydrolysis of phosphatidylinositol 4,5-bisphosphate (PIP2), generating DAG and inositol-1,4,5-trisphosphate (IP3)[2]. IP3 in turn releases Ca^{2+} from intracellular stores. Increase in Ca^{2+} takes place in two stages: initial transient release from intracellular storage sites, followed by a delayed influx across the plasma membrane[23]. Increase in cytosolic Ca^{2+} levels is one of the first detectable events induced by fMLP. Ca^{2+} works as a second messenger in chemotaxis. Change in intracellular

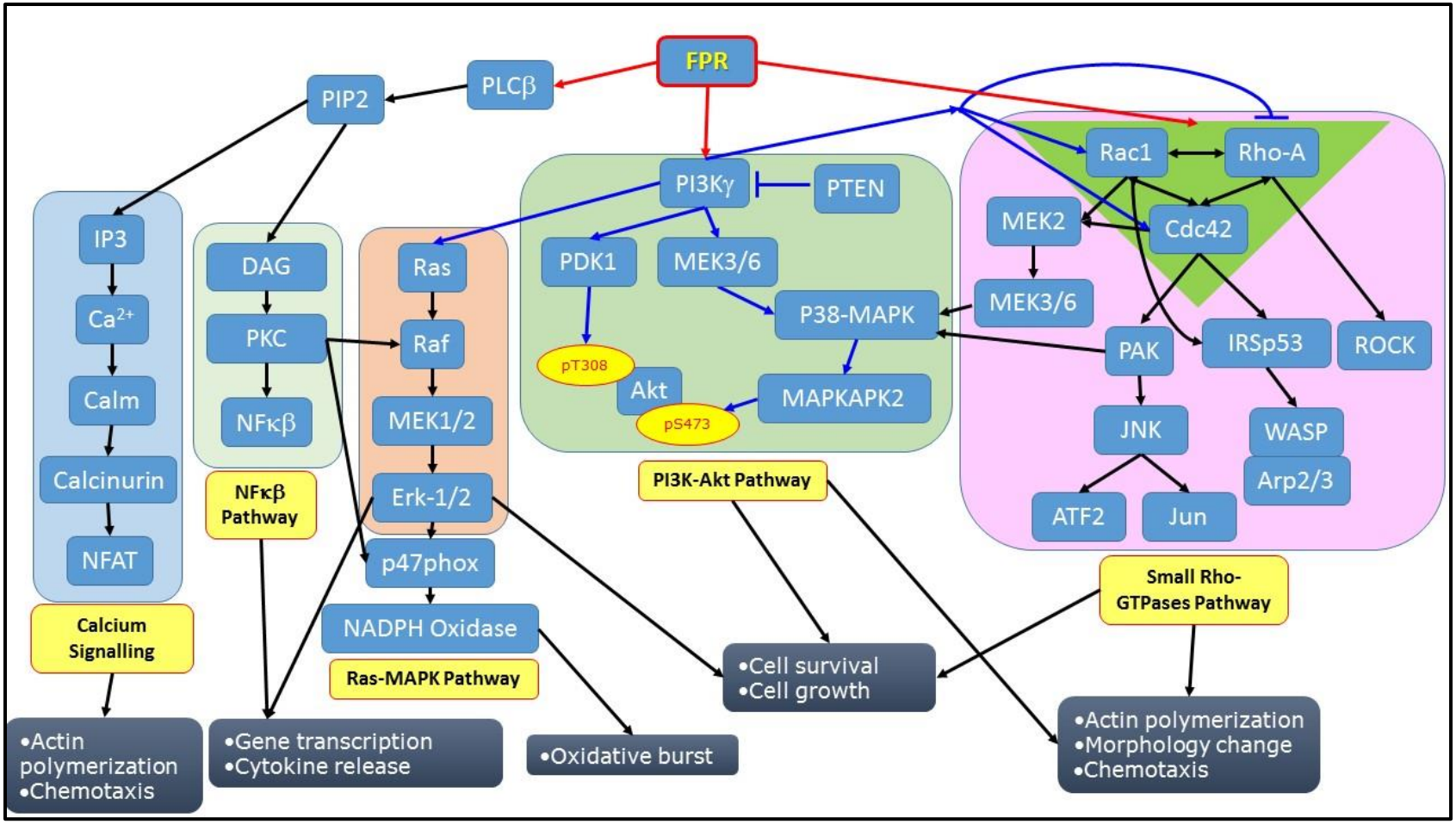

Fig IN 4: Signalling pathways activated by FPR: Upon binding to ligand, FPR activates various signalling pathways such as NFkB pathway, Calcium signalling pathway, Ras-MAPK pathway, PI3K-Akt pathway, small-RhoGTPases pathway. Activation of these pathways results in actin polymerization, chemotaxis, respiratory burst, etc.

calcium is linked with various cellular events e.g. degranulation, cellular kinase activation, regulation of cytoskeleton binding protein[24].

Activation of NFκB signalling

As mentioned above, hydrolysis of PIP2 by PLCβ generates DAG and IP3. DAG activates PKC[2]. PKC in turn activates NFκB. PKC also activates Raf and thereby activates the Raf-MEK-Erk-1/2 pathway. This pathway is also activated by Ras. fMLP, however, is proved weaker NFκB activator than LPS or TNFα, and it elicits very delayed response[25]. Browning et al. reported that fMLP activates NF-κB in human monocytes, but not in neutrophils, even after stimulation with LPS or TNF[26]. NFκB is a transcription factor that exists as a dimer[27]. NFκB dimers are kept inactive in the cytoplasm by forming a complex with cytoplasmic inhibitor proteins, collectively termed as IκB proteins[27]. Upon fMLP stimulation, multimeric IκB kinase complex (IKK) phosphorylates IκB which leads to IκB ubiquitination[2]. This process releases NFκB and it is transported to the nucleus, where it activates transcription of many proinflammatory genes[2].

Activation of PI3K-Akt pathway

Gβγ unit of FPR activates PI3K[2]. PI3K phosphorylates PIP2 to PIP3. PIP3 recruits and activates various cytosolic effectors and thereby controls chemotaxis, proliferation, oxidative burst and gene transcription. PI3K stimulates DOCK2 and P-Rex1 that activates Rac1[28].PI3K also activates Ras-Erk pathway and Akt-mTOR pathway. PI3K activates Akt by inducing its phosphorylation at two sites – T308 and S473. Phosphorylation at T308 is mediated by phosphoinositide-dependent kinase-1 (PDK1)[29] and phosphorylation at S473 is mediated by MAPKAP kinase-2 (MAPKAPK-2), which is a p38-MAPK substrate[30]. Phosphorylation of S473 stabilizes Akt in the active conformation. Akt plays the central role in the

regulation of cell differentiation, apoptosis, respiratory burst, chemotaxis and cell cycle.

Activation of MAPK pathway

The mammalian mitogen-activated protein kinases (MAPK) consist of cytoplasmic serine/ threonine kinases that participate in the transduction of signals from the surface to the interior of the cell. This group includes the extracellular signal-regulated kinase (ERK) family, the p38 kinase family, and the c-Jun N-terminal kinase family (JNK, also known as stress-activated protein kinase or SAPK). Each MAPK signalling cascade consists of at least three components, or module: a MAPK kinase kinase (MAP3K), a MAPK kinase (MAP2K), and a MAPK. Signals are transmitted through this cascade by sequential phosphorylation and activation of these components. The MAPKKK is in turn activated by interaction with a family of small GTPases[31] and/or other protein kinases connecting the MAPK cascade to the cell surface receptor or external stimuli. There are three major groups of MAPK cascades –extracellular response kinases 1 and 2 (ERK1/2), Jun N-terminal kinases (JNKs) and p38.

Extracellular response kinases 1 and 2 (ERK1/2)

ERK1/2 MAPKs are proteins of 44 and 42 kDa which are nearly 85% identical, with much greater identity in the core regions that is involved in binding to the substrates. ERK1 and ERK2 are activated by a pair of closely related mitogen and extracellular signal-regulated kinases (MEKs), MEK1 and MEK2, which are regulated by growth factor receptors and tyrosine kinases that activate through Ras[32]. Upon translocation to the nucleus, ERKs are responsible for phosphorylation of multiple substrates.

Jun N-terminal kinases (JNKs)

JNKs are encoded by three genes JNK-1, JNK-2, and JNK-3, which are alternatively spliced to form the JNK isoforms[33]. The JNKs are activated when dual phosphorylation occurs at the threonine–proline–tyrosine motifs. These are activated by GTP-binding proteins from the Rho family[31]. JNKs were originally identified as the major kinases responsible for the phosphorylation of c-Jun, leading to increased activity of the AP-1 transcription factor[34]. Other nuclear transcription factors also known to be its targets are ATF-2, Elk-1, Myc, Smad3, tumor suppressor p53, NFAT4, DPC4 and MADD, a cell death domain protein[33].

p38-MAPK

The p38 MAPKs are subject to dual phosphorylation at the threonine–glycine–tyrosine motif[35, 36]. Till date, four p38-MAPK isoforms have been identified; they share about 60%homology and two of these isoforms - p38α and p38β are ubiquitously expressed[35, 36]. The p38γ isoform is predominantly expressed in skeletal muscle, whereas p38δ gene expression is found in the lungs, kidneys, testes, pancreas and small intestine. In most of the inflammatory cells, p38α is the major activated isoform. p38 MAPK has been reported to be indispensable for chemotaxis[37].

Activation of small Rho-GTPases

The ras GTPases is a superfamily of GTPases with the molecular weight in the range of 20–30kDa[38]. They are structurally classified into five families: ras, rho, arf, rab and ran[38]. Out of these five, fMLP stimulates ras and rhoGTPases. The main members of rhoGTPase family are rhoA, rac-1 and cdc42.

Rho-GTPases exist in an inactive GDP-bound conformation and an active GTP-bound conformation[39]. Their interconversion is controlled by 1) a large family of

guanine nucleotide exchange factors (GEFs) that increase GDP/GTP exchange rate, 2) an equally large family of GTPase activating proteins (GAPs) that stimulate intrinsic GTPase activity, thereby down regulating rhoGTPases and 3) guanine dissociation inhibitors (GDIs) that sequester GDP-bound rhoGTPases in the cytoplasm and inhibit spontaneous GDP to GTP exchange. RhoGTPases modulate and control numerous aspects of actin filament dynamics and cytoskeleton structure. They link many cytoplasmic signaling effectors to actin cytoskeleton[40] and their activity influences diverse processes such as cell growth, migration, cell shape and cell fate[38, 41]. The specific mechanical and chemical cues that modulate activity of more prominent family members, rho, rac, and cdc42, to each of the above mentioned processes is likely to vary among different cell or tissue types.

RhoA is generally localized in the adhesion plaques and stress fibers. It plays important role in regulation of actomyosin contractility and in cell locomotion[42]. Active myosin II binds to actin filaments and forms actomyosin and generate actomyosin contraction. Stress-fiber assembly and actomyosin contraction are predominantly induced by RhoA[42]. Main downstream effector of RhoA which is involved in the actin dynamics is the serine/threonine kinase, ROCK. ROCK stabilizes F-actin by preventing action of actin depolymerizing factor –cofilin by cofilin phosphorylation. Activation of another downstream effector of RhoA, mDIA facilitates actin nucleation and polymerization by the actin-binding protein - profilin[43].

Rac is localized in the lamellipodia. It is the key regulator of migration because of its ability to stimulate lamellipodium extension. Rac interacts with IRSp53, which in turn interacts with WAVE, which then binds to and activates Arp2/3

complex. The Arp2/3 complex initiates polymerization of new actin filaments next to existing filaments leading to formation of a branching actin filament network[44]. IRSp53 also binds to Cdc42[45] and acts as a direct link between Cdc42 and Rac. Through IRSp53, Cdc42 can induce Rac-dependent lamellipodium extension[46]. IRSp53 can also bind to a Rho target, Dia1[47] and contribute to lamellipodium extension. Rac can also stimulate actin polymerization by promoting uncapping of actin filaments at the plasma membrane[44].

Cdc42 is seen in filopodia as it regulates filopodium formation, which is required for direction sensing during chemotaxis[48, 49]. Cdc42 initiates actin polymerization required for filopodium extension, via its interaction with WASp and N-WASp, leading to activation of the Arp2/3 complex[42].

Transactivation by FPRs

Many reports show that GPCR can utilize receptor tyrosine kinases (RTK) to mediate important cellular responses such as proliferation, differentiation and survival[50, 51]. Recent reports suggest that GPCR induced trans-activation of RTK might be important in diseases such as cancer and cardiac hypertrophy. Depending on the receptor and cell type, GPCR signaling involves activation of different subsets of RTK and thus GPCR can fine-tune their effects on target cells[52, 53]. A diverse group of agonists e.g. peptide hormones, neurotransmitters and phospholipids that do not directly interact with RTK, rather act through GPCR and induce proliferative responses and even cellular transformation in a variety of cell lines and tissues[54]. In fact, the major mitogenic activity of serum is by a GPCR ligand, lysophosphatidic acid (LPA). Such cross talk occurs in a cell type specific manner via activation of different RTK by the same GPCR ligand[53]. Ligand-independent EGFR trans-activation occurs in diverse cell types via

GPCR[55]. Tumor cells stimulated with the FPR agonist fMLP, show rapid phosphorylation of EGFR which is restricted to a single tyrosine residue Tyr992[56-59]. Studies are being carried out to know various proteins involved in this trans-activation and its significance.

Recent Developments

FPR has been shown to activate expression of VEGF and PDGF[56, 59] thus assisting the growth of tumor cells in the absence of extracellular growth factor signals. FPR in glioblastoma cells stimulates phosphorylation of STAT3 at Ser-727 and Tyr-105 residues as well as another transcription factor - hypoxia inducible factor-1α (HIF-1α). Both STAT3 and HIF-1α are implicated in the transcriptional activation of the gene coding for VEGF. It has been demonstrated that FPR induces expression of VEGF[57]. Increased FPR expression has been reported glioblastoma multiforme and anaplastic astrocytomas[60]. fMLP stimulation mediated motility, growth and angiogenesis in these. Functional expression of FPR in glioma cells plays an important role in regulating vasculogenesis by endothelial progenitor cells[61]. Chen et al. have reported that functional FPR expression was essential for sustaining growth and aggressive phenotype of glioma[62].

Cellular Transformation

Malignant cellular transformation is a process by which normal cells acquire characteristics of malignant cancer cells. Malignant cellular transformation is a multistep process, during which cells acquire various abilities to evade anticancer defense mechanisms of cells and tissues. These capabilities could broadly be divided into six major types as described by Hanahan and Weinberg[63]. These six biological capabilities are also known as "hallmarks of cancer" (Fig IN 5).

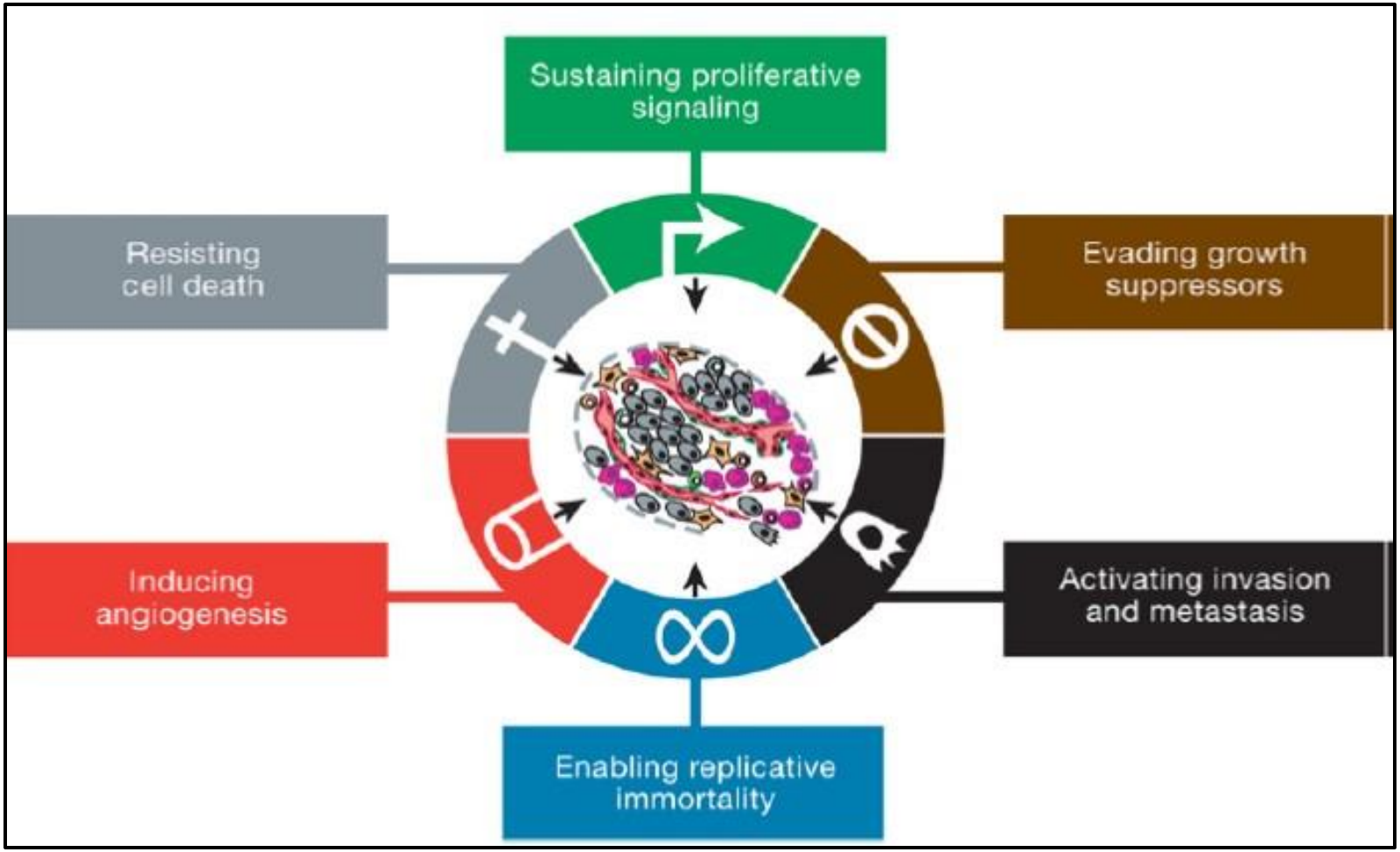

Fig IN 5: Hallmarks of cellular transformation: Six parameters described by Hanahan and Weinberg that are acquired by normal cells to transform itself to malignant cells.

Source: Cell 100: 57-70, 2010

Proliferation autonomy

To enter into the active proliferative state, normal cells require growth signals (GS). However, tumor cell enables to produce its own signals. Many oncogenes in the cancerous cells mimic normal GS. These GS work by binding to the cell surface receptors that often possess tyrosine kinase activity at the cytoplasmic end. These receptors are overexpressed in many of the cancers therefore cancer cells become hyper responsive to these signals. Hence, cancer cells start proliferation even in response to the ambient level of GS which otherwise fail to initiate proliferation in normal cells. Three strategies are evident in cancer cells for achieving self-sufficiency – alteration of extracellular GS, alteration of transcellular transducers of GS, or alteration of intracellular circuits that translate GS into action. FPR played role in cell proliferation per se as well as in trans-activation of GS receptors or cross talk with their downstream signalling as mentioned earlier. Hence FPR activity could also help the tumor cells in achieving self-sufficiency to proliferate[54, 64, 65].

Non-responsive to antigrowth signals

Various antiproliferative signals are found in normal tissues. Similar to growth signals these signals also mediate their effect on cells via transmembrane cell surface receptors. These signals maintain cell quiescence and tissue homeostasis. These antigrowth signals could inhibit cellular proliferation by two mechanisms:

1. Turn active proliferative cells into the quiescent G_0 state, so that in future when GS permit they could again be tuned into the active proliferative state.

2. Permanently inhibit the proliferative potential of cells and hold them into G0 state.

Many of these strategies to inhibit cell growth depend on the actions of tumor suppressor genes. Two of the most studied tumor suppressor genes are p53 and Rb (retinoblastoma associated). It was reported that FPR1 promoter contains p53 response element and p53 inhibit expression of FPR[66]. Hence, inactivation of p53 in cancer make FPR constitutively active and this active FPR would be capable of promoting cellular proliferation.

Escaping programed cell death (apoptosis)

Programmed cell death or apoptosis is a sequence of tightly regulated events that eliminate the cells, which are no longer required or are a threat to the organism, without releasing harmful substance. The ability of tumor cells of limitless proliferation is restricted by apoptosis. Hence, all types of tumors acquire resistance to apoptosis.

Infinite proliferative ability

Despite aforementioned abilities, a cell could proliferate only for a certain number of times and after that it stops growing. This phenomenon is known as cell senescence. Mutation in tumor suppressor genes could help the cells to proliferate for some additional generations until they enter into crisis state, which is characterized by massive cell death due to the end-to-end fusion of chromosomes[63]. However, tumor cells acquire the ability to multiply without limit, which is called immortalization. This immortalization was achieved by cancerous cells by up-regulation of telomerase enzyme.

Persistent angiogenesis

In spite of achieving limitless proliferation and independence in growth signals, a cell needs oxygen and supply of nutrients via vasculature. The process of new blood vessels formation is known as angiogenesis. To get sustained blood supply cancer cells produce angiogenic factors such as VEGF and thereby induce angiogenesis. FPR1 was shown to activate VEGF and could induce angiogenesis[59].

Invasive and metastatic potential

Cancer cells spread from the site of the primary tumor to distant organs or tissues and established new colonies. This process is known as metastasis. To achieve metastasis, cancer cells require various capabilities – motility, transmigrate through endothelial cells and tissue invasion. The role of FPR could not be ruled out in achieving first two abilities. In fact, these two capabilities could be compared to the chemotaxis of PMNL induced by activation of FPR, where FPR signalling initiated PMNL motility and transmigration. On the other hand, FPR could also help in tissue invasion. Cancer cells require extracellular proteases such as Matrix metalloproteinases (MMP) for tissue invasion. FPR had been shown to activate MMPs. Hence, fMLP could help in invasion too[67-69].

Cellular malignant transformation is a complex process which requires various changes in the cellular genome, as well as cell function. To study the role of FPR in cellular transformation, two model systems –chronic myeloid leukemia and breast cancer, were chosen. Since FPR expression has been studied extensively in myeloid cells and CML is myeloid disorder, it would be good model system to study the role of FPR. Breast cancer was chosen as model to study because there were no confirmed reports available for expression of FPR in breast cancer

whereas earlier unpublished data from our lab showed differential FPR expression in breast cancer cell line.

Chronic Myeloid Leukemia (CML)

CML is a malignant disorder of pluripotent stem cells with the predominance of mature myeloid cells and their precursors accumulating in excess in the marrow and blood. The cause of CML is unknown and most cases occur sporadically. There appears to be no genetic predisposition to the development of the disease. Some predisposition is associated with nuclear and radiation exposure, but the development of the disease has not been linked to any chemical exposure. At the molecular level CML is characterized by the bcr-abl fusion gene, creating the Philadelphia (Ph^1) chromosome[70] (Fig IN 6). The Ph^1 chromosome results from a reciprocal translocation between the long arms of chromosomes 9 and 22. This transposes the large 3' segment of the *c-abl* gene from chromosome 9q34 to the 5' part of the *bcr* gene on chromosome 22q11 in a head-to-tail fashion, creating a hybrid *bcr-ab*l gene that is transcribed into a chimeric *bcr-abl* mRNA. Chromosome 9 and 22, both possess various break points. Depending on the break points involved in the translocation, bcr-abl gene could be of four types – e1a2, b2a2, b3a2, and e19a2. These four bcr-abl genes are translated into three chimeric proteins – p190, p210 and p230. b2a2 and b3a2 mRNA are translated into a protein of same size – p210. p190 is sometimes associated with acute lymphoblastic leukemia. p210 is linked to CML while p230 is associated with chronic neutrophilic leukemia.

Classical CML has three phases - chronic, accelerated and terminal blast crisis.

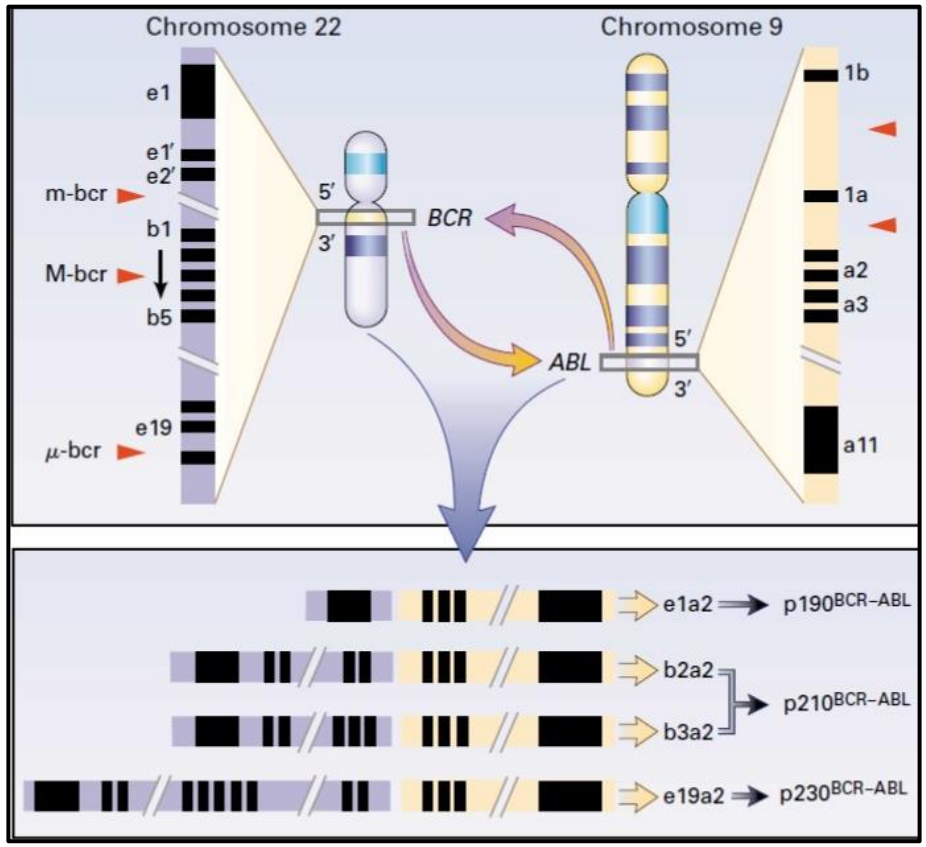

The New England Journal of Medicine 341, 164-172 (1999)

Fig IN 6: Philadelphia (Ph^1) Chromosome in CML: Ph^1 chromosome is a hallmark of CML. It results from translocation between chromosome 9 and 22. This translocation results in an oncogene bcr-abl. On the basis of break-point on bcr gene there are four bcr-abl fusion transcript named e1a2, b2a2, b3a2 and e19a2.

Source: The New England Journal of Medicine 341: 164-172, 1999

Chronic Phase

During this phase patient have less than 10% blasts cells in blood and bone marrow[71]. Most of the patients for CML are diagnosed in this phase. Duration of chronic phase depends on how early the disease was diagnosed as well as therapeutic interventions provided. During this phase, patients were treated with targeted therapy with tyrosine kinase inhibitor alone or in combination with chemotherapy. In absence of treatment the disease progresses to accelerated phase.

Accelerated Phase

During this phase more than 10% but less than 20% blasts were seen in blood and bone marrow of the patient[71]. Acquisition of chromosomal changes in addition to presence of Ph^1 chromosome and development of myelofibrosis are also included in criteria for accelerated phase. Treatment of accelerated phase chronic myelogenous leukemia may include 1) stem cell transplant 2) targeted therapy with a tyrosine kinase inhibitor 3) immune therapy (interferon) with or without chemotherapy 4) high-dose chemotherapy 5) chemotherapy and transfusion therapy to replace red blood cells, platelets, and sometimes white blood cells, to relieve symptoms and improve quality of life[71]. However, Drug treatment often becomes less effective in the advanced stages.

Blast Crisis

This is an advanced stage of CML and behaves like an acute leukemia. During blast crisis there is a rapid increase in proportion of blast cells. During this phase, patients show >20% blast cells in blood and bone marrow. Treatment of blastic phase CML may include secondary tyrosine kinase inhibitors, allogeneic transplantation and chemotherapy as palliative therapy to relieve symptoms and

improve quality of life[72]. Disease-free survival for allogeneic transplantation ranges from approximately 40 % to 50 % for accelerated phase to approximately 20 % for blast crisis. Other therapeutic agents are being developed for blast crisis and drug resistant CML (e.g., the aurora kinase inhibitors), but these are not curative[72].

Therapy for CML

There are three goals to be achieved in CML through therapeutic intervention. These are hematologic remission characterized by normalcy of blood count, cytogenetic remission characterized by 0% Ph^1 positive cells and molecular remission which is characterized by negative polymerase chain reaction (PCR) results for bcr-abl mRNA. The only curative treatment for CML is a bone marrow transplant or an allogeneic stem cell transplant, which achieve these three goals. Other than these, four main strategies were used to treat CML; targeted therapy with tyrosine kinase inhibitors, myelosuppressive or leukopheresis therapy, splenectomy and interferon alfa-2b treatment. In the first half of the 20^{th} century patients were treated predominantly with radiation therapy and later on with busulfan, hydroxycarbamide or interferon-alfa (IFN-α). From 1980 onwards, allogeneic stem cell transplantation (SCT) became the treatment of choice for eligible patients. The era of tyrosine kinase inhibitors (TKI) began in 1998 and today use of the TKI, imatinib has replaced SCT as initial therapy for patients who present with CML in chronic phase[73]. Imatinib has improved duration of hematologic and cytogenetic remissions.

Imatinib mesylate that was originally called as STI571 is commercially known as Gleevec. It works by binding to bcr-abl and blocking its function. To activate downstream signalling molecules, bcr-abl requires adenosine triphosphate (ATP),

which donates the phosphate group. ATP has a special binding site on bcr-abl close to the substrate proteins' binding site. If the ATP binding site is occupied, then ATP cannot donate the phosphate and bcr-abl can no longer activate downstream signaling proteins that promote cell division[74]. However, a small number of patients fail to respond to imatinib (primary resistance), while others respond initially and later lose their response (secondary resistance). In the last few years, new TKIs, dasatinib, nilotinib, bosutinib, ponatinib are available, which are more potent inhibitors of the bcr-abl kinase than imatinib and are useful in case of development of imatinib resistance

CML stem cell resistance

Understanding how CML cells or CML stem cells evade the effects of abl kinase inhibitors is crucial for disease eradication. According to Brian Druker, the innate resistance of leukemic cells is likely to be bcr-abl independent. Therefore, bcr-abl inhibitors as single agents may not be capable of curing patients with CML. Identifying agents that target stem cells that could be combined with bcr-abl inhibitors to eradicate disease is necessary[75].

Minimal residual disease (MRD) is to the term used for small number of residual leukemic cells that remain in patients during treatment or during remission. It is the major cause of relapse in CML. These cells can be detected only by using highly sensitive molecular biology techniques.

Possible Role of FPR in CML

In spite of being a myeloid disorder, infections are not commonly seen in CML. This could be because the increased number of PMNL seen in peripheral blood. These PMNL may arise from Ph^1 positive leukemic stem cells or normal stem cells. But, morphologically they are indistinguishable from each other. When the

functional normalcy of these cells was questioned, alterations were found at several levels in CML PMNL. CML PMNL exhibited defects in several functions such as motility, chemotaxis, transmigration, adhesion, agglutination, aggregation, phagocytosis/endocytosis and microbicidal activities[76-78]. Furthermore, CML PMNL have been reported to be defective in a panel of physiological and functional events stimulated by binding of fMLP. These include chemotaxis, actin polymerization, microtubule organization, phagocytosis, pinocytosis, degranulation, NADPH-Oxidase activity, superoxide generation and formation of H_2O_2[79-89]. CML PMNL showed defective FPR expression and downstream signalling in CML. It might be possible that FPR has role in CML pathogenesis. Therefore, the presented study was aimed to understand the role of FPR in CML, using imatinib sensitive as well as imatinib resistant CML cell lines and CML clinical samples.

Breast Cancer

Another model system chosen for the study was human breast cancer because more than 80% cancers are of epithelial origin. Breast carcinoma is the most common malignancy among women worldwide. Breast tumours are highly heterogeneous. Breast cancer could be divided into categories based on histopatholgical studies, grade and stage of tumour and expression of proteins & genes.

Histopathological classification

It is based upon characteristics seen upon light microscopy of biopsy specimens. On the basis of histopathology, breast cancer could be divided into three major types:

Invasive ductal carcinoma

This is the most common type of breast cancer. It represents 55% of breast cancer[90]. Invasive (or infiltrating) ductal carcinoma (IDC) starts in a milk duct of the breast, breaks through the wall of the duct and grows into the fatty tissue of the breast.

Ductal carcinoma in situ (DCIS)

It is also known as intra ductal carcinoma, is a pre-cancerous or non-invasive cancerous lesion of the breast. It constitutes 15-20% of all cancers[90]. DCIS means that the cancer cells are inside the ducts, but have not spread through the walls of the ducts into the surrounding breast tissue. Nearly all women diagnosed at this early stage of breast cancer can be cured.

Invasive lobular carcinoma (ILC)

ILC accounts for 5-10% of invasive breast cancers[90]. Invasive lobular carcinoma (ILC) starts in the milk-producing glands (lobules). Loss of E-cadherin is common in ILC but is also seen in other breast cancers[91].

Classification based on receptor status

Cells express receptors on their surface, cytoplasm and nucleus. Hormones are chemical messengers that bind to these receptors and cause changes in the cell. Breast cancer cells are classified on the basis of the presence or absence of three most important receptors –estrogen receptor (ER), progesterone receptor (PR), and HER2/neu. Cells with or without these receptors are called ER positive (ER+), ER negative (ER-), PR positive (PR+), PR negative (PR-), HER2 positive (HER2+), and HER2 negative (HER2-). Cells without all these receptors are called basal-like or triple negative. Another hormone receptor – androgen receptor is expressed in 80-90% of ER+ breast cancers and 40% of "triple

negative" breast cancers. Activation of androgen receptors appears to suppress breast cancer growth in ER+ cancer while in ER- breast cancer, it appears to act as growth promoter. Efforts are underway to utilize this as prognostic marker and treatment[92, 93].

Receptor status is combined with the tumour grade, to categorize breast cancer into several conceptual molecular classes:

- Basal-like: ER^-, PR^- and $HER2^-$; also called triple negative breast cancer (TNBC)[94].
- Luminal A: ER+ and low grade[95]
- Luminal B: ER+ but often high grade[95, 96]
- Luminal ER-/AR+: (overlapping with apocrine and so called molecular apocrine) - recently identified androgen responsive subtype which may respond to antihormonal treatment with bicalutamide[92]
- ERBB2/HER2+: has amplified HER2/neu[94]
- Normal breast-like[97, 98]
- Claudin-low: this class has been recently described. There is a low expression of cell-cell junction proteins, including E-cadherin[94] and frequently there is infiltration with lymphocytes[97, 99].

BRCA Genes

BRCA1 and BRCA2 genes are tumor suppressor genes. BRCA1 and BRCA2 proteins are involved in repair of DNA double-stranded breaks. Mutations in any of these genes disable the protein. Mutations in these genes may produce a hereditary breast-ovarian cancer syndrome in affected persons. 5-10% of breast cancer cases in women are attributed to BRCA1 and BRCA2 mutations where BRCA1 mutations are more common than BRCA2 mutations. Women with

mutations in either BRCA1 or BRCA2 have a 5 times higher risk of breast cancer. The risk of breast cancer is higher for women with a high-risk BRCA1 mutation than with a BRCA2 mutation. BRCA1 mutations are associated with triple-negative breast cancer, which does not respond to hormonal treatments. BRCA2 mutations are associated primarily with post-menopausal breast cancer however, highly responsive to hormonal treatments.

Possible Role of FPR in Breast Cancer

No. of reports available on study of FPR in breast cancer are negligible. Binding of fMLP and chemotaxis in response to fMLP binding was reported in breast carcinoma cell line, Walker 256[100, 101]. These cells showed chemotaxis in response to fMLP treatment in a concentration dependent manner. Binding and internalization of radiolabeled fMLP was also reported in these cells. FPR1 and FPR2 stimulation induced breast cancer cell proliferation[102]. The above-mentioned reports do provide a basis that breast cancer cells express functional FPR and stimulate chemotaxis and proliferation.

But, very little information was available about FPR per se in breast cancer. Therefore, the present studies were aimed to understand the role of FPR in breast cancer using breast cancer cell lines.

Hypothesis

In view of the defective FPR signaling and downstream cellular functions in CML PMNL at the various stages of the disease, it was hypothesized that FPR play role in CML pathogenesis as well as in disease progression

Though very little information was available about the function and expression of FPR in breast cancer, the role of FPR in breast cancer cell motility is

unambiguous. FPR expression was never shown in the breast cancer cells at molecular levels, but binding of FPR ligand fMLP and its effect on breast cancer indicated that FPR might have role in malignant transformation of breast cells. Furthermore, reports of EGFR transactivation and activation of VEGF by FPR are seen. Hence, it was hypothesized that FPR play complex role in malignant transformation of breast cells.

Drug resistance and disease recurrence are major challenges in cancer research. It's been reported that stem cell like cancer cells play role in these phenomena. Recent reports have demonstrated expression of FPR in mesenchymal stem cells and its role in their differentiation. Hence, it was postulated that FPR play role in the drug resistance of stem like cancer cells.

Aim

To investigate the role of FPR in transformed cells.

Objective

1. To study role of altered FPR expression in CML.
1. To investigate role of FPR in breast cancer.
2. To check whether FPR cross talk with other receptors.
3. To evaluate FPR as a diagnostic/prognostic marker or as a therapeutic target.

Materials

Chemicals

All chemicals and salts used unless otherwise mentioned were of analytical grade. All solutions otherwise mentioned were prepared in deionized Milli Q water (Milli Q).

Reagents were obtained from various sources as mentioned below:

Chemicals: Annexure Table-1

Bio-chemicals: Annexure Table-2

Kits: Annexure Table-3

Plastic wares: Annexure Table-4

Primary Antibodies: Annexure Table-5

Secondary Antibodies: Annexure Table-6

Fluorescent probes: Annexure Table-7

Primers: Annexure Table-8

Reagents

Inhibitors: Stock Solutions

Stock solutions were made as mentioned below and stored at -20°C. All the working stocks were prepared in complete medium/PBS. For all the experiments, the final concentration of the inhibitors mentioned below was achieved in the cell suspension. The inhibitors were used in treatment of cells for 1) cell proliferation

assays, 2) cell lysate preparation for Western blotting and 3) immunofluorescence staining.

Imatinib (M.W. - 589.7) – 5.897 mg was dissolved in 1 ml of sterile DMSO to get a 10 mM stock. The working stock of 10 μM was obtained after 1:1000 dilution of 10 mM stock. Final concentration was 1 μM after 1:10 dilution in cell suspension.

Dasatinib (M.W. – 488.0) – 0.98 mg was dissolved in 1 ml of sterile DMSO to get a 2 mM stock. 2 μM concentration was obtained after 1:1000 dilution of 2 mM stock in PBS. This 2 μM solution was diluted to 1:10 to get 0.2 μM working stock. Final concentration was 0.02 μM after 1:10 dilution in cell suspension.

Nilotinib (M.W. – 529.5) – 1.59 mg was dissolved in 1 ml of sterile DMSO to get a 3 mM stock. 3 μM concentration was obtained after 1:1000 dilution of 3 mM stock in PBS. This 3 μM solution was diluted to 1:10 to get 0.3 μM working stock. Final concentration was 0.03 μM after 1:10 dilution in cell suspension.

fMLP (M.W. – 437.55) – 4.375 mg was dissolved in 1 ml of sterile DMSO to get a 10 mM stock. The working stock of 10 μM was obtained after 1:1000 dilution of 10 mM stock. Final concentration was 1 μM after 1:10 dilution in cell suspension.

Cyclosporin H (M.W. – 1202.6) – 12.02 mg was dissolved in 1 ml of sterile DMSO to get a 10 mM stock. The working stock of 100 μM was obtained after 1:100 dilution of 10 mM stock. Final concentration was 10 μM after 1:10 dilution in cell suspension.

WKYMVm (M.W. – 855.41) – 8.554 mg was dissolved in 1 ml of sterile DMSO to get a 10 mM stock. The working stock of 10 μM was obtained after 1:1000 dilution of 10 mM stock. Final concentration was 1 μM after 1:10 dilution in cell suspension.

WRW4 (M.W. – 1104.28) –11.043 mg was dissolved in 1 ml of sterile DMSO to get a 10 mM stock. The working stock of 100 μM was obtained after 1:100 dilution of 10 mM stock. Final concentration was 10 μM after 1:10 dilution in cell suspension.

EGF (M.W. ≈ 6000) – 1 mg was dissolved in 1 ml of sterile 10 mM acetic acid to get a 1 mg/ml (≈167 μM) stock. The working stock of 1 μg/ml (≈167 nM) was obtained after 1:1000 dilution of 1 mg/ml stock with PBS containing 0.1% BSA. Final concentration was 100 ng/ml (≈16.7 nM) after 1:10 dilution in cell suspension.

AG1478 (M.W. – 315.8) – 3.158 mg was dissolved in 1 ml of sterile DMSO to get a 10 mM stock. The working stock of 5 μM was obtained after 1:2000 dilution of 10 mM stock. Final concentration was 0.5 μM after 1:10 dilution.

IL6 (M.W. ≈ 20000) – 1 mg was dissolved in 1 ml of sterile DMSO to get a 1 mg/ml (≈50 μM) stock. 1 μg/ml (≈50 nM) was obtained after 1:1000 dilution of 1 mg/ml stock. This 1 μg/ml solution was further diluted to 1:10 to get 100 ng/ml (≈5 nM) solution. Final concentration was 10 ng/ml (≈ 0.5 nM) after 1:10 dilution.

AG490 (M.W. – 294.31) – 2.943 mg was dissolved in 1 ml of sterile DMSO to get a 10 mM stock. The working stock of 200 μM was obtained after 1:50 dilution of 10 mM stock. Final concentration was 20 μM after 1:10 dilution.

PP2 (M.W. – 301.8) – 3.018 mg was dissolved in 1 ml of sterile DMSO to get a 10 mM stock. The working stock of 100 μM was obtained after 1:100 dilution of 10 mM stock. Final concentration was 10 μM after 1:10 dilution.

Cell Lines

HL60: It is a promyelocytic cell line established by S.J. Collins, et al [103]. It was established from peripheral blood leukocytes that were obtained by leukopheresis from a 36 years old Caucasian female with acute promyelocytic leukemia[103, 104]. HL60 was obtained from ATCC.

K562: K562 was established by Lozzio and Lozzio from the pleural effusion of a 53 years old female with CML in terminal blast crisis[105]. The cell population was characterized as highly undifferentiated, hematopoietic malignant cells that can be made to differentiate into recognizable progenitors of the erythrocytic, granulocytic and monocytic series. K562 cells contain at least one Ph^1 chromosome with the b3a2 bcr-abl gene arrangement[106]. K562 was obtained from ATCC.

KU812: This cell line was established by Kishi K. from the peripheral blood of a 38 years old male CML patient in blast crisis [107]. Patient was treated with busulfan for 10 years before cell line development. The patient also had an extramedullary spinal tumor which was treated with various combinations of chemotherapy with no neurological improvement [107]. This cell line was initially found to contain basophilic precursors but later it was discovered that this cell line was bipotent, containing basophilic as well as erythroide lineages[108]. The KU812 cells contain at least one Ph^1 chromosome with the b3a2 bcr-abl gene arrangement[107, 108].

KCL22: This was established by cultivation of pleural effusion cells obtained from a 32 years old woman with CML in blast crisis and expressing b2a2 fusion transcript of bcr-abl[109, 110]. This cell line was characterized as immature

undifferentiated hematopoietic cell line which showed properties of monocytes/macrophages and some characters of megakaryocytes[109, 110].

K562/SR: It was derived from K562 and is resistant to 1 μM concentration of imatinib[111].

KU812/SR: It was derived from KU812 and is resistant to 1 μM concentration of imatinib[111].

KCL22/SR: It was derived from KCL22 and is resistant to 1 μM concentration of imatinib[112].

All the above mentioned imatinib resistant (SR) cell lines did not show any mutation in the bcr-abl gene and there was no increase in the levels of bcr-abl protein and P-glycoprotein as compared to the respective parent imatinib sensitive cell lines[111, 112]. Mechanisms independent of bcr-abl signaling were involved in the imatinib resistance in all SR cells.

K562/SR, KU812, KCL22, KU812/SR and KCL22/SR cell lines were received as a kind gift from Dr. Tadashi Nagai, Jichi Medical University, Japan.

MCF-10A: This cell line is a non-tumorigenic cell line, obtained from human fibrocystic mammary tissue of a 36 years old parous premenopausal woman with no family history of breast malignancy [113]. MCF-10A has the characteristics of normal breast epithelium by the following criteria: (a) lack of tumorigenicity in nude mice; (b) three dimensional growth in collagen; (c) growth in culture that is dependent on hormones and growth factors; (d) lack of anchorage-independent growth; and (e) piling up or foci formation in confluent cultures[113]. This cell line was procured from ATCC.

MCF-7: MCF-7 is the first hormone responsive breast cancer cell line. MCF-7 is an acronym of Michigan Cancer Foundation 7, institute where the cell line was established by Soule et al [114]. This cell line was derived from pleural effusion of adenocarcinoma of 69 years old Caucasian woman. MCF-7 is positive for estrogen (ER) and progesterone (PR) receptors with no amplification of Her2/neu and expresses wild type p53[114-116]. MCF-7 is triploid to tetraploid and tuomorogenic in mice, when estrogen supplement is given. It contains WNT7B and Tx-4 oncogenes[114-116]. This cell line was a kind gift from Dr. Padma Shastry, NCCS, Pune.

MDA-MB-231: This cell line was derived from pleural effusion of adenocarcinoma of 51 years old Caucasian female[117]. This cell line is negative for ER, PR and Her2/neu. The cell line contains B type phenotype of G6PD. MDA-MB-231 is aneuploid, contains WNT7B oncogene and expresses mutated p53[115, 117]. MDA-MB-231 is tumorigenic in mice and does not need hormone supplement for tumor development [117]. This cell line was procured from ATCC.

MDA-MB-468: MDA-MB-468 cell line was derived from pleural effusion of metastatic adenocarcinoma of 51 years old black woman[117]. This cell line is also negative for ER, PR and Her2/neu[117]. MDA-MB-468 is aneuploid and expresses mutated p53[115, 117]. MDA-MB-468 is the only cell line among all the MDA-MB series of cell lines which contains A type phenotype of G6PD. MDA-MB-468 is tumorigenic in mice and does not need hormone supplement for tumor development [117]. This cell line was procured from ATCC.

T-47D: This cell line was derived from pleural effusion from metastatic site of infiltrating ductal carcinoma of mammary gland tissue of 54 years old woman.

This cell line is hypotriploid, positive for ER and PR with no amplification of Her2/neu and expresses mutated p53[115, 118]. This cell line was procured from ATCC.

Methods

Cell Culture

Reagents

All tissue culture reagents were sterilized by autoclaving (unless mentioned separately) at 15 lbs/sq. inch at 121°C for 20 min and stored at 4°C till further use.

Phosphate buffered saline (PBS) (10X):

Reagents	Quantity
80 mM Na_2HPO_4	14.5 g
10 mM KH_2PO_4	2.0 g
20 mM KCl	2.0 g
1.36 M NaCl	80.0 g

The volume was made up to 1000 ml with Milli Q after adjusting the pH to 7.4.

Trypsin-EDTA:

Reagents	Quantity
0.2 mM EDTA (disodium salt)	50 mg
5.5 mM D-Glucose	500 mg
5.36 mM KCl	200 mg
0.13 M NaCl	4 g
6 mM $NaHCO_3$	290 mg
10 mM Trypsin	125 mg

The volume was made up to 500 ml with Milli Q and sterilized by filtration through 0.45 μ Millipore filter.

Complete RPMI for hematopoietic cell lines:

Reagents	Quantity
RPMI-1640	90 ml
FBS	10 ml
Antibiotic antimycotic liquid (100x)	1 ml

Complete DMEM for MCF-7, MDA-MB-231, MDA-MB-468 and T-47D:

Reagents	Quantity
DMEM	89 ml
FBS	10 ml
10 mM HEPES pH 7.5	1 ml
Antibiotic antimycotic liquid (100x)	1 ml

Complete DMEM for MCF-10A:

Reagents	Quantity
FBS	10 ml
10 mM Hepes pH 7.5	10 ml
Antobiotic anti mycotic liquid (100x)	1 ml
MEGM SingleQuot Kit Suppl. & Growth Factors	1 unit

The volume was made up to 100 ml with DMEM and Ham's F-10 nutrient mixture in 1:1 ratio.

Freezing Medium:

Reagents	Quantity
FBS	90 %
DMSO	10 %

Freezing medium was always prepared fresh

Maintenance of cell lines

All the cell lines were maintained at 37°C in a humidified atmosphere with 5 % CO_2 in 25 cm^2 tissue culture flasks. Cells were passaged twice a week.

For passaging hematopoietic suspension cell lines, the old cell culture was centrifuged at 1000 rpm for 5 min. The cell pellet was resuspended in fresh medium. Cells were seeded at the desired density to a new flask in 5 ml fresh medium as per the table-MM1.

Imatinib resistant cell lines, K562/SR, KCL22/SR and KU812/SR were maintained under selection of 1 μM imatinib at every alternate passage i.e. imatinib was added only once in a week.

For passaging adherent breast epithelial normal and cancer cell lines, cells were washed twice with PBS to remove cell debris and serum. Cells were trypsinized by treating with 500 μl of Trypsin-EDTA / 25 cm^2 flask at room temperature approximately for 1-2 min. Cells were suspended in 2 ml of the respective complete medium and mixed well to get single cell suspension. Cells were seeded in the new flask containing 5 ml of medium at the desired density as per the table-MM1.

Table-MM1: Cell density for passaging

S/R No.	Cell line	Seeding density
1	HL-60	3×10^5 /ml
2	K562	1×10^5 /ml
3	K562/SR	1×10^5 /ml
4	KCL22	2×10^5 /ml
5	KCL22/SR	2×10^5 /ml
6	KU812	2×10^5 /ml
7	KU812/SR	2×10^5 /ml
8	MCF-10A	5×10^5 /ml
9	MCF-7	1×10^5 /ml
10	MDA-MB-231	1×10^5 /ml
11	MDA-MB-468	3×10^5 /ml
12	T47D	3×10^5 /ml

Cell Proliferation[119]

Reagents

Cell Counting Kit - 8 (CCK-8)

Protocol:

1. Cells were harvested from 70-75 % confluent flask either by centrifuging at 1000 rpm for 5 min (suspension cell lines) or by trypsinization (adherent cell lines) followed by centrifugation.
2. Supernatant was discarded and cell pellet was resuspended in 2 ml of complete medium.
3. Cell count was taken using hemocytometer and cell viability was checked by trypan blue dye exclusion method[120].

Following formula is used for calculating cells/ml and cell viability.

c = n/v

Where,

c = cell density (cells/ml)

n = number of cells counted in all four WBC squares of hemocytometer/4

v = volume counted (ml)

$c = n/10^{-4}$ or $n \times 10^4$

Total cells = Live cells + Dead cells

% Cell viability = (Live cells/Total cells) x 100

Cultures with more than 95 % cell viability were used for the experiment. Cell suspension of $1x10^5$ cells/ml density was prepared.

4. Cell suspension was dispensed in 96-well plate as described in the table-MM2. Cells were incubated at 37°C in CO_2 incubator for 24 hours before addition of test compounds or inhibitors.
5. 20 μl of the test compound or inhibitor from the working stock were added to wells, in triplicate to get the earlier –mentioned final concentrations. Same amount of the corresponding solvent dilution (DMSO in complete medium) was added in the solvent control wells to make up the total volume to 200 μl. Cells were then further incubated. Cell proliferation was measured every 24 hours after addition of the inhibitor or test compound, that is, day 0 (immediately after addition), day 1, day 2 and day 3.
6. To estimate cell growth, at the end of incubation period 10 μl of CCK-8[121] were added to wells and incubated at 37°C in CO_2 incubator for 4 hours. Wells with 200 μl complete medium were used as blank.
7. Absorbance was read at 450 nm with 650 nm as the reference wavelength.
8. % growth inhibition of cells after treatment was calculated with respect to the solvent control.

Table-MM2: Cell seeding details for cell proliferation experiment

Cell line	Cell suspension (μl/well)	Complete medium (μl /well)	No. of cells /well
K562/SR	50	130	5000
KCL22/SR	50	130	5000
KU812/SR	50	130	5000
MCF-7	50	130	5000
MDA-MB-231	50	130	5000

Percent growth inhibition of the cells was calculated as follows:

For each well, ratio of optical density at different time points with the respective reading at 0 hour time point, was calculated. The percent growth of each treated sample was calculated by considering growth in the solvent control well, equal to 100 %. The percent growth inhibition was calculated by subtracting the percent growth from 100. Thus, the inhibitory effect of the test compounds was expressed as percent growth inhibition. Experiments were done in triplicate.

Experimental setup

i. K562/SR, KCL22/SR, and KU812/SR cells were seeded into wells of 96-well plate as mentioned above and incubated at 37°C in CO_2 incubator for 24 hours. After 24 hours. 1 μM fMLP, 10 μM CsH, 1 μM imatinib or their combinations were added to the wells in triplicate. Dilution of the solvent, DMSO similar to the lowest dilution among the treatment group was added to the control wells. Cells were further incubated at 37°C in CO_2 incubator. Cells growth was monitored after 0, 24, 48 and 72 hours after treatment, by CCK-8 assay. % cell growth inhibition was calculated as mentioned above.

ii. MCF-7 and MDA-MB-231 cells were seeded into wells of 96-well plate as mentioned above and incubated at 37°C in CO_2 incubator for 24 hours. After 24 hours, cells were treated with 10 μM CsH, 10 μM WRW4 or solvent. Cells were then incubated for 1 hour at 37°C in CO_2 incubator. After 1 hour, 3 wells each of CsH treated and untreated cells, for each time point, were stimulated with 1 μM fMLP for 15 min at 37°C in CO_2 incubator. Similarly three wells treated with WRW4 and three untreated wells, for each time point were stimulated with 1 μM WKYMVm for 15 min

at 37°C in CO_2 incubator. To the solvent control wells, similar dilution of DMSO was added. After 15 min, old medium containing test compounds or solvent was replaced by complete medium. Cells were further incubated at 37°C in CO_2 incubator. Cell growth was monitored at 0, 24 and 48 hours after treatment, by CCK-8 assay and % cell growth inhibition was calculated as mentioned above.

Separation of Lymphocytes and Neutrophils from peripheral blood[122]

Reagents for Blood Processing

0.6 M KCL:

44.7 g KCL was dissolved in 800 ml of Milli Q water and volume made up to 1 liter. Solution was autoclaved and stored at 4°C.

Phosphate buffer (pH= 7.2) for Giemsa Staining:

Solution A: 27.6 g NaH2PO4.H2O was dissolved in 1 liter Milli-Q water. Solution was autoclaved and stored at 4°C.

Solution B: 28.4 g of Na2HPO4 was dissolved in 1 liter Milli-Q water. Solution was autoclaved and stored at 4°C.

For Buffered water (pH=7.2), add 140 ml solution A and 360 ml solution B.

Giemsa Stain:

Giemsa stain was diluted 1:20 with milli-Q water before use.

Method

1. Blood collected from CML patient was incubated at 37°C for 15 min to separate WBC layer or buffy coat.
2. This buffy coat was washed and diluted to 10^7 cells per 5 ml in PBS.

3. Blood collected from healthy volunteered donor was diluted 1:1 with PBS.
4. 3 ml ficoll-hypaque of density 1.077 was taken in a 15 ml centrifuge tube and 5 ml of diluted blood or diluted buffy coat (10^7 cells per 5 ml) was layered on it.
5. This was centrifuged at 400 g for 30 min with minimal break and acceleration.
6. Erythrocytes and PMNL settled down at bottom, whereas mononuclear cells settled at the interphase of ficoll-hypaque of density 1.077 and plasma.
7. Mononuclear cells were collected carefully and washed twice with PBS.
8. At the bottom of tube PMNL were present in the upper layer of pallet. This fraction was collected in a fresh tube.
9. Contaminating erythrocytes present in the PMNL fraction, were lysed by hypotonic shock.
10. This procedure was carried out on ice. To the mixture of erythrocytes and PMNL, 3 ml of chilled Milli Q was added, briefly vortexed and after 30 seconds isotonicity was restored by addition of 1 ml chilled 0.6 M KCl. Depending on the amount of cell pellet, the volumes of the lysing solutions could be varied with 3:1 proportion maintained.
11. PMNL pellet was washed with PBS.
12. Enrichment and viability of the cells were checked by Giemsa staining and trypan blue dye exclusion technique, respectively.
13. PMNL fraction showing more than 90% enrichment and more than 95% viability were used for the various experiments.

Giemsa Staining

1. Thin cell smear was prepared on glass slide and dried in air.

2. The cells were fixed with methanol for 5 min.
3. The slides were immersed in diluted Giemsa's stain for 30 min.
4. Slides were then washed with phosphate buffer.
5. Slides were then dried in air and were examined under microscope.

RNA Extraction

Reagents: RNeasy Kit (Qiagen) and TRIzol

For Monolayer Culture Cells

- Old media was discarded from the culture disk/flask and 1 ml of TRIzol Reagent was added to a 3.5 cm diameter dish/ 25 cm^2 flask. Flask/ dish was then incubated at room temperature for 15 min. Cells were then thoroughly mixed with pipette and collected in 1.5 ml centrifuge tube.

For Suspension Culture Cells

- Cells were pelleted down by centrifugation. 1 ml TRIzol was added per 10^6 to 10^7 cells. Cells were suspended thoroughly with pipette and incubated at room temperature for 15 min. Cells were then suspended again with pipette and collected in 1.5 ml centrifuge tube.

TRIzol samples were either processed for RNA, DNA and/or protein isolation or stored at –80°C till further use.

Experimental setup

Cells from 70-80% confluent K562 and HL60 cell culture were harvested. Cell pellet were resuspended in fresh medium and cells were counted. The cells were seeded as 10^6 cells/3 ml/well in 4 wells of 6 well plate. They were treated with 1 μM imatinib, 0.02 μM dasatinib, 0.03 μM nilotinib or solvent and plates were incubated for 4 hours at 37°C in CO_2 incubator. After 4 hours cells were processed for RNA extraction as mentioned above.

RNA isolation[123]

RNA was extracted by combining the protocol of TRIzol (Invitrogen) and RNeasy mini kit (Qiagen). The detailed protocol used was as follows.

14. Freshly prepared TRIzol samples were kept at room temperature for 15-20 min. Frozen samples were thawed on ice.
15. To these TRIzol samples equal volume of 70% ethanol was added and mixed by inverting the tube.
16. This mixture was loaded on RNeasy spin column and centrifuged for 15 second at 10000 rpm. Flow-through was discarded and the spin column was placed in a new collection tube.
17. 350 μl of RW1 buffer (supplied in RNeasy kit) was added to the spin column and centrifuged for 15 second at 10000 rpm. Flow-through was discarded and the spin column was placed in a new collection tube.
18. 10 μl RNase free DNase stock (supplied in RNeasy kit) was diluted with 70 μl of RDD buffer (supplied in RNeasy kit).
19. 70 μl of this diluted RNase free DNase was added on the membrane of the RNeasy spin column. The spin column was then incubated for 15 min at room temperature.
20. 350 μl of RW1 buffer was added to the spin column and it was centrifuged for 15 second at 10000 rpm. Flow through was discarded.
21. 500 μl of RPE buffer was added to the spin column and centrifuged at 10000 rpm for 15 second. Flow through was discarded.
22. 500 μl RPE buffer was again added to the spin column and the spin column was centrifuged for 2 min at 10000 rpm for complete removal of ethanol. Flow through was discarded.

23. RNeasy spin column was placed in a new 1.5 ml collection tube and 50 μl RNase free water was added on the membrane of the spin column.
24. The spin column was incubated for 1 min at room temperature and then centrifuged for 1 min at 10000 rpm. Flow through fraction contained RNA.
25. RNA purity was checked and quantitated by spectrophotometer. Absorbance (O.D.) of RNA was measured at 260 nm and 280 nm and quantitated as follows.

Concentration of RNA (μg/ml) = O.D. at 260nm X 40* X dilution factor

Note: 1 O.D. equals to 40 μg/ml RNA.

27. Ratio of A260 and A280 was also calculated and RNA having A260/A280 ratio higher than 1.9 were only used for further experiments.

cDNA Synthesis[124]

cDNA was synthesized using the RevertAid™ H-minus First Strand cDNA Synthesis Kit (Fermentas) as per manufacturer's instructions. The detailed protocol was as follows:

1. 2 μg RNA was taken for cDNA synthesis. 1 μl of 100 μM Random hexamer primers were added to RNA and volume was made up to 12 μl by nuclease free water (NFW).
2. This mixture was incubated at 70°C for 10 min and then cooled on ice for 1 min.
3. Master Mix was made with 5x reaction buffer – 4 μl, 10 mM dNTP - 2 μl, and RiboLock™ (20U/μl) - 1 μl and RevertAid™ H minus M-MuLV reverse transcriptase (200U/μl) - 1 μl.
4. 8 μl master mix was added to RNA and Random hexamer mixture.

5. This mixture was vortexed, spun-down and incubated at 42°C for 1 hour (for oligo dT primer) or incubated at 25°C for 5 min then at 42°C for 1 hour (for random hexamer).
6. The reaction was terminated by heating at 70°C for 10 min.

Real time polymerase chain reaction (QPCR) [125]

Reagent

MESA green QPCR master mix was used for QPCR.

Primers: Dried primers were reconstituted to 100 μM. This Primer stock was further diluted to working stock of 10 μM. Primers were stored at -20°C

Method

PCR reaction mix was prepared as per the following table and 10 μl was distributed in each well of MicroAMp Fast optical 96-well Reaction plate.

Reagents	1 reaction (in μl)	Final Concentration
2 X MESA green QPCR master mix	5.00	1x
10μM Primer 1	0.25	0.25 μM
10μM Primer 2	0.25	0.25 μM
cDNA	1.0	-----
NFW	2.5	-----

1. cDNA was not added to three wells. These wells would serve as non-template control (NTC) or negative control.
2. PCR plates were then placed in ABI-7500 thermal cycler.
3. The PCR reaction was run using following conditions:
    a. 95°C for 5 min — for *Taq* activation
    40 cycles of
    b. 95°C for 15 second — denaturation

c. 60°C for 1 min primer annealing and extension

4. After completion of 40 cycles, melting curve analysis was performed.

QPCR analysis[125]

Levels of the target genes were expressed relative to the expression levels of the reference genes –HPRT1 –for CML cell lines & actin –for breast cancer cell lines. mRNA level for a gene was calculated by the ΔΔCt method. For each run and for each gene a PCR cycle threshold (Ct*) value was determined using the in-built instrument software SDS v1.4.1.

*Ct Value or cycle threshold: The Ct value is defined as the number of cycles required for the fluorescent signal to cross the threshold i.e. to exceed background level. Ct level or Ct value is inversely proportional to the amount of target nucleic acid in the sample, i.e. lower the Ct value greater the amount of target nucleic acid and vice-versa.

Difference in the Ct value of the target gene and the reference gene was calculated by subtracting the later from the former and this difference was termed as ΔCt.

$\Delta Ct = (Ct_{target} - Ct_{reference})$

An average of the ΔCt values of triplicates of each sample was calculated and this values was termed as Avg (ΔCt)

ΔΔCt value was calculated for each sample from the average ΔCt values using following equation.

$\Delta\Delta Ct = Avg(\Delta Ct)_{treated} - Avg(\Delta Ct)_{untreated}$

Fold change in the gene expression of the treated sample with respect to the control or the untreated sample was calculated using the following formula.

$Fold\ Change = 2^{-\Delta\Delta Ct}$

Whole cell protein lysate preparation for Western Blotting[126]

Reagents

RIPA buffer (4X):

Reagents	Quantity
10 mM Tris	0.49 g
150 mM NaCl	3.51 g
1 mM EDTA	0.15 g
Triton X-100	4 g
Sodium deoxycholate	2.0 g
SDS	0.4 g

Volume was made up to 100 ml after adjusting pH to 7.4 with 1N HCl. Solution was sterilized by filtering through 0.45 μ filter.

Protease inhibitors:

Complete™ tablets from Roche were used. One tablet was dissolved in 2 ml of sterile Milli Q (25X).

Phosphatase inhibitors stock solutions:

1 M $Na_2HPO_4.2H_2O$: 0.356 g was dissolved in 2 ml of sterile Milli Q. Used at final concentration of 10 mM.

1 M NaF: 0.084 g was dissolved in 2 ml of sterile Milli Q. Used at final concentration of 10 mM.

100 mM Na_3VO_4: 0.037 g was dissolved in 2 ml sterile Milli Q. Used at final concentration of 10 mM.

Protease and phosphatase inhibitors were aliquoted and stored at –20°C.

RIPA lysis buffer (1X) :

For 500 μl

Reagents	Quantity
4X RIPA Buffer	125 μl
Complete™	40 μl
Milli-Q	320 μl
10 mM NaF	5 μl
1 mM Na_3VO_4	5 μl
10 mM $Na_2HPO_4.2H_2O$	5 μl

Laemmli's sample buffer (2X):

Reagents	Quantity
1 M Tris pH 6.8	1.2 ml
SDS	400 mg
Glycerol	2 ml
β–mercaptoethanol	1 ml
Bromophenol blue	10 mg

Dissolved in Milli Q and final volume was made up to 10 ml.

Lysate preparation for Western blotting

1. Cells were seeded at a density of $3x10^6$ cells/well of 6 well plate.
2. After 24 hours cells were treated with the compounds for various time point as mentioned in the table MM-3.

Table-MM3: Compounds treatment details for Western Blotting:

Compound	Final Conc.	Time	Remarks
CsH	10 μM	1 hr	Inhibitors (Pre-treatment)
WRW4	10 μM	1 hr	
AG1478	500 nM	30 min	
AG490	20 μM	1 hr	
PP2	10 μM	6 hr	
fMLP	1 μM	16 min	Stimulant (Alone or after treatment with inhibitors)
WKYMVm	1 μM	15 min	
EGF	100 ng/ml	10 min	
IL6	10 ng/ml	15 min	

3. After the treatment, cells were immediately kept on ice. Medium was removed from the well. 100 μl RIPA lysis buffer was added per well and kept for 10 min on ice.
4. Cells were then scraped off using cell scraper and collected in 1.5 ml centrifuge tube.
5. Cell lysate was further incubated on ice for 30 min with intermittent vortexing. Cell lysis was confirmed by observing a drop from this mixture under microscope.
6. Cell lysate was then centrifuged at 14000 rpm 10 min at 4^0C and supernatant was collected in a fresh 1.5 ml centrifuge tube.
7. 3 μl supernatant was taken out for protein estimation**.
8. One volume of 4X Laemmli's sample buffer was added to 3 volumes of cell lysate to get 1X and heated at 100°C for 5-10 min.
9. Lysate was allowed to cool at room temperature and then centrifuged at 12000 rpm for 5 min at room temperature.
10. 20 μl of this protein was loaded on gel for SDS page.

** Protein estimation: 3 μl of cell lysate and 300 μl of Precision Red were added in a well of 96 well plate. In another well, 3 μl lysis buffer and 300 μl of Precision Red was added and this was considered as a blank. This mixture was incubated for 1 minute at room temperature. Absorbance was measured at 600 nm on a 96-well plate reader and protein quantity was calculated as follows.

1 OD_{600nm} = 125 μg protein per ml reagent

Dilution factor = 100

Protein concentration (μg/μl) = (O.D. x 125 x 100)/1000

Western Blotting

Reagents

30 % Acrylamide-bisacrylamide

Reagents	Quantity
Acrylamide	29.2 g
Bisacrylamide	0.8 g

Dissolved in Milli Q and the volume was made to 100 ml with Milli Q. Solution was stored at 4°C in amber colored bottle.

10 % Sodium dodecyl sulphate (SDS): 10 g of SDS was dissolved in 100 ml of Milli Q.

0.5 M Tris, pH 6.8: 6.06 g of Tris was dissolved in 60 ml Milli Q. pH was adjusted to 6.8 with 2 N HCl. Volume was made up to 100 ml with Milli Q.

1.5 M Tris, pH 8.8: 18.17 g of Tris was dissolved in 60 ml Milli Q. pH was adjusted to 8.8 with 2 N HCl. Volume was made up to 100 ml with Milli Q.

10 % Ammonium per sulfate (APS): 0.1 g of APS was dissolved in 1000 μl of Milli Q.

SDS PAGE

Resolving gel

Reagents	10%
Milli Q	4 ml
30 % Acrylamide – bisacrylamide	3.3 ml
1.5 M Tris pH 8.8	2.5 ml
10 % SDS	0.1 ml
10 % APS	0.1 ml
TEMED	4 μl

Stacking Gel

Reagents	5%
Milli-Q	2.7 ml
30 % Acrylamide -bisacrylamide	0.67 ml
0.5 M Tris pH 6.8	0.5 ml
10 % SDS	40 µl
10 % APS	40 µl
TEMED	4 µl

Tank buffer (5X)

Reagents	Quantity
0.2 M Tris	30 g
1.9 M Glycine	144 g
0.5 % SDS	5 g

Dissolved in Milli-Q and the volume was made to 1000 ml with Milli Q. Diluted to 1X before use.

Transfer buffer for blotting (1X)

Reagents	Quantity
40 mM Tris	5.90 g
0.4 M Glycine	29 g
0.1 % SDS	1 g

Dissolved in Milli Q and volume was made to 800 ml with Milli Q. 200 ml of methanol was added to it before use.

Destainer: Methanol: Acetic acid: Water: 45: 10: 45

0.25 % Coomassie blue R250: 0.25 g of Coomassie blue powder was dissolved in 100 ml of destainer.

0.1 % Fast green: 0.1 g of Fast green powder was dissolved in 100 ml of destainer.

Tris Saline Tween Buffer (TBST) (10X)

Reagents	Quantity
20 mM Tris-HCl	24.228 g
130 mM NaCl	75.972 g
0.1 % Tween-20	1 ml

Tris-HCl and NaCl were dissolved in Milli Q, pH was adjusted to 7.4-7.6 with 1N HCl and volume was made up to 1000 ml with Milli Q. Diluted to 1X and then 0.1 % Tween-20 was added before use.

Buffer 1: 5 % w/v Non-fat milk in 1X TBST.

Buffer 2: 5 % w/v Bovine serum albumin (BSA) in 1X TBST.

Buffer 3: 1% w/v Non-fat milk in 1X TBST.

Protocol

1. Proteins were resolved on 10% SDS-PAGE gels using constant current at 20 mA.
2. PVDF membrane (8 cm X 9 cm) was activated in methanol for one minute and then equilibrated in transfer buffer for 5 min.
3. Proteins were transferred to pre-activated PVDF membrane at 75 mA, for 20 hours, at 4°C, using wet blotting method.
4. The PVDF membrane was stained by 0.1% fast green to confirm the protein transfer.
5. The gel was stained with 0.25 % coomassie blue to confirm complete transfer from gel.
6. The membrane was destained by using destainer and then washed once with 1X TBST.

7. The membrane was blocked using blocking buffer (buffer-1) for 2 hours, at room temperature.
8. To probe the proteins, the membrane was incubated overnight at 4ºC on rocker with the desired primary antibody at dilutions mentioned in the table-MM4.
9. The membrane was washed thrice for 10 min each with 1X TBST at room temperature, on rocker at maximum speed.
10. The membrane was then incubated for 1 hour at room temperature with 1:1000 dilution of secondary antibody as mentioned in table-MM4.
11. The membrane was washed five times for 5 min each with 1X TBST at room temperature on rocker at maximum speed.
12. Proteins were detected using the Supersignal ELISA Femto Maximum Sensitivity Kit from Thermo Scientific and images were captured using gel documentation system, BioSpectrum 500 BiochemiHR Imaging System from UVP

Densitometry

Images of the Western blots were analyzed using Visonworks Imaging Software from UVP. The bands were selected on blots using magic wand tool. Background regions were automatically selected by the software. On the basis of selection of band and background, total density* was calculated by the software. To measure the effect of treatment on protein expression, fold change in the intensity was calculated as a ratio of the total intensity of treated to that of the control. Fold changes in the range from 0.6 to 1.4 were considered as no change whereas fold changes below 0.6 and above 1.4 were considered as decreased and increased in expression, respectively.

* Total Density: The total density is the sum total of intensities of all pixels within the region, minus the background.

Total Background (default): It is equal to the sum total of the perimeter around the region marked, three pixels wide.

Table-MM4: Primary antibodies for Western blotting

Protein	Molecular Wt. (KDa)	Primary antibody		Origin	Secondary Antibody
		Buffer for antibody	Dilution		
Akt	60	Buffer-2	1:1000	Rabbit	goat anti-rabbit IgG-HRP
Akt-P-Ser473	60	Buffer-1	1:250	Mouse	goat anti-mouse IgG-HRP
Akt-P-Thr308	60	Buffer-2	1:1000	Rabbit	goat anti-rabbit IgG-HRP
Anti-Rac1 / 2 / 3	21	Buffer-2	1:500	Rabbit	goat anti-rabbit IgG-HRP
Beta-Catenin	92	Buffer-1	1:2000	Mouse	goat anti-mouse IgG-HRP
Cdc42	21	Buffer-3	1:100	Mouse	goat anti-mouse IgG-HRP
CDH-1	135	Buffer-2	1:1000	Rabbit	goat anti-rabbit IgG-HRP
EGFR	175	Buffer-2	1:1000	Rabbit	goat anti-rabbit IgG-HRP
EGFR-P-Tyr845	175	Buffer-2	1:500	Rabbit	goat anti-rabbit IgG-HRP
EGFR-P-Tyr992	175	Buffer-2	1:500	Rabbit	goat anti-rabbit IgG-HRP
Erk1/2	44/42	Buffer-2	1:1000	Rabbit	goat anti-rabbit IgG-HRP
Erk1/2-P	44/42	Buffer-2	1:1000	Rabbit	goat anti-rabbit IgG-HRP
p-38	38	Buffer-2	1:1000	Rabbit	goat anti-rabbit IgG-HRP
p38-P	38	Buffer-2	1:1000	Rabbit	goat anti-rabbit IgG-HRP
Pten	54	Buffer-2	1:1000	Rabbit	goat anti-rabbit IgG-HRP
Pten-P (Ser380/Thr382/383)	54	Buffer-2	1:1000	Rabbit	goat anti-rabbit IgG-HRP
RhoA	21	Buffer-3	1:500	Mouse	goat anti-mouse IgG-HRP
STAT3	79/86	Buffer-2	1:1000	Mouse	goat anti-mouse IgG-HRP
STAT3-P	79/86	Buffer-2	1:500	Rabbit	goat anti-rabbit IgG-HRP

Fluorescence staining

Reagents for fluorescence staining

Fixative (8 % paraformaldehyde):

- 8 g paraformaldehyde was weighed and approximately 80 ml PBS was added.
- Paraformaldehyde is not completely soluble at room temperature. So the suspension was heated and brought to boil. 100 µl 1N NaOH was added to bring the pH to 7.0 to 7.4 and volume was made to 100 ml with PBS.
- The paraformaldehyde solution thus obtained was filtered through Whatmann filter paper no. 1. It was aliquotated and stored at -20°C till use.

Triton X-100:

- 0.5 % and 1 % Triton X-100 were prepared in PBS for permeabilization of cells grown on coverslips and for cells in suspension, respectively.
- Triton X-100 tends to settle down. So before adding to cells it was vortexed thoroughly.

Reagents for Intracellular Protein Staining

Blocking buffer:

0.3% Triton X-100 and 5% goat serum were dissolved in PBS. Triton X-100 tends to settle down. So before adding to cells it was vortexed thoroughly.

Reagents for F-actin Staining Solution

FITC-Phalloidin:

- The whole vail content (~116.33 µg) of FITC-Phalloidin (MW= 1175) was dissolved in 61.8 µl methanol to obtain 1.6 X 10^{-4} M stock.
- 5 µl aliquots were made and sealed immediately to avoid evaporation of methanol.

- Aliquots were stored in dark and dry conditions, at -20°C till use.

4 % BSA:

- 0.4 g BSA was weighed and dissolved in 10 ml PBS
- It was filter sterilized. Aliquots were prepared and were stored at -20°C till use.

10 μg /μl Lysolecithin:

- 1 mg Lysolecithin was dissolved in 100 μl methanol to obtain 10 μg /μl stock.
- 5 μl aliquots were made and sealed immediately to avoid evaporation of methanol.
- Aliquots were stored at -20°C till use.

Staining Solution for F-actin: For 100 μl

Reagents	Quantity
10 μg /μl Lysolecithin	1μl
Methanol	10 μl
1X PBS	86.75 μl
4% BSA	1.25 μl
1.6 X 10^{-4}M FITC-Phalloidin	1 μl

Reagents for FPR ligand binding

n-formyl-Nle-Leu-Phe-Nle-Tyr-Lys, fluroescein derivative (FITC-fNLPNTL)

1 mg was dissolved in 824 μl Dimethylformamide (DMF) to obtain a final concentration of 1 mM. The working stock of 10 μM was obtained after 1:100 dilution of 1 mM stock in PBS. Final concentration was 1 μM after 1:10 dilution in cell suspension. The stock solution was stored at -20°C

Immuno-fluorescence staining for flow-cytometry

1. A) For adherent cells – Cells were trypsinized. For studying surface protein expression, cells were transferred to a low attachment flask in low serum (5%) medium. To regenerate the surface markers/ receptors, flasks were incubated overnight on rocker at slow speed. For staining proteins other than the surface protein, after trypsinization cells were processed from step-2.

   B) For suspension cells- processed directly from step-2
2. Cell suspension was centrifuged at 1000 rpm for 5 min to obtain cell pellet.
3. Supernatant was discarded and the cell pellet was suspended in 1 ml of PBS.
4. Using the trypan blue dye exclusion method[120], cell viability and cell counts were determined. Cultures with more than 95 % cell viability were used for the experiments.
5. The cells were washed twice with PBS containing 1% BSA and processed for staining.

Surface receptor/markers staining using antibodies

1. The cells were distributed as mentioned in table-MM5.
2. Antibodies were added in the tubes and incubated in dark at the temperature mentioned in the above table.
3. After completion of the designated incubation time, cells were washed twice with PBS and resuspended in 500 µl PBS containing 0.5% paraformaldehyde and stored at 4C until analyze by flow-cytometry.

4. Samples were analyzed on BD FACSCalibur flow cytometer using appropriate setting for respective fluorophore as mentioned in the table-MM6.

Table-MM5: Staining with fluorescently tagged antibodies for flow-cytometry

Antibody	Cell no.	Vol. of Cell suspension	Vol. of antibody	Time of Incubation	Temp. of Incubation
FPR1-FITC	10^5	25 µl	10 µl	30 min	2-8°C
FPR2-PE	10^6	25 µl	10 µl	30 min	2-8°C
FPR3-APC	$2.5x10^5$	25 µl	10 µl	30 min	room temperature
CD34-PE	10^6	90 µl	10 µl	30 min	room temperature
CD38-perCP	10^6	90 µl	10 µl	30 min	room temperature
CD117-PE	10^6	90 µl	10 µl	30 min	room temperature
CD133-PE	10^6	90 µl	10 µl	30 min	room temperature
CD44-PE	10^6	90 µl	10 µl	30 min	room temperature
CD24-FITC	10^6	90 µl	10 µl	30 min	room temperature

Table-MM6: Fluorophores, their properties and flow-cytometer setting

Dye	Excitation Maxima	Emission Maxima	Instrument Setting	
			Excitation Laser	Fl. Channel
FITC	495	519	Argon (488 nm)	FL1 (530/30 BP)
Alexa fluor 488	488	517	Argon (488 nm)	FL1 (530/30 BP)
PE	496/565	575	Argon (488 nm)	FL1 (585/42 BP)
PerCP	482	690	Argon (488 nm)	FL3 (670LP)
APC	645	660	Red Diode (635 nm)	FL4 (616/16 BP)

Indirect immunofluorescence staining of intracellular protein staining:

1. Equal volume of 8% paraformaldehyde (final concentration = 4%) was added to the 106 cells suspended in 1 ml PBS, and incubated at 37°C, for 15 min, for fixing the cells.
2. After 15 min, cells were washed twice with PBS.
3. The cells were suspended in blocking buffer and incubated for 1 hour, at room temperature.
4. The cells were spun down and the pellet was suspended in 1% BSA.
5. The cells were distributed at a density of 106 cells/90μl in flow tubes.
6. Primary antibodies were added in the tubes and incubated in dark at the temperature mentioned in the table MM7.
7. After completion of incubation period, cells were washed twice with PBS.
8. Cells were then incubated with 1:1000 diluted Alexa-488-goat anti-rabbit secondary antibody in 1% BSA for 30 min, at room temperature, in dark.

Table-MM7: Indirect immunofluorescence staining of intracellular protein for flow-cytometry:

Primary Antibody	Final dilution used	Cell no.	Incubation time	Incubation temperature
Oct-4A Rabbit mAb	1:200	10^6	Overnight	4°C
Nanog Rabbit mAb	1:200	10^6	Overnight	4°C

9. Cells were washed twice with PBS and resuspended in 500 µl PBS.
10. Samples were analyzed on BD FACSCalibur flow cytometer at appropriate settings as mentioned in the table-MM6.

Direct immunofluorescence staining of intracellular protein staining:

1. Cells were processed as mentioned above up to step 5.
2. Antibody was added in the tube and incubated in dark at the temperature mentioned in the table MM8.
3. After completion of incubation period, cells were washed twice with PBS and resuspended in 500 µl PBS.
4. Samples were analyzed on BD FACSCalibur flow cytometer at appropriate settings as mentioned in the table-MM6.

Table-MM8: Direct immunofluorescence staining of intracellular protein for flow-cytometry

Primary Antibody	Final dilution used	Cell no.	Incubation time	Incubation temperature
Mouse anti-Sox-2-PE	1:10	10^6	2 hrs	4°C

F-actin staining for flow cytometry:

1. The cells were distributed at the density of 106 cells/100 µl.
2. The cells were stimulated with fMLP (10 nM and 1 µM for 5 min, for hematopoietic cell lines and 1 µM for 16 min, for breast epithelial and breast cancer cell lines).
3. The cells were then fixed by adding equal volume of 8% paraformaldehyde (final concentration 4%), at 37°C, for 15 min.
4. The cells were washed twice with PBS and the cell pellet was suspended in 100 µl actin staining solution.
5. The cells were then incubated for 15 min, at 37°C, in dark.

6. After incubation, equal volume of 4% BSA was added to cell suspension and further incubated for 10 min at room temperature.
7. Samples were analyzed on BD FACSCalibur flow cytometer at appropriate settings as mentioned in the table-MM6.

Detection of ligand binding to FPR[127, 128]:

Protocol:

1. The cells were distributed at the density of 106 cells/90 µl.
2. 10 µl from 10 µM working stock of FITC-fNLPNTL was added to the tube whereas unstained cells served as control.
3. The cells were then incubated at 37°C in water bath, for 30 min in dark.
4. After incubation, the cells were fixed by adding equal volume of 8% paraformaldehyde (final concentration 4%), at 37°C, for 15 min.
5. The cells were then washed twice with PBS and resuspended in 500 µl PBS.
6. Samples were analyzed on FACSCalibur flow cytometer at appropriate settings as mentioned in the table-MM6.

Estimation of Calcium

Reagents

Calcium ionophore A23187: (M.W. – 523.6)

Stock solution was prepared in dry DMSO. To prepare 10 mM stock solution, 5.236 mg was dissolved in 1 ml dry DMSO. Aliquots were stored at –20°C.

Manganese chloride (MnCl2): (M.W. - 197.9)

To prepare solution of 4 mM, 1.58 g was dissolved in 2 ml Milli-Q. This 4 mM solution was diluted to 1:10 to get stock of 0.4 mM. Aliquoted and stored at 4°C.

EGTA: (M.W. - 380.25)

To prepare stock solution of 0.4 M, 1.521 g of EGTA was dissolved in 9.2 ml of 1.5 M Tris buffer, pH 8.7. pH was adjusted to 7.4 with 10 N HCl. The final volume was made to 10 ml with Milli-Q.

Fluo-4 NW Calcium Assay Kit:

Fluo-4 NW dye mix (Component A)

Probenecid, water soluble (Component B)

Assay buffer [1X Hanks' balanced salt solution (HBSS) with 20 mM HEPES]

Quantitation of Ca^{2+} release upon fMLP stimulation was measured using Fluo-4 NW calcium assay kit (Invitrogen) as per the manufacturer's instructions. Detailed protocol used was as follows:

1. Cell suspension was centrifuged at 1000 rpm for 5 min to obtain cell pellet.
2. Supernatant was discarded and cell pellet was resuspended in 1 ml of assay buffer (provided with the kit).
3. Cell viability and cell count of the cell suspension was checked using trypan blue dye exclusion method.
4. Cell count was adjusted to 2.5 x 106 cells/ml in assay buffer.
5. 50 μl cell suspension (≈125,000 cells/well) was seeded per well of 96 well plate.
6. To make 250 mM stock solution of probenecid (component B), 1 ml assay buffer was added to the one vial of component B.
7. 5 ml of assay buffer and 100 μl of 250 mM stock solution of component B was added to vial of component A to prepare 2X dye solution.
8. 50 μl of dye solution was also added to each well of 96 well plate.
9. The plate was incubated at 37°C, in CO2 incubator, for 30 min.

10. The plate were then placed in FlexStation 3 benchtop multimode microplate reader. Temperature of the FlexStation was maintained at 37°C during the complete experiment.
11. At every 2 seconds fluorescence was measured at 516 nm, using 494 nm excitation.
12. 10 μl of 1 μM fMLP was added to each well (final concentration = 100 nM) after 2nd reading.
13. Post fMLP addition readings were recorded after every 2 second up to 5 min.
14. After 5 min, 10 μl of 100 μM calcium ionophore A23187 was added to each well and readings were taken up to 2 min at every 2 second interval.
15. After 2 min 15 μl of 0.4 M EGTA was added to each well and readings were taken for further 1 min at every 2 seconds interval.
16. After 1 min 20 μl of 0.4 mM MnCl2 was added to each well and readings were taken for further 1 min at every 2 seconds interval.

Calculations for calcium estimation

Readings before fMLP addition were taken as basal calcium levels.

Relative fluorescence intensity measured at various time points was plotted against time. Highest relative fluorescence unit (RFU) readings after fMLP stimulation was termed as fMLP Max and the corresponding time was termed as t-fMLP Max. Some cell lines showed two peaks in a plot RFU v/s time. Hence, there were two fMLP Max readings, which were termed as fMLP Max-1 and fMLP Max-2 and the corresponding time points were termed as t-fMLP Max-1 and t-fMLP Max-2. Lowest RFU reading after fMLP Max was marked as fMLP Min and the corresponding time was marked as t-fMLP Min. There were two fMLP Min i.e. fMLP Min-1 and fMLP Min-2 and two corresponding t-fMLP Min i.e. t-fMLP Min-1

and t-fMLP Min-2, for the cell lines which showed two peaks in the plot. Highest RFU reading, post ionophore treatment, minimum RFU reading after EGTA & $MnCl_2$ treatments and the respective time points were also marked and named accordingly. Ratios of these RFU readings with the basal calcium reading were calculated. These RFU readings per se and ratios were compared across the cell lines.

Statistical Analysis

GraphPad Prism-5 software was used to statistically analyse all the data. All the values were expressed as mean ± SEM or median ± SEM as mentioned in various experiments.

Mainly two nonparametric statistical tests were used to calculate significance of the data.

The tests are listed below –

Wilcoxon signed-rank test:

This is a nonparametric test used to compare two related samples i.e. to compare stimulated/treated cells with unstimulated/solvent control for a given cell line. Probability value less than 0.05 was considered significant.

Mann-Whitney test:

This is a nonparametric test used to compare two independent samples. Two cell lines were compared with each other using this test. For example, MCF-10A, a normal cell line was compared with breast cancer cell line. Probability value less than 0.05 was considered significant.

Cluster Analysis [129]

A key initial step in the analysis of large data is the detection of groups of genes that exhibit similar expression patterns. The goal is to partition the elements into subsets, which are called *clusters*, so that two criteria are satisfied: *Homogeneity* -elements in the same cluster are highly similar to each other; and *separation* - elements from different clusters have low similarity to each other. Several algorithmic techniques were previously used for clustering gene expression data, including hierarchical clustering[129], self- organizing maps[130] (Tamayo et al. 1999), and graph theoretic approaches[131].

Two-way cluster analysis was carried out using Genesis software. QPCR and WB data, were used to cluster cell lines as well as genes and proteins in a given stimulation condition. Unsupervised Hierarchical clustering analysis was performed using average linkage and Euclidean distance. Data was interpreted on divisive approach. Each of these terms are explained below:

Hierarchical clustering

Hierarchical clustering is represented by a dendrogram. In Hierarchical clustering two approaches were used to generate dendrogram:

Divisive or top-down: It starts with one cluster containing all the data objects, and at each step split a cluster until only single clusters of individual objects remain.

Agglomerative or bottom-up: It initially consider each data object as an individual cluster, and at each step, merge the closest pair of clusters until all the groups are merged into one cluster.

Algorithms used for hierarchical clustering:

Complete Linkage: Distance between clusters is distance between farthest pair of points.

Single Linkage: Distance between two clusters is the distance between the closest points. Also called "neighbour joining".

Centroid Linkage: Distance between clusters is distance between centroids

Average Linkage: Distance between clusters is average distance between the cluster points

Proximity measurement:

Proximity measurement measures the similarity (or distance) between two data objects. In Hierarchical clustering Euclidean distance and Pearson correlation and 'uncentered' correlation were used for proximity measurement. In the present data, Euclidean distance was used.

Euclidean Distance: The Euclidean distance or Euclidean metric is a straight line distance between two points in Euclidean space. Euclidean distance is more appropriate for log ratio data[132].

Results and Discussion

FPR family member –FPR1 and FPR2 were extensively studied for their role as chemoattractant receptor in professional phagocytes[1, 2, 65, 133, 134] and as vomeronasal sensor[135-137]. Role of FPR1 was also studied in glioblastoma, where stage dependent increase in FPR1 expression contributed to disease pathogenesis[60]. On other hand, FPR2 was extensively studied for its role in Alzheimer's disease[138, 139] as serum amyloid A (SAA)[140] and amyloid β42 (Aβ42)[141] were found to be agonist for FPR2. Though, there was no study, which directly implicate, role of FPR in CML, events activated by FPR after binding to its ligand were found defective in CML PMNL[76-89]. Significance of these defective FPR stimulated events in CML pathogenesis was not known. In breast cancer, binding of FPR ligand to HBCC and resulting chemotaxis and motility of these cells was demonstrated[100, 101] but their significance in disease pathogenesis and role of FPR in breast cancer per se was not yet known. The aim of this study was to decipher the role of FPR in CML and breast cancer. FPR was also evaluated as candidate for diagnostic/prognostic marker as well as candidate for therapeutic target for CML and breast cancer. To study the role of FPR in these cellular malignancies, expression of FPR was checked in cell lines and clinical samples. Effect of FPR signalling activation and inhibition was checked on cell proliferation, differentiation and cancer markers. Furthermore, transactivation of RTKs by FPR1 and FPR2 was also explored.

Chronic Myeloid Leukemia

CML is a myeloproliferative disorder, characterized by presence of the Ph^1 chromosome[70]. It is one of the most extensively studied human malignancy. PMNL from CML exhibit defects in various events which are activated by the FPR. Binding of fMLP to FPR on normal PMNL activates it for host defense. This activated PMNL adheres on endothelium and transmigrates through the intercellular junction of endothelial cell monolayer[142]. This transmigration is followed migration to the target site i.e. chemotaxis. At the target site PMNL performs microbicidal action such as phagocytosis and respiratory burst[142]. PMNL from CML patients were reported to be defective in adhesion, transmigration, motility, chemotaxis, actin polymerization, phagocytosis and respiratory burst activities[76-89]. Mechanism of this defective stimulation by FPR in CML PMNL was investigated in depth. In the present study, role of FPR in these defects in CML PMNL was studied.

Expression of FPR Genes in Clinical Samples from CML Patients

To understand the defective behavior of CML PMNL, expression of FPR genes was examined in peripheral blood samples from CML patients. Peripheral blood samples from CML patients and normal donors were collected. Interphase cells and PMNLs were separated from buffy coat of peripheral blood from CML patients and normal donors, using ficoll-hypaque density gradient. In normal donors, interphase cells are mature mononuclear cells, that is, lymphocytes and monocytes (peripheral blood mononuclear cells i.e. PBMC) whereas in CML patients, the PBMCs fraction also contains immature cells and blast cells. To

know changes in the FPR gene expression CML, interphase cells and PMNL from CML patient's peripheral blood were checked for FPR genes expression and compared with that of interphase cells and PMNL from normal donors, respectively (Annexure-II).

Expression of all the FPR genes; FPR1, FPR2 and FPR3 was lower in CML patients' interphase cells as compared to that in the respective cells from normal donors (Fig-RC 1A, 1B & 1C; Table-RC 1).

Table-RC 1: Expression of FPR Genes in Clinical Samples

	Normalized Quantity			
	NL	CL	NN	CN
FPR1 (ng)	0.22 ± 0.02	0.10 ± 0.01	0.25 ± 0.04	0.19 ± 0.03
FPR2 (ng)	0.069 ± 0.017	0.060 ± 0.013	0.154 ± 0.045	0.122 ± 0.045
FPR3 (ng)	0.040 ± 0.007	0.033 ± 0.010	0.059 ± 0.013	0.060 ± 0.014
NL= Normal Interphase, CL= CML interphase, NN=Normal PMNL, CN=CML PMNL, All the values are average ± SEM (n=13)				

However, only FPR1 expression was lower in CML PMNL than that in normal PMNL. Expression of FPR2 and FPR3 were at par in CML PMNL and normal PMNL. Decrease in FPR1 was statistically significant in interphase cells as well as in PMNL (Fig-RC 1A). Expression of the FPR3 was significantly lower in CML interphase cells than in the normal interphase cells while lowered FPR2 expression in CML interphase cells wasn't statistically significant. Comparative expression of all the three receptors revealed that FPR1 was the highest expressing homologue of FPR followed by FPR2 (Fig- RC 1D; Table-RC 2). FPR3 was the least expressed FPR homologue. Although, earlier reports have suggested that FPR3 expression was not found in PMNL[4, 143, 144], FPR3 expression in PMNL was seen in the present study. This could be due to following reasons.

The studies[4, 144], which claimed that FPR3 was not present in neutrophil, were not performed on neutrophil per se but HL60 cells differentiated into neutrophils were used.

Table-RC 2: Expression of FPR 1 and FPR2 Genes with respect to FPR1 in Clinical samples

	Fold Change in Expression*			
	NL	CL	NN	CN
FPR2	0.051 ± 0.013	0.078 ± 0.019	0.057 ± 0.020	0.064 ± 0.023
FPR3	0.011 ± 0.003	0.012 ± 0.003	0.009 ± 0.004	0.018 ± 0.008
*=Fold change with respect to FPR1, All the values are average ± SEM (n=13)				

In present study, human neutrophils were used. Hence, conclusion of the present study is more reliable representations. Moreover, in the present study, real time PCR was used as a detection technique which is far more sensitive to Northern blotting, that was used in aforementioned studies[4, 144], claiming absence of FPR3 in PMNL. Devosse et al. showed minimal expression of FPR3 in PMNL[143], which is similar to the present findings as FPR3 expression was the least expressed FPR in PMNL as compared to FPR1 and FPR2.

To summarize, expression of all the FPR genes was decreased in CML patients. The decrease in the expression of the FPR1 might be the cause of the defective behavior of CML PMNL in response to fMLP stimulation. Distinct difference in expression of FPR genes in PBMC of normal and PMNL could be because of immature cells present in CML PBMC. As the disease progresses, percentage of immature cells in PBMC as well as bone marrow increases. Hence, further studies on immature CML cells would help in understanding pathogenesis of CML. Various CML cells lines are derived from bone marrow or blood samples of

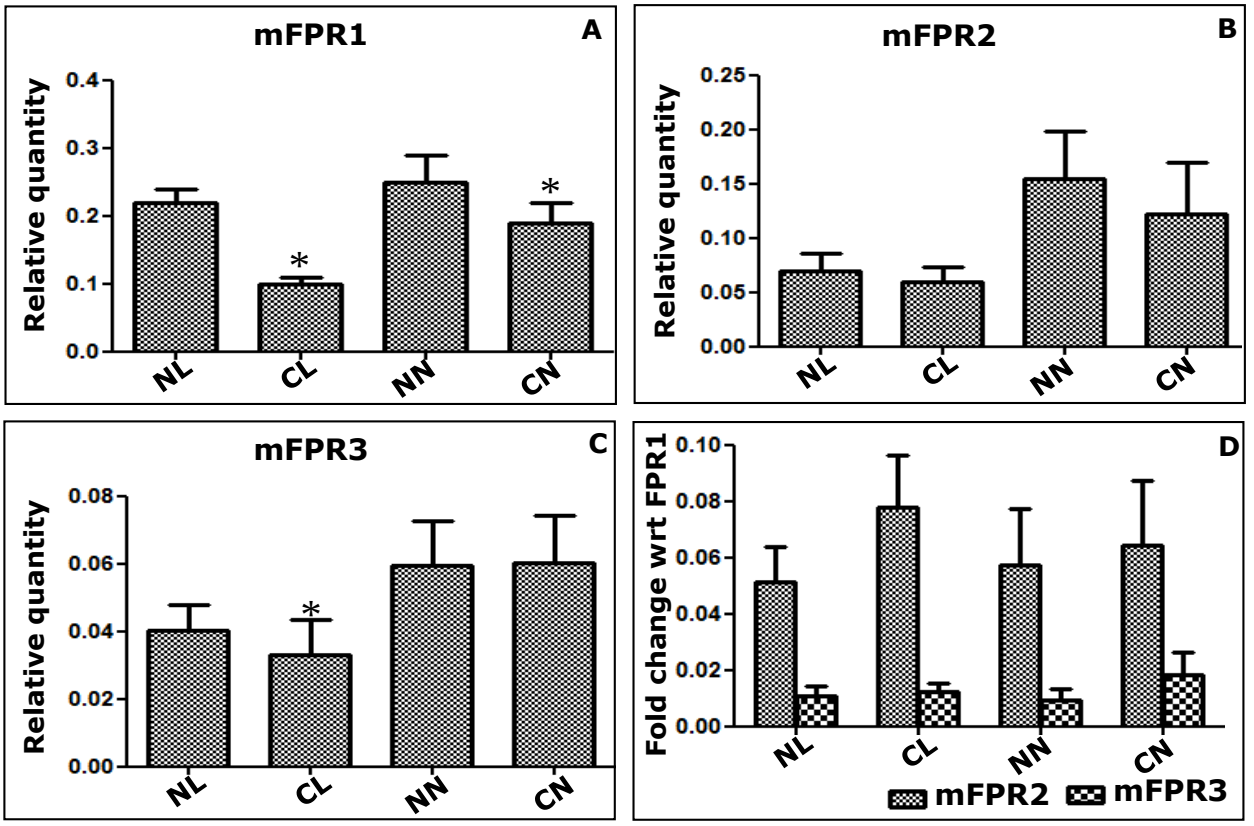

Fig-RC 1: Expression of FPR Genes in Clinical Samples: Expression of FPR1 (A), FPR2 (B) and FPR3 (C) mRNA in clinical samples; NL= normal interphase cells, CL=CML interphase cells, NN=normal PMNL, CN=CML PMNL (D) Expression of FPR2 and FRP3 mRNA in clinical samples with respect to (wrt) FPR1 mRNA. FPR expressions were normalized with actin expression. Data is presented as average fold expression ± SEM; n=13. * $p<0.05$ wrt the respective normal sample (Mann-Whitney test).

CML patients. These are at different stages of differentiation. Use of various cell lines is well accepted as models in clinical application oriented initial studies. Hence, expression of FPR genes as well as protein levels and their functionalities were checked in bcr-abl positive cell lines. Conclusions drawn on the basis of studies using more than one cell lines are more likely to resemble in vivo conditions than those based on the use of a single cell line. Therefore, to carry out these studies, a panel of cell lines was chosen which included; a) cell lines expressing b3a2 fusion transcript of bcr-abl –K562 & KU812 and the respective imatinib resistant cell lines (SR) –K562/SR & KU812/SR; b) cell line expressing b2a2 fusion transcript of bcr-abl –KCL22 and its respective imatinib resistant cell line –KCL22/SR; c) bcr-abl negative cell line –HL60.

Expression of FPR genes in Cell Lines

mRNA expression studies from the cell lines followed the similar trend as clinical samples for FPR1 and FPR2 (henceforth referred as mFPR1 and mFPR2 for FPR1 and FPR2 gene/mRNA expression, respectively), whereas FPR3 (henceforth referred as mFPR3 for FPR3 gene/mRNA expression) showed the reverse picture (Fig-RC 2A, 2B & 2C; Table-RC 3).

Table-RC 3: Expression of FPR Genes in Different Cell Lines

Genes	Fold Change in Expression						
	HL60	K562	K562/SR	KCL22	KCL22/SR	KU812	KU812/SR
mFPR1*	1.00 ± 0.00	0.46 ± 0.04	0.58 ± 0.03	0.02 ± 0.00	0.05 ± 0.01	0.02 ± 0.00	0.02 ± 0.01
mFPR2*	1.00 ± 0.00	0.007 ± 0.003	0.013 ± 0.005	0.003 ± 0.001	0.007 ± 0.001	0.001 ± 0.000	0.001 ± 0.000
mFPR2$	7.01 ± 1.57	0.11 ± 0.03	0.17 ± 0.04	1.65 ± 0.54	1.17 ± 0.36	0.34 ± 0.06	0.63 ± 0.45
mFPR3*	1.00 ± 0.00	747.95 ± 103.07	1907.41 ± 148.89	8.97 ± 0.78	12.33 ± 1.11	18.31 ± 1.28	7.15 ± 0.62
mFPR3$	0.004 ± 0.001	6.81 ± 2.49	14.10 ± 5.16	2.79 ± 1.25	1.1 ± 0.42	4.88 ± 1.37	1.85 ± 0.57
Fold change was calculated; * With respect to HL60, $ with respect to FPR, All the values are average ± SEM (n=3)							

Expression of mFPR1 and mFPR2 was higher in bcr-abl negative cell lines than that in bcr-abl positive cell line, while expression of mFPR3 was found higher in bcr-abl positive cell lines than that in CML negative cell lines. Changes in mFPR expression among bcr-abl positive and negative cell lines indicated that the bcr-abl expression might have affected expression of mFPR. It might have decreased expression of mFPR1 & mFPR2 and increased expression of mFPR3. Inhibition of mFPR1 and mFPR2 was also seen in the clinical samples but mFPR3 in cell lines did not match the results from the clinical samples. Among the three imatinib sensitive bcr-abl positive cell lines, K562 expressed the highest mFPR1, mFPR2 and mFPR3, while KU812 expressed the lowest mFPR2 and KCL22 expressed the lowest mFPR3. mFPR1 levels were at par in KCL22 and KU812 (Fig-RC 2A). On the basis of these results three bcr-abl cell lines could be categorized as follows:

	K562	**KCL22**	**KU812**
mFPR1	+++	+	+
mFPR2	+++	++	+
mFPR3	+++	+	++

CML is a stem cell disease and oncoprotein bcr-abl is essential for its pathogenesis[70]. Bcr/abl tyrosine kinase inhibitor –imatinib transformed the approach to treatment of CML[70]. Imatinib is currently accepted as the first line therapy for CML patients, regardless of the phase of disease[70]. While, imatinib is highly effective therapy against CML, a minority of patients fails or responds suboptimally to imatinib. Intrinsic and acquired resistance against imatinib has been described and recognized as the key challenge in CML research. Three imatinib resistant cell lines –K562/SR, KU812/SR and KCL22/SR were obtained from Dr. Tadashi Nagai, Jichi Medical University, Japan[111, 112]. These cell lines were generated from their respective parent cell lines –K562, KU812, and KCL22 by treatment with step-wise increasing concentration of imatinib. Genetic

analysis of these cell lines showed no mutation in bcr-abl gene, suggesting that mechanism involved in imatinib resistance in these cell lines were independent of bcr-abl[111, 112]. To study the effect of imatinib resistance on mFPR expression, imatinib resistant (SR) cell lines –K562/SR, KCL22/SR and KU812/SR were checked for the mFPR expressions and compared with their respective imatinib sensitive (S) cell lines. Various theories had been proposed for the bcr-abl independent imatinib resistance in CML. There are four proteins, which played important role in bcr-abl independent imatinib resistance. Comparative gene and proteomic analysis suggested that underexpression of Annexin A1 (ANXA1) was responsible for bcr-abl independent imatinib resistance in CML[145]. ANXA1 is a Ca^{2+} dependent phospholipid binding protein[146]. It is inhibitor of glucocorticoid induced eicosanoid synthesis and PLA2, thereby plays role in various inflammatory pathways. It is found in the gelatinase granules of PMNL. When these granules were released on cellular adhesion to the endothelium, ANXA1 was also secreted at the site. ANXA1 then bind to its receptor –FPR family, and exerts its effect. Downregulated expression of ANXA1 is also responsible for multidrug resistance in CML[147], while overexpression of ANXA1 was reported in CML blast crisis. Another study suggested the role of SH2-containing tyrosine phosphatase 1 (SHP-1) in bcr-abl independent imatinib resistance in KCL22[148]. It was shown that the expression of SHP-1 was decreased in bcr-abl independent imatinib resistance cells. Ectopic expression of SHP-1 in imatinib resistance cells restored the imatinib responsiveness. The study was also confirmed on the group of CML patient who failed to respond to imatinib. Higher expression of SHP-1 was reported in hematopoietic precursor cells. SHP-1 physically associated with bcr-abl and thereby blocked bcr-abl dependent transformation

and mediated PP2A-induced bcr-abl proteasome degradation. SHP-1 was activated by tyrosine phosphorylation upon fMLP treatment. Study by Donato et al suggested role of Src related kinase Lyn in bcr-abl independent imatinib resistance in K562[149, 150]. It was shown that Lyn was highly expressed and activated in imatinib resistant cells. The data was also confirmed in clinical samples from CML patients[149]. Inhibition of Lyn in imatinib resistant cells decreased proliferation and survival, while it had no effect on imatinib sensitive cell lines. However, the effect of Lyn on bcr-abl independent imatinib resistance seems to be SHP-1 dependent because Lyn kinase was regulated by Jak2 via SET-PP2A-SHP-1 pathway. Jak2 was activated by bcr-abl, which in turn activates SET. SET is an inhibitor of PP2A, which is an activator of SHP-1. Activated SHP-1 inhibits Lyn activation, hence Jak2 activation led to the inhibition of SHP-1. So it could not inhibit the Lyn anymore, hence resulted in activated Lyn. As it was seen that SHP-1 expression was decreased in bcr-abl independent imatinib resistance cells and this decreased SHP-1 expression could be the reason of Lyn activation in bcr-abl independent imatinib resistance cells. Another molecule, which was found, associated with acquired imatinib resistance is PKCη[151]. Upregulated PRKCH –gene encoding PKCη was found in bcr-abl independent imatinib resistant cells as well as in CML clinical samples. Its upregulation was also found in imatinib resistant CML stem cells. Combined treatment of imatinib and PKCη inhibitor kills bcr-abl independent imatinib resistant CML cells as well as CML stem cells. Taken together these observations, it would be worth noting that all these molecules were directly related to FPR. ANXA1 is the ligand for all the three FPR whereas activation of PMNL by fMLP led to the activation of SHP-1 as well as Lyn and PKCη.

Increase in the expression of all the three mFPRs –mFPR1, mFPR2, and mFPR3 was observed in SR cell line of b2a2 fusion transcript expressing cell line KCL22/SR than that in KCL22 (Fig-RC 2A, 2B & 2C; Table-RC 3). Cell lines expressing b3a2 fusion transcript of bcr-abl showed a different expression pattern between SR and S. mFPR1 level was not affected by imatinib resistance, as mFPR1 levels were at par in S and SR of K562 and KU812. mFPR2 and mFPR3 levels were higher in K562/SR than that in K562 whereas S and SR of KU812 did not show any difference in mFPR2 levels and mFPR3 levels were lower in KU812/SR than that in KU812. SR cell lines could be classified on the basis of changes in the level of mFPRs as compared to imatinib sensitive cell lines, as follows:

	K562/SR	**KCL22/SR**	**KU812/SR**
mFPR1	No Change	Increase	No Change
mFPR2	Increase	Increase	No Change
mFPR3	Increase	Increase	Decrease

When expression of all the three mFPR was compared among the cell lines, it was found that FPR3 was the highest expressed mFPR in bcr-abl positive cell lines, whereas it was the least expressed mFPR in bcr-abl negative cell line (Fig-RC 2D; Table-RC 3). mFPR2 was the highest expressed mFPR in bcr-abl negative cell line. Among bcr-abl positive cell lines, comparative expression of mFPR1 and mFPR2 was found to be linked with the type of bcr-abl fusion transcript. Cell lines expressing b3a2 fusion transcript -K562 and KU812, expressed significantly higher mFPR1 than mFPR2 whereas the levels of mFPR1 and mFPR2 were at par in KCL22 –b2a2 fusion transcript expressing cell lines. These results were completely different than the clinical samples' finding where among all the three mFPRs, mFPR1 was the highest and mFPR3 was the lowest, in both normal as well as CML samples. In imatinib resistant cell lines, b3a2 expressing cell lines

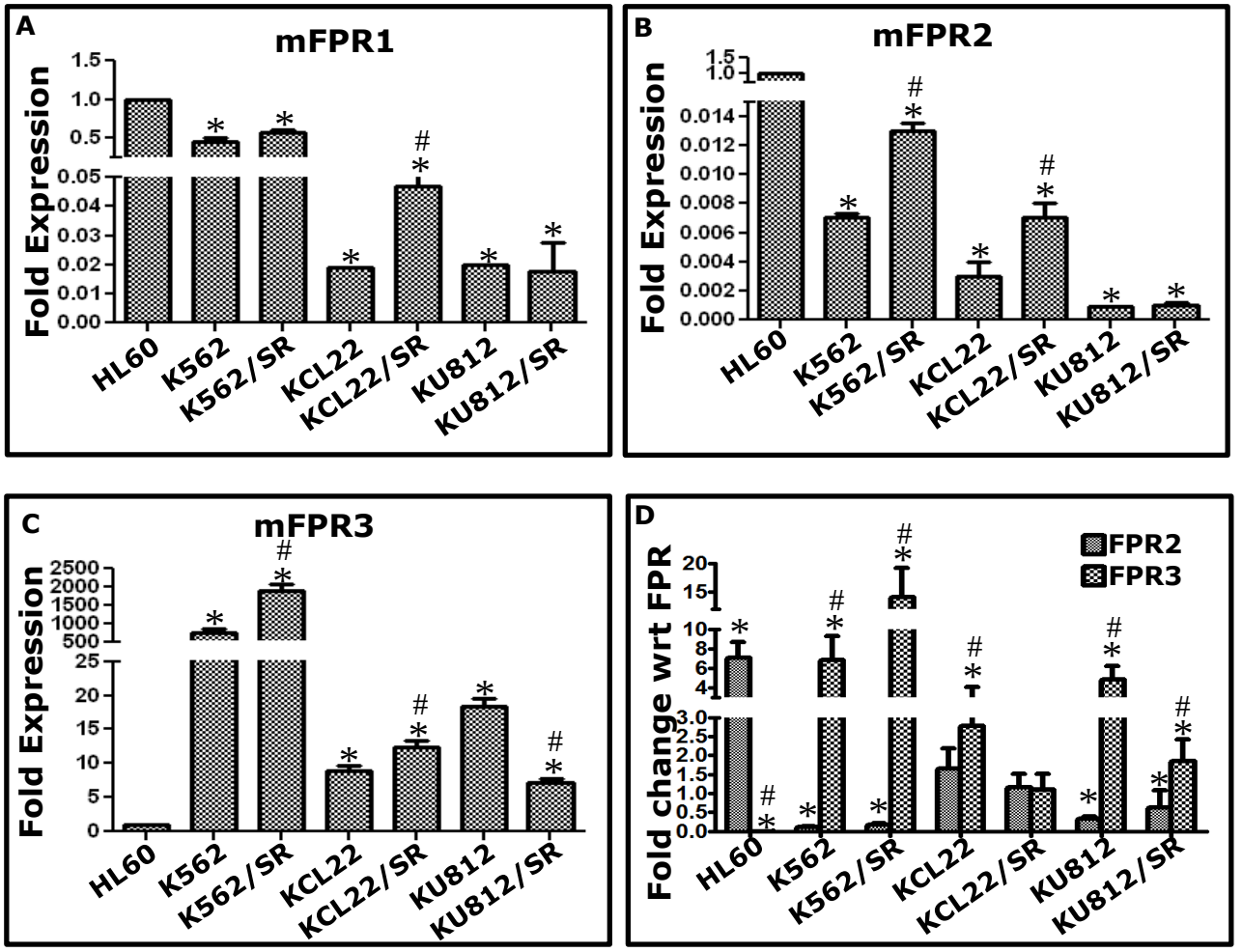

Fig-RC 2: Expression of FPR Genes in CML Cell Lines: Expression of mFPR1 (A), mFPR2 (B), mFPR3 (C), in CML cell lines with respect to the bcr-abl negative cell line HL-60 and (D) expression of mFPR2 and mFPR3 genes with respect to mFPR1, in CML cell lines and HL-60, as estimated by QPCR. Gene expressions were normalized with HPRT1 expression. Data presented as average fold change ± SEM (n=3) . For fig A, B and C statistically significant changes ~~is~~ are marked as; * $p<0.05$ wrt HL60, # $p<0.05$ wrt the respective sensitive cell line and for fig D * $p<0.05$ wrt FPR1, # $p<0.05$ wrt FPR2 (Mann-Whitney test).

did not show any change in the comparative expression of mFPR than their respective sensitive cell lines, i.e. mFPR3 showed the highest expression and mFPR2 expression was the lowest. But b2a2 fusion transcript expressing cell lines showed differences between S and SR. Expression of all the three mFPR were at par in the KCL22/SR, whereas in KCL22, FPR3 was the highest expressing mFPR followed by mFPR1 and mFPR2, whose expressions were at par.

Taken together results of mFPR from clinical samples and cell lines, it could be stated that bcr-abl expression might be affecting expression of mFPR, where expression of mFPR1 was decreased in CML clinical samples and mFPR1 and mFPR2 was decreased in CML cell lines. However, mFPR3 expression showed different results in clinical samples and cell lines. Expression of mFPR3 was higher in bcr-abl positive cell lines than that in bcr-abl negative cell lines, contrasting to the results from clinical samples. HL60 though taken as a bcr-abl negative cell line is not a normal cell line but acute promyelocytic leukemia cell line. HL60 cells are neutrophilic precursors and as it was reported that neutrophils derived from HL60 did not express mFPR3[4, 143, 144]. On other hand, all bcr-abl positive cell lines were multipotent. When comparative FPR gene expression was seen, it was clear that HL60 expressed negligible mFPR3 than mFPR1 and mFPR2, on other hand bcr-abl positive cell lines probably due to their multipotent nature expressed more mFPR3. Comparative expression pattern of all three mFPR was also different between clinical samples and cell lines. In clinical samples the highest expressing mFPR was mFPR1 sequentially followed by mFPR2 and mFPR3, in normal as well as in CML samples, whereas in cell lines comparative gene expression of mFPR not only affected by the

presence of bcr-abl gene but also by the type of bcr-abl fusion transcript present in the cell line. There could be two possible reasons for the differences between clinical sample's results and cell line results'. First, in clinical samples, CML patients' samples were compared with normal donors, whereas in the cell lines, bcr-abl positive cell lines were compared with HL60. Second, the number of immature cells was less in interphase fraction of clinical samples than that in cell lines, hence cell line data would be a better indicator of differences in gene expression between mature and immature cells.

Furthermore, differences in the FPR gene expression between imatinib sensitive and resistance cell line might also be linked with type of bcr-abl fusion gene expressed and cell line lineage. K562 contains erythrocytic, granulocytic and monocytic lineage while KU812 contains basophilic as well as erythroide lineage[105, 108]. K562 was obtained from an untreated patient whereas KU812 was developed from peripheral blood of a patient who was treated with busulfan for 10 years as well as various combination of chemotherapy for extramedullary spinal tumor[105, 107]. KU812 did not differentiate into granulocytic lineage. Hence, the effect could not resemble CML PMNL. KCL22 is also a multipotent and shows properties of monocytes/macrophages and some characters of megakaryocytes[109, 110]. b2a2 expressing cell line showed increase in all the three mFPR while b3a2 expressing cell lines showed expression pattern as per their lineage. SR cell line with granulocyte lineage showed increase in mFPR2 and mFPR3 while SR cell line with basophilic lineage showed decrease in mFPR3 than that in their respective S cell lines. Hence, changes in mFPR expression between SR and S cell lines might be linked with lineage of cell lines or type of bcr-abl fusion transcript expressed by these cell lines.

Surface Expression of FPR Protein in Cell Lines:

It was seen that expression of FPR was affected by bcr-abl expression at the genetic level. To know the effect of bcr-abl expression on FPR at protein level all the cell lines were analyzed for FPR protein expression level. FPR are surface receptors and their activity is linked to their surface expression. Hence FPR receptors present on the cell surface (sFPR) were estimated flow cytometrically, by staining with fluorescently tagged antibodies at 4°C.

Median fluorescence Intensity was compared for sFPR2 and sFPR3 because all the cell lines showed more than 95% positivity for sFPR2 and sFPR3 whereas for sFPR1, sFPR1 % cell positivity was compared among the cell lines because all the cell lines except HL60 showed lower positivity (Table-RC 4).

Table-RC 4: Expression of sFPR in Various Cell Lines

Protein		HL60	K562	K562/SR	KCL22	KCL22/SR	KU812	KU812/SR
sFPR1	MFI	33 ± 1.5	8 ± 0.3	7 ± 0.3	8 ± 0.2	8 ± 0.5	9 ± 0.4	14 ± 1.3
	% Positivity	98.8 ± 0.9	75.0 ± 2.7	72.3 ± 1.3	55.8 ± 3.3	83.9 ± 5.6	45.6 ± 2.2	70.1 ± 3.6
sFPR2	MFI	21 ± 0.9	15 ± 0.4	14 ± 1.3	13 ± 0.3	17 ± 1.2	14 ± 0.6	12 ± 0.5
	% Positivity	99.7 ± 0.3	99.3 ± 0.6	98.3 ± 0.7	99.6 ± 0.1	99.8 ± 0.1	99.5 ± 0.4	98.3 ± 0.6
sFPR3	MFI	100 ± 11.1	19 ± 1.3	13 ± 0.6	18 ± 0.5	22 ± 1.1	19 ± 0.5	16 ± 0.7
	% Positivity	96.3 ± 1.7	97.0 ± 1.4	89.6 ± 5.1	96.7 ± 0.7	93.4 ± 1.5	94.4 ± 2.0	90.7 ± 2.5
HL-60, a non-bcr-abl, promyelocytic cell line is used as a control. All the values are average ± SEM, n=3, MFI= Median Fluorescence Intensity, % positivity =% cellular positivity for given protein.								

Expression levels of all the three sFPR –sFPR1, sFPR2 and sFPR3 were significantly higher in bcr-abl negative cell line than that in bcr-abl positive cell

lines. Lowering of the sFPR1 and sFPR2 levels in CML cell lines were in line with mFPR1 and mFPR2 levels in cell lines as well as in clinical samples. sFPR3 levels did not follow the mFPR3 level in cell lines, but was similar to the clinical sample findings. Among imatinib sensitive CML cell lines, the highest % positive cells for sFPR1 were K562 while KCL22 and KU812 showed similar expression for sFPR1 (Fig-RC 3A). The expression level of sFPR2 and sFPR3 were at par in all three imatinib sensitive CML cell lines. The sFPR1 results were in line with mFPR1 results where K562 showed the highest expression and KCL22 & KU812 showed similar expression for mFPR1, but lower than K562.

However, in imatinib sensitive cell lines, sFPR2 and sFPR3 expression did not match with mFPR2 and mFPR3 results, respectively. K562 showed the highest mFPR2 and mFPR3. KCL22 showed higher mFPR2 expression than KU812 while mFPR3 expression was higher in KU812 than that in KCL22. This differential expression of mFPR2 and mFPR3 in imatinib sensitive cell lines was not reflected in sFPR 2 and sFPR3. In Imatinib resistant cell lines, significant increase in the levels of all sFPR was seen in the SR cell lines of KCL22. This was similar to the mFPR levels. K562/SR showed significant decrease in sFPR3 compared to K562, which was in contrast to the mFPR3 expression, where a significant increase in the expression was observed (Fig-RC 3C). However, no changes in sFPR1 and sFPR2 were seen between S and SR of K562 (Fig-RC 3A & 3B). Similar trend of sFPR1 and mFPR1 expression suggested that imatinib resistance did not affect FPR1 expression in K562. sFPR2 expression did not match with the mFPR2 expression. There was an increase in the mFPR2 in SR than that in S cell line of K562, while no changes in the sFPR2 were seen. These results showed that imatinib resistance differently affected the gene and protein expression of FPR2

and FPR3 in K562, while had no effect on FPR1 protein and gene expression. In KU812, significant increase in sFPR1 and decrease in sFPR3 were seen in SR compared to S whereas no change in the expression of sFPR2 was seen between KU812 S and SR cell line (Fig-RC 3C). The sFPR2 and sFPR3 results were in line with mFPR2 and mFPR3 expression, respectively, showed that imatinib resistance decrease the gene as well as protein expression of FPR3 in KU812 whereas did not affect the gene & protein expression of FPR2. The sFPR1 expression was different than mFPR1 expression. Significant increase in the expression of sFPR1 was seen in SR than that in S cell line while no changes in the expression of mFPR1 were observed. Above results could be summarized as follows.

	K562	**KCL22**	**KU812**
mFPR1	+++	+	+
mFPR2	+++	++	+
mFPR3	+++	+	++
sFPR1	+++	++	++
sFPR2	+++	+++	+++
sFPR3	+++	+++	+++

	K562/SR	**KCL22/SR**	**KU812/SR**
mFPR1	No Change	Increase	No Change
sFPR1	No Change	Increase	Increase
mFPR2	Increase	Increase	No Change
sFPR2	No Change	Increase	No Change
mFPR3	Increase	Increase	Decrease
sFPR3	Decrease	Increase	Decrease

Expression of all the three sFPRs was lower in CML cell lines than that in non-CML cell line. Thus, expression of bcr-abl was associated with the expression of sFPR. Since the expression of sFPR1 was similar to the expression of mFPR1, it could be said that, bcr-abl expression might be affecting transcription of FPR1 and the effect on transcription was translated in protein expression. Bcr-abl

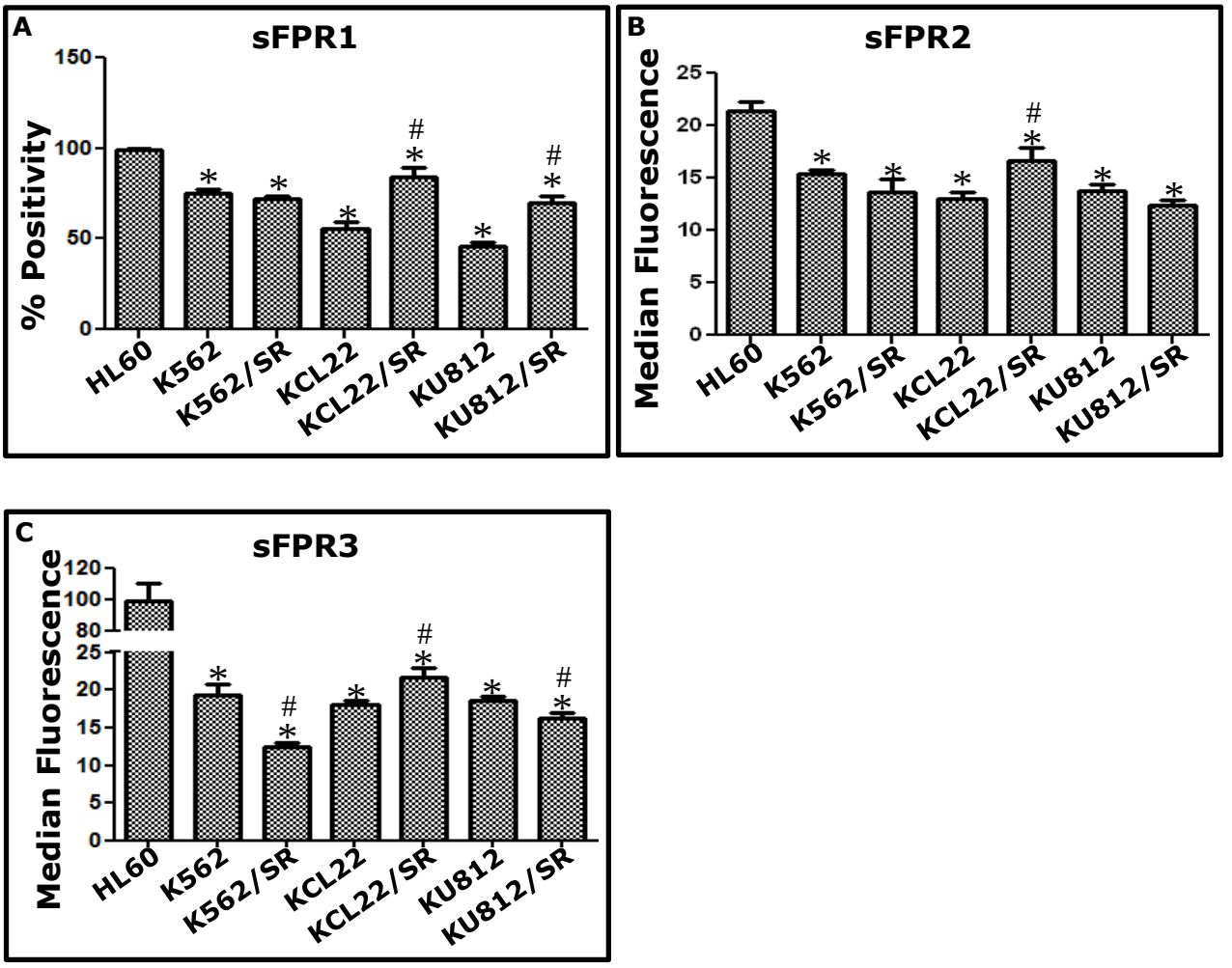

Fig-RC 3: Expression of sFPR in CML Cell Lines: Expression of sFPR1 (A), sFPR2 (B) and sFPR3 (C) proteins in CML cell lines and HL60 as indicated. Data presented as (A) average % positive population ± SEM (B & C) average Median Fluorescence Intensity ± SEM.* $p<0.05$ wrt HL60, # $p<0.05$ wrt the respective sensitive cell line (Mann-Whitney test).

expression might exert different effect on transcription and translation of FPR2 and FPR3, hence the results of gene expression for FPR2 and FPR3 were different than protein expression. There are many reports suggesting that mRNA and protein expression usually does not matched. A global analysis of mRNA and protein abundance in 3 human cancer cell lines –brain glioblastoma (U-251MG), squamous cell carcinoma (A-431) and bone osteosarcoma (U-2 OS) was performed by Lundberg et al[152]. Using digital RNA seq and triple-SILAC method. Although this paper focused on the differences between the cell line types, supplementary figure showed three correlation plot between mRNA transcripts and protein levels for three cell lines. The Spearman correlation coefficient for mRNA and protein expression were 0.42, 0.42 and 0.43 respectively for U-2 OS (n=5210), A-431 (n=5158), U-251MG (n=5197). Tien et al. measured steady state levels of protein (ICAT/MS) and mRNA (Agilent microarrays) in multipotent mouse EML cells and their differentiated progeny MPRO cells[153]. The abundance ratios of 425 proteins were mapped to the corresponding mRNA expression levels. The correlation coefficient R^2 between mRNA and protein was 0.35 for all the genes examined. Vogel et al. pointed out that transcription, mRNA decay, translation and protein degradation are key processes, which determined steady state protein concentrations[154]. They measured protein using shotgun MS and mRNA levels using microarrays for 1025 genes from human medulloblastoma cells harvested at steady state logarithmic growth. A plot of protein versus mRNA level for these proteins gave an R^2 value of 0.29. Schwanhausser, et al. in 2011 performed a definitive global analysis of protein versus mRNA levels in NIH3T3 mouse fibroblasts[155]. The group used metabolic pulse labeling (SILAC) followed by mass spectrometry to measure protein turnover and 4-thiouridine to

measure mRNA turnover in exponentially growing, non-synchronized cells. They calculated absolute cellular mRNA copy number based on number of sequencing reads in the unfractionated sample. They also calculated absolute protein copy numbers from the mass spectrometry data, by summing peak intensities of all peptides matching to a specific protein. The log-log plot of mRNA versus protein showed a R^2 value of 0.41. Removal of less reproducible data points did not improve the correlation, but rather brought R^2 to about 0.3. These reports clearly showed that mRNA level could not predict or correlated with the protein levels. Hence, the differences in the expression data of mRNA and protein of FPR could be attributed to various biological factors.

These results also showed that the effect of imatinib resistance on FPR was dependent on bcr-abl fusion types as in b2a2 expressing cell lines increase in all the three mFPR & sFPR was seen, but in b3a2 expressing cell lines effect of imatinib resistant was different on different FPR and also different on mRNA & protein expression of these FPR. Various studies have examined the influence of type of fusion transcript (b3a2 versus b2a2) on duration of survival or chronic phase. The issue is debatable till date, since some evidences are in favor[156-158] and some are against[159-164] to the hypothesis that a link exists between type of fusion transcript and disease feature. It was very well reviewed by Melo J, where it was mentioned that if the number of patients were increased in the studies favoring hypothesis, the difference in disease feature due to type of fusion transcript became insignificant[165]. Similar situation was observed where association of thrombopoiesis with type of fusion transcript was shown. It was reported that patients with b3a2 fusion transcript had significantly higher number of platelets[166-168]. However, other studies did not corroborated with

these finding[163, 169, 170]. It was also reported that the study supporting this claim had smaller sample size and therefore was prone to statistical error.

All the cell lines were also studied for the co-expression patterns of the three sFPR homologues. Since, sFPR2 and sFPR3 showed more than 95% cellular positivity in all the cell lines, it was sFPR1 cellular positivity which altered the co-expression patterns of sFPR. Dual positivity for sFPR1 & sFPR2, sFPR1 & sFPR3 and triple positivity for all the cell lines displayed a similar pattern (Fig-RC 4A, 4B & 4D; Table-RC 5).

Table-RC 5: Co-expression of sFPR by Flow Cytometry

Protein	% Positivity						
	HL60	K562	K562/SR	KCL22	KCL22/SR	KU812	KU812/SR
sFPR1 & sFPR2	97.7 ± 1.5	77.3 ± 4.3	64.7 ± 6.5	50.8 ± 7.7	87.1 ± 5.4	32.1 ± 1.4	55.7 ± 2.2
sFPR1 & sFPR3	94.4 ± 2.5	69.9 ± 2.5	50.5 ± 4.9	53.6 ± 2.6	78.8 ± 3.3	32.5 ± 2.0	56.2 ± 2.1
sFPR2 & sFPR3	94.5 ± 2.3	92.0 ± 4.4	74.6 ± 12.7	95.9 ± 1.3	92.5 ± 1.0	90.1 ± 3.0	87.0 ± 3.9
sFPR1, sFPR2 & sFPR3	93.7 ± 2.8	72.6 ± 2.5	50.9 ± 5.3	28.1 ± 5.3	80.0 ± 4.9	31.7 ± 1.6	54.4 ± 1.9
HL-60, a non-bcr-abl, promyelocytic cell line is used as a control. All the values are average ± SEM, n=3, % positivity =% cellular positivity for given proteins.							

Bcr-abl negative cell line HL60 had a higher % of cells co-expressing sFPR1 & sFPR2, sFPR1 & sFPR3 and triple positivity than all the CML cell lines. Among imatinib sensitive bcr-abl positive cell lines, K562 showed the highest number of cells co-expressing sFPR1 & sFPR2, sFPR1 & sFPR3 and triple positivity, whereas

KU812 showed the least number of cells co-expressing sFPR1 & sFPR2, sFPR1 & sFPR3 and triple positivity. Co-expression of sFPR2 & sFPR3 were at par in all the three CML cell lines (Fig-RC 4C). In imatinib resistant K562, decrease in co-expression of sFPR1 & sFPR2, sFPR1 & sFPR3, sFPR2 & sFPR3 and triple positivity was seen (Fig-RC 4A, 4B, 4C & 4D). There was an increase in the co-expression of sFPR1 & sFPR2, sFPR1 & sFPR3 and triple positivity in SR than that in S in KCL22 and KU812 (Fig-RC 4A, 4B & 4D). No changes in the co-expression pattern of sFPR2 & sFPR3 were seen between SR and S of KU812 and KCL22, whereas a decrease in the co-expression of sFPR2 & sFPR3 were seen in SR compared to S, in K562 (Fig-RC 4C).

Above results showed that bcr-abl expression affecting the co-expression pattern of sFPR1 & sFPR2, sFPR1 & sFPR3 and sFPR1, sFPR2 & sFPR3, as there was decrease in these co-expressions in bcr-abl positive cell lines than that in bcr-abl negative cell lines. However, bcr-abl did not affect the co-expression of sFPR2 & sFPR3. Furthermore, the imatinib resistant also affected the co-expression pattern, but this effect was cell line dependent.

	K562	**KCL22**	**KU812**
mFPR1	+++	+	+
mFPR2	+++	++	+
mFPR3	+++	+	++
sFPR1	+++	++	++
sFPR2	+++	+++	+++
sFPR3	+++	+++	+++
sFPR1 & sFPR2	+++	++	+
sFPR1 & sFPR3	+++	++	+
sFPR2 & sFPR3	+++	+++	+++
sFPR1, sFPR2 & sFPR3	+++	++	+

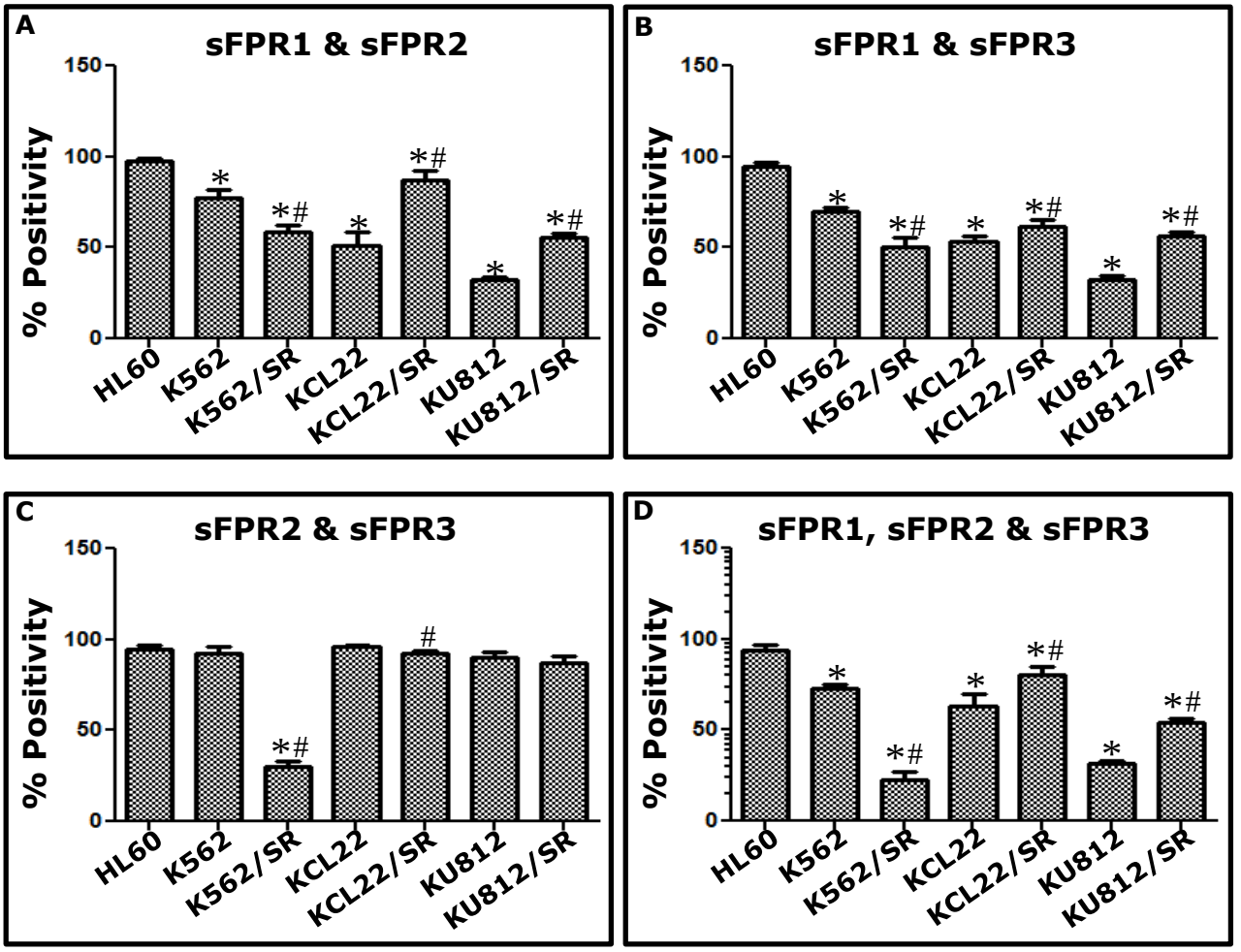

Fig-RC 4: Co-Expression of sFPR in CML Cell Lines: Co-expression of sFPR1 & sFPR2 (A), sFPR1 & sFPR3 (B), sFPR2 & sFPR3 (C) and sFPR1, sFPR2 & sFPR3 triple positive (D) in CML cell lines and HL60 as estimated by flow cytometry. Data presented as average % positive population ± SEM (n=3). * $p<0.05$ wrt HL60, # $p<0.05$ wrt the respective sensitive cell line (Mann-Whitney test).

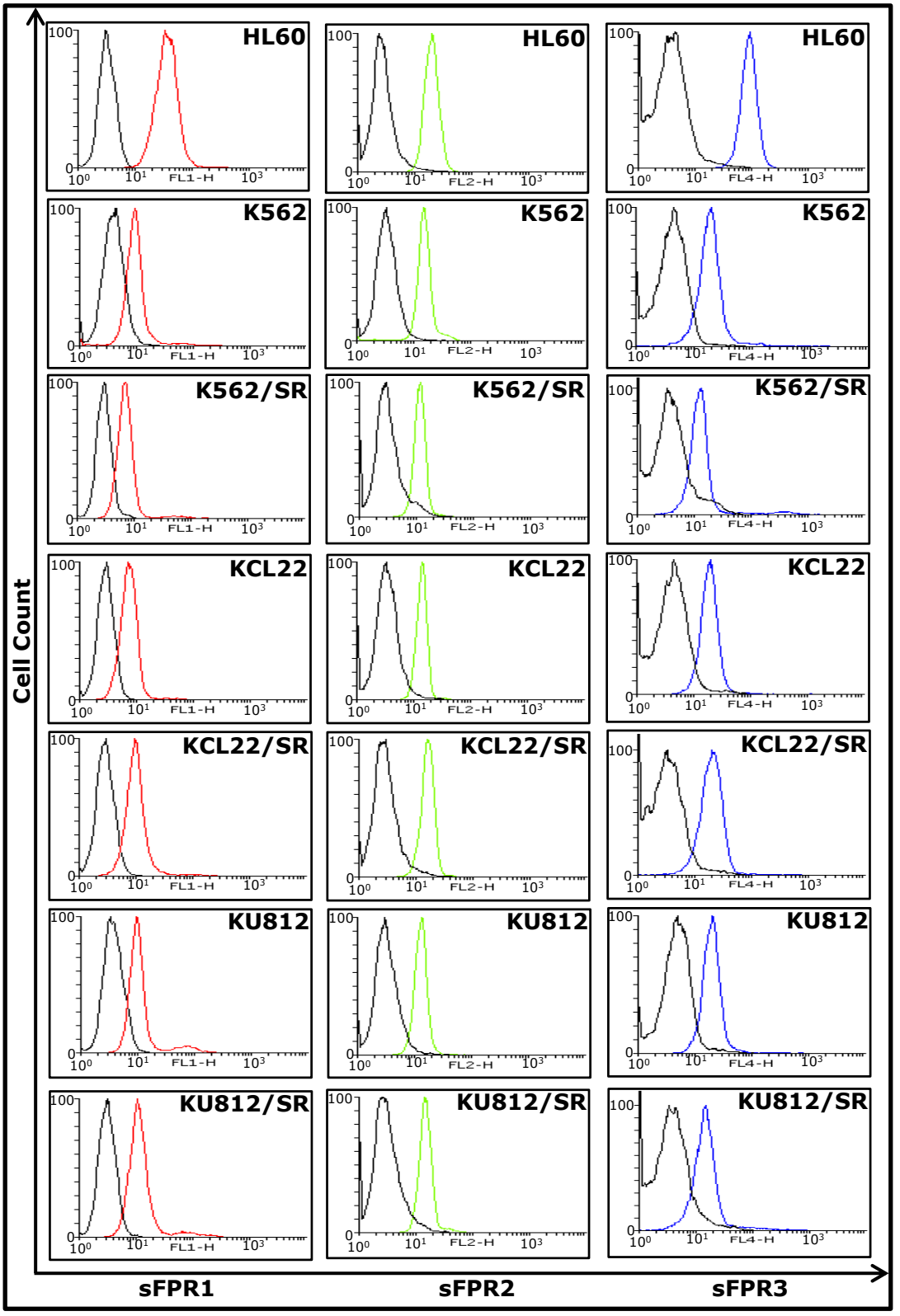

Fig-RC 5: Expression of sFPR in CML Cell Lines: Histogram overlays showing surface expression of sFPR1, sFPR2 and sFPR3 in CML cell lines and HL60 as indicated. In each overlay plot, black solid line indicates unstained isotype control while colored lines indicate cells stained for sFPR1 (red), sFPR2 (green), and sFPR3 (blue).

	K562/SR	KCL22/SR	KU812/SR
mFPR1	No Change	Increase	No Change
sFPR1	No Change	Increase	Increase
mFPR2	Increase	Increase	No Change
sFPR2	No Change	Increase	No Change
mFPR3	Increase	Increase	Decrease
sFPR3	Decrease	Increase	Decrease
sFPR1 & sFPR2	Decrease	Increase	Increase
sFPR1 & sFPR3	Decrease	Increase	Increase
sFPR2 & sFPR3	Decrease	No Change	No Change

Bcr-abl Expression

Above results had shown that expression of FPR did change in CML. To see whether this change in expression of FPR was connected with the expression of bcr-abl gene or protein, expression of bcr-abl was studied in all the CML cell lines.

mRNA

As already mentioned, there were two sets of cell lines as per the expression of bcr-abl fusion proteins. One set with b3a2 fusion expressing cell lines –K562 & KU812 and another set with b2a2 expressing cell line –KCL22. Among b3a2 expressing cell lines K562 and KU812, bcr-abl expression was higher in KU812 than that in K562 (Fig-RC 6A; Table-RC 6).

All the three SR cell lines showed lowered bcr-abl than their respective S cell line (Fig-RC 6A & 6B). The higher expression of bcr-abl in KU812 than that in K562 was opposite of all the mFPR expression, sFPR1 expression, sFPR1& sFPR2 co-expression, sFPR1 & sFPR3 co-expression and sFPR1, sFPR2 & sFPR3 co-expression results. This indicates that bcr-abl expression showed an inverse relationship with FPR expression.

Table-RC 6: Expression of bcr-abl genes in CML cell lines

Genes	Fold Change in Expression					
	K562*	K562/SR*	KCL22$	KCL22/SR$	KU812*	KU812/SR*
Bcr-abl#	1.00 ± 0.00	0.25 ± 0.02	N.A.	N.A.	1.54 ± 0.18	0.08 ± 0.02
Bcr-abl@	1.00 ± 0.00	0.25 ± 0.02	1.00 ± 0.00	0.03 ± 0.00	1.00 ± 0.00	0.06 ± 0.01

Fold change was calculated; # with respect to K562, @ with respect to the respective sensitive cell lines. N.A.: Not applicable, All the values are average ± SEM (n=3); * cell lines were tested for b3a2 fusion transcript, $ cell lines were tested for b2a2 fusion transcript.

In imatinib resistant cell lines decrease in the expression of bcr-abl was seen. There was increase in the expression of all the three mFPR and sFPR in b2a2 fusion transcript expressing SR cell line than that in S cell line, while bcr-abl gene expression was lower in b2a2 fusion transcript expressing SR cell line than that in its S cell line. It indicate an inverse relationship of bcr-abl gene with mFPR and SFPR in b2a2 fusion transcript expressing cell line. In b3a2 expressing cells, bcr-abl expression and FPR expression, were not opposite to each other. In K562, bcr-abl gene expression was reverse to mFPR2 and mFPR3 expression. However, bcr-abl expression in the SR and S cell lines of K562, was in line with the expression of sFPR3, sFPR1 & sFPR2, sFPR1 & sFPR3 and sFPR1, sFPR2 and sFPR3 co-expression patterns. In KU812, bcr-abl gene expression change was reverse to sFPR1, sFPR1 & sFPR2, sFPR1 & sFPR3 and sFPR1, sFPR2 and sFPR3 expression between SR and S cell lines while in line with the expression pattern of mFPR3 and sFPR3. It could be drawn from these results that bcr-abl expression that S and SR cell line expressing b2a2 fusion transcript had an inverse relationship with all three FPR gene and protein expression. Between SR and S cell lines, expressing b3a2 fusion transcript, relation between FPR and bcr-

abl gene was cell line dependent. However sFPR3 expression pattern matched with bcr-abl gene expression between SR and S cell lines of both b3a2 fusion transcript expressing cell lines. The results for imatinib sensitive cell lines are summarized in following table.

	K562	KCL22	KU812
mFPR1	+++	+	+
mFPR2	+++	++	+
mFPR3	+++	+	++
sFPR1	+++	++	++
sFPR2	+++	+++	+++
sFPR3	+++	+++	+++
sFPR1 & sFPR2	+++	++	+
sFPR1 & sFPR3	+++	++	+
sFPR2 & sFPR3	+++	+++	+++
sFPR1, sFPR2 & sFPR3	+++	++	+
Bcr-abl gene	++	NA	+++

The results for imatinib resistant cell lines with respect to their sensitive cell lines are summarized in following table.

	K562/SR	KCL22/SR	KU812/SR
mFPR1	No Change	Increase	No Change
sFPR1	No Change	Increase	Increase
mFPR2	Increase	Increase	No Change
sFPR2	No Change	Increase	No Change
mFPR3	Increase	Increase	Decrease
sFPR3	Decrease	Increase	Decrease
sFPR1 & sFPR2	Decrease	Increase	Increase
sFPR1 & sFPR3	Decrease	Increase	Increase
sFPR2 & sFPR3	Decrease	No Change	No Change
Bcr-abl gene	Decrease	Decrease	Decrease

Protein

To see the bcr-abl protein expression levels in the cell lines, all the cell lines were subjected to the Western blot analysis and total bcr-abl protein was probed using c-abl antibody. Density for the 210 kDa band was measured. The band

density of all the cell lines were ratioed to the band density of K562 and cell lines were compared for bcr-abl expression.

The highest bcr-abl protein among imatinib sensitive cell lines was expressed by K562, followed by KU812 (Fig-RC 6C; Table-RC 7). The lowest bcr-abl protein among imatinib sensitive cell lines was expressed by KCL22. K562/SR showed decreased expression of bcr-abl protein than that in K562 while SR cell lines of KCL22 and KU812 showed higher expression of bcr-abl protein than that in their respective S cell lines. The highest expression of bcr-abl protein by K562, among all the S cell lines was in line with all the three mFPR and sFPR1 expression results. In b3a2 fusion transcript expressing cell lines –K562 and KU812, K562 expressed higher bcr-abl protein than that in KU812 which was opposite of bcr-abl gene expression results, but in line with the FPR gene expression, sFPR1 & sFPR2, sFPR1 & sFPR3 and sFPR1, sFPR2 and sFPR3 co-expressions. Higher expression of bcr-abl protein by KU812 than that in KCL22 was similar to the mFPR3 expression, but in contrast to the mFPR2, sFPR1 & sFPR2, sFPR1 & sFPR3 and sFPR1, sFPR2 and sFPR3 co-expression results.

Decreased expression of bcr-abl in K562/SR than that in K562 was matched with bcr-abl gene, sFPR3, sFPR1 & sFPR2, sFPR1 & sFPR3, sFPR2 & sFPR3 and sFPR1, sFPR2 and sFPR3 co-expression results, but opposite of the mFPR2 and mFPR3 expression. The increase of bcr-abl protein in KU812/SR than that in KU812 was in contrast to bcr-abl gene expression as well as mFPR3 and sFPR3 expression, but matched with the sFPR1, sFPR1 & sFPR2, sFPR1 & sFPR3 and sFPR1, sFPR2

Table-RC 7: Expression of bcr-abl Protein

Protein	Fold Change					
	K562	K562/SR	KCL22	KCL22/SR	KU812	KU812/SR
Bcr-abl	1.0 ± 0.0	0.6 ± 0.04	0.4 ± 0.28	0.8 ± 0.13	0.9 ± 0.19	1.5 ± 0.04
Normalized with respect to K562, All the values are average ± SEM (n=3)						

and sFPR3 co-expression. There was also increase in the bcr-abl protein in KCL22/SR than that in KCL22. This was in contrast to bcr-abl gene expression, but matched with all mFPR and sFPR. Also, this was matched with the co-expression of sFPR1 & sFPR2, sFPR1 & sFPR3 and sFPR1, sFPR2 and sFPR3. The results are summarized as follows:

	K562	**KCL22**	**KU812**
mFPR1	+++	+	+
mFPR2	+++	++	+
mFPR3	+++	+	++
sFPR1	+++	++	++
sFPR2	+++	+++	+++
sFPR3	+++	+++	+++
sFPR1 & sFPR2	+++	++	+
sFPR1 & sFPR3	+++	++	+
sFPR2 & sFPR3	+++	+++	+++
sFPR1, sFPR2 & sFPR3	+++	++	+
Bcr-abl gene	++	NA	+++
Bcr-abl Protein	+++	+	++

The results for imatinib resistant cell lines with respect to their sensitive cell lines are summarized in following table.

	K562/SR	**KCL22/SR**	**KU812/SR**
mFPR1	No Change	Increase	No Change
sFPR1	No Change	Increase	Increase
mFPR2	Increase	Increase	No Change
sFPR2	No Change	Increase	No Change
mFPR3	Increase	Increase	Decrease
sFPR3	Decrease	Increase	Decrease
sFPR1 & sFPR2	Decrease	Increase	Increase
sFPR1 & sFPR3	Decrease	Increase	Increase
sFPR2 & sFPR3	Decrease	No Change	No Change
Bcr-abl gene	Decrease	Decrease	Decrease
Bcr-abl Protein	Decrease	Increase	Increase

The published reports said that there were no changes in the bcr-abl gene expression between SR and S cell lines but no data has been presented, hence we could not comment on the different results[111, 112]. Furthermore, these papers also said that there was not any change in the bcr-abl protein, but we had found

Fig-7

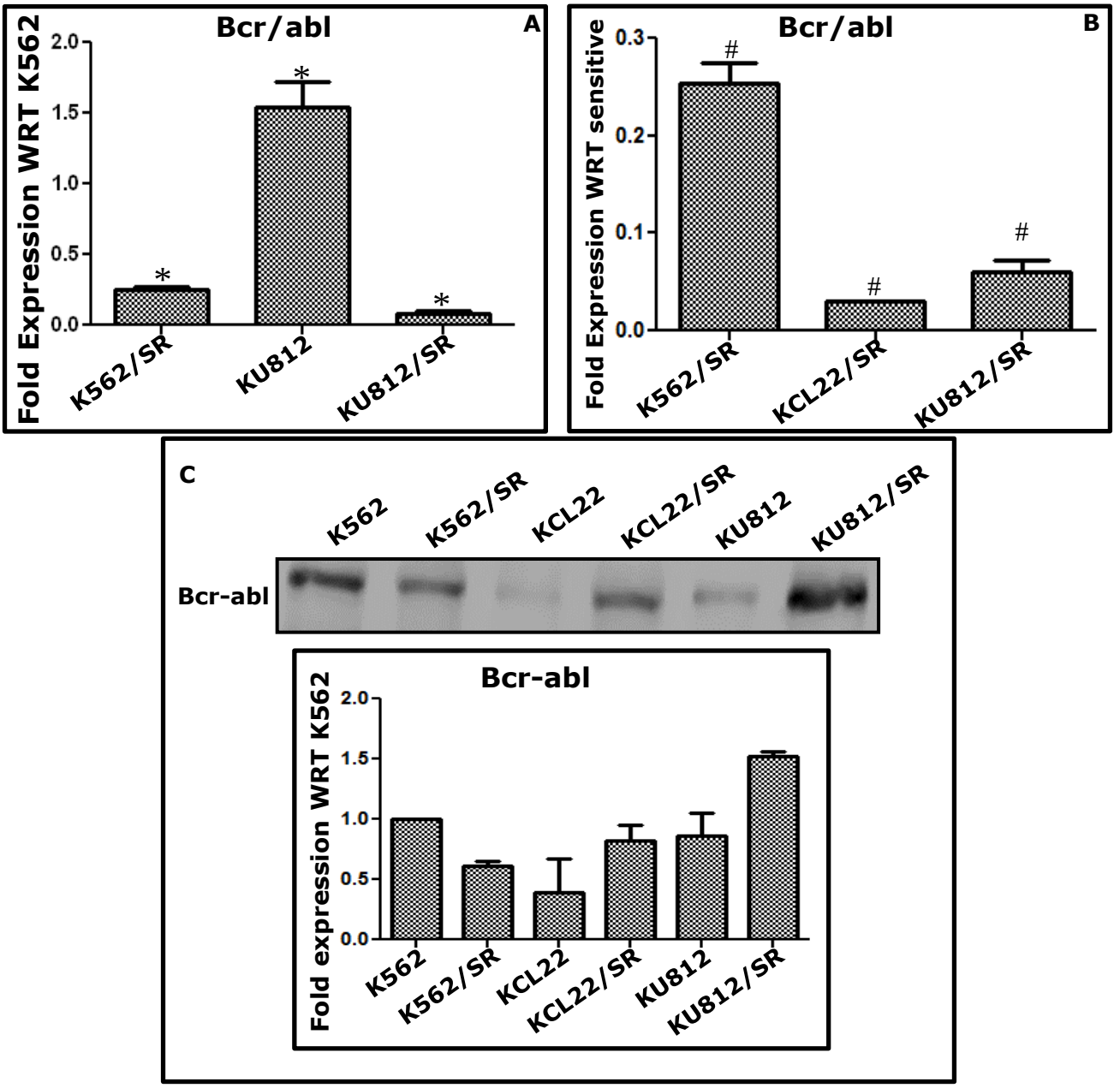

Fig-RC 6: Expression of bcr-abl in CML Cell Lines: (A) Expression of bcr-abl gene (b3a2 fusion transcript) in CML cell lines with respect to that in the K562 cell line. (B) Expression of bcr-abl in imatinib resistant cell lines with respect to the respective imatinib sensitive cell lines. Gene expressions were normalized with HPRT1 expression. Data presented as average fold expression ± SEM (n=3). (C) Expression of bcr-abl protein in CML cell lines. Experiment was done in triplicate and a representative blot is presented. Densitometry data from the Western blots is presented as an average fold expression wrt K562 ± SEM. * $p<0.05$ wrt K562, # $p<0.05$ wrt respective the sensitive cell line (Mann-Whitney test).

that there was decrease in bcr-abl protein in K562/SR than that in K562 and increase in bcr-abl protein in KCL22/SR and KU812/SR as compared to KCL22 and KU812 respectively. The aforementioned paper by Miyoshi et al. and Ohmine et al. had presented data only for KCL22 & KCL22/SR but not for K562 & K562/SR and KU812 & KU812/SR[111, 112]. In KCL22, the protein expression was normalized against GAPDH[59], which is not a suitable loading control in imatinib resistant bcr-abl positive cells[171] because imatinib resistant cells overexpressed GAPDH, a mechanism used by cells to prevent caspase independent cell death. Hence, fast green image should be produced to confirm equal loading. The Western blot image in the paper by Ohmine et al. showed increase in bcr-abl protein expression in KCL22/SR similar to our finding but when it was normalized with the GAPDH, the increase was neutralized. Lee et al. have showed that there was decrease in the bcr-abl protein and mRNA expression in imatinib resistance cell line of K562 upon acquiring bcr-abl mutation independent imatinib resistance[172]. They proposed that loss of target might be the mechanism of imatinib resistance. Recently Karimiani et al. showed that imatinib resistance increased adhesion in K562 cells[173]. These adherent K562 cells showed increase in bcr-abl mRNA. These two reports showed contrasting results indicating that the imatinib resistance was acquired by different mechanism. Taken together, these results it could be said that bcr-abl protein expression and mRNA expressions were opposite of each other except for the K562 and K562/SR. This indicates that gene and protein expression of bcr-abl might be regulated by a different mechanism. Association of imatinib resistance with the bcr-abl gene and protein expression is different and varies from cell line to cell line. B2a2 expressing cell line showed an increase in the expression of bcr-abl protein in SR

cell line than that in S cell, while in b3a2 expressing cell lines, the difference between expression of bcr-abl gene and protein in SR and S cell line varied depending on cell line.

Expression of Hematopoietic Stem Cell Markers

CML is a myeloproliferative disease characterized by bcr-abl oncoprotein. Bcr-abl is a constitutively active tyrosine kinase that has been targeted by TKIs (tyrosine kinase inhibitors). Imatinib is the front-line therapeutic against bcr-abl TK. Intrinsic and acquired resistance to imatinib pose a challenge to the complete cure of the disease. Scientific evidences accumulated over the time have attributed imatinib resistance to presence of CML hematopoietic stem cells (HSC)[174, 175]. HSC were identified by the presence of selective markers on their cell surface. Most of these markers belong to cluster of differentiation series. Most commonly used markers for human HSC are $CD34^+$, $CD38^-$, and $CD117^+$ [73,176]. Since differences in the FPR expression between imatinib resistant and sensitive cell lines were seen in the above results, presence of HSC markers (CD34 and CD117) and differentiation marker for hematopoietic cells (CD38) was studied in these cell lines. Furthermore, correlation of expression of these markers with imatinib resistance, FPR expressions and bcr-abl expression was checked. % cell positivity above 10% was considered as positive expression.

CD34

CD34 is a cluster of differentiation molecules that is expressed on early hematopoietic and vascular associated tissues[177]. Using fluorescently tagged antibody, expression of CD34 and percent of cells expressing CD34 (% positivity) was studied in all the cell lines. % positivity below 10% was considered as negative.

HL60, KCL22, and KU812 were negative for CD34 as the % cell positivity were less than 10% (Fig-RC 7A & 7D; Table-RC 8). Only one bcr-abl positive, imatinib sensitive cell line –K562 showed 30% positivity for CD34. In imatinib resistant cell lines, decrease in the CD34 cellular positivity were observed in the SR cell lines of K562 compared to S cell line, whereas a remarkable increase in the CD34 cellular positivity was observed in the SR cell lines of KCL22 and KU812 compared to their respective S cell lines. When above results were compared with the FPR and bcr-abl expression, it was found that CD34 expression was very much similar to the expression pattern of mFPR1 in imatinib sensitive cell lines, where K562 expressed the highest amount of mFPR1 and KCL22 and KU812 were negligible.

Table-RC 8: Expression of CD Markers

Protein	% Positive Cells						
	HL60	K562	K562/SR	KCL22	KCL22/SR	KU812	KU812/SR
CD34	9.3 ± 2.0	30.0 ± 3.1	17.6 ± 2.6	5.9 ± 0.5	65.9 ± 9.4	9.7 ± 0.5	65.1 ± 5.2
CD38	97.3 ± 0.5	14.1 ± 2.5	10.2 ± 0.8	5.1 ± 0.5	68.7 ± 5.4	16.6 ± 2.8	55.1 ± 1.2
CD117	62.4 ± 4.9	73.6 ± 12.2	74.4 ± 13.1	27.2 ± 1.3	96.2 ± 1.7	46.2 ± 5.2	92.5 ± 1.7
All the values are average ± SEM (n=3)							

The highest expression of CD34 in K562, among imatinib sensitive, CML cell lines was also similar to expression patterns of all other mFPR, sFPR1, bcr-abl protein, co-expression of sFPR1 & sFPR2, sFPR1 & sFPR3 and sFPR1, sFPR2 and sFPR3. When the results of SR and S cell lines were compared with the previous results, CD34 expression pattern for the SR and S cell line of K562 matched with the expression of sFPR3, bcr-abl mRNA & protein expression and co-expression pattern of sFPR1 & sFPR2, sFPR1 & sFPR3, sFPR2 & sFPR3 and sFPR1, sFPR2 &

sFPR3 but was opposite of mFPR2 and mFPR3 expression. CD34 expression pattern of SR and S cell line of KCL22 matched with the expression pattern of all the three mFPR, sFPR, bcr-abl protein expression and co-expression pattern of sFPR1 & sFPR2, sFPR1 & sFPR3 and sFPR1, sFPR2 & sFPR3. Results of CD34 expression between SR and S cell line of KU812 matched with the expression changes of sFPR1, bcr-abl protein and co-expression of sFPR1 & sFPR2, sFPR1 & sFPR3 and sFPR1, sFPR2 & sFPR3. It was in contrast to the expression patterns of mFPR3, sFPR3 and bcr-abl gene.

From above data, it may be suggested that in imatinib sensitive cell lines, mFPR1 and between SR and S cell lines bcr-abl protein, showed the expression correlation with CD34. However, more evidences will be required to confirm it. Furthermore, all the imatinib resistant cell lines showed the positivity for the CD34 whereas the only one out of three imatinib sensitive cell lines showed the positivity for CD34. Since CD34 expression was correlated with the HSC, it could be said the imatinib resistant cells had more stemness properties than imatinib sensitive cell lines.

CD38

CD38 (cluster of differentiation 38), also known as cyclic ADP ribose hydrolase is a glycoprotein found on the surface of many immune cells (white blood cells), including $CD4^+$& $CD8^+$ B lymphocytes and natural killer cells[178]. CD38 is a multifunctional ectoenzyme that catalyzes synthesis and hydrolysis of cyclic ADP-ribose (cADPR) from NAD^+ to ADP-ribose[178-180]. These reaction products are essential for the regulation of intracellular Ca^{2+}[178-180]. Since chemotaxis of neutrophils to fMLP is dependent on Ca^{2+} mobilization and is mediated by cyclic ADP-ribose, CD38 controls chemotaxis of neutrophils to fMLP through its

production of cyclic ADP-ribose, and acts as a critical regulator of inflammation and innate immune response[178-180]. CD38 is also used as a negative marker for HSC identification. Since, it was earlier reported from our lab that CML neutrophils were defective in Ca^{2+} signalling, it would be interesting to see the levels of CD38 markers in the CML cell lines. Using fluorescently tagged antibody, expression of CD38 and percent of cells expressing CD38 (% positivity) were studied in all the cell lines. % positivity below 10% was considered as negative.

Among all the cell lines tested b2a2 fusion transcript expressing cell line, KCL22 was found negative for the expression of CD38 as the % positivity was less than 10% (Fig-RC 7B & 7D;Table-RC 8). All the bcr-abl positive cell lines showed lower % positivity for the CD38 than that in bcr-abl negative, promyelocytic cell line HL-60. Very few cells in K562 and KU812 cell lines (i.e. 14.1 and 16.6, respectively) were positive for the CD38. SR and S cell lines of K562 showed similar cellular positivity for CD38. However, the SR cell lines of KU812 and KCL22 showed an increase in the CD38 cellular positivity than that in their respective S cell lines.

The higher expression of CD38 in HL60 than that in CML cell lines was similar to all the mFPR and sFPR expression pattern. Furthermore, no change in the expression level of CD38 between SR and S cell line of K562 was similar to the expression pattern of mFPR1, sFPR1 and sFPR2. An increase in the expression of CD38 in SR than S cell lines of KCL22 and KU812 was similar to the CD34 expression pattern.

CD38 data clearly showed that bcr-abl positive cell lines were less differentiated than HL60. Furthermore, the expression of CD38, among imatinib sensitive, bcr-abl positive cell lines, was limited to b3a2 fusion transcript expressing cell lines.

CD117

CD117 is a cytokine receptor or receptor tyrosine kinase type III expressed on the surface of HSC, multipotent progenitors (MPP), and common myeloid progenitors (CMP) as well as other cell types[181]. CD117 is also known as mast/stem cell growth factor receptor (SCFR), proto-oncogene c-Kit and tyrosine-protein kinase Kit[181].

All the cell lines tested, showed expression of CD117, however distinction was not seen between bcr-abl negative and positive cell lines (Fig-RC 7C & 7D;Table-RC 8). The highest CD117 positive cells among imatinib sensitive CML cell lines, was expressed by K562 followed by KU812. KCL22 showed the least cellular positivity for the CD117. Similar to CD38, there was no difference in cellular positivity for CD117, between SR and S cell lines of K562 while increase in the CD117 positive cells was observed in the SR cell lines of KCL22 and KU812 than their respective S cell lines. The highest expression of CD117 by K562 among imatinib sensitive cell lines was similar to the expression of mFPR1, mFPR2, mFPR3, sFPR1, bcr-abl protein, CD34 and co-expression of sFPR1 & sFPR2, sFPR1 & sFPR3 and sFPR1, sFPR2 and sFPR3. The differences in the expression of CD117 between SR and S cells of all three cell lines were similar to the differences in sFPR1 expression between SR and S cell lines. Increase in the CD117 positivity in the SR cell line of KCL22 was similar to all the mFPR, sFPR, bcr-abl protein, CD34, and co-expression of sFPR1 & sFPR2, sFPR1 & sFPR3 and sFPR1, sFPR2 and sFPR3. Increase in the cells showing positivity for the CD117

in SR cell line than that in S cell line of KU812 was similar to the sFPR1, bcr-abl protein, CD34 and co-expression of sFPR1 & sFPR2, sFPR1 & sFPR3 and sFPR1, sFPR2 and sFPR3.

The above result showed that there was no distinction in CD117 expression of bcr-abl positive and negative cell lines. However, among bcr-abl positive, imatinib sensitive cell lines, its expression might be dependent on the type of bcr-abl fusion transcript. B2a2 expressing cell line showed the least CD117 cellular positivity. In imatinib resistant cell lines, its expression increased in two out of three cell lines and found to be similar to the CD38 and bcr-abl protein expression pattern.

On the basis of these CD markers expression the phenotype of cell lines could now be expressed as follows:

HL60	$CD34^{--}/CD38^{++}/CD117^{++}$
K562	$CD34^{++}/CD38^{low}/CD117^{++}$
K562/SR	$CD34^{low}/CD38^{low}/CD117^{++}$
KCL22	$CD34^{--}/CD38^{--}/CD117^{++}$
KCL22/SR	$CD34^{++}/CD38^{++}/CD117^{++}$
KU812	$CD34^{low}/CD38^{low}/CD117^{++}$
KU812/SR	$CD34^{++}/CD38^{++}/CD117^{++}$

CD markers expression pattern confirmed the lineage of these cell lines as HL60 was negative for CD34 and strongly positive for CD38 and CD117 –characteristic feature of promyelocyte[182]. Among imatinib sensitive CML cell lines, only K562 showed positivity for CD34 while KCL22 and KU812 were negative for CD34. K562 also showed positivity for CD38 and CD117 while KU812 showed marginal positivity for CD38 but strong positivity for CD117. KCL22 showed only CD117

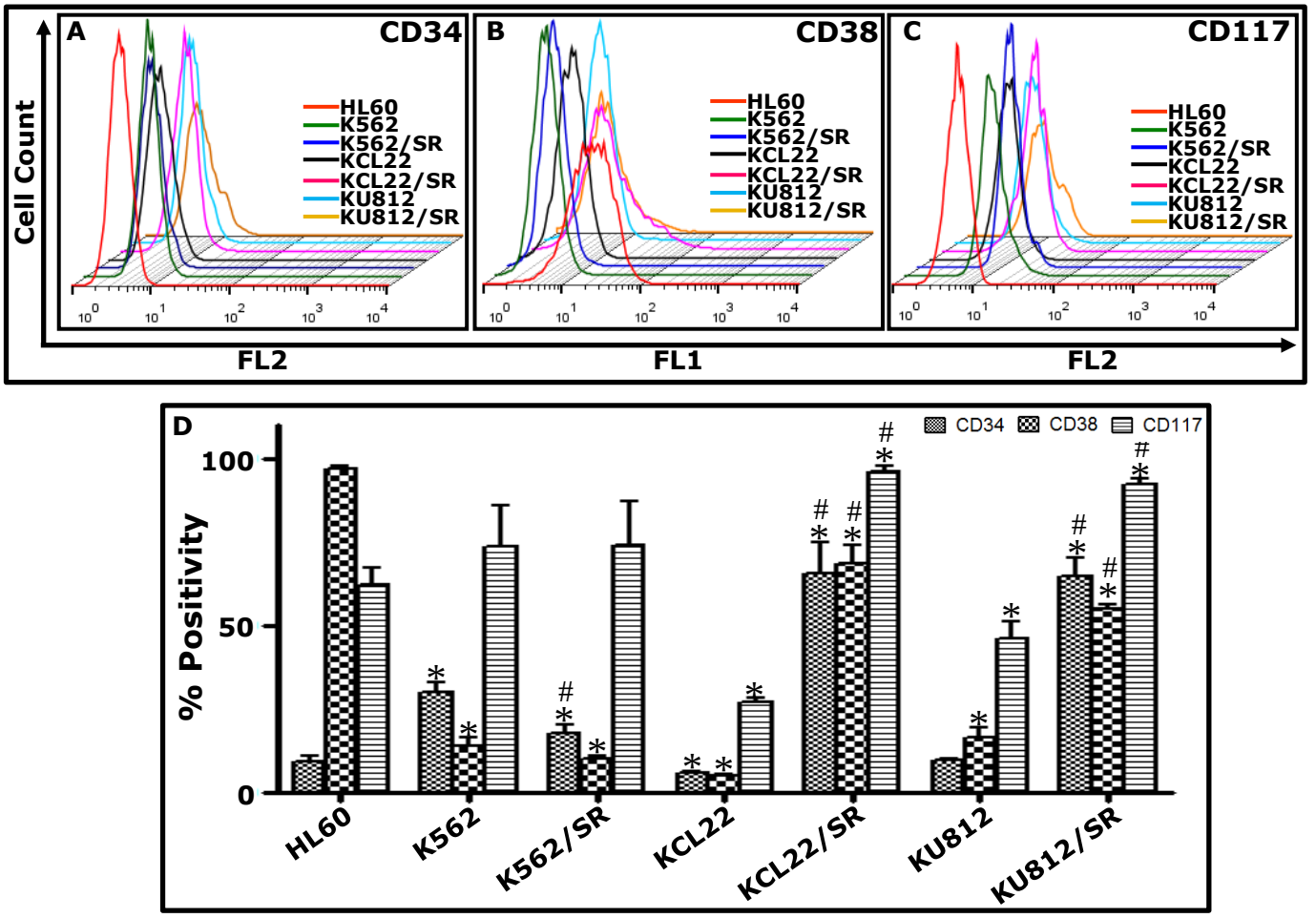

Fig-RC 7: Expression of CD Markers in CML Cell Lines: Representative 3D-histogram overlays showing surface expression of (A) CD34, (B) CD38 and (C) CD117 in CML cell lines and HL60 as indicated. (D) Bar plot showing average percent positive cells ± SEM of each cell line for all the three CD markers is plotted (n=3) * $p<0.05$ wrt HL60, # $p<0.05$ wrt respective sensitive cell line (Mann-Whitney test).

positivity. K562 has features of myeloblasts, KCL22 showed features of promonocytes and KU812 showed features of early basophilic origin[182].

	K562	KCL22	KU812
mFPR1	+++	+	+
mFPR2	+++	++	+
mFPR3	+++	+	++
sFPR1	+++	++	++
sFPR2	+++	+++	+++
sFPR3	+++	+++	+++
sFPR1 & sFPR2	+++	++	+
sFPR1 & sFPR3	+++	++	+
sFPR2 & sFPR3	+++	+++	+++
sFPR1, sFPR2 & sFPR3	+++	++	+
Bcr-abl gene	++	NA	+++
Bcr-abl Protein	+++	+	++
CD34	+++	+	+
CD38	++	+	++
CD117	+++	+	++

To summarize the CD expression results, it could be said that all the bcr-abl positive cell lines were less differentiated than bcr-abl negative cell lines. K562/SR showed lowered CD34 than K562, while CD38 and CD117 expressions were at par in both the cell lines. It showed that in K562/SR, imatinib resistance was not due to quiescent CML stem cells. K562/SR showed decrease in bcr-abl gene, and bcr-abl protein expression. This indicate that loss of target could be the reason for imatinib resistance in K562/SR. KCL22/SR, showed increase in all the three CD markers than that in KCL22. This cell line had also shown increase in the level of bcr-abl protein and all three mFPR and sFPR. Increase in the target protein with increased cellular stemness might be responsible for the imatinib resistance of this cell line. Furthermore, increase in the expression of FPR might be promoting imatinib resistance because as mentioned earlier molecules that play role in acquiring imatinib resistance, have shown direct link with FPR. KU812/SR, also showed increase in all the three CD markers than that

in KU812. Similar to KCL22/SR, this cell line also showed increase in the expression of bcr-abl protein. Hence, the mechanism for the resistance for both of these cell lines were same except KU812/SR had involvement of different FPR. There was increase in sFPR1 and decrease in sFPR3 in KU812/SR, which showed that these two proteins also played role in imatinib resistance in this cell lines. The results for imatinib resistant cell lines with respect to their sensitive cell lines are summarized in following table.

	K562/SR	**KCL22/SR**	**KU812/SR**
mFPR1	No Change	Increase	No Change
sFPR1	No Change	Increase	Increase
mFPR2	Increase	Increase	No Change
sFPR2	No Change	Increase	No Change
mFPR3	Increase	Increase	Decrease
sFPR3	Decrease	Increase	Decrease
sFPR1 & sFPR2	Decrease	Increase	Increase
sFPR1 & sFPR3	Decrease	Increase	Increase
sFPR2 & sFPR3	Decrease	No Change	No Change
Bcr-abl gene	Decrease	Decrease	Decrease
Bcr-abl Protein	Decrease	Increase	Increase
CD34	Decrease	Increase	Increase
CD38	No Change	Increase	Increase
CD117	No Change	Increase	Increase

Ligand Binding

The first step in any ligand mediated receptor signalling is binding of the receptors to their ligand. This leads to the activation of downstream signalling cascade. It was earlier reported by our group that CML neutrophils were defective in ligand binding. Since we have found that CML cell lines had shown differences in their expression of FPR mRNA as well as protein as compared to the bcr-abl negative cell lines, these receptors were checked for their ligand binding ability by using fluorescent ligand. FITC-fNLPNTL is a fluorescently tagged ligand with high affinity for FPR1 and FPR2. Hence, FITC-fNLPNTL was used to investigate the ligand binding ability of FPR receptors in CML cell lines.

Cells were incubated with 1.0 μM ligand at 37°C for 1 hr and ligand binding was checked by flow-cytometry.

All the cell lines showed 100% positivity for ligand binding (Fig-RC 8A & 8B; Table-RC 9). Among all the cell lines, bcr-abl negative cell line –HL60 showed the lowest binding to the ligand whereas all the bcr-abl positive cell lines showed significantly higher binding to the ligand, which was in contrast to mFPR1, mFPR2 and sFPR expression. In FPR expression studies in normal PMNL, it has been shown that in addition to the surface receptors, an intracytoplasmic pool of receptors exists. Hence, at physiological temperature, the receptor trafficking may occur, i.e. the surface receptors are endocytosed and receptors from the intracytoplasmic pool translocated to the surface. Staining of sFPR1 and sFPR2 was done at 4°C and ligand binding was done at 37°C. Therefore, binding assay carried out at 37°C could be considered as an estimation of the total number of receptors in cell lines. Taken into account both, surface expression and ligand binding assay data, it could be said that though expression of sFPR1 and sFPR2 was lower in CML cell lines, the total receptor pool or functional receptor pool was higher. The % cell positivity for the sFPR1 was more than 95% only for HL-60. All other cell lines showed cellular positivity less than HL-60. Among bcr-abl positive cell lines, KU812, showed the highest binding to the ligand while K562 showed the lowest ligand binding, again contrasting to the sFPR expressions.

Table-RC 9: Binding of fNLPNTL-FITC

	MFI						
	HL60	K562	K562/SR	KCL22	KCL22/SR	KU812	KU812/SR
fNLPNTL-FITC	34.5 ± 1.7	53.1 ± 4.3	50.3 ± 1.6	76.1 ± 0.8	71.1 ± 0.7	121.5 ± 10.9	66.8 ± 5.8
All the values are average ± SEM (n=3)							

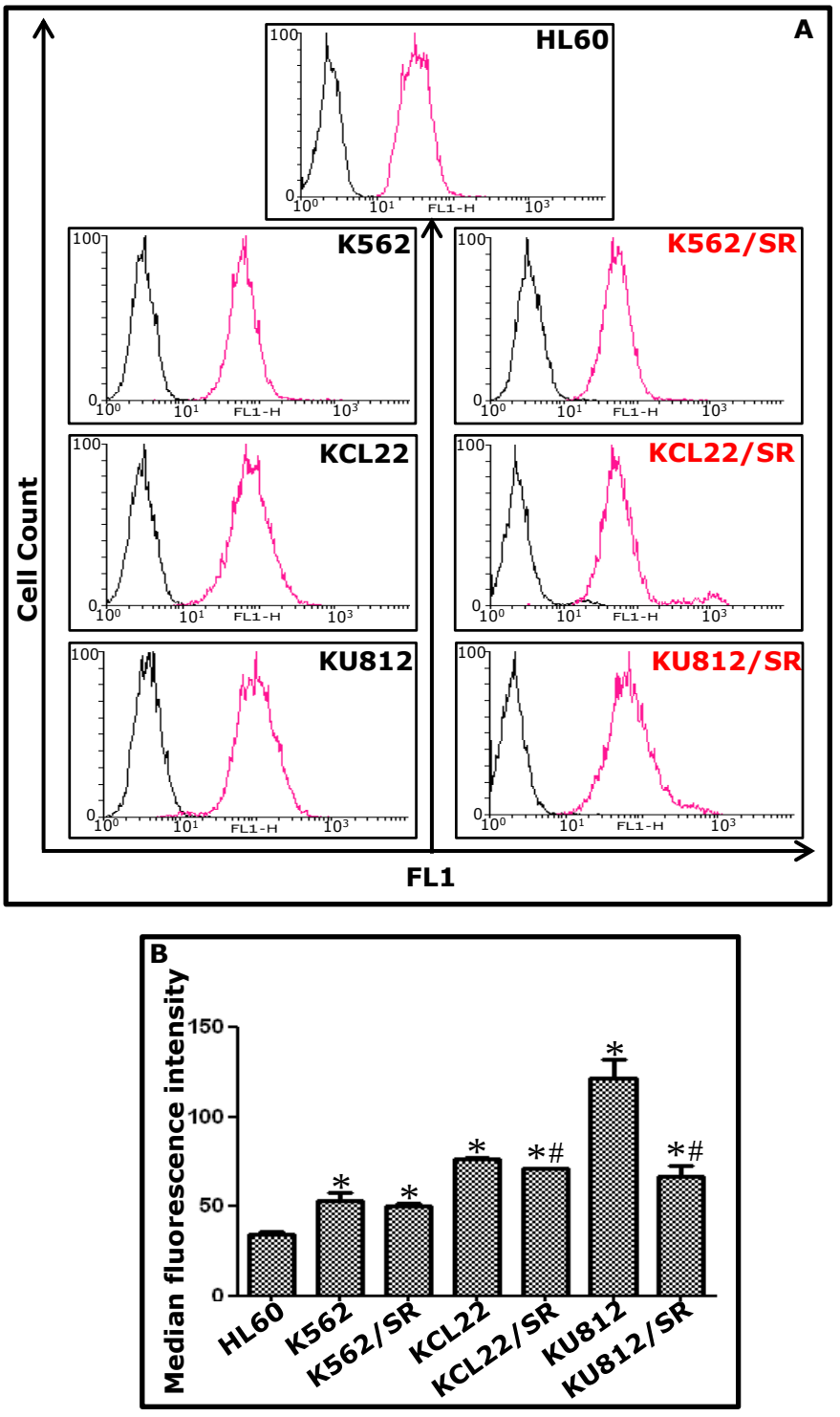

Fig-RC 8: fNLPNTL-FITC Ligand Binding: fNLPNTL-FITC ligand binding to CML cell lines - (A) Representative histogram overlays showing fNLPNTL-FITC binding in all the CML cell lines and HL-60 as indicated. In each plot black solid line represents unstained isotype control, pink line represents cells stained by fNLPNTL-FITC. (B) Bar plot showing average MFI ± SEM of fNLPNTL-FITC treated CML cell lines and HL60, as estimated by flow cytometry (n=3) . * $p<0.05$ wrt HL60, # $p<0.05$ wrt the respective sensitive cell line (Mann-Whitney test).

Receptor ligand dynamics is an important step in understanding the activation of the cells by external stimuli. Studies by Fletcher and Gallin, and Perez et al., have indicated that for PMNL to continuously sense a chemotactic gradient and move along the gradient, continuous occupancy of FPR or recovery of FPR on the membrane is required[183-185]. FPR expressed on PMNL are present on the cell membrane as well and as an intracytoplasmic pool[183, 186, 187]. Studies by Sengelov et al., using a high affinity, photoactivable, radioiodinated derivative of fMLFK-^{125}I-B-ASD demonstrated that the compartment in human PMNL that is mobilized most easily and fastest, the secretory vesicles, is a major reservoir of FPR[188]. Earlier studies from our group showed defective functional responses upon FPR activation, hence ligand binding ability of CML cell lines was also checked. Earlier report by Baker et al., has shown lower formyl peptide binding to PMNL from CML patients in chronic phase[77]. Another report from our laboratory has shown lower number of FPR in CML PMNL at 4°C. However, the association and dissociation constants of normal and CML were comparable[87]. In present study, CML cell lines showed higher ligand binding despite lower sFPR expression than bcr-abl negative cell line –HL60. As mentioned earlier, though bcr-abl positive cell lines were compared with the bcr-abl negative cell line –HL60. Being a cancerous cell line –HL60 could also exhibit defect in the ligand binding to FPR, hence higher ligand binding was observed in CML cell lines, while CML PMNL showed lower ligand binding than normal PMNL. Furthermore, cell lines have more immature cells, while PMNL are highly differentiated cells. As per the CD marker expression, all the CML cell lines were less differentiated than HL60. Hence, the receptor status and its kinetics could probably differ as per differentiation status. This difference would also affect the receptor expression

as well as affinity of the receptor to the ligand. There would also be various reasons for the difference in the surface protein level obtained from antibody staining and ligand binding data. Observations from different studies have shown that not all the receptors present on the cell bind to the ligand. Sklar et al., have shown using fNLPNTL-FL that only 1-2 % of FPR are occupied [186]. Hence, detection of FPR using antibodies, aids in studying the receptor in totality in contrast to only the ligand bound receptor when detected using labelled ligand. Studies of antibody binding assume 1:1 receptor and antibody binding, while ligand did not bind to receptor in 1:1 ratio. Furthermore, staining of sFPR1 and sFPR2 was done at 4°C and ligand binding was done at 37°C. As mentioned, FPR is present on cell membrane as well as present as a cytoplasmic pool. At 4°C receptor internalization, translocation and upregulation was inhibited hence only surface receptors were available for binding, while at 37°C surface as well as cytoplasmic pool of receptor would be available. Study form Hoffman et.al showed that binding of FNLPNTL-FL at 37°C was 1.5 to 2.5 times higher than the quantity bound at 4°C. The reason for cited was a rapid movement of receptors from an internal pool to the plasma membrane surface and/or a physical change in surface receptor due to temperature that may expose a previously hidden binding pocket to the ligand. Among imatinib sensitive cell lines, highest ligand binding was observed in KU812, while K562 showed the least ligand binding. Differences in the level of ligand binding among the CML cell lines could be attributed to their lineages. There were no study comparing the FPR status among various fractions of blood cells, but given the fact that there were difference in the level of FPR expression and ligand binding, it might be possible that different hematopoietic cell might have different FPR expression level

and/or ligand binding affinity. KCL22/SR and KU812/SR showed lower ligand binding than their respective imatinib sensitive cell lines, while ligand binding was at par in K562 and K562/SR. In KCL22/SR and KU812/SR, imatinib resistance might be affecting the ligand binding affinity of FPR or the receptor folding was defective so that ligand binding pocket might not be freely accessible to ligand.

Signaling of FPR

It was shown in our previous results that expression of mFPR1 and mFPR2 as well as sFPR1, sFPR2 and sFPR3 expression was lowered in bcr-abl cell lines. However, the ligand binding of the bcr-abl positive cell lines was higher than the bcr-abl negative cell line. To see if downstream signaling of FPR was affected by the change in FPR expressions, the downstream events, activated by binding of ligand to the FPR were studied in all the cell lines.

Release of calcium is one of the earliest events in FPR activation pathway followed by actin polymerization. It has been reported that CML PMNL were defective in both Ca^{2+} signalling as well as actin polymerization. Hence, both the phenomena were studied in all the cell lines.

Calcium signaling:

Binding of the chemoattractants to their receptors on PMNL transmits signals across the plasma membrane, initiating phosphorylation cascade and changes in Ca^{2+} concentration, that are crucial to cell activation. Both calcium release from the intracellular stores and the calcium influx from the extracellular space contribute to the rise in Ca^{2+} levels. This Ca^{2+} in turn regulates chemoattractant receptor availability in PMNL[189]. Calcium from the extracellular space enters the

cell cytoplasm through various types of channels, i.e. voltage operated Ca^{2+} channels (VOCCs), ligand gated non-specific cation channels (LGCCs) and receptor activated Ca^{2+} channels (RACCs). Calcium can also be released from internal Ca^{2+} stores through inositol 1,4,5-triphosphate (IP_3) or ryanodine receptors and is replenished by store operated channels (SOCs)[190]. Two distinct Ca^{2+} storage sites have been identified in PMNL. One site was located peripherally under the plasma membrane and the other in the juxtranuclear space. The central Ca^{2+} storage site released Ca^{2+} in response to fMLP, whereas engagement and clustering of CD11b/CD18 integrins caused Ca^{2+} release from the peripheral stores[191]. The peripheral stores of Ca^{2+} are known to be regulated by the cytoskeleton interactions[192]. The rise in Ca^{2+} concentration is caused by mobilization of Ca^{2+} from intracellular stores to the cytosol followed by an immediate increase in plasma membrane permeability to extracellular calcium. Efflux of Ca^{2+} is mediated by calmodulin dependent calcium adenosine triphosphatase (Ca-ATPase). Ca-ATPase probably serves as the regulatory and homeostatic mechanism required to maintain low Ca^{2+} concentrations. When the cytosolic Ca^{2+} concentration is increased by either fMLP or ionophore, efflux of Ca^{2+} from the cell occurs as a result of calmodulin mediated activation of Ca-ATPase[193].

Mobilization of Ca^{2+} is upstream to various biochemical and functional events in PMNL stimulated by various chemoattractants. Since there were differences in the expression of FPR in CML cell lines and their ligand binding, study on mobilization of Ca^{2+} in response to fMLP was performed. The cell lines were loaded with fluo-4 and changes in relative fluorescence in response to activation by the ligand – fMLP, were recorded using a spectrophotometer.

Basal

Except K562, all the bcr-abl positive cell lines showed significantly higher basal Ca^{2+} level than the bcr-abl negative cell line HL-60. K562 showed basal Ca^{2+} level at par with HL-60 (Fig-RC 9; Table-RC 10) . There were not significant difference in the basal Ca^{2+} levels, between SR and S cell lines of KCL22 and KU812, whereas significantly higher Ca^{2+} levels were observed in the SR cell line of K562 as compared to the S cell line.

fMLP stimulation

Ca^{2+} levels: After stimulation with fMLP, all the cell lines showed the increase in Ca^{2+} levels with respect to their respective basal levels (Fig-RC 10 & 11; Table-RC 11). In bcr-abl negative cell line HL60, Ca^{2+} levels increased and reached at the peak by 18s which came down at 22s and again increased showing the second peak at 44s (Fig-RC 10). These high levels were maintained for a longer duration. Ca^{2+} levels were back to the basal levels at 131s (Fig-RC 10). This type of two peaked response after stimulation with fMLP is a characteristic feature of neutrophils. Among bcr-abl positive, imatinib sensitive cell lines, only KU812 followed this two peaks pattern upon fMLP stimulation. In HL60, the first increase in Ca^{2+} level was not statistically significant with respect to the basal level, but the second peak was significantly higher than the basal Ca^{2+} level (Fig-RC 11A). In KU812 both the peaks showing increase in Ca^{2+} levels, were significantly higher than the basal Ca^{2+} level. K562 and KCL22, both showed the single peak pattern. Increase in the Ca^{2+} level of K562 and KCL22 was significantly higher than their respective basal Ca^{2+} level. The peak of Ca^{2+} level increase in K562, in response to fMLP, was at par with the first peak of HL60. KCL22 showed significantly higher increase in the Ca^{2+} level, in response to fMLP

stimulation, than that in HL60. Among imatinib resistant cell lines, both b3a2 fusion transcript expressing SR cell lines –K562/SR and KU812/SR showed the two peak pattern, upon fMLP stimulation similar to that in HL60. Both the peaks of increase in Ca^{2+} levels for K562/SR and KU812/SR were significantly higher than their respective basal Ca^{2+} level. The first peak of increase in Ca^{2+} levels for K562/SR was at par with the peak of increase in Ca^{2+} levels for K562. Increase in Ca^{2+} levels in both the peak of KU812/SR were lower than the respective peak of Ca^{2+} levels increase in KU812. SR cell line with b2a2 fusion transcript –KCL22/SR showed only one peak pattern, similar to its S cell line. This increase in the Ca^{2+} level in KCL22/SR, upon fMLP stimulation was significantly higher than its basal level, but lower than the increase in the Ca^{2+} level in KCL22.

All the cell lines were treated with the ionophore A23187 as a positive control. Ionophore is an artificial mobile ion carrier that normally acts as an ion-exchange shuttle molecule transporting one divalent calcium ion into the cell in exchange of two H^+. All the cell lines showed remarkable increase in the Ca^{2+} level after ionophore treatment, indicating that the cells were healthy and their Ca^{2+} channels were open.

Quenching of Ca^{2+} level with EGTA showed decrease in Ca^{2+} levels in all the cell lines below their basal level. $MnCl_2$ treatment did not show any further decrease in Ca^{2+} levels in the EGTA treated cells.

Table-RC 10: Calcium Levels in Various Cell Lines

		HL60		K562		K562/SR		KCL22		KCL22/SR		KU812		KU812/SR	
		RFU	Time* (Sec.)	RFU	Time* (Sec.)	RFU	Time* (Sec.)	RFU	Time* (Sec.)	RFU	Time* (Sec.)	RFU	Time* (Sec.)	RFU	Time* (Sec.)
Basal		300237 ± 20935	N.A	297757 ± 25568	N.A	516227 ± 43825	N.A	399480 ± 31244	N.A	437901 ± 33774	N.A	444349 ± 35435	N.A	519281 ± 32680	N.A
fMLP	Max-1	319875 ± 20337	18.4 ± 0.58	339038 ± 33378	18.2 ± 0.79	559565 ± 48055	17.8 ± 1.14	477962 ± 41550	65.6 ± 5.86	467321 ± 35758	17.1 ± 1.27	496995 ± 37132	16.5 ± 2.09	540665 ± 34005	18.7 ± 1.07
	Min-1	291798 ± 16437	22.3 ± 0.43	293283 ± 25006	24.9 ± 1.29	519721 ± 44490	23.1 ± 1.47	433203 ± 41515	128.0 ± 12.44	421922 ± 34524	21.5 ± 1.00	449942 ± 36650	25.6 ± 5.14	502506 ± 31994	23.1 ± 0.95
	Max-2	322685 ± 19705	43.8 ± 2.06	N.F.	N.F.	554327 ± 62507	221.8 ± 18.73	N.F.	N.F.	N.F.	N.F.	496271 ± 61492	95.8 ± 14.24	550516 ± 36890	60.41 ± 5.78
	Min-2	285326 ± 18565	131.2 ± 6.16	N.F.	N.F.	523475 ± 59470	264.1 ± 14.65	N.F.	N.F.	N.F.	N.F.	461220 ± 59545	131.9 ± 16.58	517151 ± 34737	128.8 ± 5.93
Ionophore		727577 ± 22176	68.3 ± 2.5	493877 ± 42589	109.6 ± 7.65	849293 ± 47810	82.9 ± 4.99	615789 ± 34959	50.7 ± 6.69	681711 ± 16725	56.5 ± 5.35	824781 ± 78154	123.9 ± 3.53	845775 ± 33206	72.0 ± 8.55
EGTA		154805 ± 8099	28.2 ± 3.76	114980 ± 13035	33.2 ± 2.37	156082 ± 9952	28.9 ± 2.78	137541 ± 8466	27.1 ± 3.77	127763 ± 8034	25.3 ± 2.88	152056 ± 9847	21.01 ± 2.05	183650 ± 9942	20.8 ± 2.64
MnCl2		157884 ± 9328	18.0 ± 1.51	136076 ± 4986	18.4 ± 1.70	174259 ± 5345	18.4 ± 0.89	181305 ± 9405	17.8 ± 1.01	216560 ± 15329	16.3 ± 2.33	214813 ± 11040	17.0 ± 1.55	237534 ± 14658	14.6 ± 1.35
* Time after addition of each compound, All the values are average ± SEM (n=3)															

Table-RC 11: Changes in Calcium Levels upon fMLP stimulation

Ratio wrt Basal		**HL60**	**K562**	**K562/SR**	**KCL22**	**KCL22/SR**	**KU812**	**KU812/SR**
fMLP	**Max-1**	1.08 ± 0.04	1.13 ± 0.03	1.08 ± 0.01	1.18 ± 0.04	1.07 ± 0.01	1.12 ± 0.03	1.04 ± 0.01
	Min-1	0.99 ± 0.05	0.98 ± 0.01	1.00 ± 0.02	1.06 ± 0.02	0.96 ± 0.01	1.01 ± 0.01	0.97 ± 0.01
fMLP	**Max-2**	1.08 ± 0.02	N.F.	1.12 ± 0.02	N.F.	N.F.	1.10 ± 0.01	1.06 ± 0.01
	Min-2	0.95 ± 0.01	N.F.	1.06 ± 0.02	N.F.	N.F.	1.02 ± 0.01	0.99 ± 0.01
Ionophore		2.72 ± 0.21	1.82 ± 0.12	1.72 ± 0.12	1.61 ± 0.12	1.82 ± 0.12	1.94 ± 0.21	1.83 ± 0.08
EGTA		0.57 ± 0.04	0.42 ± 0.02	0.32 ± 0.03	0.27 ± 0.01	0.37 ± 0.01	0.36 ± 0.02	0.48 ± 0.03
MnCl2		0.58 ± 0.04	0.52 ± 0.03	0.36 ± 0.02	0.37 ± 0.03	0.62 ± 0.03	0.51 ± 0.04	0.62 ± 0.03
All the values are average ± SEM (n=3)								

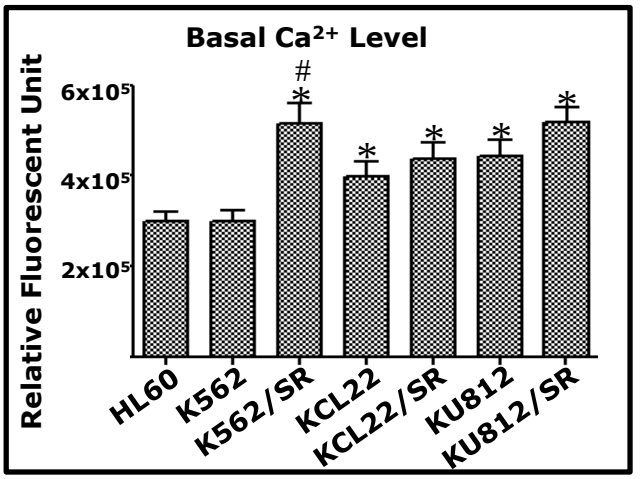

Fig-RC 9: Basal Ca^{2+} levels: Basal Ca^{2+} levels in CML cell lines and HL60 measured by using Fluo4. Data presented is average relative fluorescence unit ± SEM for each cell line (n=3). * $p<0.05$ wrt HL60, # $p<0.05$ wrt the respective sensitive cell line (Mann-Whitney test).

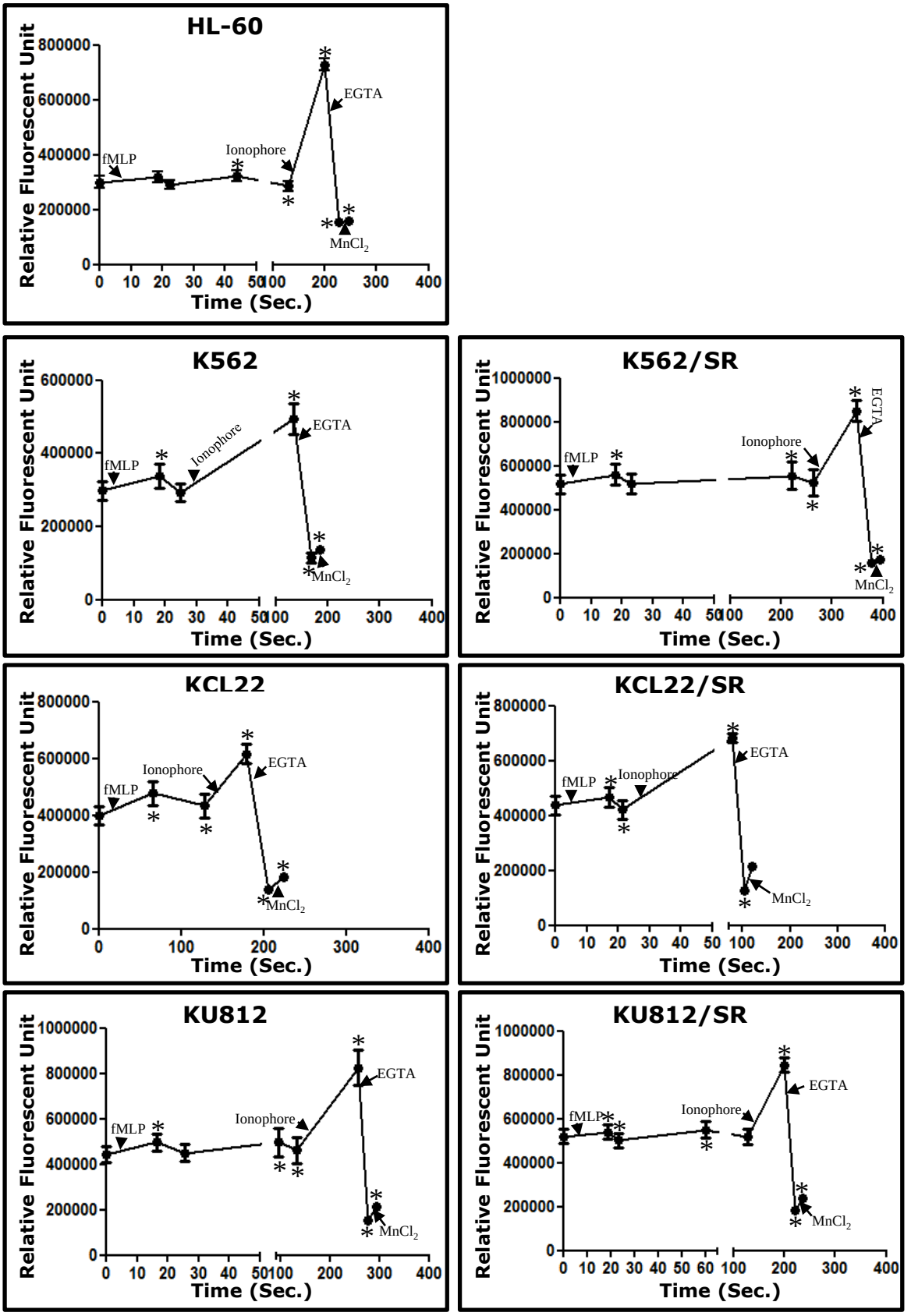

Fig-RC 10: Change in Calcium Levels upon fMLP Stimulation: Histograms showing Ca^{2+} levels in CML cell lines and HL-60 as indicated. Data presented as average relative fluorescence unit ± SEM of each cell lines as indicated (n=3). * $p<0.05$ wrt the basal calcium level (Wilcoxon paired test)

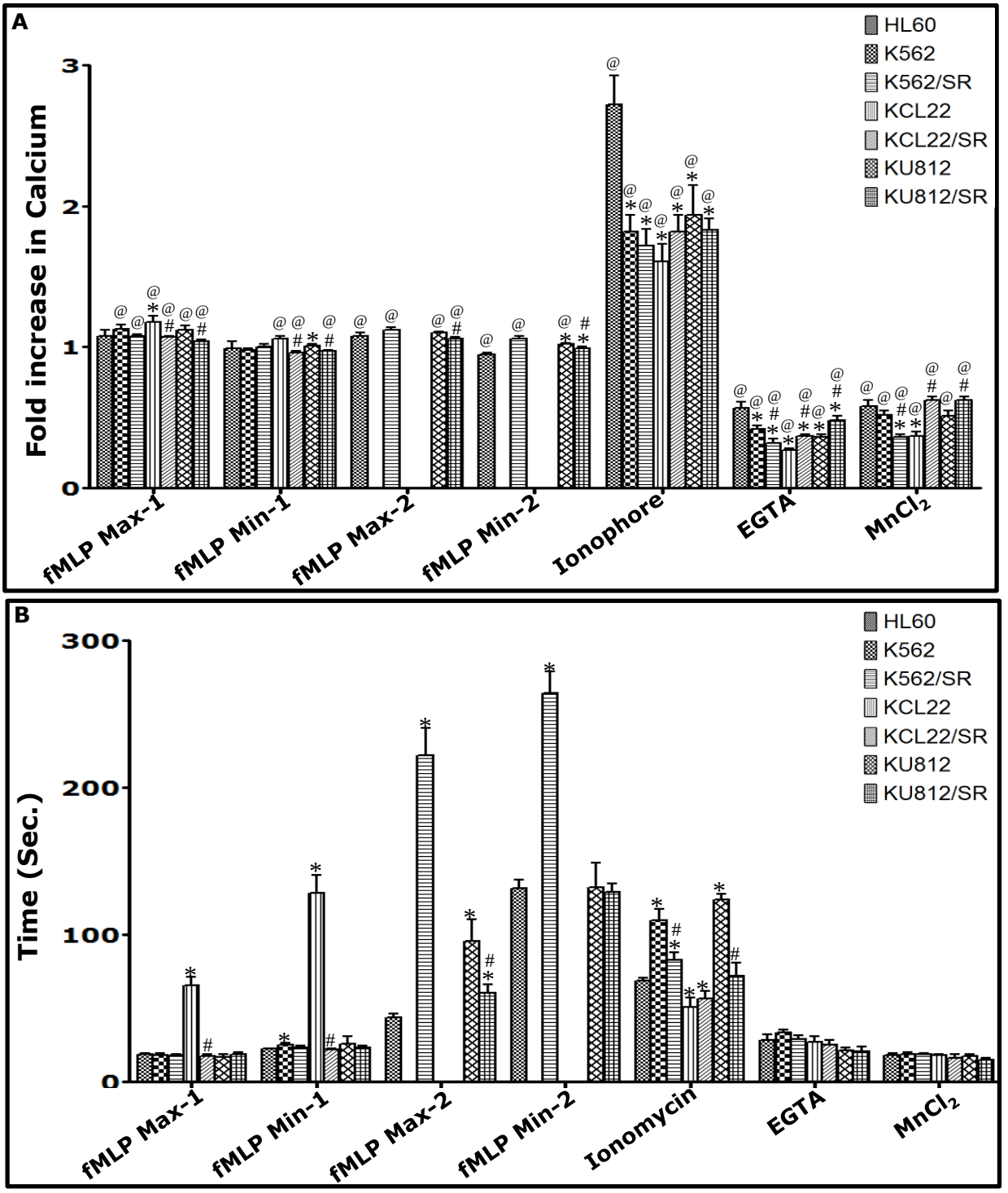

Fig-RC 11: Time Kinetics of Calcium in CML Cell Lines: Flurometric analysis of calcium release in responses to fMLP treatment in CML cell lines and HL60. (A) Average increase in OD from baseline ± SEM for each cell line was plotted (n=3). (B) Time required to reach the peak or minimum value after various treatments for each cell line is plotted as average time in sec ± SEM (n=3). * $p<0.05$ wrt HL60, # $p<0.05$ wrt the respective sensitive cell line (Mann-Whitney test). @ $p<0.05$ wrt the basal Ca2+ levels (Wilcoxon paired test)

Time Kinetics: Time required by the cell lines to reach up to first peak was similar for the HL60 and b3a2 fusion transcript expressing, imatinib sensitive as well as imatinib resistant cell lines (Fig-RC 11B; Table-RC 10). B2a2 fusion transcript expressing, imatinib sensitive cell line KCL22 was the slowest cell line to respond to fMLP. As mentioned earlier among imatinib sensitive cell lines, only KU812 showed the two peak pattern for Ca^{2+} signalling. KU812 required a longer time to reach to the second peak as compared to HL60. Among the SR cell lines, only b3a2 expressing cell lines showed the two peak pattern. Both these SR cell lines –K562/SR and KU812/SR too took longer time to reach to the second peak than that taken by HL60. Between both of the SR cell lines, K562/SR took longer time to reach to the second peak than KU812/SR. KU812/SR required more time to reach to the second peak compared to its S cell line. B2a2 fusion transcript expressing SR cell line, was faster responding than its S cell line.

Post ionophore treatment, imatinib sensitive cell lines with b3a2 fusion transcript were slow responding and took longer time than HL60 to reach the peak Ca^{2+} level, whereas imatinib sensitive and resistant cell line with b2a2 fusion transcript were the fastest responding and took less time than taken by HL60 to reach peak Ca^{2+} levels. SR cell lines of b3a2 were faster to reach to peak Ca^{2+} levels after ionophore treatment than their respective S cell lines. Quenching of the cell lines with the EGTA took similar time for all the cell lines.

Above result showed that all the CML cell lines responded to fMLP and showed increase in the Ca^{2+} levels. Though increase in the Ca^{2+} levels was to a lesser extent, it was significantly higher than their respective basal levels. The range for the fold increase of Ca^{2+} levels in CML cell lines were 1.04-1.18. This fold increase in the Ca^{2+} levels upon fMLP stimulation, in CML cell lines was very

much lower than the increase in the CML PMNL, where fold increase was reported 1.45-2.7[194]. Similarly, bcr-abl negative cell line HL60 also showed the lower increase in the Ca^{2+} levels post fMLP stimulation than that in normal PMNL as well as CML PMNL[194]. Less activation of calcium in cell lines than the respective PMNL could be due to their less differentiated status. As already mentioned HL60 is a promyelocytic cell line, which justifies its different behavior than PMNL. However the two peak pattern of Ca^{2+} release of PMNL was seen in HL60. Montero et al. reported that undifferentiated HL-60 did not show any increase in Ca^{2+} levels upon fMLP stimulation[195]. Cowen et al. showed 1.5 fold increase in Ca^{2+} level in undifferentiated HL60 after stimulating with 30 μM fMLP[196]. Our results matched with the report of Cowen et al., as there was very light increase in the Ca^{2+} level in HL60 upon fMLP stimulation. HL-60 showed calcium release time kinetics similar to b3a2 expressing cell lines suggesting that expression of b3a2 bcr-abl does not affect calcium release time kinetics. But type of bcr-abl fusion transcripts might be playing a role in alteration of Ca^{2+} signalling in CML. b2a2 fusion transcript expressing, S cell line was the slowest responder to the fMLP while all other cell lines required similar time to reach to the first peak after fMLP stimulation. Differences among the cell lines in the expression of sFPR and ligand binding were not reflected in calcium signalling. Hence, it could be said that calcium release upon fMLP stimulation in CML cell lines might be independent of the FPR expression levels and extent of ligand binding.

CD38 is a 42-kDa type II transmembrane glycoprotein that catalyzes the synthesis and hydrolysis of[178-180] three molecules — cyclic adenosine diphosphate ribose (cADPR), adenosine diphosphate ribose (ADPR), and nicotinic acid adenine

dinucleotide (NAADP). These molecules are essential for the regulation of intracellular Ca^{2+}[178-180]. cADPR produced by the enzymatic reaction of CD38, is able to mobilize the calcium release from ryanodine receptor gated stores. Fujita et al reported that fMLP treatment to PMNL decreased the CD38 protein in neutrophil, but increased its release in conditioned media in a p38-MAPK dependent manner. However, fMLP did not affect the mRNA expression of CD38. Sanchez et al had shown that CD38 controlled neutrophil chemotaxis to fMLP through production of cyclic ADP-ribose, by controlling calcium signalling. Hence the above calcium signalling data was compared with the CD38 expression data of these cell lines. Any correlation was not found between the CD38 expression and calcium release upon fMLP stimulation in CML cell lines, except that the lowest CD38 expressing cell line –KCL22 was the slowest fMLP responder. It could be suggested from these results that in CML cell lines, Ca signalling upon fMLP treatment was independent of bcr-abl expression, CD38 expression, FPR expression and extent of FPR ligand binding.

Actin polymerization

Actin polymerization is one of the downstream events after FPR activation. To study actin polymerization in CML cell lines, cells were stimulated with fMLP or solvent and F-actin was quantitated flow-cytometrically before and after stimulation using FITC-phalloidin.

Basal

Basal F-actin quantity was maximum in the bcr-abl negative cell line HL-60 (Fig-RC 12A & 12B; Table-RC 12). All the bcr-abl positive cell lines showed basal levels of F-actin significantly lower than that in HL-60, this was similar to that in

CML PMNL[85, 88]. Among bcr-abl positive cell lines, both the b3a2 fusion transcript expressing cell lines showed lower basal F-actin than that in b2a2 fusion transcript expressing cell lines. Both the b3a2 fusion transcript expressing, imatinib sensitive cell lines were at par with respect to their basal F-actin levels.

Table-RC 12: **F-actin in Various Cell Lines**

	MFI						
	HL60	K562	K562/SR	KCL22	KCL22/SR	KU812	KU812/SR
Control	259.9 ± 10.3	59.4 ± 1.41	63.6 ± 0.38	120.4 ± 1.57	97.6 ± 0.77	74.6 ± 2.14	128.3 ± 1.39
10^{-8} M fMLP	428.5 ± 12.86	103.4 ± 1.12	135.9 ± 3.53	173.7 ± 3.38	134.2 ± 1.46	112.5 ± 7.75	209.6 ± 9.84
10^{-6} M fMLP	393.1 ± 15.61	110.8 ± 3.45	111.2 ± 1.01	187.9 ± 6.02	150.8 ± 1.19	132.7 ± 3.80	234.5 ± 5.93
All the values are average ± SEM (n=3)							

Their SR cell lines, especially KU812/SR showed higher levels of basal F-actin than that in their respective S cell line while lower levels of the basal F-actin were seen in the SR cell line of b2a2 fusion transcript expressing cell line than that in the respective S cell line.

Stimulation with 10^{-8} M fMLP

Cells were stimulated with two different concentrations of fMLP (10^{-8} M and 10^{-6} M). Normal PMNL had shown concentration dependent increase in F-actin content from 10^{-11} M to 10^{-8} M[197]. At concentrations above 10^{-8} M, significant changes were not seen in the F-actin level of normal PMNL than that with 10^{-8} M fMLP stimulation[197]. There are no reports on actin polymerization in CML PMNL in response to various concentrations of fMLP. However, there are reports on difference in stimulation of F-actin polymerization between normal PMNL and

CML PMNL after treatment with 10^{-8} M fMLP[86]. CML PMNL showed lower and slower F-actin polymerization than that in normal PMNL[86].

On stimulation with 10^{-8} M fMLP, 1.5 to 2 fold increase in the F-actin was observed in all the cell lines (Fig-RC 12C; Table-RC 12). Distinct differences in F-actin polymerization between bcr-abl negative and bcr-abl positive cell lines in response to 10^{-8} M fMLP was not seen. Among imatinib sensitive cell lines highest change in F-actin content was seen in K562. KCL22 and KU812 showed the least stimulation of actin polymerization in response to 10^{-8} M fMLP. Between SR and S cell lines, the SR cell lines with b3a2 fusion transcript showed higher stimulation of actin polymerization than that in their respective S cell lines, whereas SR and S cell line with b2a2 fusion transcript showed at par stimulation of actin polymerization.

Stimulation with 10^{-6} M fMLP

Upon stimulation with 10^{-6} M fMLP, b3a2 fusion transcript expressing cell lines showed higher stimulation of actin polymerization than that in bcr-abl negative cell line HL60. b2a2 fusion transcript expressing cell line showed stimulation of actin polymerization similar to HL60 in response to 10^{-6}M fMLP (Fig-RC 12C; Table-RC 12). There were no differences in stimulation of actin polymerization upon 10^{-6} M fMLP treatment, between the SR and S cell lines of KCL22 and KU812. The SR cell line of K562 showed the slightly lower stimulation of actin polymerization than that in S cell line, but this difference was statistically significant.

Binding of chemotactic peptide to polymorphonuclear leucocytes (PMNL) results in rapid changes in the cytoskeleton of the cells finally leading to a directed movement of the cells towards the source of chemoattractant. A very early

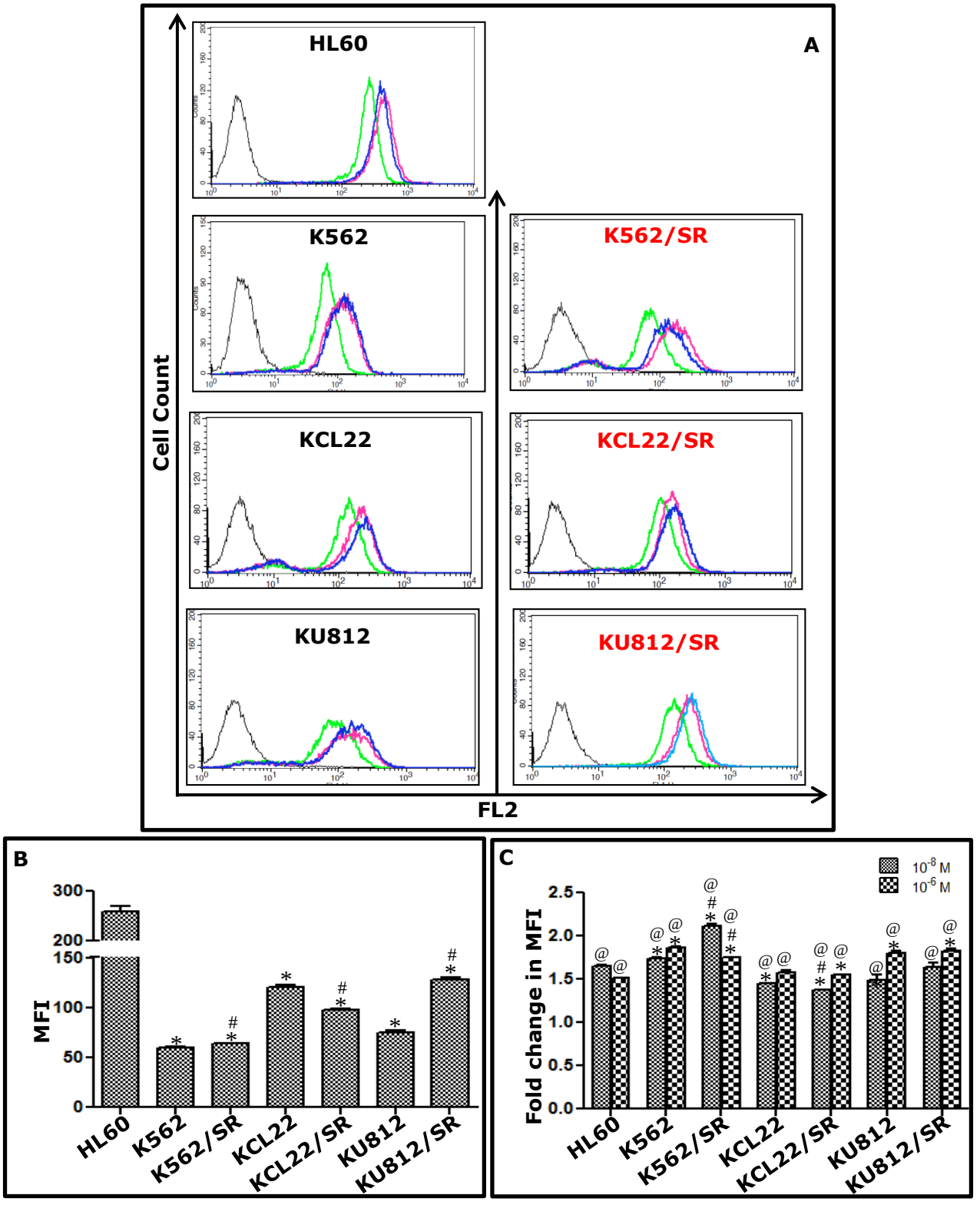

Fig-RC 12: F-actin Quantitation by Flow Cytometry: F-actin quantitation in CML cell lines and HL-60 by flow cytometry (A) Representative histogram overlays of FITC-phalloidin intensity in unstimulated and fMLP stimulated cells. In each plot black solid line represents unstained isotype control, green line represents unstimulated control and cells stimulated with 10^{-8}M and 10^{-6}M fMLP are represented by pink line and blue line, respectively (B) Bar plot showing basal F-actin expressed as average MFI ± SEM of FITC-phalloidin stained various cell lines (n=3). (C) Bar plot showing change in F-actin content after fMLP (10^{-6}M and 10^{-8}M) stimulation as a fold change in the median fluorescence intensity ± SEM (n=3) * $p<0.05$ wrt HL60, # $p<0.05$ wrt the respective sensitive cell line (Mann-Whitney test). @ $p<0.1$ wrt the basal F-actin level (Wilcoxon paired test)

event in changes in the cytoskeletal organization is the polymerization of cytoplasmic G-actin to F-actin, which forms the motile apparatus of the cells. Earlier work from our laboratory has shown that PMNL from CML patients in active phase of the disease and also during subsequent remission do not exhibit chemotaxis after stimulation with the synthetic chemotactic peptide fMLP[80, 83]. F-actin plays a force-generating and structural role in nonmuscle cell motility[197-199]. Many chemoattractants such as fMLP and TPA are known to stimulate polymerization of actin in PMNL[200, 201]. Polymerization of actin stimulated by chemoattractants involved, an immediate phase of polymerization lasting few seconds followed by depolymerisation[197, 202-204]. The F-actin present in the cells gets reorganized after stimulation[197, 203, 205, 206]. Most of the F-actin gets concentrated in the peripheral region, especially in the lamellipodium and uropods. Existence of two subpopulations among the normal PMNL cells on the basis of NBD-ph binding has been shown by Downey et al.[207]. Factors such as type of chemoattractant used, actin binding proteins, pH, osmolarity, and level of chemo-attractant receptor occupancy are known to modulate the rate and extent of polymerization of actin and F-actin organization[206]. Hsu and Becker attributed abnormal gelation and contraction of extracts of PMNL from CML patients, to the absence of CaZ+-dependent regulatory factor[208]. Boxer and Stossel observed that PMNL from CML patients had less myosin, which was different from normal myosin[209]. A polymerization inhibiting protein has been reported in leukemic myeloblasts[210]. Changes in actin related gelation in crude extracts from myeloid leukemic cell line M1 have also been observed[211]. Earlier studies from our group had shown defective actin polymerization in PMNL from CML patients[86]. CML PMNL showed lower actin polymerization in upon fMLP

stimulation. An impairment of PMNL locomotion and ingestion has been shown to be associated with abnormally functioning actin[198, 212] and it has been postulated that actin dysfunction might be responsible for aberrant PMNL movements. From studies on F-actin content in neonates and adults it was suggested that abnormalities in microfilament organization of neonatal cells may in part, be responsible for their reduced chemotactic response[212]. In both these reports[198, 212] the basal F-actin content in PMNL from the patients and neonates was comparable to that of normal cells but the rate and extent of polymerization into F-actin after stimulation was lower than in normal PMNL. Naik et al. reported that, normal PMNL showed the increase of 1.14 fold with respect to its basal level, upon 10^{-8} M fMLP stimulation at 5 min while the decrease in F-actin content was seen in CML PMNL at similar time point after fMLP stimulation[85]. The highest increase in F-actin in normal PMNL and CML PMNL was recorded at 30s post fMLP stimulation. At 30s of fMLP stimulation normal PMNL showed 1.24 fold increase in F-actin whereas CML PMNL showed 1.14 fold than basal level[85]. In the present experiment, bcr-abl negative cell line showed increase of 1.6 fold to its basal level, in F-actin content upon stimulation with similar concentration of fMLP for 5 min, while fold increase in F-actin in bcr-abl positive cell lines in the said conditions ranged from 1.4-2.1 fold. Various studies published from our group have shown defects in F-actin polymerization in CML PMNL upon chemoattractant stimulation. Anklesaria et al. and Naik et al. showed that CML PMNL were defective in chemotaxis towards fMLP during active phases as well as in remission phase of the disease[79, 83]. Naik et al. showed that CML PMNL showed slow as well as lesser actin polymerization[85]. Furthermore, CML PMNL showed different F-actin organization than that in normal PMNL. Tarachandani et al.

showed that amount of actin was significantly lower in CML PMNL[88]. In the present results too, CML cell lines showed lowered basal F-actin than that in non-CML cell line HL60. Actin polymerization upon fMLP stimulation did not match with the reported results of CML and normal PMNL. As seen earlier, HL60 did not behave like normal PMNL probably due to its leukemic origin. In context of F-actin polymerization also, HL60 showed different behavior. Moreover, CML cell lines have more undifferentiated cells than CML PMNL. HL60 showed decrease in the extent of stimulation of actin polymerization in response to increasing concentration of fMLP. In contrast, except K562/SR, all the CML cell lines showed concentration dependent increase in the actin polymerization. At 10 nM fMLP stimulation HL60 showed higher F-actin polymerization than that in imatinib sensitive and resistant KCL22 and KU812 cell line while imatinib resistant and sensitive cell line of K562 showed higher F-actin polymerization than HL60. At 1 μM fMLP stimulation CML cell lines showed higher F-actin polymerization than that in HL60. In past, various group have already reported the defects in actin polymerization in HL60 upon fMLP stimulation. Marinovich et al. showed very little actin polymerization in undifferentiated HL60 upon fMLP stimulation[213]. Meyer et al., Rao et al., and Cui et al. showed no actin polymerization in HL60 upon fMLP stimulation[214-216]. These reports confirmed that undifferentiated HL60 showed little or no F-actin polymerization. Hence, HL-60 is not a good control cell line for actin polymerization studies. However, among CML cell lines results could be compared between b2a2 and b3a2 expressing cell lines as well as imatinib sensitive verses imatinib resistance cell lines. The lowest increase in F-actin upon fMLP stimulation was seen in b2a2 expressing cell line. Also, At 10^{-8} M fMLP stimulation, imatinib resistant cell lines

of b3a2 fusion transcript showed a lesser increase in F-actin content than their respective S cell lines while difference was not observed between b2a2 expressing, S and SR cell line. From these observations, it could be said that bcr-abl fusion transcript type might be affecting the signalling downstream FPR.

Effect of bcr-abl Tyr-Kinase Inhibitor (TKI) on FPR Expression

Imatinib is a bcr-abl TKI and is used as the first line of treatment for CML. It was observed that imatinib sensitive and resistant cell lines differ in the FPR expression. Since, these cell lines were maintained under continuous selection medium containing imatinib, differences found between imatinib resistant and sensitive cell lines could be the effect of imatinib treatment instead of imatinib resistance. Studies were carried out to confirm that the changes in the FPR expression in the imatinib resistant cell lines were not due to imatinib treatment, but were result of imatinib resistance. Imatinib sensitive, bcr-abl positive cell line K562 was treated with imatinib and expression of FPR & bcr-abl genes were checked. Bcr-abl negative cell line, HL60 was used to confirm, that the effect of imatinib is a result of bcr-abl tyrosine kinase inhibition and is not due to any other side effect. In addition to imatinib, two more bcr-abl TKI –dasatinib and nilotinib, were used to further confirm the specificity of imatinib resistance effect. Less than 50% change in the gene expression was not considered.

Imatinib

Upon imatinib treatment, significant increase in the expression of all the three FPR and bcr-abl was observed in K562 wherein FPR1 increase was the maximum (Fig-RC 13A; Table-RC 13). In HL60, upon treatment with imatinib, noteworthy

changes were not observed in any of the tested gene (Fig-RC 13B). K562/SR and K562 cell lines did not show any differences in FPR1 gene expression whereas significantly higher expression of FPR2 and FPR3 genes was observed in K562/SR as compared to K562. Similarly FPR2 and FPR3 expression is higher in other SR cell lines i.e. KU812/SR and KCl22/SR as compared to KU812 and KCL22, respectively. This suggests association between increased FPR2 and FPR3 with imatinib resistance.

Dasatinib

Dasatinib is a second generation bcr-abl TKI and can be used as the first line therapy for bcr-abl positive CML. Treatment of dasatinib did not show noteworthy effect on expression of any genes tested, in both the cell lines (Fig-RC 13A & 13B;Table-RC 13).

Nilotinib

Nilotinib is also a bcr-abl TKI and it is used for the treatment of imatinib resistant bcr-abl positive CML. Nilotinib treatment did not exerts any effect on expression of the genes tested, in both the cell lines (Fig-RC 13A & 13B; Table-RC 13).

Table-RC13: Effect of bcr-abl tyrosine kinase inhibitor on gene expression

Treatment Gene	Fold Change in Expression											
	Imatinib				Dasatinib				Nilotinib			
	FPR1	FPR2	FPR3	Bcr-abl	FPR1	FPR2	FPR2	Bcr-abl	FPR1	FPR2	FPR2	Bcr-abl
K562	14.9 ± 5.8	2.5 ± 0.16	1.7 ± 0.42	1.8 ± 0.03	1.0 ± 0.05	1.0 ± 0.03	0.7 ± 0.06	1.0 ± 0.05	1.2 ± 0.04	1.1 ± 0.08	1.1 ± 0.06	1.04 ± 0.02
HL60	1.1 ± 0.03	0.9 ± 0.01	0.9 ± 0.09	N.A.	1.3 ± 0.06	1.0 ± 0.03	1.5 ± 0.05	N.A.	1.0 ± 0.1	0.8 ± 0.03	0.8 ± 0.01	N.A.
All the values are average ± SEM (n=3)												

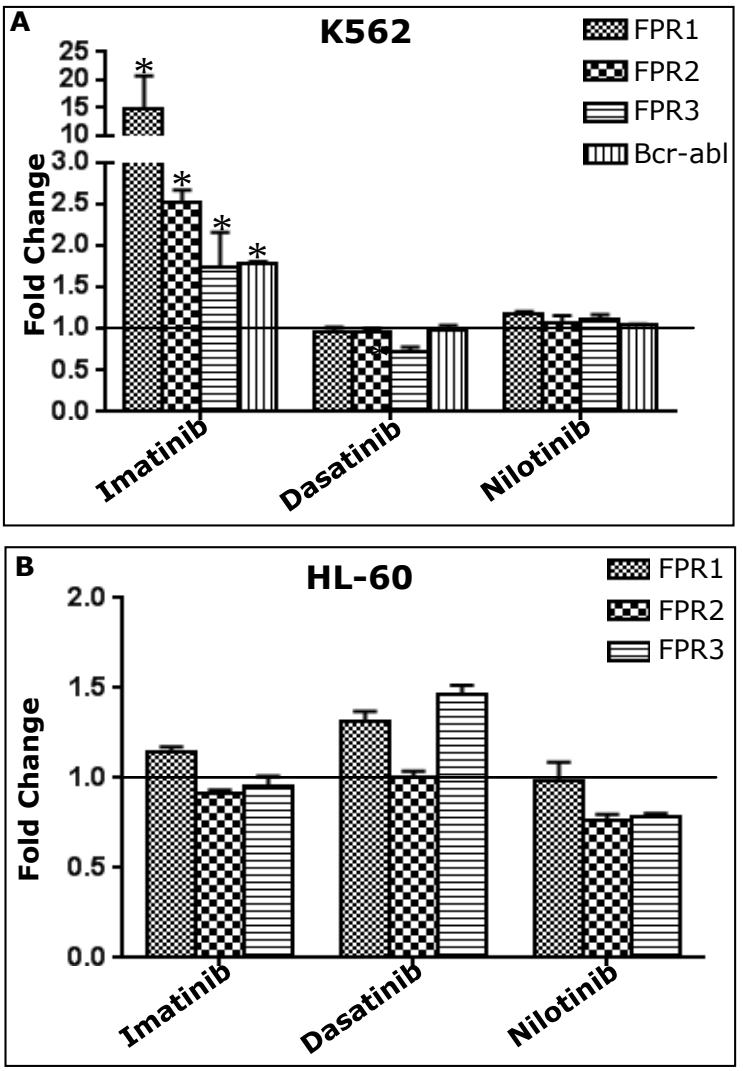

Fig-RC 13: **Effect of bcr-abl Tyrosine Kinase Inhibitors on Expression of Various Genes:** Effect of bcr-abl tyrosine kinase inhibitors on expression of FPR1, FPR2, FPR3 and bcr-abl genes in K562 (A) and HL60 (B). Data presented as average fold change ± SEM (n=3). * $p<0.05$ wrt the untreated cells (Willcoxon paired test).

Above results suggested that changes in the expression of FPR1 gene upon imatinib treatment were imatinib specific effect on the bcr-abl positive cells. This was not due to inhibition of expression of bcr-abl tyrosine kinase because other bcr-abl TKI did not show this effect. Similar changes were not seen in the bcr-abl negative cell line -HL60, hence this effect was specific to bcr-abl positive cell line. Since this this type of differences in the expression of FPR1 was not observed between K562 and K562/SR cell lines, it could be said that this might be the effect of transient treatment of imatinib. Imatinib, though preferentially inhibits abl kinase of bcr-abl, it also have many off targets. Most prominent off-targets for imatinib were c-kit, PDGFR and NAD(P)H:quinone oxidoreductase (NQO2)[217]. There could be possibility that inhibition of any of these proteins could result into increase in mFPR1 expression. Since there were no increase in mFPR1 in K562/SR than K562, it might be possible that imatinib resistant cell other mechanisms might be preventing imatinib induced increase of mFPR1. Changes in the expression of FPR2 and FPR3 genes in K562 after imatinib treatment, were similar to the differences between the SR and S cell lines. Hence, it could be suggested that changes in expression of these two genes might be associated with the acquisition of imatinib resistance. Furthermore, changes in these two genes after imatinib treatment were specific to imatinib treatment of the bcr-abl positive cell line as such changes were not observed after treatment with any other bcr-abl TKI and not observed in HL60. Increase in the expression of bcr-abl gene upon imatinib treatment and lower expression of bcr-abl gene expression in SR cell line compared to S cell line, demonstrated that increase in the bcr-abl gene expression might be the effect of transient imatinib treatment, while lower expression of bcr-abl in K562/SR, could be

imatinib resistance specific effect. However, none of these effects could be considered as the result of bcr-abl tyrosine kinase inhibitors, in general because other bcr-abl TKI did not show any such effect.

Effect of bcr-abl Tyr-Kinase Inhibitor, FPR1 Agonist and FPR1 Antagonist on Imatinib Resistant Cell Proliferation

Imatinib is a very potent inhibitor of CML cell proliferation, but some CML cells acquire the resistance to imatinib. All the three SR cell lines showed differences in expression of FPR genes and protein as compared to their respective S cell lines, indicating that FPR expression might be affected by imatinib resistance. To study role of FPR in imatinib resistance, impact of imatinib on the growth of imatinib resistant cell lines was checked by coupling stimulation or inhibition of FPR signaling with imatinib treatment. All the three imatinib resistant cell lines K562/SR, KU812/SR, KCL22/SR were treated with imatinib, FPR1 agonist –fMLP and a specific inhibitor of FPR1[218] –cyclosporine H (CsH) and their combinations. Since, bcr-abl protein has half-life of 48 hrs, the cell growth was checked at 24 hrs, 48 hrs and 72 hrs.

In K562/SR, which has highest expression of all the three FPR receptors, growth inhibition was seen after treatment with all –fMLP, CsH and imatinib and inhibitory effect of all these treatment was almost at par (Fig-RC 14A; Table-RC 14). Treatment with the combination of fMLP-imatinib and CsH-imatinib showed more growth inhibition than that seen after individual treatments. The inhibitory effect of the CsH-imatinib combination was maximum and almost double than the individual anti-proliferative effect of both.

Table-RC 14: Effect of FPR and bcr-abl on cell proliferation

		% Growth Inhibition				
		fMLP	CsH	Imatinib	fMLP + Imatinib	CsH + Imatinib
K562/SR	24 Hrs	14.1 ± 2.4	18.5 ± 1.9	19.9 ± 3.4	28.5 ± 3.4	38.1 ± 4.1
	48 Hrs	19.6 ± 1.4	20.0 ± 3.3	25.3 ± 1.2	36.4 ± 2.1	44.7 ± 2.9
	72 Hrs	16.1 ± 1.2	27.4 ± 2.3	24.9 ± 1.6	27.2 ± 2.6	47.7 ± 2.4
KU812/SR	24 Hrs	-0.6 ± 3.3	12.1 ± 5.3	8.4 ± 2.9	-5.2 ± 4.0	11.7 ± 7.7
	48 Hrs	-5.4 ± 3.8	7.8 ± 5.0	19.7 ± 1.8	14.7 ± 2.4	34.9 ± 3.0
	72 Hrs	4.8 ± 1.0	29.3 ± 4.0	28.0 ± 1.6	20.4 ± 2.2	39.3 ± 7.1
KCL22/SR	24 Hrs	4.8 ± 2.8	18.6 ± 3.5	16.7 ± 1.9	-3.2 ± 3.6	30.6 ± 3.3
	48 Hrs	11.2 ± 2.0	21.7 ± 5.1	31.1 ± 2.5	35.5 ± 2.6	43.5 ± 3.1
	72 Hrs	2.8 ± 1.4	25.9 ± 1.9	25.2 ± 1.1	26.8 ± 2.5	35.9 ± 2.5
All the values are average ± SEM (n=3)						

In KU812/SR, which had the lowest expression of all the three FPR receptors growth inhibitory effect of fMLP was not seen at any of the time points and same was true for CsH at 48 hrs (Fig-RC 14B; Table-RC 9). CsH treatment showed cellular growth inhibition at 72 hrs as much as that shown by imatinib at the same time point. Combination of fMLP-imatinib showed slightly lower growth inhibitory effect than the effect of imatinib alone. However CsH-imatinib combination which shuts down signalling of FPR1 and bcr-abl both, appeared to be more lethal and effective than their individual treatments.

In KCL22/SR, fMLP had no effect on cell growth (Fig-RC 14C; Table-RC 9). Cell growth inhibition by CsH and imatinib was at par. Combination of fMLP-imatinib

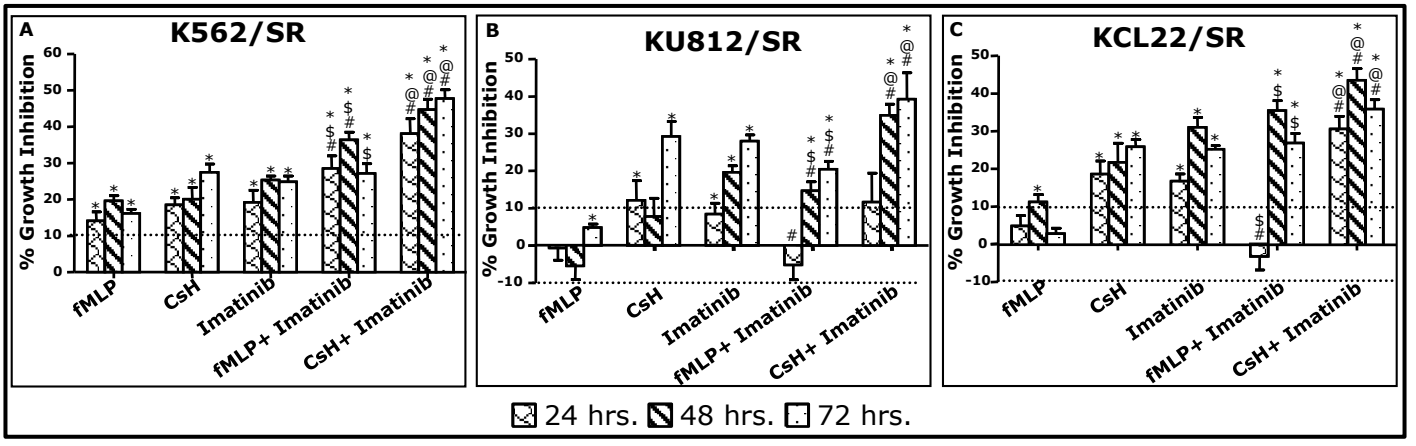

Fig-RC 14: Effect of FPR and bcr-abl Signalling on Cell Proliferation: Effect of FPR agonist – fMLP, FPR antagonist –CsH, bcr-abl tyrosine kinase inhibitor –imatinib and their combinations on proliferation of imatinib resistant cell lines -K562/SR (A), KCL22/SR (B), and KU812/SR (C). Data presented as average % growth inhibition ± SEM. * $p<0.05$ wrt the solvent control, $ $p<0.05$ wrt to fMLP, @ $p<0.05$ wrt to CsH, # $p<0.05$ wrt to imatinib (Willcoxon paired test).

did not show any effect on cell growth at 24 hrs. Since, imatinib alone, had shown inhibition of growth at this time point, it could be said that fMLP nullified the effect of imatinib at 24 hrs time point. At 48 & 72 hrs inhibitory effect of fMLP-imatinib was same as that of imatinib treatment. In this cell line too, CsH almost doubled the effect of imatinib at 24 hrs and 41% and 44% higher than imatinib treatment at 48 hrs and 72 hrs, respectively.

Thus effect of FPR stimulation by fMLP, alone or in combination with imatinib, was cell line specific. Inhibition of FPR1 signaling by CsH had an additive effect on the growth inhibitory effect of imatinib in imatinib resistant cell lines.

To summarize, the above presented results showed that there was decrease in the expression of FPR in bcr-abl positive cells, though there was inverse relationship between the expression of FPR and expression of bcr-abl gene and protein. On the basis of CD markers expression data, it could be said that bcr-abl positive cell lines were less differentiated than bcr-abl negative cell lines. HL60 did not behave like normal PMNL in some experiments for example expression of mFPR3 was lower in HL60 than bcr-abl positive cell lines while normal PMNL expressed higher mFPR3 than CML PMNL. Despite higher sFPR expression, HL60 showed decreased FPR ligand binding while normal PMNL were reported to have higher ligand binding than CML PMNL[87]. Similarly, increase in the Ca^{2+} level, upon fMLP stimulation was at par in bcr-abl positive and negative cell lines except for KCL22, while normal PMNL showed more increase in Ca^{2+} than that in CML PMNL[194]. This could be because of two reasons; one is its oncogenic origin and second its differentiation status with respect to normal PMNL. Being promyelocytic, HL-60 is less differentiated than the PMNL.

Among bcr-abl positive cell lines, as mentioned there were two groups on the basis of expression of bcr-abl fusion transcript. K562 and KU812 expressed b3a2 fusion transcript whereas KCL22 expressed b2a2 fusion transcript. Their expression pattern should represent the effect of the presence of a particular fusion transcript. KCL22, the b2a2 fusion transcript expressing cell line, turned out to be different then b3a2 expressing cell lines. It was negative for the presence of CD34, CD38 and had the least expression of CD117. Among FPRs, it had the least expression of mFPR3. It also expressed the least amount of bcr-abl protein. It contained the highest basal actin among bcr-abl positive, imatinib sensitive cell lines and it showed the highest increase in the Ca^{2+} level upon fMLP stimulation. B3a2 fusion transcript expressing cell lines did not show similarities with respect to all the parameters. It could be explained by the fact that both the cell lines expressing b3a2 fusion transcript were of different hematopoietic lineages. K562 was pluripotent cell line that could be differentiated into erythrocytic and granulocytic while KU812 could be differentiated into basophilic and erythroide lineage[105, 108]. Furthermore, K562 was developed from bone marrow of an untreated patient, whereas KU812 was developed from peripheral blood of a patient who was treated with busulfan for 10 years as well as various combinations of chemotherapy for extramedullary spinal tumor. Hence K562 would be a better indicator for b3a2 specific effect on basal gene expression, than KU812. It was evident from the results that K562, expressed the highest mFPR and sFPR1 among all the bcr-abl positive, imatinib sensitive cell lines. It also expressed the highest percentage of the cells co-expressing the sFPRs. K562 also expressed the highest percentage of cells positive for CD34, CD38 and CD117 among all the bcr-abl positive, imatinib sensitive cell lines. On the other

hand KU812 was more similar to KCL22 than K562. Hence it could be concluded that presence of specific type of bcr-abl fusion transcripts have different effect on expression of various gene and it also affects behavior of CML cell lines.

Comparison between pairs of imatinib resistant and sensitive cell lines, showed that change in expression pattern of CD34, bcr-abl protein, percent of cells co-expressing sFPR1 & sFPR2, sFPR1 & sFPR3 and sFPR1, sFPR2 & sFPR3 were similar for all the three pairs of S and SR. SR cell line of b2a2 fusion transcript expressing cell line, showed increase in the expression of all the three mFPR, sFPR, bcr-abl protein, CD34, CD38 and CD117 compared to S cell line. Similar to the trend of imatinib sensitive cell lines, changes between SR and S cell lines expressing b3a2 expressing imatinib were cell line dependent.

To understand the mechanism behind the imatinib resistance, the imatinib sensitive cell line was treated with imatinib and gene expression of FPR1, FPR2, FPR3, and bcr-abl was checked. It was concluded that in K562, expression of FPR2 and FPR3 gene might play role in imatinib resistance. Furthermore, when imatinib resistant cell lines were treated with combination with imatinib and FPR1 antagonist –CsH, it was found that CsH doubled the growth inhibitory effect of imatinib. In short, FPR expression showed an inverse relationship with bcr-abl mRNA expression. FPR expression was very well associated with the increased expression of stemness and imatinib resistance. Hence, it could be suggested that FPR might play role in imatinib resistance of stem like CML cells.

Breast Cancer

Earlier, expression of FPR was thought to be restricted to hematopoietic cells involved in the first line of immunity. However, over the past years, data from several groups have reported their expression in many cell types other than hematopoietic cells, such as mesenchymal stem cells (MSCs)[20], dendritic cells[219], astrocytes[220], hepatocytes[21]. However, their biological significance in these cell types is not well understood. To understand the role of FPR in solid tumors, breast cancer was chosen as a system. Breast cancer is the most common cancer in women worldwide. It accounts for 22.9% of all the cancers in women.

It is also the principle cause of death from cancer among women globally. In U.S., Breast cancer affects 1 in eight women during their lives[221]. In India, breast cancer incidence rate ranges from 6.2 - 39.5 females per 100,000[222]. Countrywide, relative proportion of breast cancer (incidence of breast cancer/total number of cancer registries) in female varied from 14.4% in Guwahati to 30.3% in Mumbai.

Classification of the cell lines based on their properties

As already mentioned, use of various cell lines is well accepted as models in preliminary clinical application oriented studies. Conclusions drawn based on studies using more than one cell lines are more likely to resemble in vivo conditions than those based on the use of a single cell line. Therefore, to study role of FPR in breast cancer, a panel of human breast cancer cell lines (HBCC) along with one non-cancerous cell line of breast epithelial origin as a control, was chosen. Properties of the selected cell lines are tabulated in Table-RB 1. Cell lines were selected based on their growth rate, hormone receptor status, and tumorigenicity.

Table-RB 1: Properties of the selected cell lines

Characters	MCF-10A	MCF-7	MDA-MB-231	MDA-MB-468	T47D
Cancerous	No	Yes	Yes	Yes	Yes
Cell growth rate	Slow -	Fast	Fast	Slow	Slow
Hormone receptors –ER-PR	negative	positive	negative	negative	positive
Her2	Low	Low	Negative	Negative	Negative
Cancer subtype	Not applicable	Adenocarcinoma	Adenocarcinoma	Adenocarcinoma	Infiltrating ductal carcinoma
Racial Origin	Unknown	Caucasian	Caucasian	Black	Unknown
p53	Wild Type	Wild Type	R280K Mutation[223]	R273H Mutation[224]	F194F Mutation[224]
Ploidy	Near Diploid	Hypertriploid to hypertetraploid	Aneuploid	Aneuploid	Hypertriploid
Tumorigenicity	Non tumorigenic	Tumorigenic, but with hormonal supplement	Tumorigenic	Tumorigenic	Tumorigenic

Basal expression of FPR in HBCC

To start with, basal expression of the FPR (mFPR as well as sFPR) was studied in all the HBCC and the expression was then compared to the respective expression in the normal breast epithelial cell line –MCF-10A.

Gene expression

Expression of mFPR1 was significantly higher in normal breast epithelial cell line MCF-10A than that in all the HBCC (Fig-RB 1A, Table-RB 1).

Table-RB 1: Basal Expression of FPR Genes

Fold Change					
	MCF-10A	**MCF-7**	**MDA-MB-231**	**MDA-MB-468**	**T47D**
mFPR1*	1.00 ± 0.00	0.12 ± 0.01	0.26 ± 0.01	0.12 ± 0.004	0.07 ± 0.002
mFPR2*	1.00 ± 0.00	4.16 ± 0.28	2.16 ± 0.10	4.75 ± 0.09	2.76 ± 0.09
mFPR2$	0.02 ± 0.00	0.68 ± 0.05	0.15 ± 0.01	0.64 ± 0.04	0.68 ± 0.04
mFPR3*	1.00 ± 0.00	6.70 ± 0.28	2.59 ± 0.17	6.03 ± 0.16	4.42 ± 0.26
mFPR3$	0.01 ± 0.0003	0.28 ± 0.02	0.05 ± 0.002	0.22 ± 0.02	0.30 ± 0.02
Fold change calculated - * with respect to MCF-10A, $ with respect to FPR1					

Among the HBCC, expression of mFPR1 was the highest in the triple negative cell line MDA-MB-231. MCF-7, MDA-MB-468, and T47D showed similar expression of FPR1. Unlike mFPR1, mFPR2 expression was higher in HBCC than that in MCF-10A (Fig-RB 1B, Table-RB 1). Furthermore, among HBCC the least mFPR2 was expressed by MDA-MB-231, which expressed the highest mFPR1 among HBCC. Expression of mFPR2 was at par in MCF-7 and MDA-MB-468 and was the highest among all the cell lines. Expression pattern of mFPR3 was similar to the mFPR2 expression pattern. Expression of mFPR3 was also higher in HBCC than that in MCF-10A (Fig-RB 1C, Table-RB 1). Among HBCC, lowest mFPR3 expression was in MDA-MB-231. This was similar to mFPR2 expression, but in contrast of mFPR1 expression. The highest mFPR3 was seen in MCF-7 and

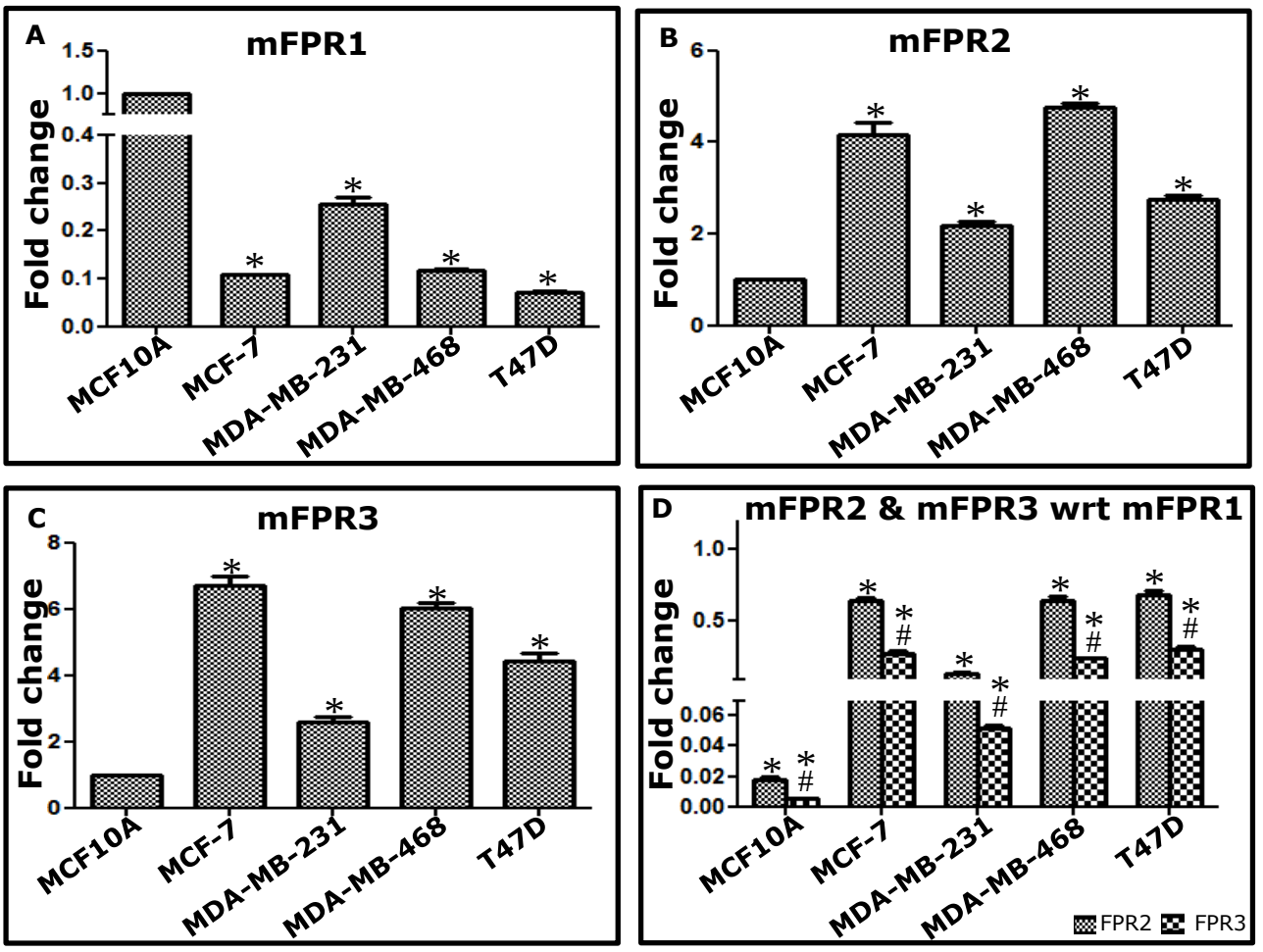

Fig-RB 1: Expression of FPR Genes in HBCC: Expression of mFPR1 (A), mFPR2 (B) and mFPR3 (C) in various HBCC with respect to normal breast epithelial cell line MCF-10A and (D) expression of mFPR2 and mFPR3 with respect to mFPR1 as estimated by QPCR. Gene expressions were normalized using expression of housekeeping gene GAPDH. Data is presented as average fold change ± SEM (n=3). For fig A, B and C statistically significant changes is marked as; * $p<0.05$ wrt MCF-10A (Mann-Whitney test) and for fig D * $p<0.05$ wrt FPR1 # $p<0.05$ wrt FPR2 (Mann-Whitney test).

MDA-MB-468 followed by T47D. Comparative expression of all the three receptors showed that mFPR1 was the highest expressed receptor in all the cell lines followed by mFPR2 and mFPR3 (Fig-RB 1D, Table-RB 1). However, expression of mFPR2 and mFPR3 was negligible as compared to mFPR1 in MCF-10A whereas the comparative expression of mFPR2 and mFPR3 was higher and reached 0.2-0.5 fold of mFPR1 in all the HBCC except MDA-MB-231. mFPR2 and mFPR3 expression in MDA-MB-231 was 0.15 and 0.05 fold of its mFPR1 expression, respectively. These results of mFPR expression have shown that expression of mFPR1 was decreased while mFPR2 & mFPR3 expression was increased in HBCC than that in normal breast cell line MCF-10A. Based on these expressions, cell lines and genes were clustered (Fig-RB 2A). The dendrogram for the genes branches into two clusters, namely, cluster-I and cluster-II. Cluster-I included only one gene mFPR1, while mFPR2 and mFPR3 fall into cluster-II. Cell line dendrogram also branched into two clusters at the first level. This cluster analysis showed that expression pattern of mFPR1, mFPR2 and mFPR3 was similar in the members of the cluster. Based on similarity in expression pattern of all the three mFPR, at level I, MCF-7 & MDA-MB-468 formed one group and MDA-MB-231 & T47D formed another group. MCF-10A, as expected did not show similarity in mFPR expression pattern with any of the HBCC. However, at the level II, it was clustered with MDA-MB-231 & T47D, probably because of its lower expression of mFPR2 and mFPR3.

Protein

To see whether the differences in the gene expression of FPRs were translated into protein expression, all the cell lines were flow cytometrically analyzed for

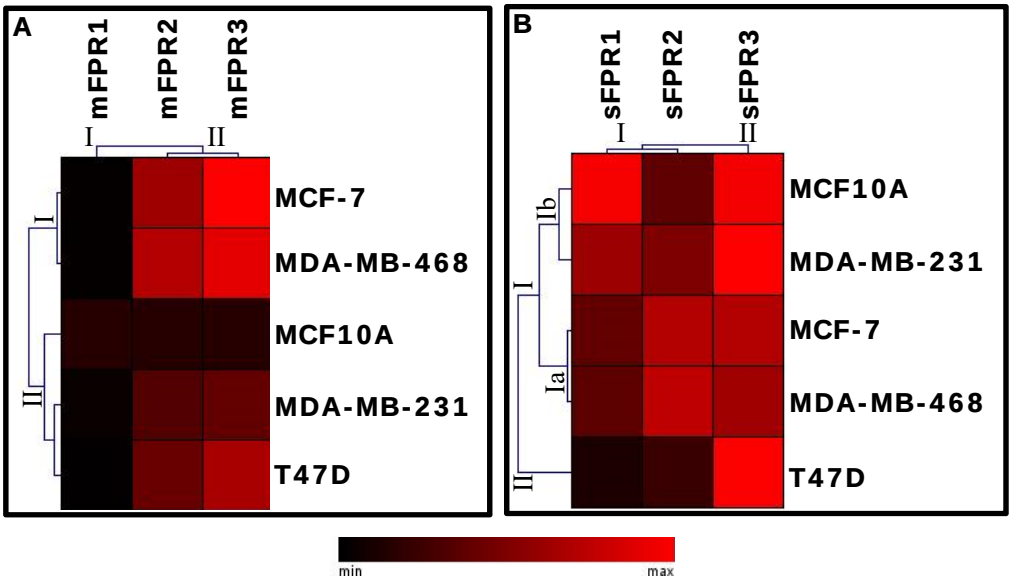

Fig-RB 2: Clustering of Expression of FPR: Two way hierarchical cluster of gene expression data (A) and surface protein expression data (B), using average linkage clustering and default distance setting using Genesis software.

expression of sFPR, using labelled antibodies as described in materials and methods.

All the cell lines showed presence of all the three FPR on surface (Fig-RB 3).

Table-RB 2: Expression of sFPR

Cell Lines		MCF-10A	MCF-7	MDA-MB-231	MDA-MB-468	T47D
FPR1	Median	17.9 ± 0.7	7.7 ± 1.3	12.0 ± 0.1	6.1 ± 0.3	6.6 ± 1.1
	% Positivity	94.3 ± 0.5	37.6 ± 3.4	60.0 ± 1.0	35.2 ± 1.5	11.0 ± 0.8
FPR2	Median	6.8 ± 0.3	10.8 ± 0.4	12.1 ± 0.3	8.9 ± 0.6	7.9 ± 0.1
	% Positivity	36.9 ± 2.1	68.6 ± 3.7	48.4 ± 2.3	72.9 ± 5.7	22.1 ± 1.6
FPR3	Median	22.5 ± 0.6	18.8 ± 3.0	28.1 ± 0.2	11.1 ± 0.8	19.7 ± 1.4
	% Positivity	93.4 ± 1.0	68.3 ± 12.2	97.2 ± 0.3	61.1 ± 10.4	96.7 ± 0.9

Similar to mFPR1 expression, sFPR1 expression was highest in MCF10A (Fig-RB 4A, Table-RB 2). Almost all the cells (about 95%) of MCF-10A showed expression of FPR1. Among the HBCC, the highest % positivity for sFPR1 i.e. % of cells expressing sFPR1 was seen in MDA-MB-231, followed by MCF-7 and MDA-MB-468, which were at par. T47D showed the lowest % positivity for sFPR1. Results of sFPR2 did not follow the pattern of mFPR2 expression. In all the HBCC except T47D, % positivity for sFPR2 was significantly higher than MCF-10A (Fig-RB 4B, Table-RB 2). About 70% cells of the MDA-MB-468 and MCF-7 were positive for sFPR2, which were the highest among all the cell lines. These were followed by MDA-MB-231, which showed 48% cell positivity for the sFPR2. T47D showed the least % positivity for the sFPR2 too. Distinct expression pattern was not observed in the MFI of MCF10A and HBCC. Results of sFPR3 expression were completely different from mFPR3 expression results. Distinct differentiating pattern between expression of sFPR in HBCC and normal breast epithelial cell line was not observed. % positivity for sFPR3 in MCF-10A was at

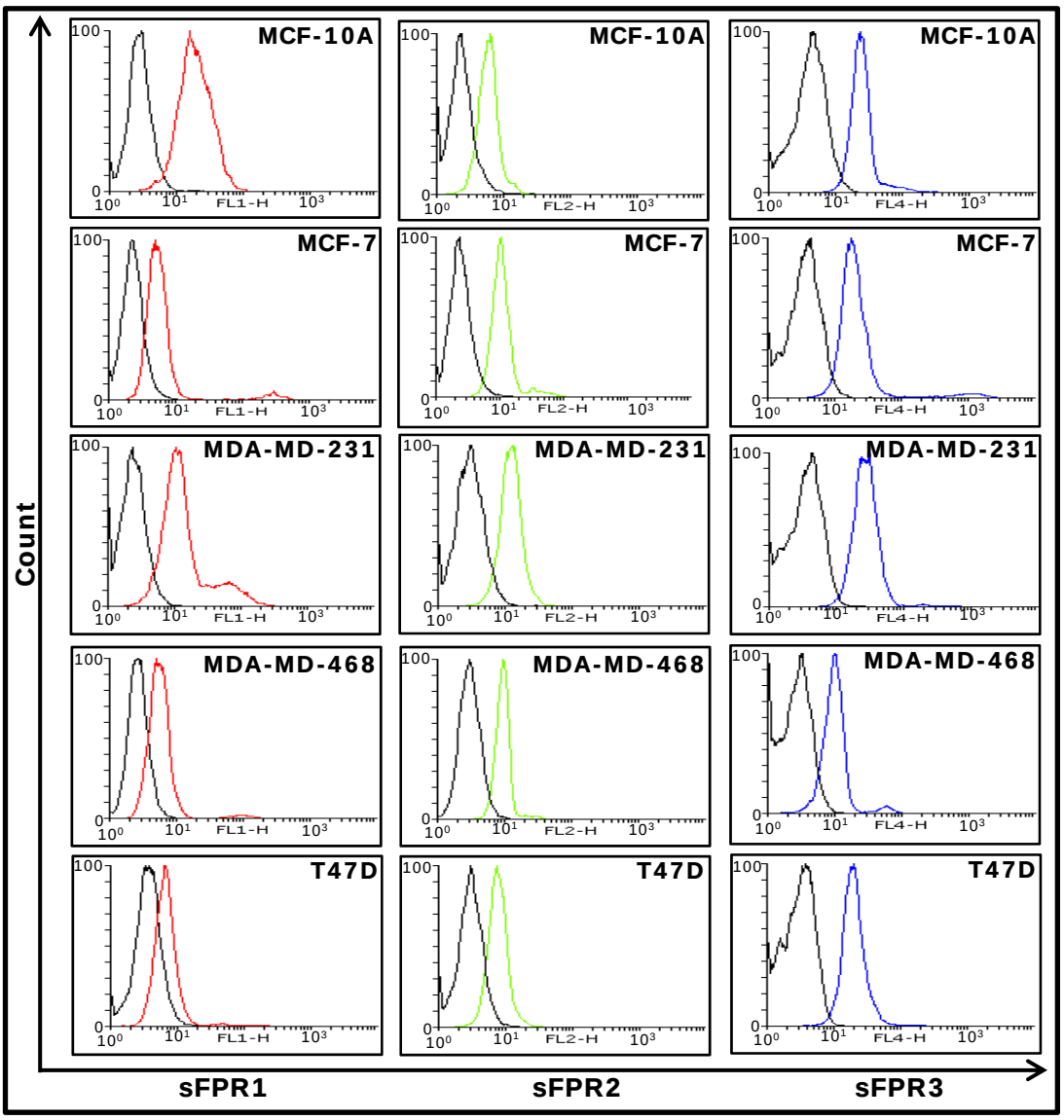

Fig-RB 3: Expression of sFPR in HBCC: Representative histogram overlays showing surface expression of sFPR1, sFPR2 and sFPR3 in HBCC and MCF-10A as indicated. In each overlay plot, black solid line indicates unstained isotype control while colored lines indicate cells stained for sFPR1 (red), sFPR2 (green), and sFPR3 (blue)

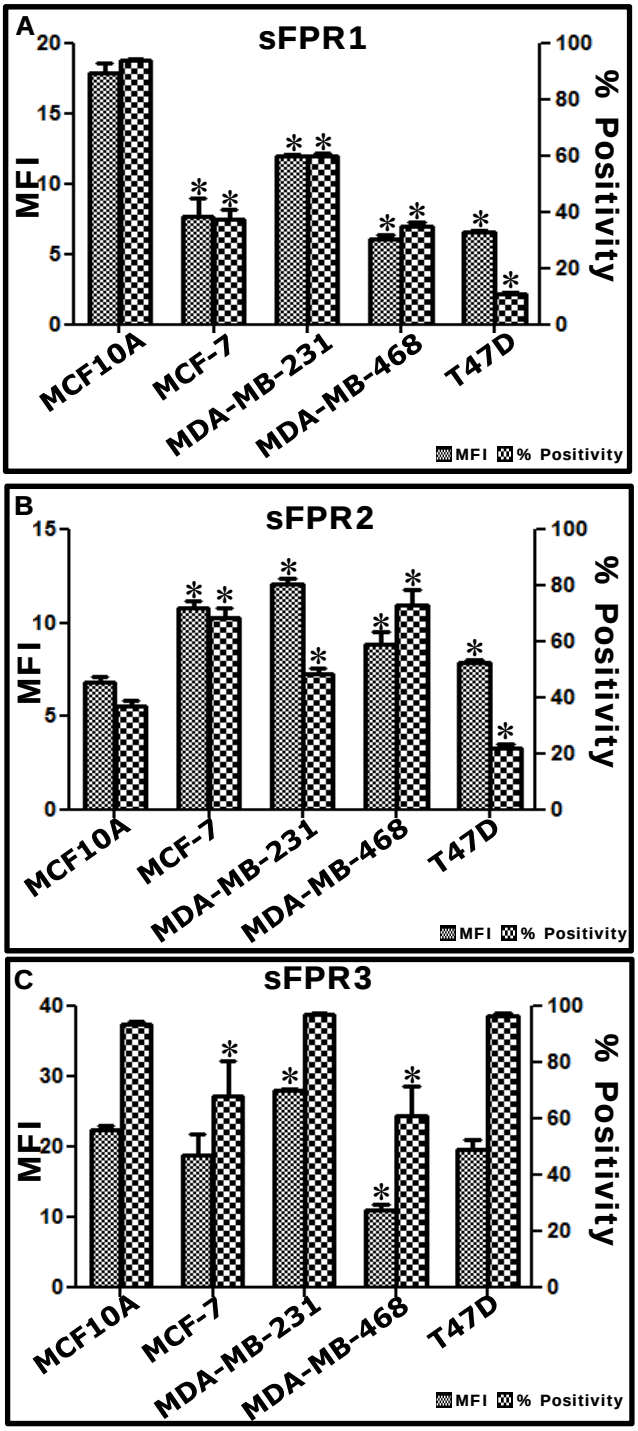

Fig-RB 4: Expression of sFPR in HBCC: Expression of sFPR1 (A), sFPR2 (B) and sFPR3 (C) proteins in HBCC and MCF-10A as indicated. Data presented as Average (% positivity & MFI as indicated) ± SEM (n=3).* $p<0.05$ wrt MCF-10A (Mann-Whitney test).

par with MDA-MB-231 and T47D (Fig-RB 4C, Table-RB 2). They showed more than 90% cellular positivity. MCF-7 and MDA-MB-468 were at par and showed 68% and 61% positivity for sFPR3, respectively. Opposite to % positivity, MFI for sFPR2 in MDA-MB-231 was higher than that in MCF-10A. MFI for sFPR2 in MCF-10A was at par with sFPR2 MFI in MCF-7 and T47D. It is clear from this data that similar to mFPR expression, reduction in % positivity for sFPR1 and increase in % positivity for sFPR2 was observed in the HBCC. In other words, pattern of mFPR was not translated to sFPR.

This data was also subjected to two-way, unsupervised hierarchical clustering. Similar to gene expression clustering, protein expression dendrogram also branched into two main clusters. But in proteins, cluster-I grouped sFPR1 and sFPR2 (Fig-RB 2C). Due to the distinct expression pattern, sFPR3 was a single protein cluster –cluster-II. At the top of the hierarchy, the cell line dendrogram branched into two clusters (labelled I, and II). Cluster-I was further branched into two sub-clusters –cluster-Ia and cluster-Ib. Cluster-Ia grouped MDA-MB-468 and MCF-7 while Ib contained MCF-10A and MDA-MB-231. T47D was included in cluster-II. In cell lines, surface expression pattern of all the three FPR was similar in MCF-7 and MDA-MB-468. These two cell lines also showed similar gene expression pattern for all the three FPR. Surprisingly, normal breast epithelial cell line – MCF-10A and HBCC – MDA-MB-231 showed similar surface expression pattern for sFPR2 and sFPR3. Though, MDA-MB-231 and MCF-10A did not form cluster on the basis of expression of mRNA as well as sFPR data at the first level, they were close to each other and clustered at the second level. Expression pattern for sFPR in T47D did not show similarity with any of the HBCC studied.

FPR family members have been extensively studied for their role in innate immunity[1, 2]. FPR mediates chemotaxis of professional phagocytes at the site of infection or injury, which is followed by inflammatory response[1, 2]. It has also been proposed that FPR might have role in wound healing[225]. In spite of their well characterized role in host immune response, FPR expression was not restricted to hematopoietic cells. In past various reports have demonstrated expression of FPR in cells of non-hematopoietic origin. Expression of FPR by immunohistochemistry was reported in epithelial cells especially those with secretory functions, some endocrine cells e.g., follicular cells, smooth muscle, endothelial cells, neurons of motor, sensory, cerebellar system and those of parasympathetic & sympathetic[13]. Various reports have shown the expression of functional FPR in human coronary arteries, intestinal epithelia, lung fibroblast, lens epithelial cells, liver cells, astrocytes, primary tracheobronchial cell line, amnion derived WISH cell line and human lens cell line FHL124[19, 21, 60, 226-229]. Human cancer and cancer cell lines –rat breast carcinoma cell line Walker-256, hepatoma cell line HepG2, astrocytoma cell line SNB75 & U87, lung cell line A549, colorectal adenocarcinoma cell line SKCO15, grade IV human glioblastoma multiform, human anaplastic astrocytoma grade-II, ovarian cancer, gastric cancer, and melanoma also expressed functional FPR[18, 21, 60, 100, 230-235]. Varani et al. have shown that fMLP –ligand for FPR, increases adherence of rat breast carcinoma cell line Walker-256[236]. Walker-256 cell line showed increased migration and cell swelling upon fMLP stimulation[237-239]. Intraperitoneal injection of fMLP to rat bearing circulating Walker-256 cells induced localization of the tumor cells in peritoneal mesentries and subsequent formation of tumor at these sites[240, 241]. Rayner et al. and Marasco et al. have shown the binding of fMLP to

Walker-256 cell lines[100, 101]. McCoy et al. showed expression of functional FPR in human liver cells and hepatoma cell line HepG2[21]. In these cells FPR mediated changes in hepatic acute phase genes in time dependent and agonist's concentration dependent manners. This regulation of hepatic acute phase genes by FPR is different than other regulators of hepatic acute phase genes because unlike others it is desensitized at higher concentration of fMLP. Binding of fMLP to human amnion derived WISH cells induced release of prostaglandin (PG) E2[229]. This release of PGE2 by fMLP in WISH cells was cox-2, PLA2 and PLC dependent. Stimulation of FPR in astrocytoma cell lines SNB75 and U87 induced cell migration, calcium mobilization and increased secretion of IL6[230]. It was also reported that FPR was not expressed by less aggressive gliomas or by normal astrocytes but primary grade IV glioblastoma multiforme and grade II anaplastic astrocytomas showed expression of FPR[60]. fMLP stimulation induces motility, growth and angiogenesis in them. Chen et al. reported that functional FPR expression was essential for sustaining the growth and aggressive phenotype of glioma[62]. Expression of functional FPR in glioma cells plays an important role in regulating vasculogenesis by endothelial progenitor cells[61]. FPR is responsible for increased motility of human glioblastoma cells and formation of highly invasive tumors[242]. LL-37/hCAP-18 has been shown to accelerate tumor growth via FPR2 in ovarian cancer cells[232]. High ANXA1 (endogenous ligand for FPR) was associated with highly invasive, peritoneal metastasis and poorer overall survival in gastric cancer patients[243]. FPR induced EMT, proliferation, resistance to apoptosis and migration in gastric cancer (GC) cells in culture. It was also reported that FPR1 inhibits angiogenesis in GC cells. Hence, silencing of FPR1 gene in GC cells increased cell proliferation and xenograft growth due to

increased vessel density[234]. Hif-1α and VEGF mRNA expressions were higher in FPR1 silenced xenografts. Production of proangiogenic factors was also higher in FPR1 silenced xenografts. These presented reports suggested that FPR might act in more complex manner than expected. Apart from cancer and normal cell lines, expression of FPR was also reported in mesenchymal stem cells[20, 244]. Stimulation of FPR by fMLP in MSC triggers osteoblastic commitment while inhibits adipogenic commitment[245]. During osteoblastic differentiation of MSC, significant increase in the expression of FPR1 but not FPR2 and FPR3 was reported. Earlier binding of fMLP and chemotaxis in response to that fMLP binding was reported in rat breast carcinoma cell line Walker 256[100, 101]. These cells showed chemotaxis in response to fMLP treatment in a concentrated dependent manner. Binding and internalization of radiolabeled fMLP was also reported in these cells. Another report showed that FPR1 and FPR2 stimulation induced cell proliferation in breast cancer[102]. Any of the reports had not mentioned about status of FPR mRNA expression in breast cancer cells, but aforementioned reports do demonstrate that breast cancer cells could express functional FPR. This is the first report of mRNA and protein expression of all three FPR in HBCC and normal breast epithelial cell line. All the HBCC and normal breast epithelial cell line MCF-10A, expressed mRNA and protein of FPR1, FPR2 and FPR3. Expression of mFPR1 was significantly higher in normal breast epithelial cell line MCF-10A than that in all the HBCC, while mFPR2 and mFPR3 expression was higher in HBCC than that in MCF-10A. Comparative expression of all the three receptors showed that mFPR1 was the highest expressed receptor in all the cell lines followed by mFPR2 and mFPR3. Decrease of mFPR1 and increase of mFPR2 & mFPR3 expression was seen in HBCC than that in normal

breast cell line MCF-10A. Similar to mFPR1 expression, sFPR1 expression was also the highest in MCF10A. sFPR2 expression was higher than that in MCF-10A in all the HBCC except T47D. Results of sFPR3 were completely different from mFPR3 expression results, where distinguishing pattern between HBCC and normal breast epithelial cell lines was not observed. Zhou et al. reported increase in the expression of FPR1 in cancer cell line compared to normal tissue[60]. Similar observations were reported by VanCompernolle et al. where mRNA expression of FPR1 and FPR2 were higher in human fibrosarcoma cell line HT1080 than normal lung fibroblast cell MRC-5 and normal skin fibroblast WS1[19]. They also estimated the number of total receptor by equilibrium binding assay with FPR1 and FPR2 ligand fNLPNTL. Since they used <2 nM concentration for the ligand, they claimed that low affinity FRP2 receptor did not affect the results and ligand will only bind to FPR1, however no experimental evidence was produce in support of this claim. Total number of receptor calculated were higher in normal lung fibroblast cell MRC-5 than that in fibrosarcoma cell line HT1080. Our results for mFPR1 are in contrast with these two reports while for mFPR2 they are in line with results reported by VanCompernolle et al.. It could be that breast cancer cell lines due to their different tissue origin behave differently. Moreover, Zhou et al[60] have compared U87 cell lines with human astrocytes and not with cell line. It is well established fact that due continuous culture, cell lines develop various features which are different from their origin cell type. Hence, this could be one of the factor for differences in expression of FPR between U87 and astrocyte. Similarly VanCompernolle et al.[19] have compared the HT-1080 cell line with lung and skin fibroblast cell line while HT-1080 was developed from the fibrosarcoma adjacent to acetabulum. Cells from different parts of the body

could have different gene expression patterns. Hence, comparing HT1080 with lung and skin fibroblast couldn't be right. In the present study normal breast epithelial cell line was compared with the breast cancer cell lines, where decrease in mFPR1 and sFPR1 was seen in tumor cell lines. It is already mentioned that the use of various cell lines is well accepted as models in clinical application oriented initial studies. Conclusions drawn on the basis of studies, using more than one cell lines are more likely to resemble in vivo conditions than those based on the use of a single cell line. Therefore, conclusions drawn from the present study on the role of FPR in breast cancer, using a panel of human breast cancer cell lines (HBCC) along with one non-cancerous cell line, are more reliable. It was seen that mFPR1 and sFPR1 levels decreased in the HBCC, while increase in expression of mFPR2 and sFPR2 was observed. Expression of mFPR1 was significantly higher in normal breast epithelial cell line MCF-10A than that in all the HBCC, while mFPR2 and mFPR3 expression was higher in HBCC than that in MCF-10A. Decrease of mFPR1 and increase of mFPR2 & mFPR3 expression was seen in HBCC than that in normal breast cell line MCF-10A. Similar to mFPR1 expression, sFPR1 expression was also the highest in MCF10A. sFPR2 expression was higher than that in MCF-10A in all the HBCC except T47D. Results of sFPR3 were completely different from mFPR3 expression results, where distinguishing pattern between HBCC and normal breast epithelial cell lines was not observed. Aggressiveness and metastatic nature of HBCC seems to be affected by balance of sFPR1 and sFPR2 expression level. MDA-MB-231, which is most aggressive, fast growing and highly metastatic cell line, showed the highest expression sFPR1 and sFPR2 while the slow growing and least aggressive cell line T47D showed the least sFPR1 and sFPR2. MCF-7 and MDA-MB-468,

moderately aggressive cell lines express high sFPR2 but low sFPR1. It showed that similar to glioma FPR also contributing to the aggressive nature of HBCC.

Ligand binding

The first step of any receptor signalling is binding of the receptor to its ligand, which leads to the activation of downstream signalling cascade. After binding to the ligand, FPR is internalized and dissociated from the ligand. This internalization and dissociation of FPR was temperature dependent[128]. At 4°C, there was complete abolition of receptor internalization and maximum internalization was observed at 37°C. It was also reported that neutrophil contains an intracellular pool of FPR that could be mobilized to surface upon stimulation[183]. Hence, ligand-binding assay carried out at 37°C, could be taken as an estimation of the total number of receptors in cells in question. Above results had shown differences in the expression of sFPR in HBCC, as well as in mRNA levels, hence their ligand binding ability was checked using fluorescent fNLPNTL. All the HBCC except T47D showed significantly higher ligand binding than that in normal breast cell line MCF-10A (Fig-RB 5A & 5B, Table-RB 4). T47D showed the minimum ligand binding among all the HBCC and it was at par with that in MCF-10A. Among the rest of the HBCC, ligand binding in MCF-7 and MDA-MB-231 was at par while MDA-MB-468 showed maximum ligand binding.

Table-RB 4: Binding of fNLPNTL-FITC

Cell lines	MCF-10A	MCF-7	MDA-MB-231	MDA-MB-468	T47D
Median	18.3 ± 0.2	25.3 ± 1.7	27.1 ± 0.2	33.6 ± 1.0	16.9 ± 1.2
% Positivity	88.9 ± 0.5	96.0 ± 0.5	99.7 ± 0.1	100.0 ± 0.0	98.6 ± 1.3

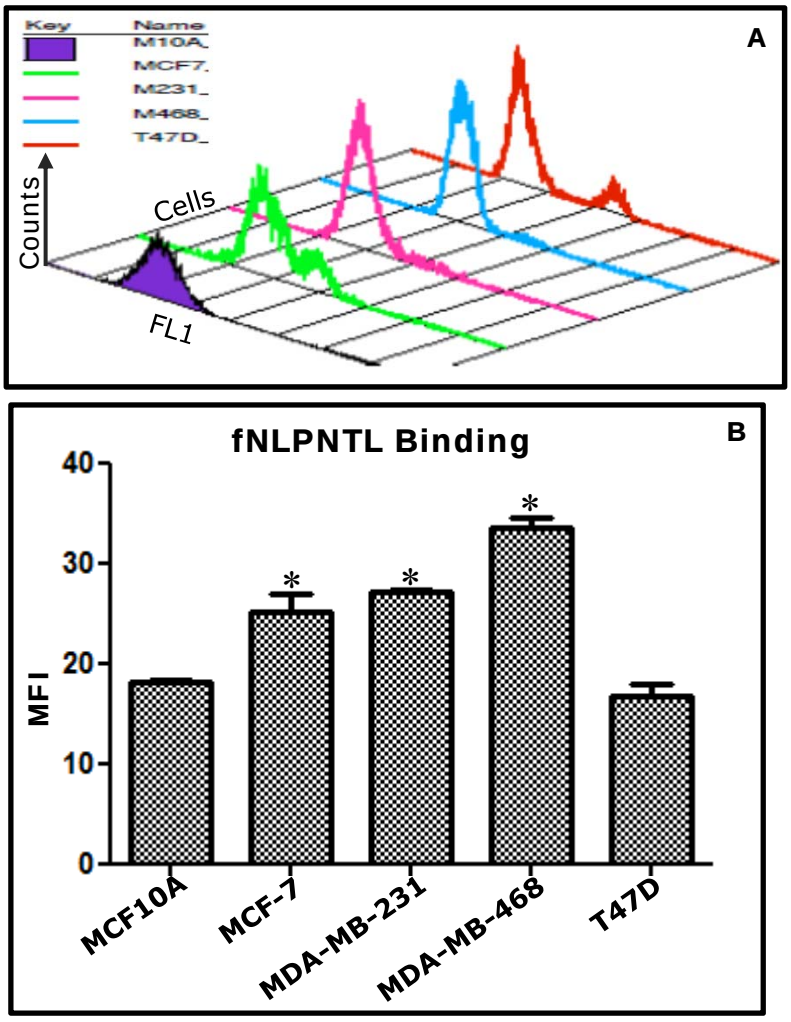

Fig-RB 5: fNLPNTL-FITC Ligand Binding: fNLPNTL-FITC ligand binding to breast cancer cell lines - (A) Representative histogram overlay showing fNLPNTL-FITC binding in HBCC and MCF-10A as indicated. (B) Bar plot showing average MFI ± SEM of fNLPNTL-FITC in HBCC and MCF-10A (n=3). * $p<0.05$ wrt MCF10A (Mann-Whitney test)

Relevance, importance and mechanism of FPR ligand binding to its receptor has been discussed extensively in CML section. As mentioned there, only 1-2% of FPR sites are occupied using fNLPNTL-FL. Hence, detection of FPR using antibodies, aids in studying the receptor in totality. In contrast, only ligand bound receptors are detected using labelled ligand[186]. In present work staining of the cells with antibody was done at 4°C and thus receptor internalization, translocation and upregulation was inhibited. At this temperature, only surface receptors were available for antibody binding. On other hand, ligand binding experiments were performed at 37°C. Hence, surface as well as cytoplasmic pool of the receptors was available for ligand binding. In view of these, surface staining results of FPR showed the receptor expressed on the cell membrane, while ligand binding estimated the total pool of the receptors i.e. surface and cytoplasmic. All HBCC except T47D showed higher ligand binding than that in MCF-10A. Though, this ligand binds to both FPR1 and FPR2, it generally show preference to FPR1 over FPR2. Since surface receptor expression and gene expression status showed that HBCC expressed lower FPR1 but higher FPR2 than MCF-10A, it would be imperative that the ligand binding would be at par between MCF-10A and HBCC, but HBCC showed higher ligand binding than normal cell line. Similar observations were seen in the CML results that bcr-abl positive cell lines showed higher ligand binding than that in bcr-abl negative cell line. It could be possible that the ligand binding affinity of cancerous cell lines might have increased. This hypothesis is supported by the fact that one of the hallmark of cancerous cells is that they become hypersensitive to extracellular signals[63]. This hypersensitivity is believed to be achieved by either receptor

overexpression or by increasing affinity to the signal. Among, HBCC, the highest ligand binding was observed in MDA-MB-468, while the lowest ligand binding was observed by T47D. T47D expressed the lowest sFPR1 and sFPR2, hence it was obvious that this cell line would show the least ligand binding.MDA-MB-468 did not express the highest sFPR1 or sFPR2. Since, ligand binding experiments were performed at 37°C and at this temperature cytoplasmic pool is available for ligand binding; it could be possible that MDA-MB-468 would have higher cytoplasmic pool for FPR which are available for binding, thus MDA-MB-468 showed the highest FPR ligand binding. Differences in MFI by ligand binding by MCF_7, MDA-MB_231 and MDA-MB-468 were marginal. But it is noteworthy that though % positivity for FPR1 and FPR2 seen by antibody was in the range of 11-73%, almost 100% positivity was seen for ligand binding. This suggested that in HBCC, either both FPR1 and FPR2 bound to the ligand or many cells in the population had sFPR1 that could not bind to the antibody or by addition of ligand, cytoplasmic FPR1 were cycled to the membrane and could bind the ligand. In view of lower % positivity if T47D for FPR1 and FPR2 only later two explanations could be accepted. Use of labelled ligand specific for FPR2 to explore ligand binding to FPR2 could aid in distinctly distinguishing HBCC from normal and grade them as per their aggressiveness.

Signaling of FPR

Actin polymerization

Actin polymerization is one of the downstream events after FPR activation. Actin is one of the major cytoskeletal component in cells. Exposure of PMNL to FPR ligand fMLP causes polymerization of monomeric globular G-actin to filamentous F-actin leading to chemotactic motility. First basal actin gene expression in HBCC

and in MCF-10A was studied using qRT-PCR. Then, F-actin was quantitated using fluorescent-tagged actin binding phalloidin.

Except T47D, all HBCC expressed lower actin gene than that in MCF-10A (Fig-RB 6A). Among HBCC, the highest expression of actin gene was in T47D followed by MDA-MB-231. The lowest expression of actin gene was in MDA-MB-468 and MCF-7. When these cell lines were stained with fluorescently tagged phalloidin, it was found that all the HBCC showed significantly lower basal F-actin than the normal breast cell line, MCF-10A (Fig-RB 6B & 6C, Table-RB 5). Among HBCC, highest basal level of F-actin was found in T47D followed by MCF-7, MDA-MB-468, and MDA-MB-231. After stimulation with 10^{-6} M fMLP, significant decrease in F-actin content was observed in MCF-10A, and MCF-7 (Fig-RB 6C & 6D, Table-RB 5). MDA-MB-231 and MDA-MB-468 showed significant increase in F-actin content after fMLP stimulation, while T47D did not show any change in F-actin content upon fMLP stimulation.

fMLP stimulation is known to increase F-actin quantity in PMNL and other cells, but two out of five cell lines showed decrease and one cell line did not show any change in F-actin content, upon fMLP stimulation. MDA-MB-231, which expressed the highest mFPR1 and sFPR1 among all the HBCC, showed the highest increase in F-actin quantity. When these results were compared with actin gene expression data and ligand binding data, it was found that MDA-MB-468 showed lower actin gene expression (Fig-RB 6A). This probably resulted in very little change in F-actin on fMLP treatment. On other hand, T47D, which showed the highest actin gene expression and the lowest FPR ligand binding, did not show any change in F-actin, on fMLP treatment. It might be possible that a

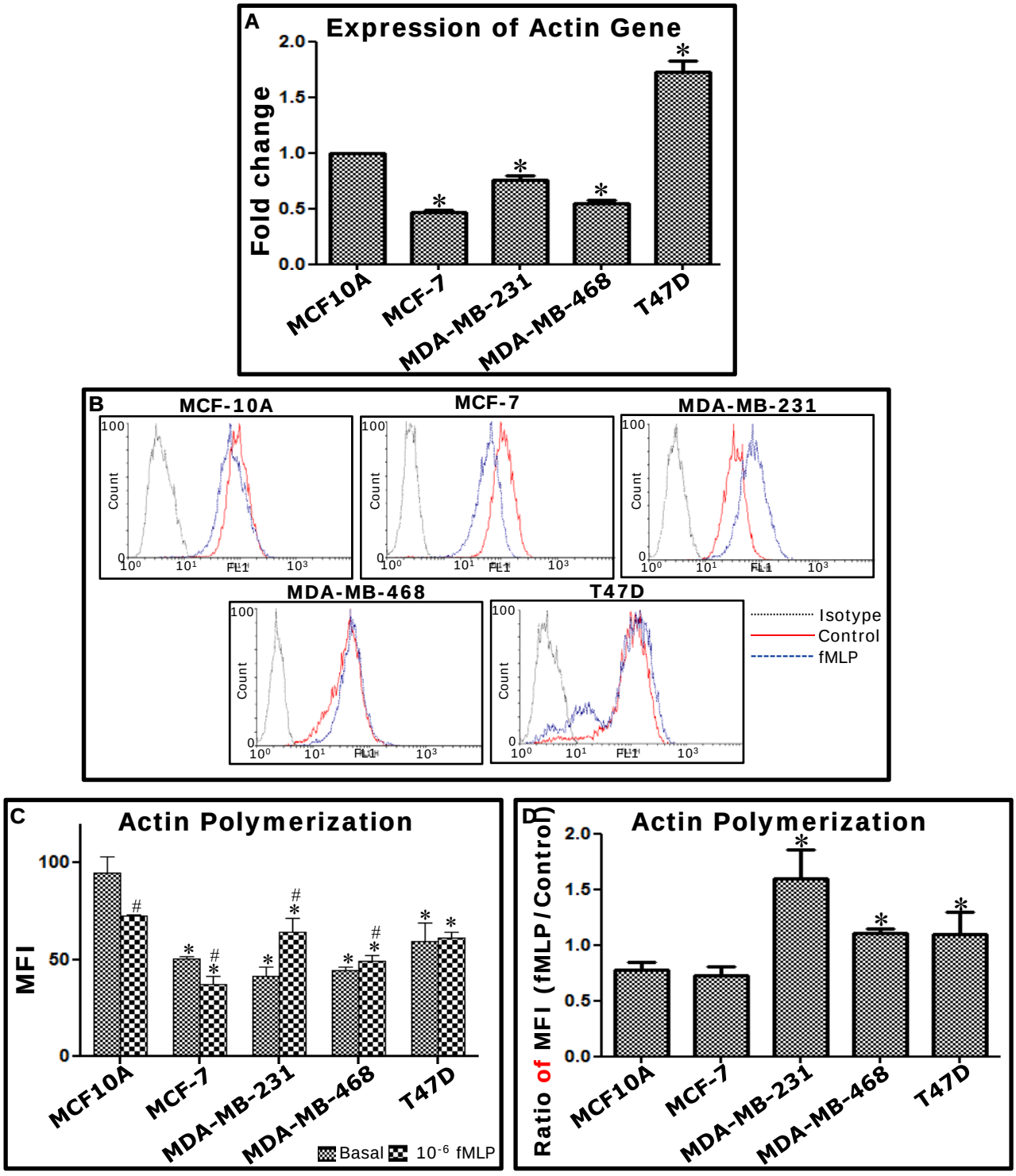

Fig-RB 6: Actin Gene Expression and F-actin Quantitation: (A) Expression of actin gene in HBCC with respect to the normal breast epithelial cell line MCF-10A is estimated by QPCR. Gene expressions were normalized using expression of housekeeping gene GAPDH. Data is presented as average fold change ± SEM (n=3). (B) Representative flow cytometry histogram overlays of FITC-phalloidin intensity in unstimulated (control) and fMLP stimulated cells as indicated (C) Bar plots showing F-actin expressed as average MFI ± SEM (n=3) (D) Bar plots showing change in F-actin content after stimulation with 10^{-6}M fMLP, expressed as average relative fold change in MFI with respect to the basal F-actin content ± SEM (n=3). * $p<0.05$ wrt MCF-10A (Mann-Whitney test), # $p<0.01$ wrt basal actin level (Wilcoxon pair test)

minimum number of ligand molecules are required to bind to the cell in order to bring any change in F-actin content.

Table-RB 5: F-actin quantitation

Treatment	Median Fluorescent Intensity (MFI)				
	MCF-10A	MCF-7	MDA-MB-231	MDA-MB-468	T47D
Solvent (Control)	94.9 ± 8.1	50.7 ± 0.7	41.4 ± 5.0	44.4 ± 1.6	59.4 ± 9.8
10^{-6} M fMLP	72.6 ± 0.6	37.1 ± 4.7	64.4 ± 7.0	49.4 ± 2.8	61.6 ± 2.8
Ratio fMLP/Control	0.78 ± 0.07	0.73 ± 0.08	1.60 ± 0.26	1.11 ± 0.04	1.07 ± 0.2

To understand the decrease in F-actin content, MCF-7 –the only HBCC, which had shown decrease in F-actin content after fMLP stimulation, was stained for F-actin using TRITC-phalloidin, after fMLP stimulation. Unstimulated cells were used as control. Images of stained cells were captured using a laser confocal microscope (Fig-RB 7). Upon fMLP stimulation, distinct changes in the MCF-7 morphology were observed (Fig-RB 7A & 7E). Cells were epithelioid and spreaded before fMLP treatment, but after fMLP stimulation, decrease in cell size was observed. Many cellular projections were seen at the cell periphery after fMLP stimulation. Control cells showed diffused cytoplasmic F-actin concentrated at the cellular periphery with cytoplasmic stress fibers (Fig-RB 7B & 7C). In fMLP treated cells decrease in cytoplasmic and peripheral F-actin was seen (Fig-RB 7F & 7G). Stress fibers disappeared in fMLP treated cells. F-actin was more concentrated in the long, thick, spike like cellular projections. fMLP treated cells, were less spreaded and showed reduced adhesion to substratum as well as

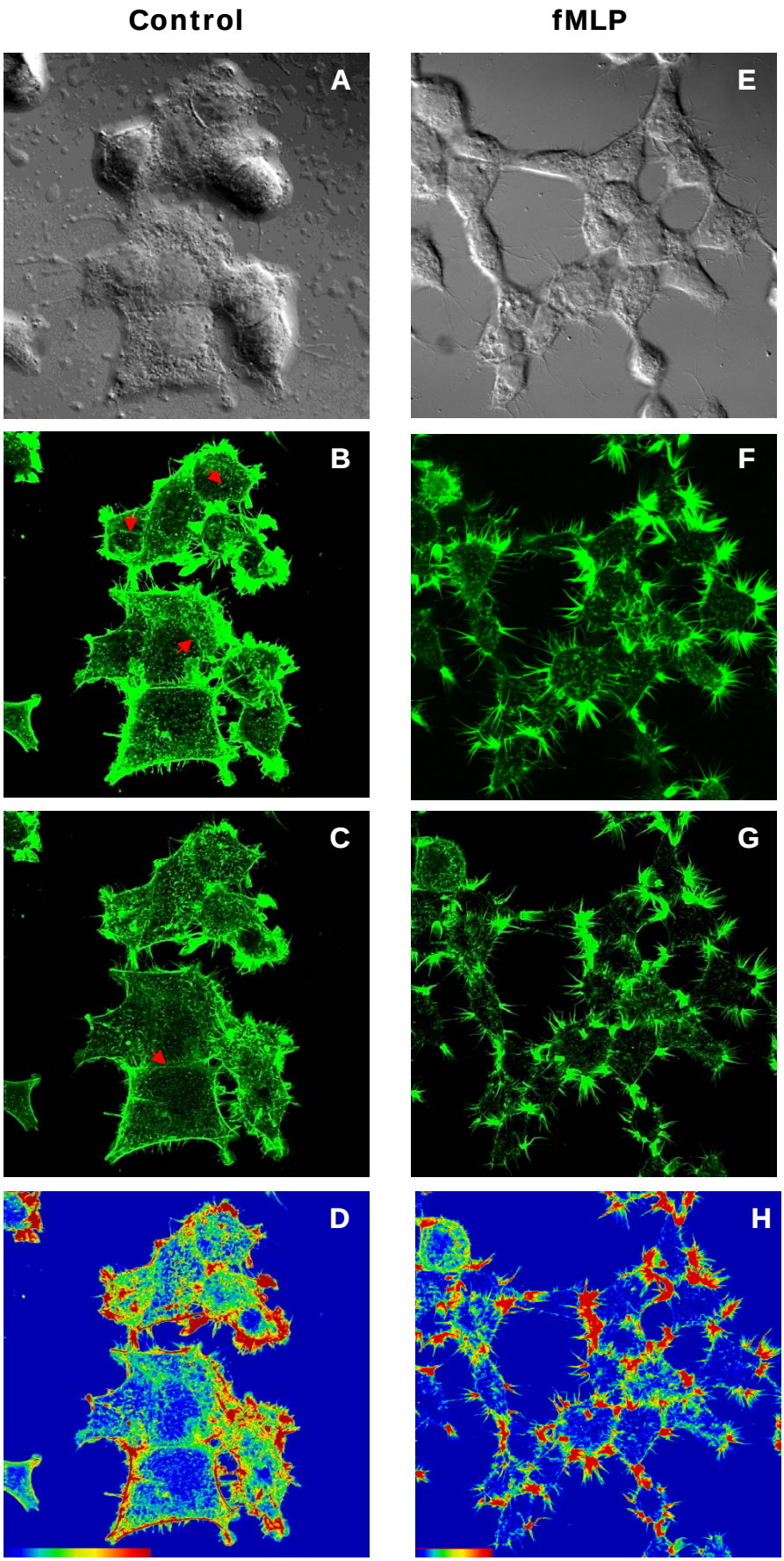

Fig-RB 7: F-actin in MCF-7: Representative images of MCF-7 cells stained with TRITC-phalloidin (pseudo green color), captured by laser confocal microscopy, wherein A, B, C & D are control cells while E, F, G & H are fMLP treated. (A) & (E) are in DIC mode while others are in fluorescence mode. (B) & (F): Middle planes (4/7) of the 3D images (C) & (G): 3D projections (D) & (H) intensity LUT - rainbow color palette for 3D projections, where blue and red indicate minimum and maximum fluorescence intensity, respectively. Red arrows in panels B and C show stress fibers.

reduced cell-cell adhesion. An overall decrease in F-actin was seen in fMLP-stimulated cells than that in control (Fig-RB 7D & 7H). It was clear from the images that after fMLP stimulation, decrease in F-actin quantity in MCF-7 cells was associated with the loss of epithelioid morphology of the cells and decrease in cell spreading. This could be the induction of epithelial-mesenchymal transition (EMT). Furthermore, increase in length and number of projections after fMLP stimulation, could be an indication of acquisition of more motile and invasive characteristics.

As mentioned in CML section that binding of chemotactic peptide to polymorphonuclear leucocytes (PMNL) results in rapid changes in the cytoskeletal system of the cells finally leading to a directed movement of the cells towards the source of chemoattractant. A very early event in changes in the cytoskeletal organization is the polymerization of cytoplasmic G-actin to F-actin, which forms the motile apparatus of the cells. All the HBCC studied are metastatic cell lines and showed migration when stimulated with various stimulator, however, effect of fMLP on breast cancer migration was not looked into[246]. The present study showed that fMLP stimulation affected F-actin polymerization levels in HBCC, although all cell lines behaves differently. Effect of fMLP varies from cell line to cell line and therefore, the underlying mechanisms could be different in each cell line. MCF-10A, MCF-7 and T47D showed decrease in F-actin content upon fMLP stimulation while there were increase in F-actin content in MDA-MB-231 and MDA-MB-468 upon fMLP stimulation. The highest increase in F-actin content upon fMLP stimulation was seen in MDA-MB-231 cell line, which expressed the highest mFPR1 and sFPR1. MDA-MB-468 showed marginal increase in the F-actin level upon fMLP

stimulation. T47D showed two population upon fMLP stimulation, one population showed decrease in the F-actin content while one population showed marginal increase in F-actin. fMLP stimulation showed increase in F-actin in neutrophil but in MCF-10A and MCF-7 decrease in F-actin was observed. When MCF-7 was examined under laser confocal microscope it was found that decrease in F-actin in this cell line was associated with change in cell line shape and loss of cell-cell contact, which indicate acquisition of motile and invasive characteristic by the cell line. Probably in the cells, increase or decrease in F-actin might be dependent on cells' basal F-actin architecture that is whether it requires decrease in F-actin or increase in F-actin in order to migrate. Though further investigations are needed, it could be said from these observations that fMLP was probably inducing epithelial to mesenchymal transition in MCF-7 cell line.

Status of markers for Cell differentiation

Growing evidences have suggested that solid tumors are heterogeneous in nature. These cancers are driven by the population of cells that display stem cell properties. These cells are known as cancer stem cells (CSC) or tumor initiating cells. This small population of breast cancer is also termed as breast cancer initiating cells. In breast cancers, the cell surface markers CD44 and CD24 are commonly used to define a population enriched in CSCs[247-249]. The $CD24^{-}$ /$CD44^{+}$ breast CSCs possess the ability to self-renew and to differentiate when injected into the mammary fat pad of NOD/SCID mice, resulting in engrafted mammary tumor formation and progression[247]. Although the $CD24^{-}$ /$CD44^{+}$ phenotypic markers have been extensively used to isolate breast CSCs in different cancer subtypes especially basal-like tumors[250], a recent study showed that both $CD24^{-}$ /$CD44^{+}$and $CD24^{+}$ /$CD44^{+}$cell populations in ERα–negative breast tumors are

tumorigenic in murine xenograft models[251]. Expression of $CD24^-$ /$CD44^+$ population was higher in MCF-10A than that in HBCC. Among HBCC, MDA-MB-468 and T47D were negative for the $CD24^-$ /$CD44^+$ population. After pioneering studies of Al-Hajj et al. in human breast cancer, $CD24^-$ /$CD44^+$ cells were recognized as prospective CSC[247]. This was subsequently supported by Sheridan et al., but it was suggested that this phenotype alone may not be appropriate to envisage metastasis though these cells showed higher expression of genes that are required for tissue invasion[252]. Later on, large body of evidence demonstrated that this phenotype is not expressed in all the breast cancers emphasizing the need for identification of other breast CSC markers[250, 253, 254]. In MDA-MB-468 cell line high expression of $CD44^+$/$CD24^+$ cells with basal/epithelial phenotype are reported[44]. Our results complemented this finding. It is very well accepted that $CD24^-$ /$CD44^+$ exhibit undifferentiated cell properties and $CD44^+$/$CD24^+$ exhibit highly differentiated basal/epithelial cell properties[44]. However, mechanism of tumor induction by cell lines like MDA-MB-468 with high CD24 expression remains unclear. MDA-MB-468 is enriched with $CD44^+$ /$CD24^+$ cells, which are not invasive. It is assumed that some $CD44^+$/$CD24^-$ cells in this cell line are progressed to $CD44^+$/$CD24^+$ phenotype after metastasis showing an interconversion of $CD24^+$ to $CD24^-$[252]. Recent studies for migration, colony formation and invasion in MDA-MB-468 by $CD44^+$ cells complimented the CD24 interconversion and regulatory concept[255]. Meyer et al. supported the possibility of interconversion between the phenotypes and suggested that epithelial like $CD44^+$/$CD24^+$ can readily give rise to $CD44^+$/$CD24^-$ cells during tumor initiation[256]. Based on the these concepts, Shi et al. demonstrated in human epithelial ovarian cancer, that $CD44^+$/$CD24^-$ cells showed CSC-like properties

and differentiated to $CD44^{+}/CD24^{+}$[257]. Regardless of the positivity or negativity of CD44 and CD24, the cells expressing these markers in breast cancer were acknowledged with invasive properties but lacking metastatic genes[252]. Although many studies showed the vital role of CD44 in metastasis[258, 259], contrastingly, Lopez et al.[260] demonstrated that CD44 can inhibit metastasis in the breast cancer. Similar contradictory views are reported for CD24 too. Baumann et al.[261] showed CD24 promotes invasion, while Schabath et al.[262] demonstrated expression of CD24 inhibiting the invasion and metastasis.

After the discovery of induced pluripotency by Yamanaka et al and subsequent research in the field, few transcription factors - Oct-3/4, Sox-2, Nanog, Nestin, Klf-4, & cMyc and their role in pluripotency were studied in depth[263-265]. Among these transcription factors Oct-3/4, Sox2 and Nanog are considered as the main player in cellular pluripotency. In the above results, it was seen that in CML expression of FPRs was linked to cellular stemness. Hence, in HBCC too, the status of these stemness markers was tested at mRNA as well as protein levels and effect of FPR ligand was checked on their protein expression.

mRNA

cMyc

cMyc is one of the Yamanaka factors[264] that was used for the generation of iPS cells. Later, it was found that the omission of cMyc had no effect on generation of iPS cells[266]. Hence, there is a debate on the importance of cMyc in stemness of cells. cMyc is a transcription factor that plays role in cell cycle, apoptosis and cellular transformation[267-269]. In HBCC, pattern of expression of cMyc gene was opposite of FPR1 gene expression. Expression of cMyc was highest in T47D, which had the lowest expression of FPR1 gene and protein, whereas cMyc gene

expression was least in MDA-MB-231, which had shown the highest expression of FPR1 gene and protein among all the HBCC (Fig-RB 8A, Table-RB 6). All the HBCC except T47D, showed expression of cMyc less than that in normal breast cell line MCF-10A.

Table-RB 6: Basal Expression of Stemness Marker Genes

	Fold Change wrt MCF-10A			
	MCF-7	**MDA-MB-231**	**MDA-MB-468**	**T47D**
cMyc	0.70 ± 0.04	0.35 ± 0.02	0.82 ± 0.06	1.34 ± 0.06
Klf4	3.08 ± 0.24	0.62 ± 0.06	6.28 ± 0.10	2.77 ± 0.10
Nanog	6.39 ± 0.38	1.81 ± 0.11	10.58 ± 0.57	4.78 ± 0.25
Nestin	7.67 ± 0.24	11.14 ± 0.47	15.96 ± 1.05	8.13 ± 0.47
Oct-3/4	3.62 ± 0.21	1.41 ± 0.08	5.00 ± 0.37	4.43 ± 0.24
Sox2	43.87 ± 2.45	2.69 ± 0.20	58.94 ± 3.43	31.49 ± 1.31

Klf-4

Kruppel-like factor 4 (KLF4) is a transcription factors that plays role in cell proliferation, cellular differentiation, apoptosis[270, 271]. It also works as a tumor suppressor gene in some of the cancers[271]. Klf-4 was identified and used by Yamanaka et al. in the generation of iPS cells[264]. It is a good indicator of cellular stemness in embryonic as well as in mesenchymal stem cells[270].

All the HBCC except MDA-MB-231 showed higher expression of klf-4 than normal breast epithelial cell line MCF-10A (Fig-RB 8B, Table-RB 6). MDA-MB-231 showed the lowest expression of klf-4 whereas MDA-MB-468 expressed the highest expression of klf-4. mRNA expression level of klf-4 in ER-PR positive cell lines MCF-7 and T47D were found at par with each other, but more than triple negative cell lines –MDA-MB-231 and less than MDA-MB-468.

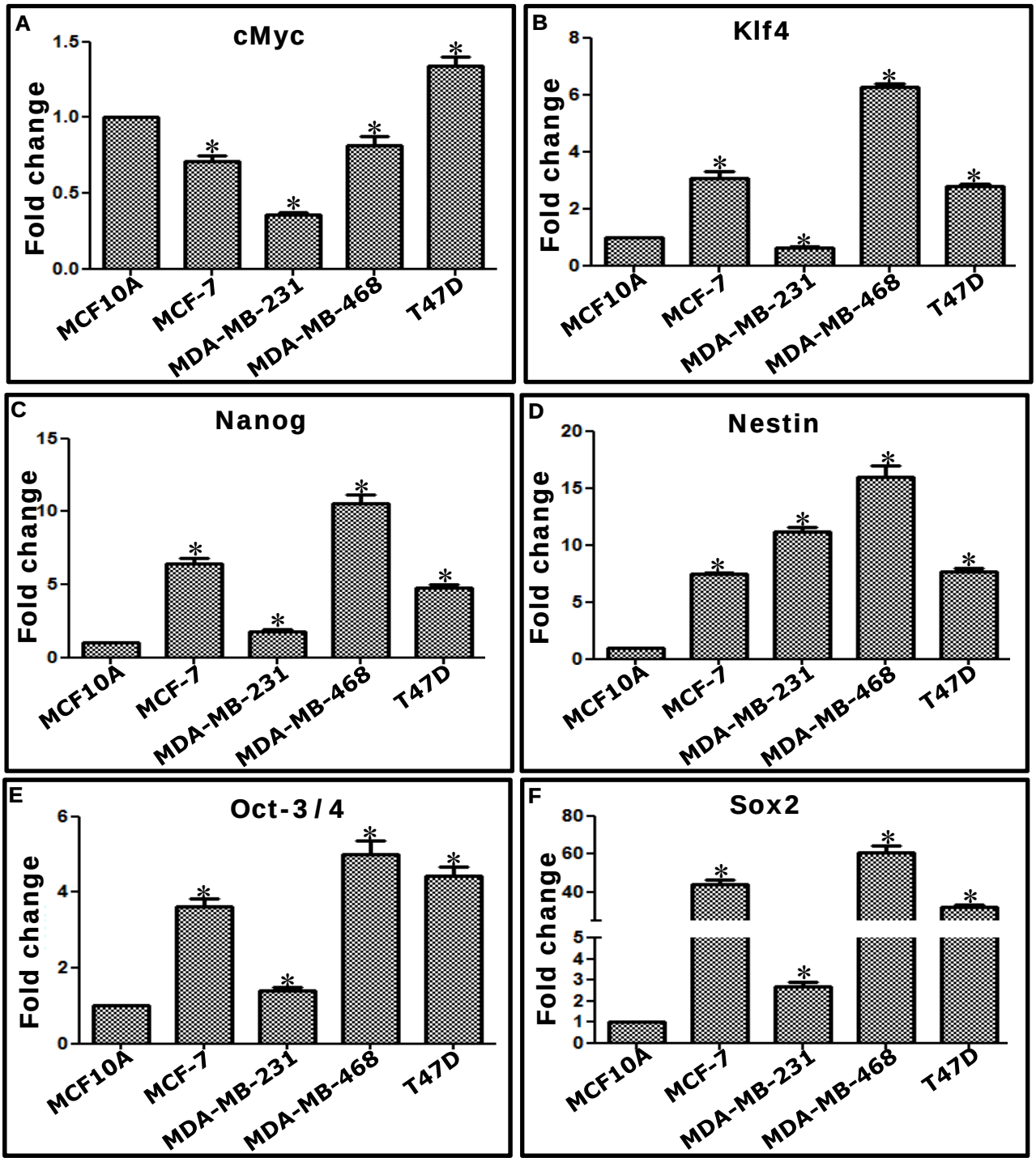

Fig-RB 8: Expression of Stem Cell Marker Genes in HBCC: Expression of cMyc (A), Klf4 (B), Nanog (C), Nestin (D), Oct-3/4 (E), and Sox2 (F) genes in HBCC with respect to the normal breast epithelial cell line MCF-10A, as estimated by QPCR. Gene expressions were normalized with GAPDH expression. Data is presented as average fold change ± SEM (n=3). * $p<0.05$ wrt MCF-10A (Mann-Whitney test).

Nanog

In embryonic stem cells, along with oct-3/4 and sox-2, nanog is required for maintaining pluripotency[272, 273]. Nanog is the transcription factor that is involved in self-renewal of embryonic stem cells[272].

Expression of nanog was higher in all the HBCC than the normal breast epithelial cell line, MCF-10A (Fig-RB 8C, Table-RB 6). The expression pattern of nanog in breast cancer cells was similar to that in klf-4. The highest expression of nanog was shown by MDA-MB-468 followed by MCF-7 and T47D. MDA-MB-231 showed the lowest expression of nanog.

Nestin

Nestin was reported as a protein marker for neural stem cells and follicular stem cells, but recently its expression was also reported in breast stem cells[274-276].

In our experiments, the mRNA expression of nestin was higher in all the HBCC than normal breast epithelial cell line (Fig-RB 8D, Table-RB 6). Among HBCC, the highest expression was shown by MDA-MB-468, which was followed by MDA-MB-231. Gene expression levels of nestin in both ER-PR positive cell lines MCF-7 and T47D were found at par, but were lower than that in the triple negative cell lines –MDA-MB-231 and MDA-MB-468.

Oct-3/4

Oct-3/4 is one of the Yamanaka factors and is critically involved in the self-renewal of undifferentiated embryonic stem cells[264]. Oct-3/4 is used as a marker for stem cells.

It had been observed in the present studies that expression level of oct-3/4 gene was higher in all the HBCC than that in breast normal epithelial cell line MCF-10A. This was similar to nanog and klf4 (Fig-RB 8E, Table-RB 6). The highest

expression of oct-3/4 was shown by MDA-MB-468 and the lowest expression was shown by MDA-MB-231. Oct-3/4 expression in T47D was slightly higher than that in MCF-7, but was less than that in MDA-MB-468.

Sox-2

SRY (sex determining region Y)-box 2 also known as Sox-2 is a transcription factor, which is necessary for maintaining pluripotency of embryonic stem cells[264].

Expression pattern of sox-2 in HBCC was similar to oct-3/4, klf4, and nanog except that the difference in the expression was higher between HBCC and normal epithelial cell line (Fig-RB 8F, Table-RB 6). All the HBCC expressed higher sox-2 gene than normal breast epithelial cell line MCF-10A. Similar to other stem cell markers, the highest expression of sox-2 was shown by MDA-MB-468 and minimum by MDA-MB-231. Sox-2 gene expression in MCF-7 was lower than MDA-MB-468, but higher than T47D.

When the relative expression patterns of these genes among HBCC were compared with the results of FPR expression, it was observed that the expression pattern of klf4, nanog, oct-3/4 and sox2 were similar to the gene expression patterns of FPR2 and FPR3 (Fig-RB 9A & 9B). Moreover, similar to FPR2 and FPR3 expression of these genes in all the HBCC except that of klf4 in MDA-MB-231 was 1.5 or more fold higher than that in MCF-10A. Gene expression data of the stem cell markers was subjected to the hierarchical clustering using default distance setting. At the top of the hierarchy, the dendrogram was divided into two major clusters (labelled I, and II) (Fig-RB 10A). Cluster-I contained only one gene –Sox2 for which increase in expression was extremely high in HBCC than that in MCF-10A. Cluster-II was further

branched into two sub-clusters –cluster-IIa and cluster-IIb. Cluster-IIa was also a single gene cluster that included nestin, for which increase in expression was very high in HBCC than that in MCF-10A, but was lower than that for Sox-2. Cluster-IIb was a group of three small clusters, which were close to each other. This cluster included four genes –oct-3/4, klf4, nanog, and cMyc. For the cell lines, dendrogram branched into two major clusters (labelled I & II). Cluster-I included two completely different cell lines, one triple negative HBCC, MDA-MB-231 and a normal breast epithelial cell line, MCF-10A. These two cells lines had shown lower expression as compared to other HBCC. Cluster-II was further branched into two sub-clusters –cluster-IIa and cluster-IIb. Cluster-IIa contained only one cell line –MDA-MB-468, which showed highest expression for all the genes except cmyc when compared with all the cell lines. While cluster IIb included both ER-PR positive cell line –MCF-7 & T47D, in which expression levels of all the genes studied were close to each other. Thus, both the ER-PR positive cell lines were in one cluster, but the triple negative cell lines were in different clusters. Hence, it could be said that expression of stem cell marker genes might be affected by or related to ER-PR dual positivity. Expression levels of Yamanaka factors – Oct-3/4, Sox2 and klf4 as well as stem cell marker genes –nanog and nestin in ER-PR dual positivity HBCC are comparable and significantly higher than the normal breast epithelial cell line. In triple negative HBCC too, expression of all these genes except klf4 is higher than that in the normal breast epithelial cell line, but expression levels vary from each other considerably.

Further, gene expression data of stem cell markers and FPR were clustered together. Clustering of the cell lines was same as that when done with stem cell

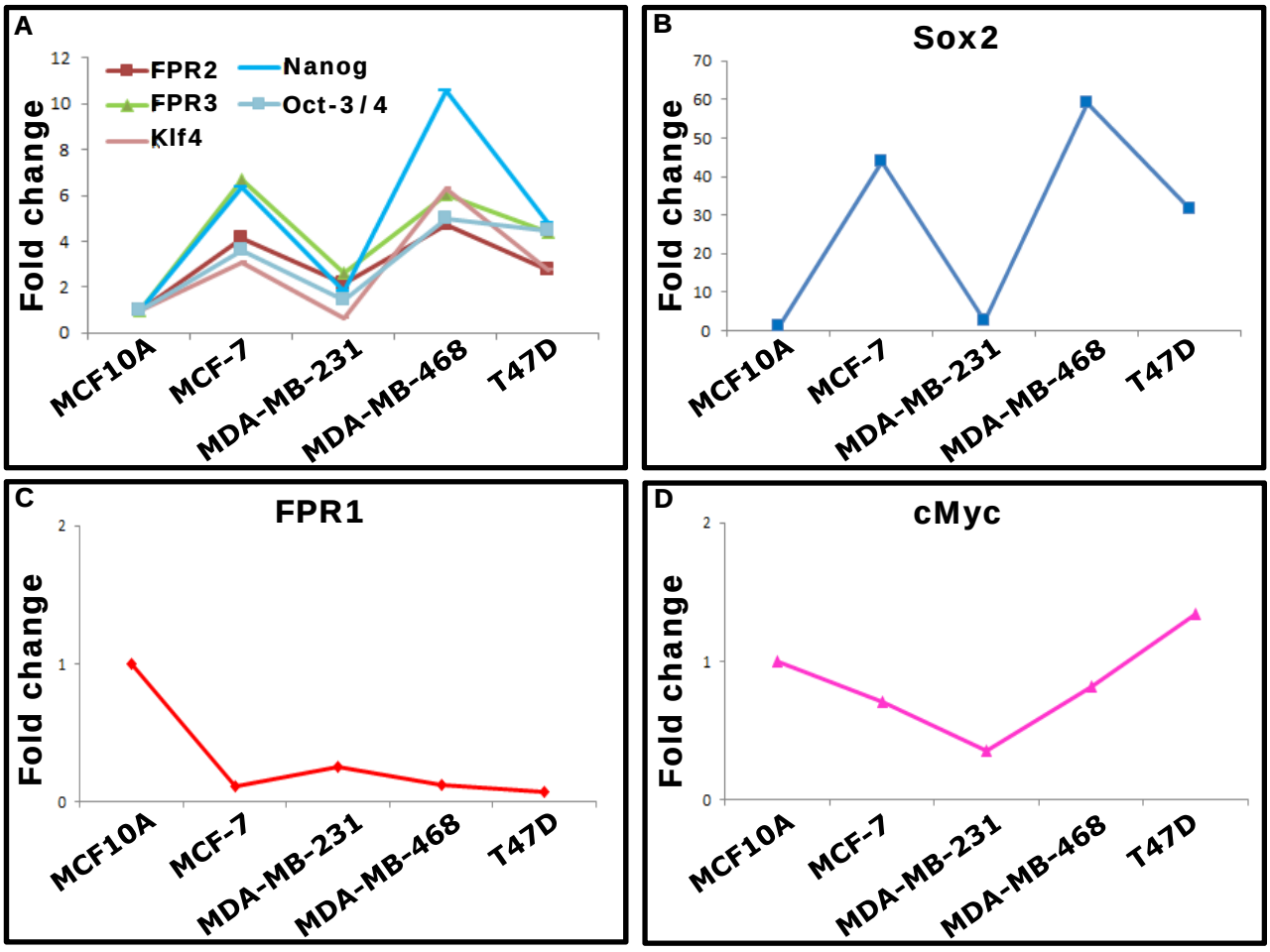

Fig-RB 9: Comparative Gene Expression Patterns in HBCC: Line plots of expression of various genes are showing trends in the expression patterns among different HBCC and MCF-10A. Line plots showed similarity pattern for expression of FPR2, FPR3, Klf4, Nanog, & Oct-3/4 (A), and patterns of Sox2 (B), FPR1 (C) and cMyc (D).

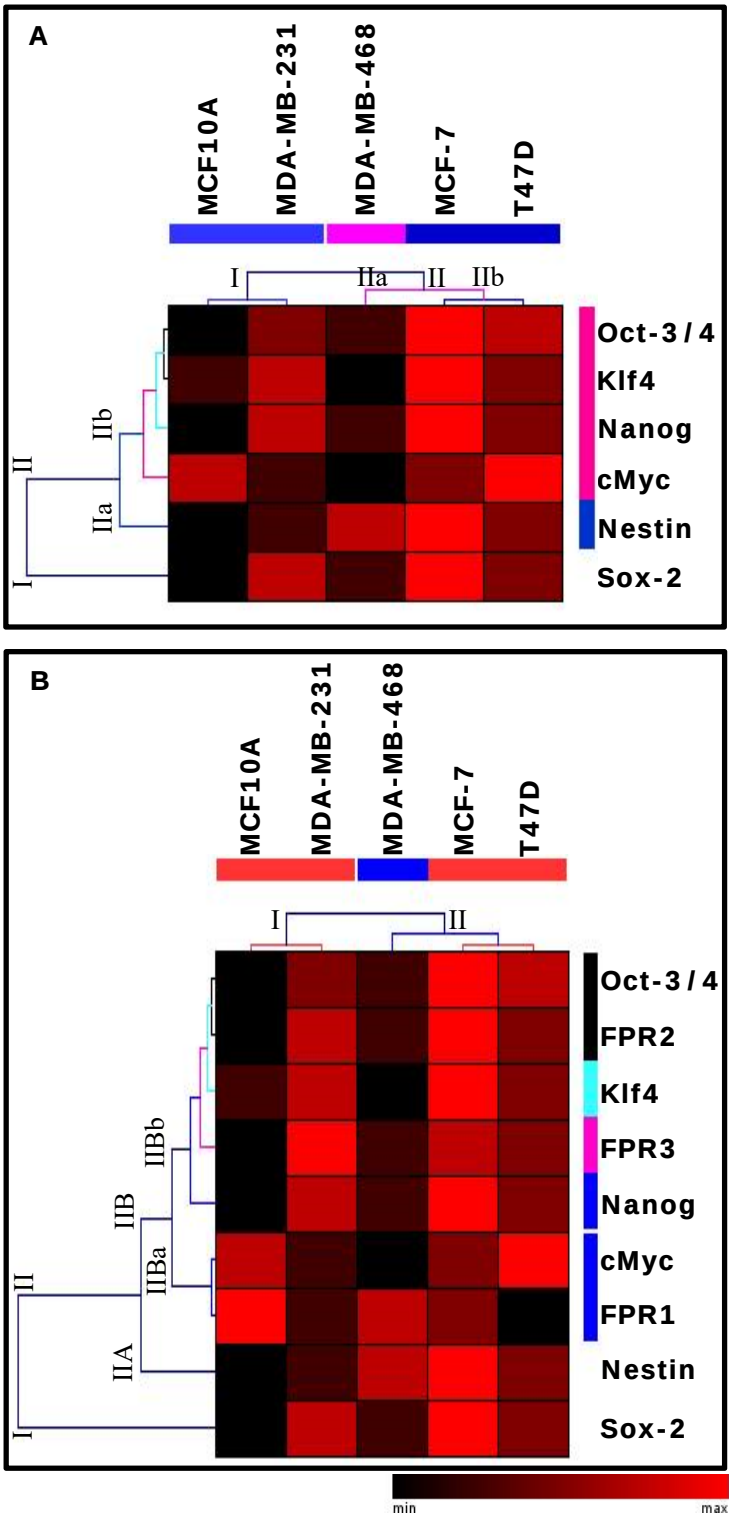

Fig-RB 10: Two way hierarchical clustering of genes: Two way hierarchical cluster of gene expression data using average linkage clustering and default distance setting using Genesis software. (A) Clustering of genes for stem cell markers and cell lines and (B) Clustering of genes of stem cell markers & FPR and cell lines.

markers alone. Two major clusters, one with MCF-10A & MDA-MB-231 and another with MCF-7, T47D, and MDA-MB-468 (Fig-RB 10B) were seen. This again indicated association of ER-PR positivity on gene expression pattern of HBCC. Dendrogram for gene clustering branches into two major clusters -I, and II, which was similar to previous clustering. Cluster-I was single gene cluster and included only Sox-2. Cluster-II was further branched into to clusters – cluster-IIA and cluster-IIb. Cluster-IIA was again a single gene cluster and included nestin. Further branching subdivided the cluster-IIB into two subordinate clusters -IIBa & IIBb. Cluster-IIBa formed a group of two genes - FPR1 and cMyc, which showed similar expression pattern in HBCC. Cluster-IIBb was a group of few small and close clusters. It included three stem cell marker genes -oct-3/4, klf4, and nanog, along with FRP2 and FPR3. It indicated that expression pattern of FPR2 closely matched with the expression pattern of oct-3/4, which was serially followed by klf4, FPR3 and nanog. Hence, it could be said that expression of these genes might be affected by or related to each other.

Protein

It was seen that the gene expression pattern of the stem cell markers closely resembled the expression pattern of FPRs. Hence, expression of three main Yamanaka factors and CD markers -CD24 & CD44 was studied in the HBCC before and after treatment of fMLP, to see if activation of FPR receptors has any effect on the expression patterns of these stem cell markers at the protein level. % positivity below 10% was considered as negative for all the markers.

Oct-3/4

Expression of Oct-3/4 was highest in MDA-MB-468, followed by T47D and MCF-10A (Fig-RB 11A & 12, Table-RB 7). Expression of Oct-3/4 was not seen in MCF-

7 & was very low in MDA-MB-231. After treatment with fMLP there was increase in the Oct-3/4 in % positive cells in all the cell lines except MDA-MB-231, which became negative (Fig-RB 12A & 12B, Table-RB 7). After fMLP treatment, Oct-3/4 expression was induced in MCF-7, wherein 48% cellular positivity was observed. Others showed increase in % positivity of cells as well as slight increase in expression.

Nanog

Similar to nanog m-RNA expression and Oct-3/4 protein expression, nanog protein expression was highest in MDA-MB-468 (Fig-RB 11B, Table-RB 7). More than 90% MDA-MB-468 cells were positive for nanog. However, other cell lines did not follow the mRNA expression pattern for nanog. MDA-MB-468 and T47D were the only two HBCC that were positive for the nanog. Both MCF-7 and MDA-MB-231 were negative for nanog protein expression. In MCF-10A, 35% cells showed weak positivity for nanog. After fMLP treatment, nanog expression slightly increased in all the cell lines except MDA-MB-231 (Fig-RB 11B & 11E). In MDA-MB-231, even after fMLP treatment, the cells remained negative for nanog. After fMLP stimulation, 23.3% MCF-7 cell showed positivity. After fMLP stimulation, MCF-10A, MDA-MB-468, and T47D showed 1.13, 1.14, and 1.26 fold increase in MFI and 13%, 5.5% and 16% increase in cell positivity, respectively. Thus, considerable increase (>10%) in nanog expressing cells is observed in normal breast epithelial cell line and triple positive HBCC.

Sox-2

Expression of Sox-2 was not seen in any of the cell lines, except MCF-7. Only MCF-7 showed very weak expression of Sox-2 in about 10% cells (Fig-RB 11C, Table-RB 7). After fMLP treatment, Sox-2 expression was observed in MCF-7,

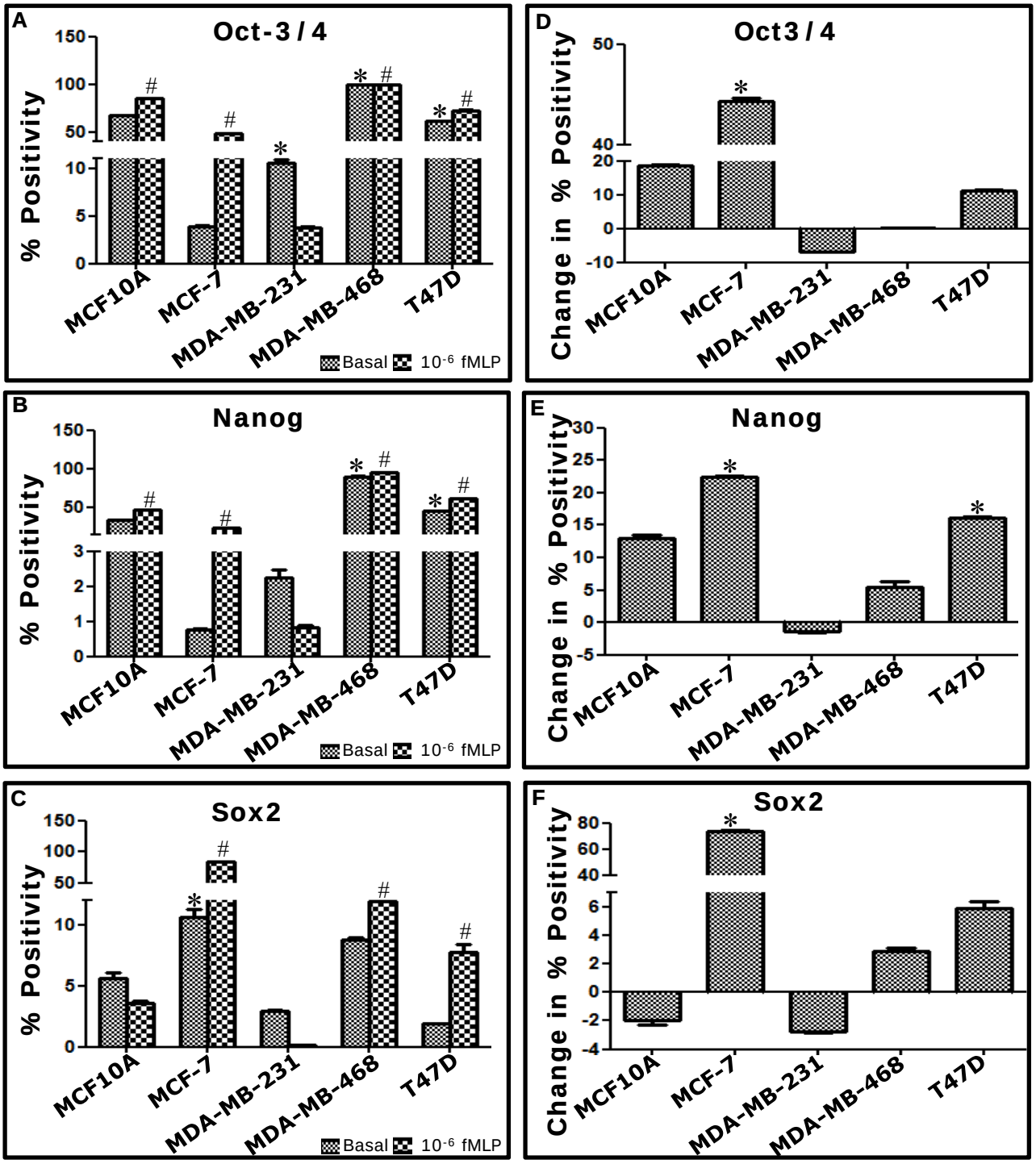

Fig-RB 11: Expression of stem cell markers proteins in HBCC: Bar plots showing average % positive cells ± SEM for Oct-3/4 (A), Nanog (B), & Sox2 (C) in HBCC and MCF-10A (n=3). Increase in the expression of stem cell markers after fMLP treatment is presented as change in percent positivity (% positivity after fMLP treatment - % positivity in control) for Oct-3/4 (D), Nanog (E), & Sox2 (F) (n=3). * $p<0.05$ wrt MCF-10A (Mann-Whitney test), # $p<0.01$ wrt the respective control (Wilcoxon pair test).

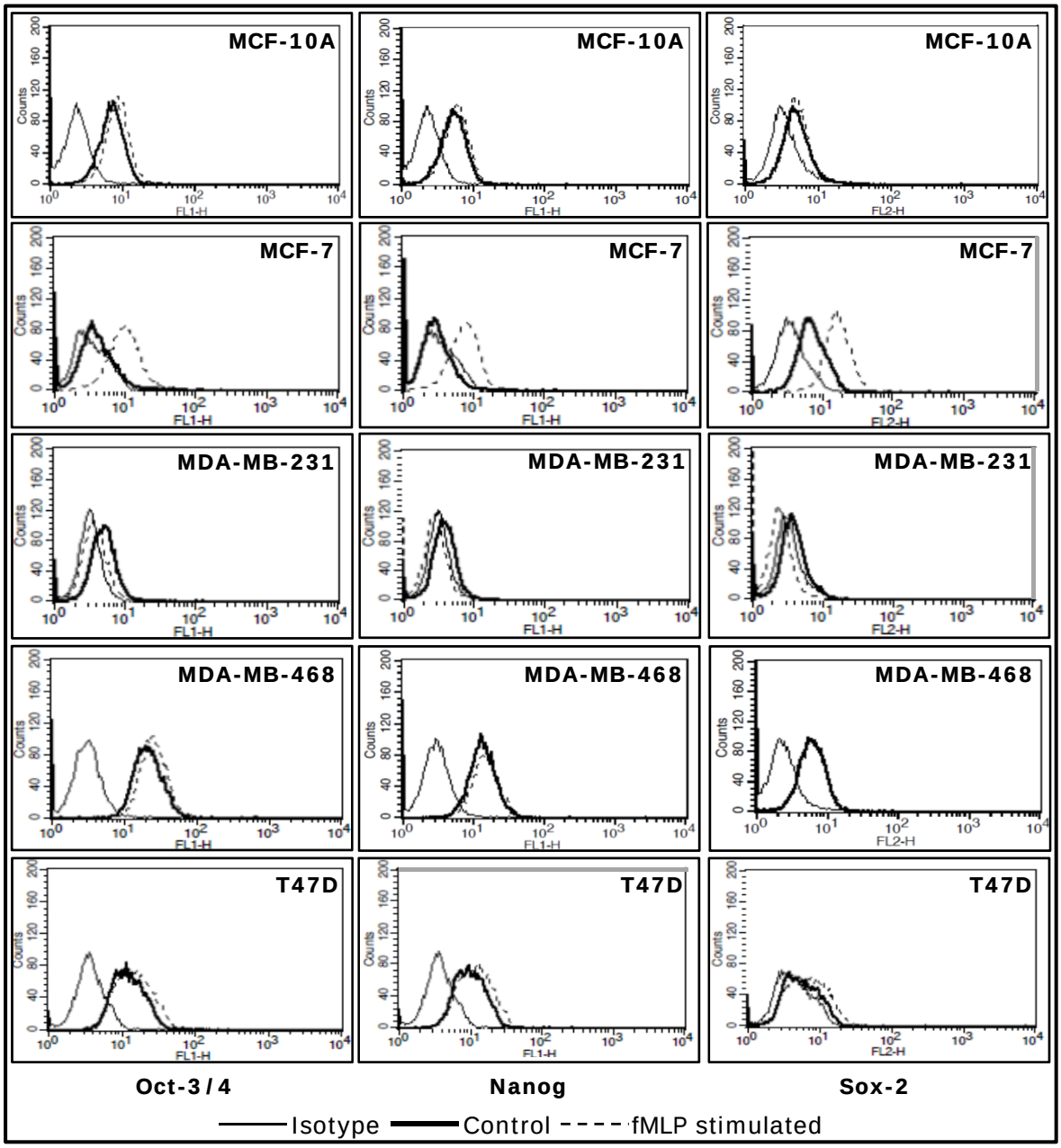

Fig-RB 12: Expression of stem cell markers proteins: Representative histogram overlays showing expression of Oct-3/4, Nanog & Sox2 in HBCC and MCF-10A as indicated.

where MFI increased from 6.2 to 15.9, a 2.6 fold increase and % positivity rose from 10.6% to 85% (Fig-RB 11C & 11F). All other cell lines remained negative for Sox-2 expression even after fMLP treatment.

It can be seen in the above results that there were differences in the expression pattern of stemness markers in the HBCC. Except MDA-MB-231, there was always increase in the expression of stemness markers or % positive cells, after fMLP treatment. Among all, MCF-7 had responded strongly to fMLP treatment where expression of Nanog, Oct-3/4, and Sox-2 had shown a noteworthy increase after fMLP treatment.

Basal levels of Oct-3/4, Nanog & Sox-2 protein and their increase after fMLP appeared to be independent of sFPR expression. MDA-MB-231, which had high sFPR1 and sFPR3, were negative for Oct-3/4, Nanog, and Sox-2 and fMLP treatment did not have any effect on expression of these proteins. Whereas T47D with high sFPR3 showed expression of Oct-3/4 and Nanog and after fMLP treatment, only slight increase in both these markers was seen. Cell lines with high sFPR2 -MCF-7 and MDA-MB-468 too had contrasting basal levels for Oct-3/4 and Nanog however, both of them were negative for Sox-2. Increase in Oct-3/4, Nanog, and Sox-2 expression was seen in MCF-7, but only slight increase was seen in MDA-MB-468. Furthermore, the levels of these stemness markers were also independent of ER-PR status as two triple negative cell lines -MDA-MB-231, MDA-MB-468, and two ER-PR positive cell lines MCF-7 and T47D showed contrasting levels of these markers between themselves. However, it was worth noting that triple positive cell line with, high mFPR2 & sFPR2 and good FPR ligand binding –MCF-7 showed induction of Oct-3/4, Nanog and Sox-2 upon fMLP stimulation while other triple positive and FPR2 positive cell line, T47D which

express the lower mFPR2 & sFPR2 and ligand binding than that of MCF7 showed only slight increase in Oct-3/4 & Nanog. Hence, it could be postulated that fMLP after binding to FPR2 induced expression of Oct-3/4, Nanog, and Sox-2.

$CD44^{++}/CD24^{--}$

In breast cancer $CD44^{++}/CD24^{--}$ population is considered undifferentiated population and $CD44^{++}/CD24^{--}$ is used as a maker for breast cancer stem cells[277]. In our experiments, all the HBCC showed less positivity for $CD44^{++}/CD24^{--}$ than normal epithelial cell line (Fig-RB 13 & 14, Table-RB 7). In MCF-10A, 32% cells were $CD44^{++}/CD24^{--}$ while only 20% and 16% cell population of MCF-7 and MDA-MB-231 showed $CD44^{++}/CD24^{--}$ phenotype. MDA-MB-468 and T47D were negative for $CD44^{++}/CD24^{--}$. After fMLP treatment, significant increase in the cells showing $CD44^{++}/CD24^{--}$ phenotype was observed in MCF-10A. The % positivity reached to 61% from 32%. In MCF-7 and MDA-MB-231, changes in the $CD44^{++}/CD24^{--}$ population were not observed after fMLP treatment. The $CD44^{++}/CD24^{--}$ phenotype seems to be modulated by FPR1 in normal breast cell line as MCF-10A highest sFPR1 expressing cell line showed the tremendous increase after fMLP treatment, but HBCC were unaffected. When results of $CD44^{++}/CD24^{-}$ expression were compared with the results of Oct-3/4, Sox-2 and Nanog protein expression it was found that both these results were opposite to each other. Since $CD44^{++}/CD24^{--}$, Oct-3/4, Sox-2 and Nanog are indicator of cellular stemness, their results were expected be at par. However, it was found that highest Oct-3/4 and Nanog expressing cell line –MDA-MB-468 did not show $CD44^{++}/CD24^{--}$ population. MCF-7 and MDA-MB-231, which were negative for Oct-3/4, Sox-2, and Nanog were positive for $CD44^{++}/CD24^{--}$.

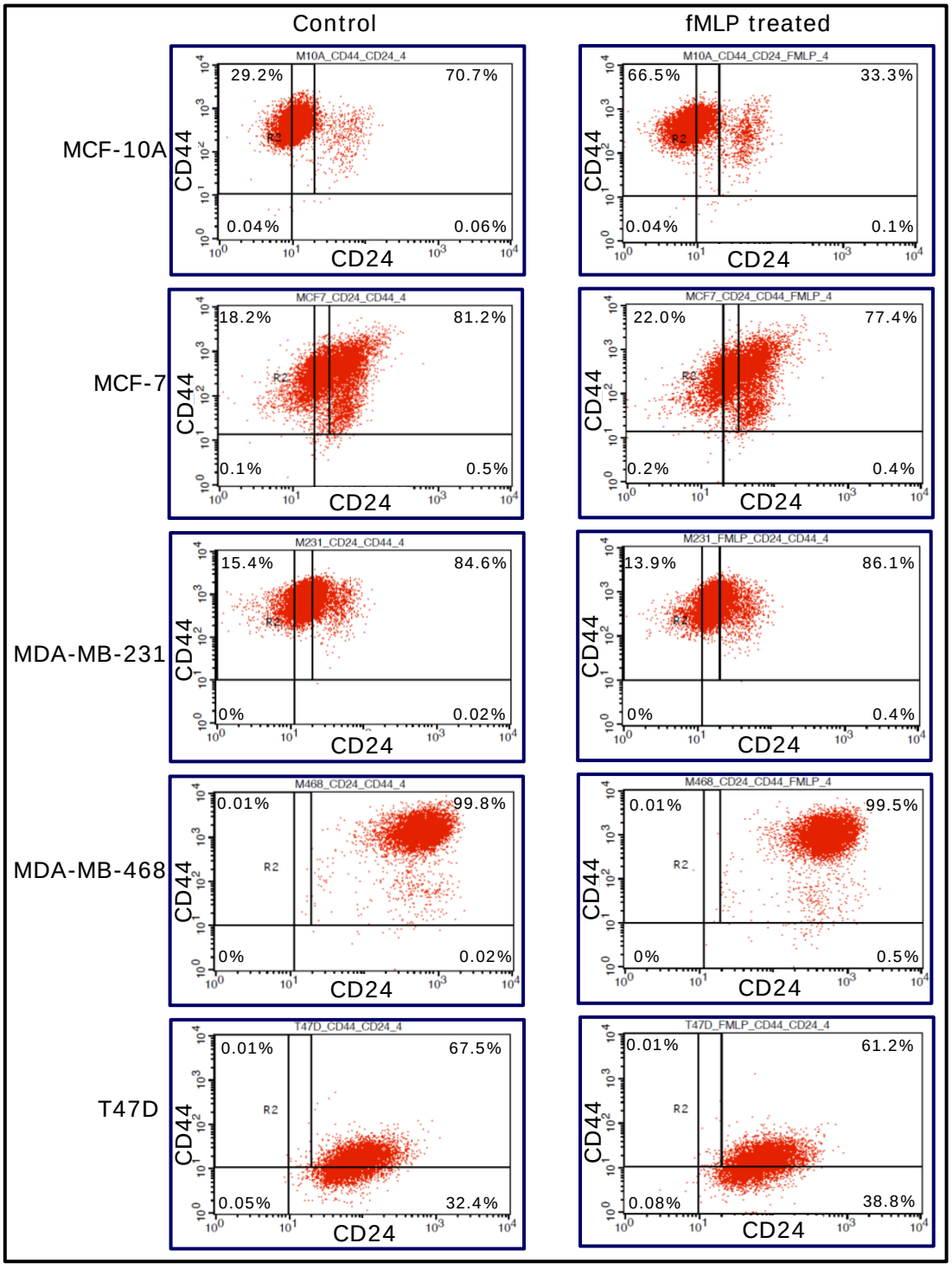

Fig-RB 13: Detection of $CD44^{++}/CD24^{--}$ population: Representative dot-plots of HBCC and MCF-10A cells stained for CD24 and CD44 before and after fMLP treatment. No. in quadrants indicate % positive cells.

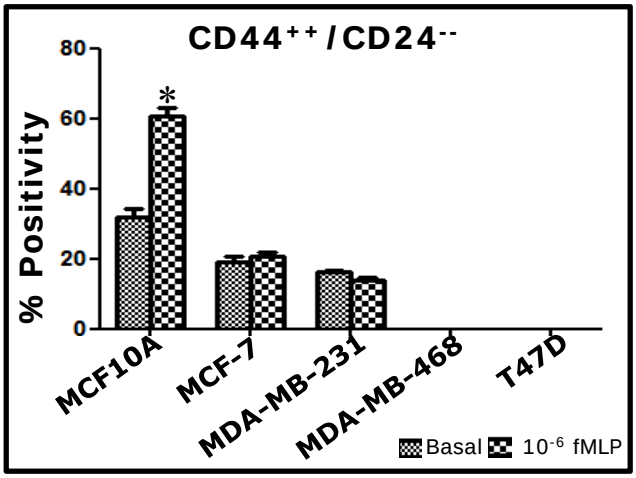

Fig-RB 14: Estimation of $CD44^{++}/CD24^{--}$: Bar plots showing % cells that have $CD44^{++}/CD24^{--}$ phenotype in HBCC and MCF-10A. Data is presented as average ± SEM (n=3). * $p<0.05$ wrt the respective control (Wilcoxon pair test).

Table-RB 7: Surface expression of stem cell markers

Cell lines / Treatment		MCF-10A		MCF-7		MDA-MB-231		MDA-MB-468		T47D	
		Control	fMLP	Control	fMLP	Control	fMLP	Control	fMLP	Control	fMLP
Oct-3/4	Median	7.0 ± 0.02	8.7 ± 0.04	3.6 ± 0.01	9.7 ± 0.04	4.6 ± 0.01	3.6 ± 0.01	19.5 ± 0.26	24.4 ± 0.32	11.4 ± 0.04	14.0 ± 0.08
	% Positivity	67.0 ± 0.23	85.8 ± 0.12	3.9 ± 0.08	48.2 ± 0.37	10.6 ± 3.7	3.7 ± 0.13	99.4 ± 0.07	99.9 ± 0.11	61.6 ± 0.5	72.9 ± 0.19
Nanog	Median	5.2 ± 0.02	5.8 ± 0.02	2.7 ± 0.01	7.4 ± 0.02	3.6 ± 0.01	2.8 ± 0.01	12.8 ± 0.22	14.6 ± 0.11	9.3 ± 0.04	11.7 ± 0.04
	% Positivity	34.6 ± 0.30	47.6 ± 0.28	0.8 ± 0.03	23.3 ± 0.12	2.3 ± 0.23	0.8 ± 0.07	90.3 ± 0.68	95.8 ± 0.14	45.3 ± 0.25	61.6 ± 0.17
Sox-2	Median	3.3 ± 0.36	3.4 ± 0.42	6.2 ± 0.12	15.9 ± 0.11	3.5 ± 0.01	2.4 ± 0.01	5.9 ± 0.05	6.4 ± 0.10	5.2 ± 0.05	6.3 ± 0.19
	% Positivity	5.6 ± 0.50	3.6 ± 0.17	10.6 ± 0.70	85.0 ± 0.32	2.9 ± 0.12	0.2 ± 0.02	8.8 ± 0.14	11.9 ± 0.62	1.9 ± 0.03	7.8 ± 0.63
$CD44^{++}/CD24^{--}$	% Positivity	32.0 ± 2.36	60.6 ± 2.39	19.2 ± 1.25	20.8 ± 0.92	16.2 ± 0.55	14.1 ± 0.45	0.01 ± 0.01	0.0 ± 0.00	0.01 ± 0.003	0.02 ± 0.01

In view of the above observations, there is need for further investigation to determine the true breast cancer stemness marker.

We have demonstrated that mRNA expression of four stemness marker Nanog, Nestin, Oct-3/4, and Sox-2 was higher in HBCC. Expression of Klf-4 was higher in HBCC except MDA-MB-231 than MCF-10A, while expression of cMyc was lower in HBCC except T47D than MCF-10A. When protein expression was examined for the three main Yamanaka factors –Oct-3/4, Sox-2 and Nanog, it was seen that MCF-7 and MDA-MB-231 were negative for all three while MDA-MB-468, T47D and MCF-10A expressed Oct-3/4 and nanog, but were negative for Sox-2. These results indicate that breast cancer cell lines showed higher expression of transcription factors involved in cellular pluripotency while normal breast epithelial cell line MCF-10A showed higher expression of cell surface markers for pluripotency. MDA-MB-468, turns out to be the most stem (like) cells among HBCC as it has the highest expression of klf-4, nanog, nestin and oct-3/4 genes and Oct-3/4 and Nanog protein. However this cell lines did not showed any cellular positivity for $CD44^{++}/CD24^{--}$. In view of the varied results for the stem cell markers, selecting most suited marker is difficult and needs further characterization of the cell lines using functional tests for cellular stemness. mRNA expression pattern of KLf4, Oct-3/4 and Sox2was similar to mFPR2 and mFPR3 expression. Expression pattern of cMyc in HBCC was inverse to mFPR1. These observations strengthened our hypothesis that FPR played role in cellular stemness in HBCC. This hypothesis was confirmed by the results when fMLP stimulation showed increase in the protein expression of Oct-3/4, Nanog, Sox-2, and cellular positivity for $CD44^{++}/CD24^{-}$phenotype. However the increase in these markers upon fMLP stimulation in HBCC was cell line dependent. The

highest responsive cell line for increase in Oct-3/4, Nanog and Sox-2 was MCF-7, while for $CD44^{++}/CD24^{-}$phenotype MCF-10A showed the highest increase. MDA-MB-231 was the only cell line which was non-responsive to fMLP stimulation. Increase in the expression of Sox-2 was the highest upon fMLP stimulation in MCF-7 among the three marker. Oct-4 and Nanog expression were reported to be significantly associated with tumor pathology and poor prognosis in breast cancer patients[278]. When nanog was co-expressed with Wnt-1 in the mouse mammary gland, it promoted mammary tumorigenesis and metastasis[279]. Nanog and Oct4 are expressed at high levels in multiple types of cancers, including breast cancer[280-284]. Recent findings have shown that the pluripotency factor Nanog is overexpressed in poorly differentiated breast cancers and its expression correlated with poor prognosis[285]. Additionally, it was found that the co-expression of Nanog and Oct4 promotes the EMT and enhances cancer stem-like properties in lung adenocarcinoma cells[281]. In MCF7 cells, overexpression of Nanog1 or NanogP8 was found to promote cancer stem cell characteristics[286]. Sox2 is expressed in early stage breast tumors[287, 288]. Over-expression of Sox2 increased mammosphere formation, Sox2 knockdown prevented mammosphere formation and delayed tumor formation in xenograft tumor initiation models[288]. Sox2 expression has been observed in 43% of basal cell-like breast carcinomas, suggesting a role in conferring a less differentiated phenotype[289]. Sox2 expression has been reported from normal mammary stem cells when cultured as mammospheres and is lost as the cells differentiate in vitro[290]. Sox2 expression was seen in mammospheres obtained from human breast tumor cell cultures, and from MCF7 and T47D cells[288]. These reports suggested that expression of Oct-3/4, Nanog and Sox2 involved in promoting stem cell

characteristic in breast cancer cells. Since stimulation of FPR by fMLP increased expression of these three proteins in HBCC, FPR probably involved in inducing stem cell phenotype in breast cancer cells too.

Basal expression of E-cadherin, Cox-2 and PTEN in HBCC

Apart from the FPR and stemness or differentiation marker genes, expression of three more genes –E-cadherin, cox-2 and pten was checked in HBCC. These genes are used as marker genes in breast cancer[291-295]. Role of these genes was very well established in breast cancer pathogenesis. These genes also showed functional association with FPR[142, 296-298].

Epithelial cadherin (E-Cadherin)

Cadherin-1 or E-cadherin, which is also known as CAM 120/80 or uvomorulin, is encoded by the CDH1 gene, in humans. E-cadherin is a calcium-dependent cell-cell adhesion glycoprotein[299]. Mutations in this gene are correlated with gastric, breast, colorectal, thyroid, and ovarian cancers[300, 301]. Loss of function of E-cadherin is thought to contribute to cancer progression by increasing proliferation, invasion and/or metastasis[300, 301].

In the present studies, normal breast epithelial cell line MCF-10A did not show expression of E-cadherin mRNA, whereas all the HBCC expressed E-cadherin (Fig-RB 15A, Table-RB 8). Expression of E-cadherin gene was negligible in MDA-MB-231, whereas it was very high in T47D. Expression of E-cadherin was at par in MCF-7 and MDA-MB-468. Expression of E-cadherin was inversely related to the expression of FPR1 (Fig-RB 16C, 16D & 16E). The highest FPR1 expressing cell lines MCF-10A and MDA-MB-231 did not express considerable E-cadherin and the least FPR1 expressing cell line T47D showed the highest expression of E-cadherin.

Table-RB 8: Basal Expression of Genes for Signalling Molecules

Fold Change					
	MCF-10A	**MCF-7**	**MDA-MB-231**	**MDA-MB-468**	**T47D**
CDH-1@	Absent	1.00 ± 0.00	0.07 ± 0.01	1.02 ± 0.02	365.2 ± 22.8
Cox-2*	1.00 ± 0.00	0.7 ± 0.08	2.05 ± 0.07	0.82 ± 0.02	1.55 ± 0.21
Pten*	1.00 ± 0.00	1.35 ± 0.03	0.64 ± 0.06	1.69 ± 0.13	4.66 ± 0.12
@ With respect to MCF-7, * With respect to MCF-10A, N.F.: Not found					

It has been reported earlier that <70-80% confluent MCF-10A did not express E-cadherin[302]. Among HBCC, lowest E-cadherin was expressed by MDA-MB-231, while T47D expressed the highest. Cadherin-1 also known as E-cadherin, CAM 120/80 or uvomorulin. E-cadherin is a calcium-dependent cell-cell adhesion glycoprotein[299]. Mutations in this gene are correlated with gastric, breast, colorectal, thyroid, and ovarian cancers[300, 301]. Loss of function of E-cadherin is thought to contribute to cancer progression by increasing proliferation, invasion, and/or metastasis[300, 301]. E-cadherin is also used as a diagnostic marker for breast cancer. E-cadherin expression is also dependent on cellular confluency, hence care was taken during cell harvesting. All the cell lines were ~60-70% confluent while harvested for mRNA to examine E-cadherin expression. Normal breast epithelial cell line –MCF-10A did not express E-cadherin. Since loss of E-cadherin was associated with the aggressiveness of the cancer and MDA-MB-231 is the most aggressive cell line among all HBCC tested, the lowest E-cadherin expression in MDA-MB-231 is justified. However, it's worth noting that E-cadherin expression showed inverse relationship with mFPR1 while matched with

the expression pattern of FPR2 and FPR3. This could be another indication of probable role of FPR in breast cancer.

Cyclooxygenase-2 (Cox-2)

Cox-2 is also known as Prostaglandin-endoperoxide synthase 2 and prostaglandin G/H synthase. Cox-2 is not expressed under normal conditions in most of the cells, but high expression is found during inflammation[303]. Expression of cox-2 is very well associated with various parameters of aggressive breast cancer[303] such as mutagenesis, mitogenesis, angiogenesis, reduced apoptosis, metastasis and immunosuppression.

In our studies, expression of cox-2 did not show distinction between HBCC and normal epithelial cell line (Fig-RB 15B, Table-RB 8). Expression of cox-2 in MDA-MB-231 and T47D was significantly higher than that in MCF-10A. It was maximum in MDA-MB-231, followed by T47D. Expression of cox-2 was significantly lower in MCF-7 than that in MCF-10A. Expression of cox-2 in MDA-MB-468 and MCF-10A were at par. The expression pattern of the cox-2 gene matched with the expression pattern of the FPR1 gene in HBCC except for T47D (Fig-RB 15E). The highest FPR1 expressing HBCC – MDA-MB-231, also expressed the highest cox-2. However, in contrast to mFPR1, T47D showed higher expression of cox-2 than that in MDA-MB-468, MCF-7 and MCF10A.

Virchow et al.[304] first suggested that chronic inflammation leads to cancer development by increasing cellular proliferation[305]. Since then various carcinogenesis theories have been proposed involving inflammatory stimuli and mediators of wound healing[306, 307]. The recent developments have relighted interest in the link between inflammation and cancer, and various models of carcinogenesis have been proposed involving inflammatory stimuli and COX-2

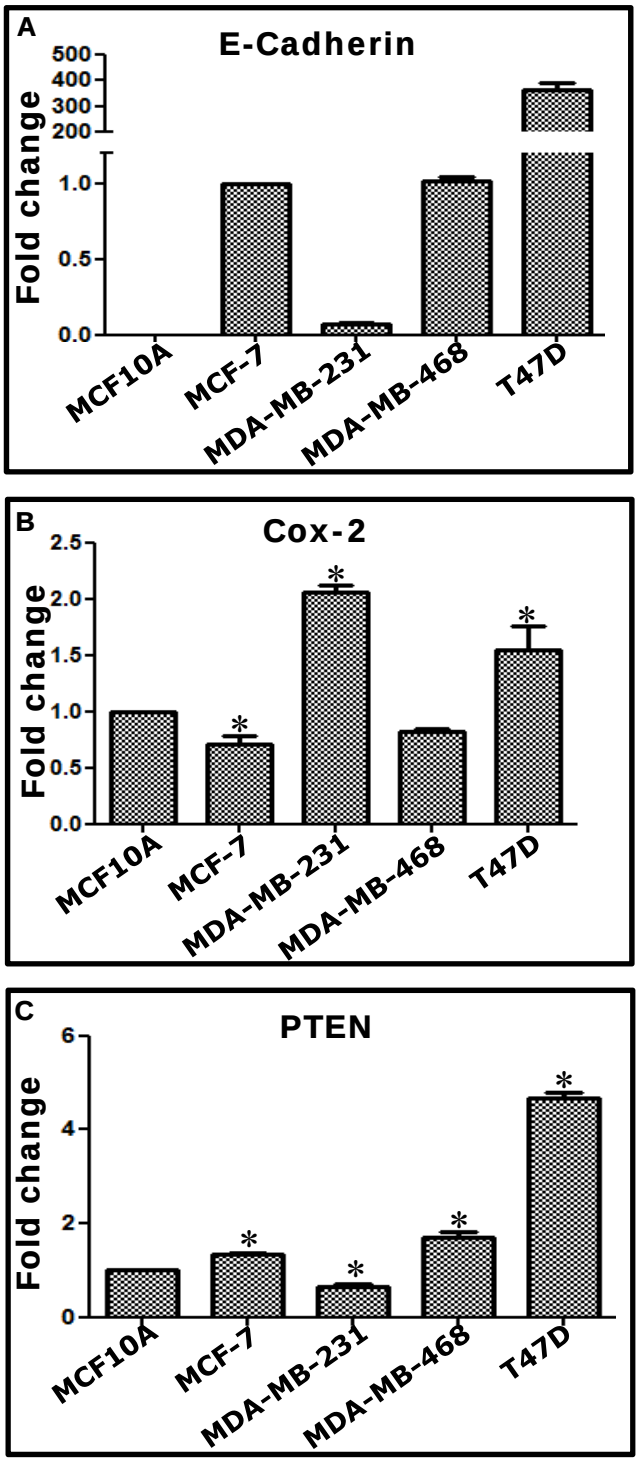

Fig-RB 15: Basal expression of E-cadherin, Cox-2 and PTEN in HBCC: Expression of E-cadherin (A), Cox-2 (B) and Pten (C) in various HBCC with respect to the normal breast epithelial cell line MCF-10A, as estimated by QPCR. Gene expressions were normalized with GAPDH expression. Data is presented as average fold change ± SEM (n=3); * $p<0.05$ wrt MCF-10A (Mann-Whitney test).

expression[303]. Cox-2 is also known as Prostaglandin-endoperoxide synthase 2 and prostaglandin G/H synthase. In most of the cells, Cox-2 is not expressed under normal conditions but high expression is found during inflammation[303]. As expected the highly aggressive cell line MDA-MB-231, which showed the highest expression of FPR1, expressed the highest cox-2 gene. Cox-2 gene expression levels in MCF-7 and MDA-MB-468 were at par with MCF-10A, while T47D expressed higher cox-2 than these three cell lines. Normal breast tissues usually do not express cox-2, hence expression of the cox-2 in MCF-10A was unusual. During cell line development process various changes were observed due to which cell line behaves differently than its parental tissue. This could be the reason that MCF-10A being normal epithelial cell line express cox-2. Expression of cox-2 is very well associated with various parameters of aggressive breast cancer[303] such as mutagenesis, mitogenesis, angiogenesis, reduced apoptosis, metastasis and immunosuppression. FPR1 and FPR2 activation with their ligand also induced cox-2 production. fMLP binding to human amnion derived WISH cells induced release of (PG)E2 via cox-2 activation[229]. Similarly activation of FPR2 by SAA in monocyte induced cox-2 production which in turn induced production of cytokine CCL2[308]. As mentioned in earlier reports that activation of FPR by its ligand induced cox-2 production. Our results also complimented those finding as cluster analysis showed close correlation between expression of FPR1 and cox-2 gene.

PTEN

Phosphatase and tensin homolog (PTEN) acts as a tumor suppressor gene through its phosphatase action[309]. This phosphatase is involved in the regulation of the cell cycle. It prevents cells from growing and dividing too rapidly[309]. It

negatively regulates intracellular levels of phosphatidylinositol-3,4,5-trisphosphate in cells and functions as a tumor suppressor by negatively regulating Akt/PKB signalling pathway[309].

All the HBCC except MDA-MB-231 showed higher expression of pten mRNA than that in MCF-10A. The highest pten expression was seen in T47D while its expression in MCF-7 and MDA-MB-468 was at par. MDA-MB-231 showed the least expression of the pten gene (Fig-RB 15C, Table-RB 8). In HBCC, expression pattern of pten was also inversely related to the expression of FPR1 and it matched with the expression pattern of cMyc (Fig-RB 16E & 16F). The highest FPR1 expressing cell lines MCF-10A and MDA-MB-231 expressed lower pten and the least FPR1 expressing cell line T47D showed the highest expression of pten.

Phosphatase and tensin homolog (PTEN) acts as a tumor suppressor gene through its phosphatase action[309]. This phosphatase is involved in the regulation of the cell cycle. It prevents cells from growing and dividing too rapidly[309]. It negatively regulates intracellular levels of phosphatidylinositol-3,4,5-trisphosphate in cells and functions as a tumor suppressor by negatively regulating Akt/PKB signalling pathway[309]. All other HBCC showed higher pten gene expression that that in MCF-10A. In line with the previous results, MDA-MB-231 again showed characteristic feature of highly aggressive of metastatic cell line as among all the cell lines it showed the least expression of pten gene. T47D, which is the most slow growing cell line among all the HBCC showed the highest pten expression. This suggested that pten mRNA expression might be inverse to cell proliferation in HBCC. In cluster analysis, pten gene was clustered with FPR1, which showed close correlation between expression of FPR1 and pten gene expression in HBCC. PTEN played an important role in fMLP mediated

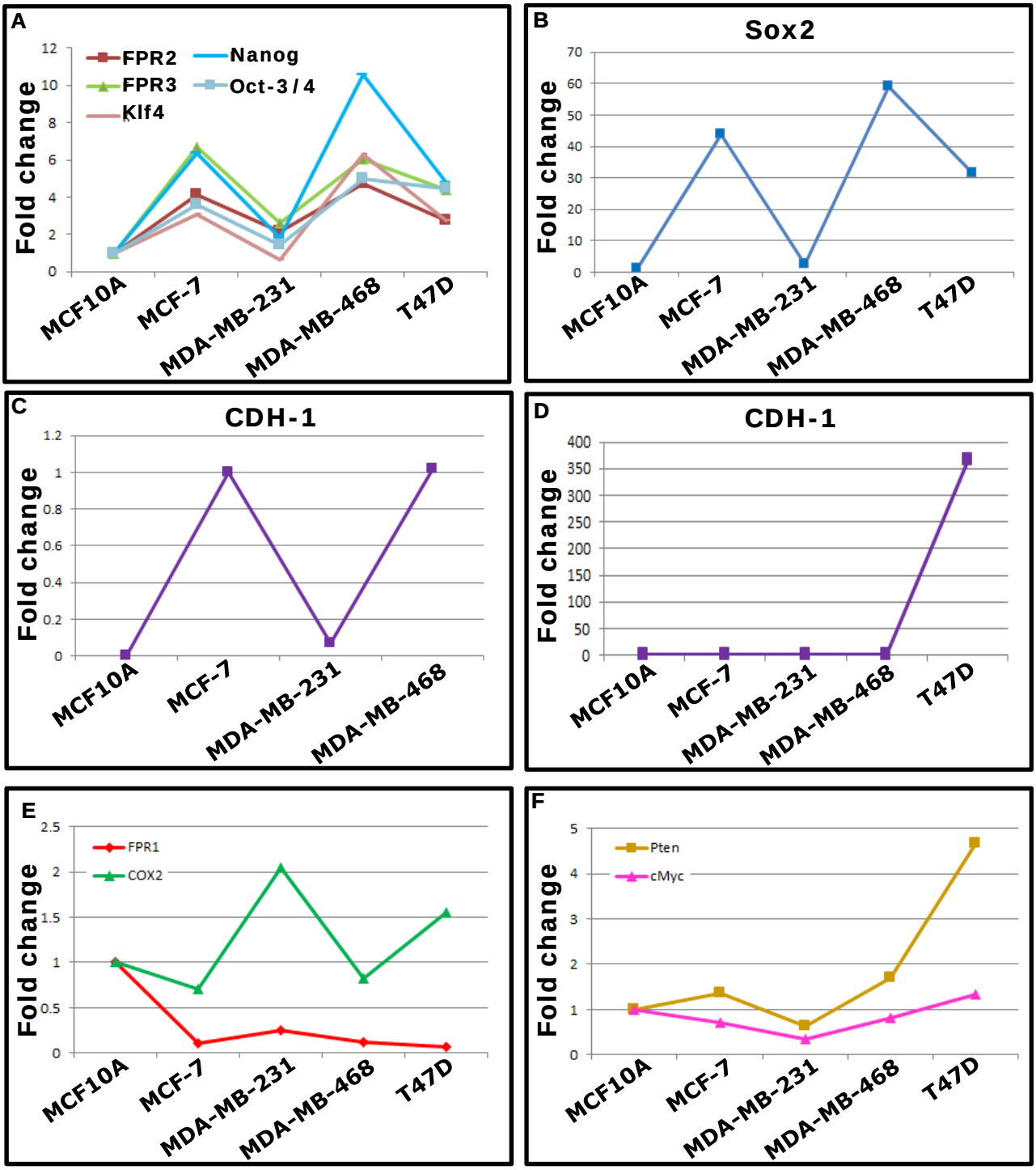

Fig-RB 16: Comparative Gene Expression Patterns in HBCC: Line plots of expression of various genes showing similar trends in the expression patterns among different HBCC and MCF-10A. (A) Line plots showed similarity pattern for gene expression of FPR2, FPR3, Klf4, Nanog, & Oct-3/4. Gene expression pattern of Sox2 (B), CHD-1 (C 7 D), FPR & COX2 (E) PTEN & cMyc (F) are seen.

chemotaxis of PMNL[310]. fMLP binding activated PI3K, which induced the conversation of PIP2 in PIP3 and thereby stimulated chemotaxis[142, 310]. On other hand fMLP also activated p38-MAPK which activated PTEN. PTEN localized to the sides and rear end of the crawling cell, converted PIP3 back to PIP2 in areas of the cell away from the leading edge and insulated those areas from receiving any other signals[142, 310]. In breast and other cancers loss of PTEN function was reported. Loss of PTEN in cancer led to the increased concentration of PIP3, which resulted in constitutive activation of downstream component of PI3K pathway leading to cell motility[311]. Cluster analysis showed that FPR1 and pten gene expressions were closely related. It was observed that overall gene expression pattern for all the genes studied in HBCC, MCF-7 and MDA-MB-468 were at par for the most of the genes, whereas MDA-MB-231 and T47D were distinctly different. Complete gene expression data from the present study, including mFPR expression data, stem cell marker expression data, and basal expression of E-cadherin, cox-2 & pten were subjected to two way, unsupervised hierarchical clustering. At the top of the hierarchy, cell lines formed two main clusters – cluster-I and cluster-II (Fig-RB 17). Cluster-I was further branched into two sub-clusters –cluster-IA and cluster-IB. Cluster-IA consist of normal epithelial cell line –MCF-10A and triple negative cell line –MDA-MB-231. ER-PR positive cell line MCF-7 and triple negative cell line –MDA-MB-468 fell in cluster-Ib. Gene expression pattern of T47D was distinctly different from rest of the cell lines, hence it formed its own separate cluster –cluster-II. This observation indicated that on the basis of gene expressions MCF-7 & MDA-MB-468 and MDA-MB-231 & MCF-10A showed similar expression pattern while T47D did not matched with the expression pattern of any of them. At the genes, the

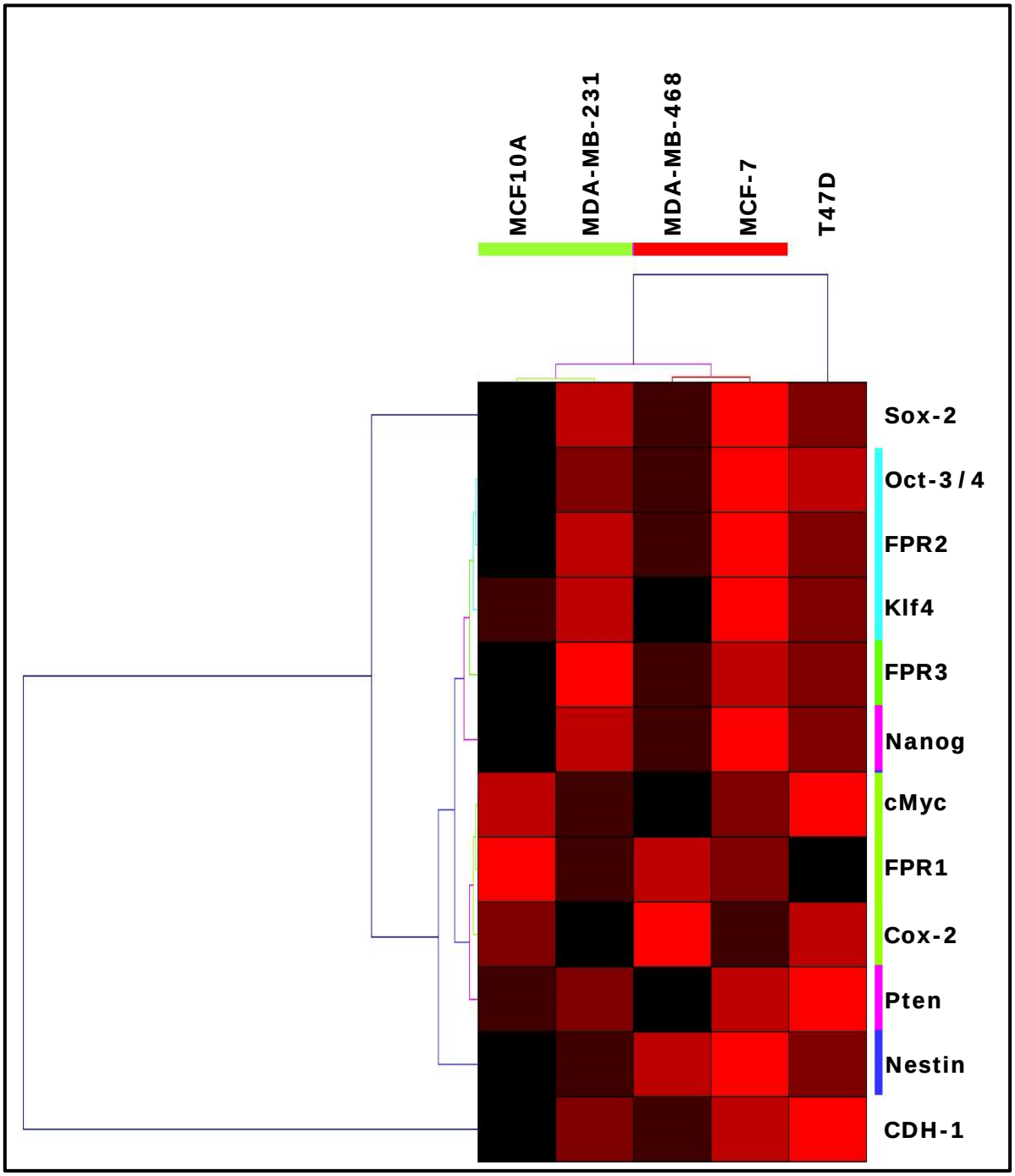

Fig-RB 17: Clustering of genes: Two way hierarchical cluster of gene expression data using average linkage clustering and default distance setting using Genesis software.

dendrogram branched into two main clusters namely Cluster-I and cluster-II. Cluster-I was single gene cluster and contained only E-cadherin. Cluster-II was further branched into two sub-clusters; cluster-IIA and cluster-IIB. Cluster-IIA divided into two groups –cluster-IIA-a and IIA-b. Cluster-IIA-a was a single gene cluster and contained only nestin. Cluster-IIA-b was further divided into two subordinate groups –group-IIA-b1 and group-IIA-b2. Group-IIA-b1 was group of three small and close cluster contained four genes –cMyc, FPR1, cox-2, and pten.

Among the genes in this group, cMyc and cox-2 are known to have role in cell proliferation and tumorigenesis[267-269, 312] while pten is involved in cell cycle regulation. On hierarchy, FPR1 was more close to cox-2 and cMyc; hence, it might be involved in cell proliferation and tumorigenesis. Group-IIA-b2 was group of few small and closely associated clusters. It contained oct-3/4, FPR2, Klf4, FPR3, and nanog. Apart from FPR2 and FPR3, rest three genes are associated with cellular stemness. Hence, from this observation it may be inferred that FPR2 and FPR3 might have role in cellular stemness. Expression patterns of E-cadherin, sox2 and nestin were completely different from the rest of the genes and hence they fell into separate clusters. Thus, the cluster analysis revealed the new possible role of FPR genes in the breast cancer. FPR2 and FPR3 might have role in stemness while FPR1 could be involved in cell proliferation.

Expression of FPR family genes as well as proteins was found to be altered in HBCC. Correlation of expression of FPR family genes with the stem cell marker genes was evident. Furthermore, binding of ligand to FPR and subsequent downstream events were also found to be altered in HBCC as compared to that in normal as well as among HBCC. It was seen that stimulation of FPR by its

ligand led to the increase in expression of stemness marker in triple positive, $CD44^{++}/CD24^{--}$ and high sFPR expressing cell lines MCF-7 and T47D. In view of these results, it would be interesting to look deep into FPR signalling and role of FPR in HBCC cell proliferation. Based on the above results, two fast growing cell lines, MCF-7 and MDA-MB-231 were chosen for further mechanistic studies to decipher the role of FPR in breast cancer transformation. The rationale of choosing these two cell lines were as follows:

1) MCF-7 is ER-PR and Her-2 positive cell line whereas MDA-MB-231 is triple negative.
2) These two cell lines represents different clusters for FPR gene and protein expression
3) They also represent two different clusters for stemness markers gene expression clusters.
4) They showed equal binding to FPR ligand fNLPNTL-FITC but responded differently for actin polymerization.
5) MCF-7 strongly responded to fMLP and showed increase in Oc-3/4, Nanog, and Sox-2 after fMLP stimulation but MDA-MB-231 did not respond to fMLP with respect to expression of these stemness markers.
6) Among all the HBCC, only these two cell lines showed $CD44^{++}/CD24^{-}$ population, which is considered as other parameter for stemness, especially for breast epithelial cells.
7) MCF-7 has wild type p53 gene while MDA-MB-231 expressed mutated p53.

Receptor cross talk in HBCC

As mentioned in the introduction, in recent years, expression of FPR has been reported in various cell types. However, signalling events activated by stimulation of FPR1 and FPR2 are known only in the hematopoietic cells. Since in the present studies, FPR expression was shown in the breast cancer cell lines; signalling stimulated by ligand binding to the FPR was investigated in breast cancer. Cross talk between FPR1 and EGFR has been reported in glioblastoma[59], but its existence in other cell systems is not explored. Hence, studies were carried out to investigate if such cross talk exists in breast cancer. Finally, it was also investigated whether the downstream molecules, were directly activated by FPR1/FPR2 stimulation or due to receptor cross talk.

Thus, following queries were addressed:

1. Which signalling pathways are stimulated by FPR1 and FPR2 after ligand binding?
2. Is there any cross talk between FPR1 and FPR2?
3. Is there any cross talk between FPR and growth factor receptor –EGFR in HBCC?
4. Is there any cross talk between FPR and cytokine receptor IL6R in HBCC?

To answer these questions, MCF-7 and MDA-MB-231 were treated with CsH (FPR1 inhibitor[313]), WRW4 (FPR2 inhibitor[314]), AG490 (JAK-STAT inhibitor[315]), AG1478 (EGFR inhibitor[316]), PP2 (Src kinase inhibitor[317]) or solvent. All these treated cells were then stimulated by either fMLP, WKYMVm, EGF, IL6 or solvent (solvent control). These cells were then analyzed by Western blotting for various molecules. To answer the aforementioned queries following signalling molecules were studied (Fig-RB 18).

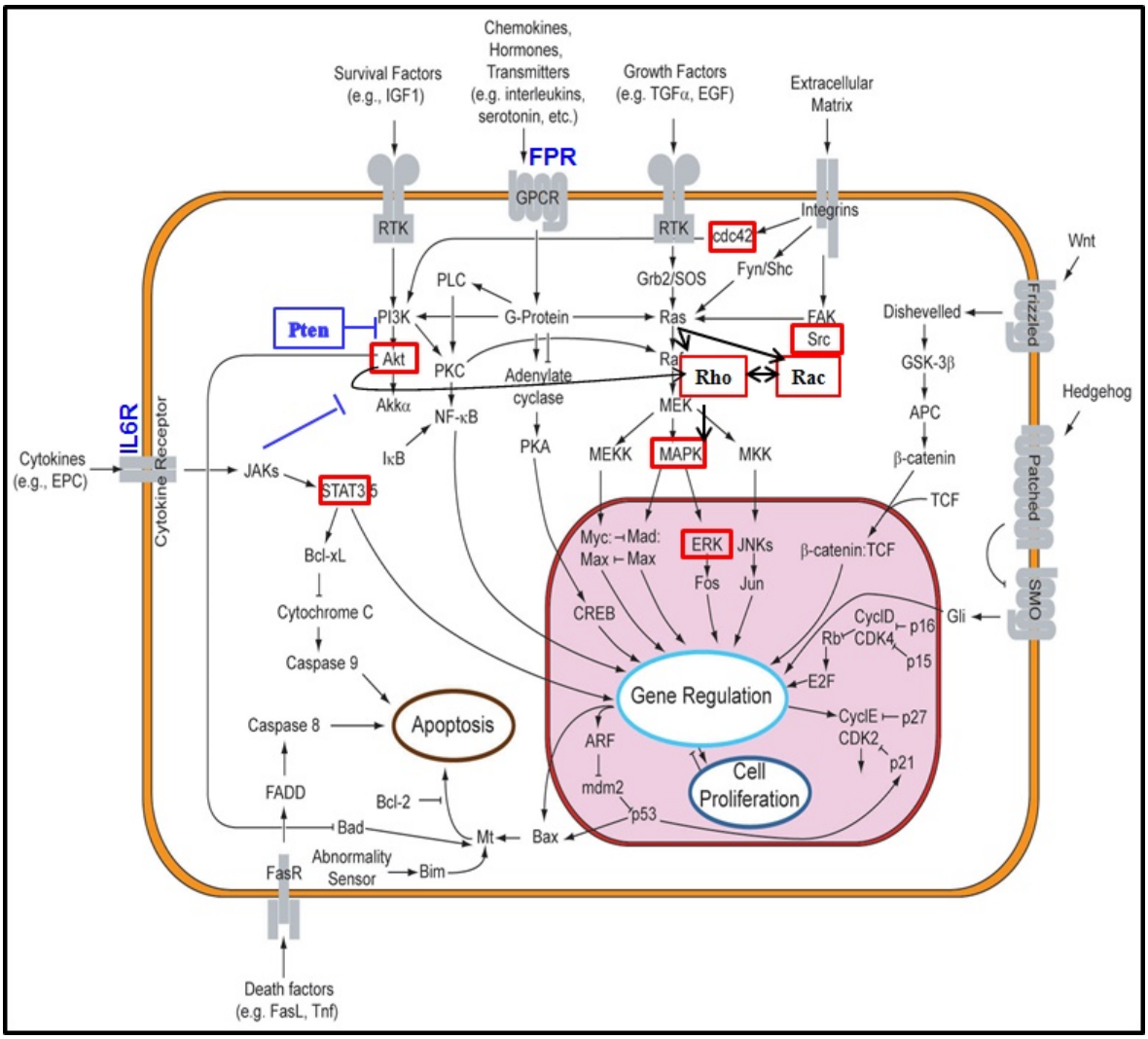

Fig-RB 18: Intracellular signalling pathway

1) EGFR transactivation: EGFR is a transmembrane glycoprotein, which is widely expressed in most of the cell types. It is a member of ErbB family[318]. Upon ligand binding, EGFR undergoes receptor dimerization, which activates its intrinsic intracellular tyrosine kinase activity[318]. Because of this activation, EGFR undergoes autophosphorylation at several tyrosine residues e.g. Y845, Y992, etc.[319]. Activation of EGFR by autophosphorylation activates downstream signalling which regulates various cellular processes such as growth, survival, proliferation and differentiation[318]. Unregulated, constitutive activity of EGFR has been associated with various kinds of cancer[320, 321]. As mentioned earlier, EGFR cross talk with FPR1 has been reported in glioblastoma[59] and monocytes[58]. Its existence was explored in breast cancer.
2) JAK-STAT3 activation: The Janus kinase/signal transducers and activators of transcription (JAK/STAT) pathway is the principal signalling pathway utilized by various and cytokines[322]. There are four JAK and seven STAT proteins present in mammalian cells[322]. Among these, JAK2-STAT3 signalling plays an important role in linking inflammation and cancer[323, 324]. STAT3 phosphorylation is the hallmark of JAK2-STAT3 signalling[322]. STAT3 phosphorylation is also reported by the activation of FPR1, FPR2 and EGFR signalling[325-327]. However, it is not clear if this STAT3 phosphorylation is result of receptor signalling cross talk or these receptors directly activate STAT3.
3) small Rho-GTPases: RhoA, Rac1 and Cdc42 are members of the Rho family of small GTPases acting as a signalling molecule, regulating various cellular processes, including cell division, proliferation, differentiation,

survival, motility, vesicle transport, nuclear assembly and dynamics of cytoskeleton[328]. These small GTP binding proteins were thought to be activated by either PI3K via PIP3 or by $G_{\beta\gamma}$ subunit of FPR via GTPases activating proteins (GAP)[329]. Activation of small Rho-GTPases by EGFR via Vav2 has been reported[330]. In PMNL after activation through FPR, these Rho GTPases activate downstream signalling which is involved in oxidative burst, actin rearrangement, activation of MAPKs etc. Furthermore, activation of small Rho-GTPases was required for activation of JAK-STAT signalling by GPCR[331]

4) PI3K-Akt pathway: PI3K-Akt pathway is important cellular pathway that controls cell cycle and promotes cell survival and growth in response to extracellular signals. It is directly related to cellular proliferation and cancer. PI3K activation phosphorylates and activates Akt, which can have number of downstream effect. PI3K-Akt pathway has natural inhibitor called PTEN, which prevents conversion of PIP2 to PIP3. Both PTEN and Akt activation were checked in the presented work.

   PTEN: PTEN (also known as MMAC and TEP1) is a tumor suppressor gene[309]. PTEN mutations have been implicated in a variety of human cancers[311]. PTEN negatively regulates PI3K signalling by dephosphorylating the lipid signalling intermediate PIP3 thus leading to inhibition of PI3K-dependent activation of AKT[311]. Defective PTEN function leads to the PIP3 accumulation in cells and to constitutive activation of its downstream signals[311].

   Akt: Akt, also known as protein kinase B (PKB), is a serine/threonine-specific protein kinase that plays a key role in multiple cellular processes

such as glucose metabolism, apoptosis, cell proliferation, transcription and cell migration[332]. Upon activation of PI3K by fMLP, Akt is recruited to the plasma membrane, where it undergoes phosphorylation on two sites: threonine 308 (Thr308) in the kinase domain by the phosphoinositide-dependent kinase-1 (PDK1)[29] and serine 473 (Ser473) in the C-terminal domain by MAPKAP kinase-2 (MAPKAPK-2), a p38-MAPK substrate[30]. Though Akt is a central molecule in PI3K-mTOR pathway, PI3K independent activation of Akt has also been reported[333]. Akt has been shown to contribute to chemotaxis and to the respiratory burst in fMLP-stimulated neutrophils[334]. Activation of Akt was found to be linked with the resistance to hormone therapy in metastatic breast cancers[335, 336].

5) Ras-MAPK-Erk-1/2 pathway: Ras-MAPK pathway is a pathway that communicates signals from receptor expressed on cell surface to DNA in cell nucleus. This pathway that controls cellular proliferation could be activated by various cell receptors. Two MAPK were checked in the presented work:

   p38-MAPK: p38-mitogen-activated protein kinases (p38-MAPK) are a class of evolutionarily conserved serine/threonine mitogen-activated protein kinases (MAPKs) that link extracellular signals to the intracellular machinery and regulate various cellular processes[35]. p38-MAPK activation is dependent on PI3K and phospholipase C [36]. Small Rho-GTPases could also activate p38-MAPK[337]. Activation of p38-MAPK is necessary for fMLP-mediated stimulation of respiratory burst activity[338]. Activated p38-MAPK also helps in proper localization of activated PTEN in the circumference of

PMNL other than leading edge[142]. PTEN then prioritize chemotactic cues and thereby prevents the distraction in migrating PMNL[310].

Erk-1/2: ERK1 and ERK2 are serine/threonine kinases that participate in the Ras-Raf-MEK-ERK signal transduction cascade. This cascade participates in the regulation of a large variety of processes including cell adhesion, cell cycle progression, cell migration, cell survival, differentiation, metabolism, proliferation and transcription[339].

Stimulation with fMLP

EGFR

After treatment with fMLP increase in phosphorylation of EGFR was seen in MCF-7 at Y845 (Fig-RB 19). This activation was unaffected by the pre-treatment of CsH. In WRW4 pre-treated cells, the phosphorylation levels were higher than that in the solvent control, but slight increase was also seen in the total protein level. Hence, the ratio of phospho and total protein in WRW4 pre-treated cells was comparable to that of the solvent control. PEGFR-Y845 levels were comparable to the solvent control, in cells pre-treated with AG490, AG1478 and PP2, in spite of increase in total EGFR expression. These results suggested that this activation of EGFR by fMLP in MCF-7 was mediated by FPR2, JAK2, EGFR and Src-kinase.

In MDA-MB-231 too, fMLP treatment led to the activation of EGFR as increase in the phosphorylation of EGFR was seen (Fig-RB 19). Further increase in levels of pEGFR-Y845 was seen in the cells pre-treated with CsH, WRW4 AG490 and PP2. The highest level of pEGFR-Y845 upon fMLP treatment was seen in the cells pre-treated with AG490. These observations are suggestive of inhibitory or negative regulatory role of FPR2, JAK2 and Src-kinase. Cells pre-treated with AG1478

showed pEGFR-Y845 levels slightly lower than that in fMLP treated cells but still higher than the solvent control. This suggested that increase in pEGFR-Y845 level in MDA-MB-231 upon fMLP treatment could be mediated by EGFR to some extent.

STAT3

Upon fMLP treatment, change in the STAT3 phosphorylation was not seen in MCF-7 (Fig-RB 19). Decrease in the STAT3 phosphorylation was observed in cells pre-treated with CsH, AG490, AG1478 and PP2. These results indicated that in fMLP treated MCF-7 along with FPR1, JAK2, EGFR and Src-kinase were required for maintaining STAT3 phosphorylation at the basal level.

In MDA-MB-231, fMLP treatment decreased the level of pSTAT3 (Fig-RB 19). This decrease was partially recovered in CsH and AG490 pre-treated cells, whereas pSTAT3 levels were back to the level of solvent control in PP2 pre-treated cells. These results suggested that in fMLP treated MDA-MB-231 cells, FPR1 mediated decrease in pSTAT3 involves JAK2 and Src-kinase.

Rac-1

Upon fMLP treatment, change in the expression of Rac-1 was not seen in MCF-7 cell line as compared to that in the solvent control (Fig-RB19). However, increase in Rac-1 was observed in the cells pre-treated with CsH and AG1478 and decrease in the expression of Rac-1 was seen upon fMLP stimulation in AG490 pre-treated cells. This indicated that fMLP stimulation could increase expression of Rac-1 in MCF-7 via JAK2 and by cross-activating EGFR, provided FPR1 pathway is inhibited. In MDA-MB-231 too, fMLP treatment did not show any change in Rac-1 expression as compared to that in the solvent control (Fig-RB 19). However, increase in Rac-1 expression upon fMLP treatment was seen in

WRW4, AG1478 and PP2 pre-treated cells. This observation suggested that FPR2, EGFR and Src-kinase negatively regulate Rac-1 expression in fMLP treated MDA-MB-231.

RhoA

Upon fMLP treatment, increase in the expression of RhoA was observed in MCF-7 cell line as compared to that in solvent control (Fig-RB 19). This increase in the expression of RhoA was not inhibited by the treatment of any of the inhibitors used in the study. It suggested that increase in RhoA upon fMLP treatment in MCF-7 involved some unknown mechanism.

In MDA-MB-231, fMLP treatment led to increase in RhoA (Fig-RB 19). This increase in the RhoA was inhibited in CsH and AG490 pre-treated cells, while partial inhibition was observed in AG1478 and PP2 pre-treated cells. This suggested that along with FPR1, JAK2, EGFR and Src-kinase were involved in increase in RhoA expression, in fMLP treated in MDA-MB-231.

Cdc42

Upon fMLP stimulation, changes in the expression of Cdc42 were not seen in MCF-7 cell line as compared to that in the solvent control (Fig-RB 19). Though there were no changes in Cdc42 after fMLP stimulation in MCF-7, decrease in the expression of Cdc42 upon fMLP treatment was seen in WRW4 and AG1478 pre-treated cells. Furthermore, increase in Cdc42 expression upon fMLP treatment was observed in PP2 pre-treated cells than that in the fMLP treated cells. This indicated that cells could have maintained expression of Cdc42 to the basal level in fMLP treated cells via FPR2 and EGFR. On the contrary, Src-kinase might have inhibitory role. In MDA-MB-231, fMLP treatment led to slight decrease in Cdc42 than that in the solvent control (Fig-RB 19). This decrease in Cdc42 expression

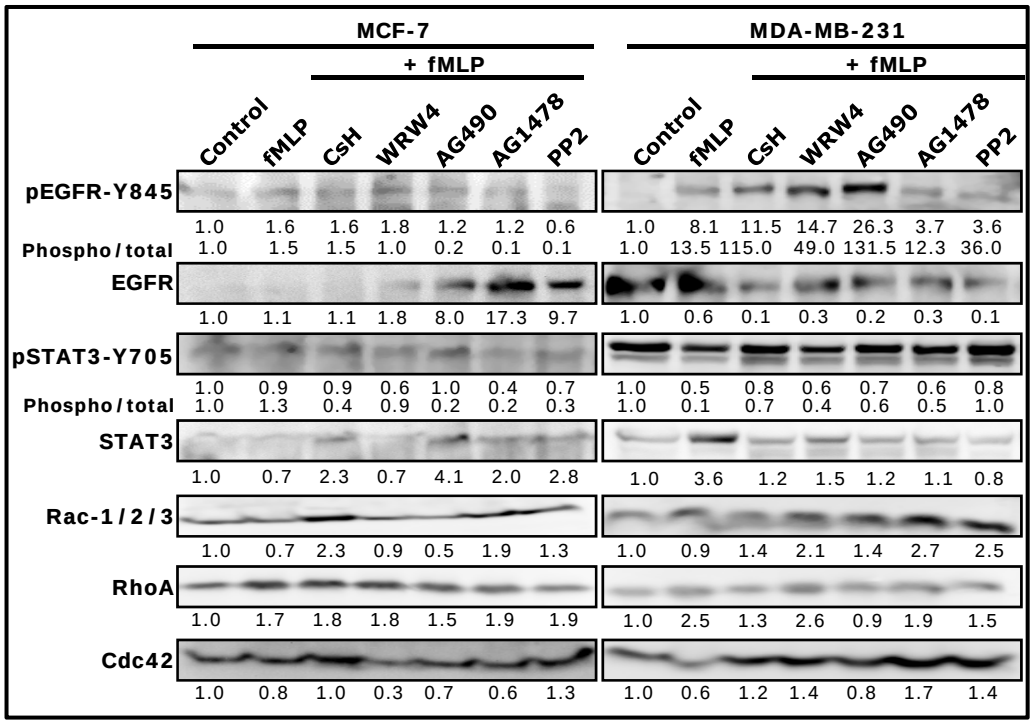

Fig-RB 19: fMLP Stimulation: Effect of fMLP was studied on various proteins in MCF-7 and MDA-MB-231 by Western blotting. Band density of the treatment group was compared to that of the solvent control to get fold change in expression. Fold change in expression of phospho protein was normalized with the fold change in expression of total protein to get absolute change in phospho protein. Each experiment was done in triplicate and representative blots are shown.

was inhibited in cells pre-treated with CsH, WRW4 and PP2. Furthermore, increase in the expression of Cdc42 was observed in AG1478 pre-treated cells. In addition to role of FPR1 in slight decrease in Cdc42 expression upon fMLP treatment, role of FPR2 and EGFR cross talk with FPR1 is indicated by these results. Moreover, Src-kinase is also involved as a player in the signalling pathway.

PTEN

fMLP treatment caused decrease in the phosphorylation level of PTEN in MCF-7 cells (Fig-RB 20). This decrease in PTEN phosphorylation was partially inhibited by the pre-treatment of CsH and AG1478, while increase in the PTEN phosphorylation was observed in cells pre-treated with PP2. These observations indicated cross talk with EGFR and signalling by Src-kinase in FPR1 mediated decrease in the PTEN phosphorylation. Since the decrease in PTEN phosphorylation was not completely inhibited by CsH and AG1478 pre-treatment, there could be a possibility of involvement of some other signalling pathway involving Src-kinase.

In MDA-MB-231, fMLP treatment did not affect phosphorylation level of PTEN. Though fMLP failed to activate the PTEN, increase in the PTEN phosphorylation was observed in the cells pre-treated with CsH, WRW4, AG490, AG1478 and PP2 (Fig-RB 20). This means that fMLP could activate PTEN by some unknown signalling pathway, if FPR1 per se or FPR2, JAK2, EGFR and Src-kinase signalling was inhibited.

p38-MAPK

In MCF-7, fMLP treatment led to increased p38-MAPK phosphorylation (Fig-RB 20). Further increase in p38 -MAPK phosphorylation was observed in CsH, WRW4

and AG490 pre-treated cells. This suggested that in addition to FPR1, fMLP induced p38-MAPK phosphorylation by some unknown pathway, which was inhibited by FPR1, FPR2 and JAK2.

In MDA-MB-231, fMLP treatment failed to change phosphorylation levels of p38-MAPK (Fig-RB 20). However, increase in p38-MAPK phosphorylation was observed in cells pre-treated with CsH, AG1478 and PP2. Decrease in p38-MAPK phosphorylation upon fMLP treatment was observed in the cells pre-treated with AG490. These observations indicated that p38-MAPK phosphorylation levels in fMLP treated MDA-MB-231 were maintained by inhibition of FPR1, EGFR and Src-kinase signalling and by activation of JAK2.

Akt

Akt-T308

In MCF-7, change in level of pAkt-T308 was not seen upon fMLP treatment (Fig-RB 20). However, decrease in pAkt-T308 level upon fMLP treatment was seen in WRW4 and PP2 pre-treated MCF-7 cells. These results showed that FPR2 and Src-kinase helped in maintaining basal pAkt-T308 level in MCF-7.

In contrast to MCF-7 results, fMLP treatment caused increase in pAkt-T308 level in MDA-MB-231 (Fig-RB 20). Increase in the level of pAkt-T308, upon fMLP stimulation, was inhibited by the pre-treatment of CsH, while further increase in the pAkt-T308 level was observed in WRW4, AG490 and PP2. These results indicated that fMLP induced increase in pAkt-308 was mediated by FPR1 and was negatively regulated by FPR2, JAK2 and Src-kinase.

Akt-S473

Change in level of pAkt-S473 was not seen in MCF-7 upon fMLP treatment (Fig-RB 20). Increase in the level of pAkt-S473 upon fMLP treatment was seen in CsH and PP2 pre-treated MCF-7 cells, while decrease in the level of pAkt-S473 upon fMLP treatment was observed in WRW4, AG490 and AG1478 pre-treated MCF-7 cells. These results suggested that in fMLP treated MCF-7 cells, maintenance of pAkt-S473 to the basal levels is, by inhibition of FPR1 and Src-kinase signalling. Moreover, cross talk of FPR1 with FPR2 and EGFR involving JAK2 might be playing role too.

There was increase in Akt phosphorylation at S473 in MDA-MB-21 upon fMLP treatment (Fig-RB 20). Increase in pAkt-S473, upon fMLP stimulation was completely inhibited by CsH pre-treatment. However, partial inhibition of pAkt-S473 was also seen in AG490, AG1478 and PP2 pre-treated cells. It suggested that increase in the pAkt-S473 in MDA-MB-231 upon fMLP stimulation was mediated by FPR1 its cross talk with EGFR and Src-kinase also played a role in this increase.

Erk-1/2

In MCF-7, fMLP treatment led to the activation of Erk-1/2 by inducing phosphorylation (Fig-RB 20). In MCF-7, this phosphorylation was partially inhibited by the pre-treatment of CsH and WRW4, while complete inhibition of Erk-1/2 phosphorylation was observed in cells pre-treated with AG490, AG1478 and PP2. This indicated that not only FPR1 but FPR2, JAK2, EGFR and Src-kinase signalling also had a role in the activation of Erk-1/2 by fMLP.

Similar to MCF-7, fMLP activated Erk-1/2 in MDA-MB-231 too (Fig-RB 20). In MDA-MB-231, Erk-1/2 phosphorylation was further increased in the cells pre-treated with CsH, WRW4 and PP2 while inhibition of Erk-1/2 phosphorylation was

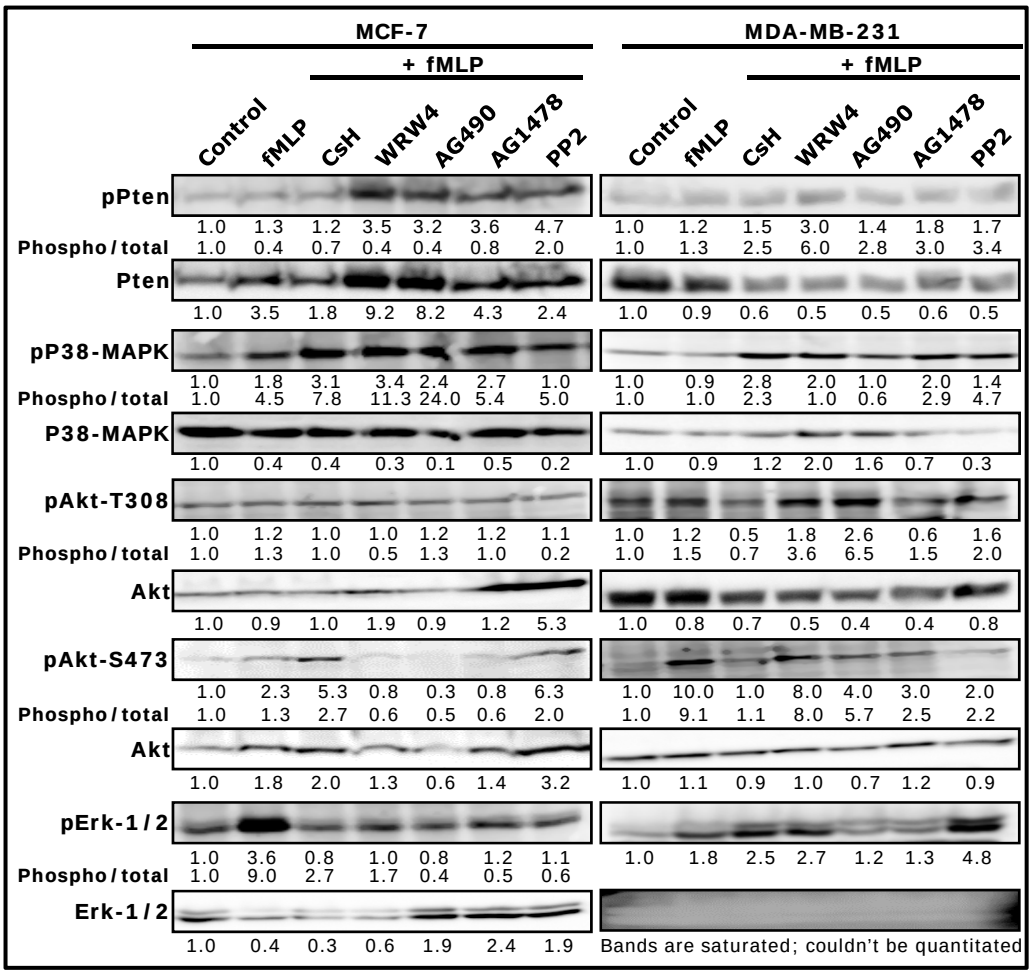

Fig-RB 20: fMLP Stimulation: Effect of fMLP was studied on various proteins in MCF-7 and MDA-MB-231 by Western blotting. Band density of the treatment group was compared to that of the solvent control to get fold change in expression. Fold change in expression of phospho protein was normalized with the fold change in expression of total protein to get absolute change in phospho protein. Each experiment was done in triplicate and representative blots are shown.

seen in AG490 and AG1478 pre-treated cells. These observations indicated that in MDA-MB-231 activation of Erk-1/2 upon fMLP stimulation was mediated by cross talk

with EGFR and JAK2 activation and was negatively regulated by FPR1, FPR2 and Src-kinase.

fMLP summary

MCF-7

Effect of fMLP treatment to MCF-7 is summarized in Table-RB 9 and Fig-RB 21A. As seen fMLP activated FPR1 which transactivated FPR2 and EGFR, ultimately leading to activation of JAK-STAT, Ras-MAPK-Erk-1/2 and Ras-Rho GTPase pathway. These pathways are known to play role in cell proliferation while Ras-Rho-GTPases pathway is involved in cell motility too. Thus, on fMLP stimulation, FPR1 seemed to play role in motility as well as proliferation of MCF-7.

Table-RB 9: Effect of fMLP on MCF-7

Signalling molecules	Effect of fMLP	Contributors to the effect	Negative regulators
EGFR-845	**Increase**	FPR2, EGFR, JAK2, Src-kinase	------
STAT-3-Y705	*No effect*	FPR1, EGFR, JAK2, Src-kinase	------
Rac	*No effect*	JAK2	FPR1, EGFR
RhoA	**Increase**	------	------
Cdc42	*No effect*	FPR2, EGFR*	Src-kinase
Pten	**Decrease**	FPR1*, EGFR*, Src-kinase	------
p38-MAPK	**Increase**	------	FPR1, FPR2, JAK2
Akt-T308	*No effect*	FPR2, Src-kinase	------
Akt-S473	*No effect*	FPR2, JAK2, EGFR	FPR1, Src-kinase
Erk-1/2	**Increase**	EGFR, JAK2, Src-kinase	------

MDA-MB-231

Similar to MCF-7, fMLP treatment activated FPR1, which transactivated FPR2 and EGFR in MDA-MB-231 too (Fig-RB 21B, Table-RB 10). This resulted into activation of PI3K-Akt pathway, Ras-Rho-GTPase pathway and Ras-MAPK-Erk-1/2 pathway and deactivation of JAK-STAT pathway. All activated pathways are known to play role in cell proliferation while PI3K-Akt and Ras-Rho-GTPases pathways are also involved in cell motility. Thus, FPR1 might be playing role in proliferation and motility in MDA-MB-231, similar to MCF-7.

Major difference in fMLP stimulated signalling in MCF-7 and MDA-MB-231 are activation of PI3K-Akt pathway and deactivation of JAK-STAT pathway in MDA-MB-231. Hence, it is proposed that PI3K-Akt pathway might be contributing to higher metastasis and drug resistance exhibited by MDA-MB-231 as compared to MCF-7.

Table-RB 10: Effect of fMLP on MDA-MB-231

Signalling molecules	Effect of fMLP	Contributors to the effect	Negative regulators
EGFR-845	**Increase**	EGFR*	FPR1, FPR2, JAK2, Src-kinase
STAT-3-Y705	**Decrease**	FPR1, JAK2*, Src-kinase	------
Rac	*No effect*	-----	FPR2, EGFR, Src-kinase
RhoA	**Increase**	FPR1, JAK2, EGFR*, Src-kinase*	------
Cdc42	**Decrease***	FPR1, FPR2, EGFR, Src-kinase	------
Pten	*No effect*	------	FPR1, FPR2, JAK2, EGFR, Src-kinase
p38-MAPK	*No effect*	JAK2	FPR1, EGFR, Src-kinase
Akt-T308	**Increase**	FPR1	FPR2, JAK2, Src-kinase
Akt-S473	**Increase**	FPR1, JAK2*, EGFR*, Src-kinase	------
Erk-1/2	**Increase**	EGFR, JAK2	FPR1, FPR2, Src-kinase

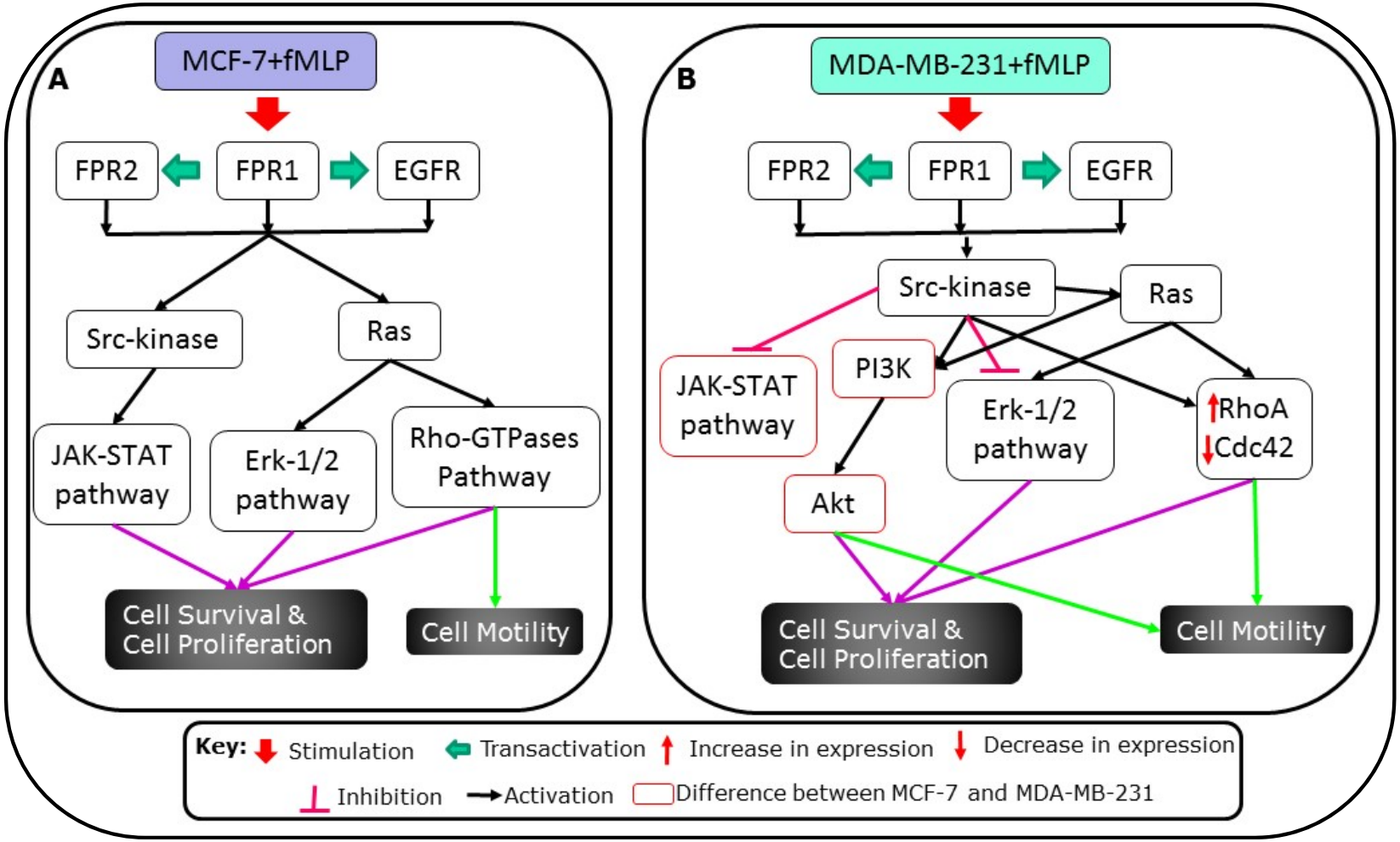

Fig-RB 21: Effect of fMLP treatment on signalling pathways in MCF-7 and MDA-MB-231 and probable resultant cellular events

Stimulation with WKYMVm

EGFR

Upon WKYMVm treatment, increase in EGFR phosphorylation was not seen in MCF-7 (Fig-RB 22). However, decrease in the pEGFR-Y845 level upon WKYMVm treatment was observed in CsH and PP2 pre-treated MCF-7 cells. These result suggested that in MCF-7, FPR1 and Src-kinase are required to maintain basal phosphorylation levels of EGFR at Y845.

In MDA-MB-231, phosphorylation of EGFR was seen after WKYMVm stimulation (Fig-RB 22). Further increase in pEGFR-Y845 level was seen in CsH pre-treated and WKYMVm stimulated cells. Partial inhibition of increase in pEGFR-Y845 was seen in AG1478 pre-treated cells while complete abolition of phosphorylation was observed in PP2 pre-treated cells. This indicated that WKYMVm utilize trans-activated EGFR and Src-kinase was involved in facilitating phosphorylation of EGFR at Y845.

STAT3

WKYMVm treatment did not affect the level of pSTAT3 in MCF-7. However, cells pre-treated with WRW4, AG1478 and PP2 (Fig-RB 22) showed decrease in pSTAT3. It suggested that in MCF-7, FPR2, EGFR and Src-kinase are required for maintaining pSTAT3 level.

In MDA-MB-231 also, WKYMVm treatment caused decrease in pSTAT3 level (Fig-RB 22). This decrease was partially neutralized by the pre-treatment of WRW4 and AG490. Increase in pSTAT3 level was observed in the cells pre-treated with CsH. These results indicated that decrease in pSTAT3 upon WKYMVm treatment in MDA-MB-231 was caused by both FPR1 and FPR2. Transactivation of FPR1

seemed to have a major role between the two. Moreover, JAK2 was also involved.

Rac-1

WKYMVm treatment inhibited expression of Rac-1 in MCF-7 cell lines (Fig-RB 22). This decrease in the expression of Rac-1 was not affected by treatment of any inhibitors used in the study. It indicated that WKYMVm induced decrease of Rac-1 protein expression in MCF-7 was mediated by some unknown signalling mechanism.

In MDA-MB-231, WKYMVm treatment show increased expression of Rac-1 (Fig-RB 22). This increase in Rac-1 upon WKYMVm treatment was partially inhibited by in WRW4, AG490, AG1478 and PP2 pre-treated cells. It indicated that increase in Rac-1 upon WKYMVm treatment was dependent on FPR2, EGFR, JAK2 and Src-kinase.

RhoA

WKYMVm treatment inhibited expression of RhoA in MCF-7 cell lines (Fig-RB 22). The inhibitory effect of WKYMVm on RhoA expression was increased in cells pre-treated with AG490, AG1478 and PP2 whereas partial inhibition of the decrease in RhoA expression upon WKYMVm treatment was observed in CsH pre-treated cells. It suggested that WKYMVm induced decrease in RhoA expression was partially mediated by FPR1. EGFR, JAK2 and Src-kinase negatively regulated FPR2 mediated decrease of RhoA upon WKYMVm treatment, in MCF-7 cell line.

In MDA-MB-231, WKYMVm treatment showed increase in the expression of RhoA (Fig-RB 22). Increase in the RhoA expression upon WKYMVm stimulation was inhibited in CsH, AG1478 and PP2 pre-treated cells. These results showed that increase in the expression of RhoA upon WKYMVm treatment majorly required

cross talk with FPR1 and EGFR and is not directly mediated by FPR2. Moreover, Src-kinase plays role in this increase.

Cdc42

WKYMVm treatment inhibited Cdc42 expression in MCF-7 cell lines (Fig-RB 22). Similar to Rac-1, this decrease in Cdc42 expression was not affected by pre-treatment of any inhibitors. This suggested that the decrease in the expression of Cdc42 upon WKYMVm stimulation of MCF-7 cells was independent of all the tested signalling pathways.

In MDA-MB-231, WKYMVm treatment did not show changes in Cdc42 expression (Fig-RB 22). However, there was increase in the Cdc42 protein expression upon WKYMVm treatment in PP2 pre-treated cells. This suggested that in MDA-MB-231, Src-kinase could be maintaining expression of Cdc42 upon WKYMVm treatment.

PTEN

WKYMVm treatment posed no effect on PTEN phosphorylation in MCF-7 cells (Fig-RB 23). However, Decrease in the PTEN phosphorylation upon WKYMVm treatment was observed in the cells pre-treated with WRW4 and increase in PTEN phosphorylation was seen in AG490 pre-treated cells. It indicated that when stimulated with WKYMVm JAK2 acts as a negative regulator in maintaining steady levels of PTEN.

In MDA-MB-231, WKYMVm treatment caused decrease in PTEN phosphorylation (Fig-RB 23). This decrease in PTEN phosphorylation upon WKYMVm treatment was inhibited in WRW4 and PP2 pre-treated cells. It suggested that the decrease in PTEN phosphorylation by WKYMVm in MDA-MB-231 involved Src-kinase signalling. Partial recovery of pPTEN in cells pretreated with CsH and AG490

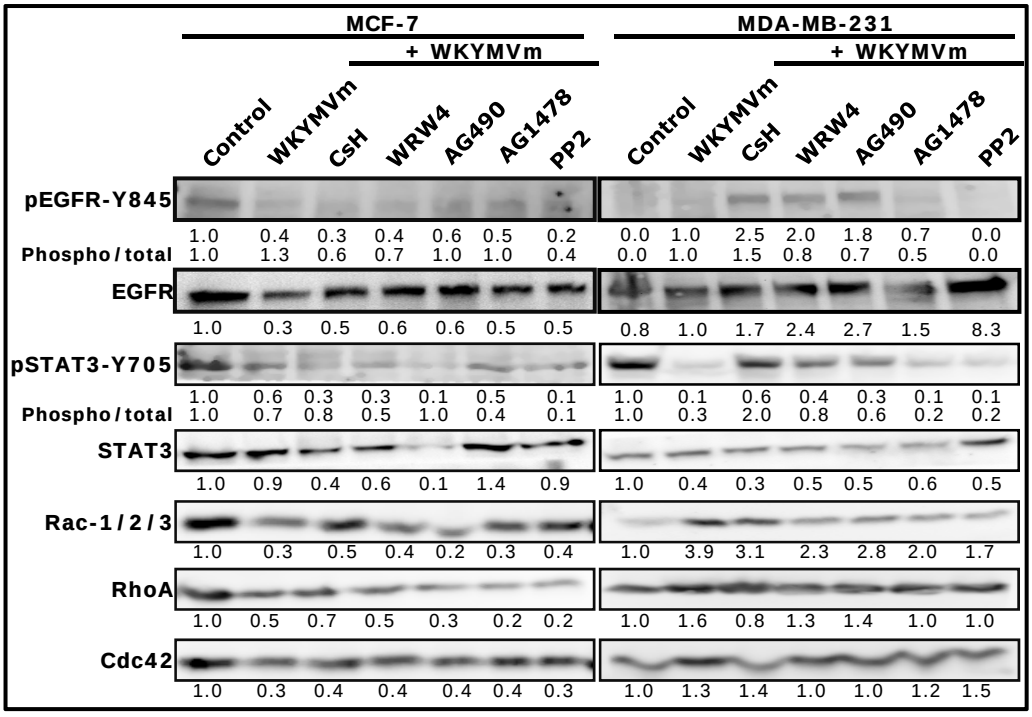

Fig-RB 22: WKYMVm Stimulation: Effect of WKYMVm was studied on various proteins in MCF-7 and MDA-MB-231 by Western blotting. Band density of the treatment group was compared to that of the solvent control to get fold change in expression. Fold change in expression of phospho protein was normalized with the fold change in expression of total protein to get absolute change in phospho protein. Each experiment was done in triplicate and representative blots are shown.

indicated negative regulation of WKYMVm induced PTEN signalling in MDA-MB-231.

p38-MAPK

WKYMVm stimulation led to the activation of p38-MAPK in MCF-7(Fig-RB 23). Further increase in p38-MAPK phosphorylation upon WKYMVm treatment was observed in cells pre-treated with CsH, WRW4, AG490 and AG1478, while partial decrease in p38-MAPK phosphorylation upon WKYMVm treatment was observed in cells pre-treated with PP2. It indicated that WKYMVm induced p38-MAPK phosphorylation, which involved Src-kinase signalling to some extent, was negatively regulated by FPR1, FPR2, JAK2 and EGFR.

In MDA-MB-231, increase in PTEN phosphorylation was observed upon WKYMVm treatment (Fig-RB 23). Further increase in p38-MAPK phosphorylation upon WKYMVm treatment was observed in cells with CsH, WRW4, AG490, AG1478 and PP2 pre-treatment. This indicated that activation of p38-MAPK upon WKYMVm stimulation was negatively regulated by FPR1, JAK2, EGFR, Src-kinase and also by FPR2 per se probably after reaching a threshold.

Akt

Akt-T308

WKYMVm treatment had no effect on pAkt-T308 level (Fig-RB 23). Furthermore, decrease in pAkt-T308 level upon WKYMVm treatment was observed in AG1478 and PP2 pre-treated cells. Increase in the pAkt-T308 upon WKYMVm treatment was seen in CsH and WRW4 pre-treated cells. These results suggested that WKYMVm could increase pAkt-T308 level by EGFR and Src-kinase if FPR1 and FPR2 were inhibited.

Decrease in pAkt-T308 level was observed upon WKYMVm treatment (Fig-RB 23). This decrease in pAkt-T308 upon WKYMVm treatment was partially inhibited in cells pre-treated with CsH, WRW4 and AG490. It suggested that WKYMVm induced decrease in pAkt-T308 via FPR1, FPR2 and JAK2.

Akt-S473

WKYMVm treatment to MCF-7 induced phosphorylation at S473 (Fig-RB 23). Increase in pAkt-S473 level upon WKYMVm treatment was inhibited by the pre-treatment of CsH, AG490, AG1478 and PP2 but not by WRW4. This indicated that increase in pAkt-S473 upon WKYMVm treatment in MCF-7 was mediated through cross talk with FPR1 and EGFR. Signalling of JAK2 and Src-kinase is also involved.

In MDA-MB-231 too, WKYMVm treatment induced Akt phosphorylation only at Ser-473 (Fig-RB 23). Increase in pAkt-S473 level upon WKYMVm treatment in MDA-MB-231 was inhibited by the pre-treatment of CsH, AG1478 and PP2. It indicated that the increase in pAkt-S473 level in MDA-MB-231 upon WKYMVm treatment was mediated by cross talk with FPR1 and EGFR than FPR2 per se. Moreover, Src-kinase is involved in signalling pathway.

Erk-1/2

WKYMVm treatment led to increase in phosphorylation of Erk-1/2 in MCF-7 (Fig-RB 23). This phosphorylation was further increased in the cells pre-treated with CsH. Partial inhibition of phosphorylation was seen in cells pre-treated with WRW4 and PP2 while decrease in Erk-1/2 phosphorylation upon WKYMVm treatment was observed in AG490 and AG1478 pre-treated cells. It indicated that along with FPR2; JAK2, EGFR and Src-kinase were involved in WKYMVm induced Erk-1/2 phosphorylation, which was negatively regulated by FPR1.

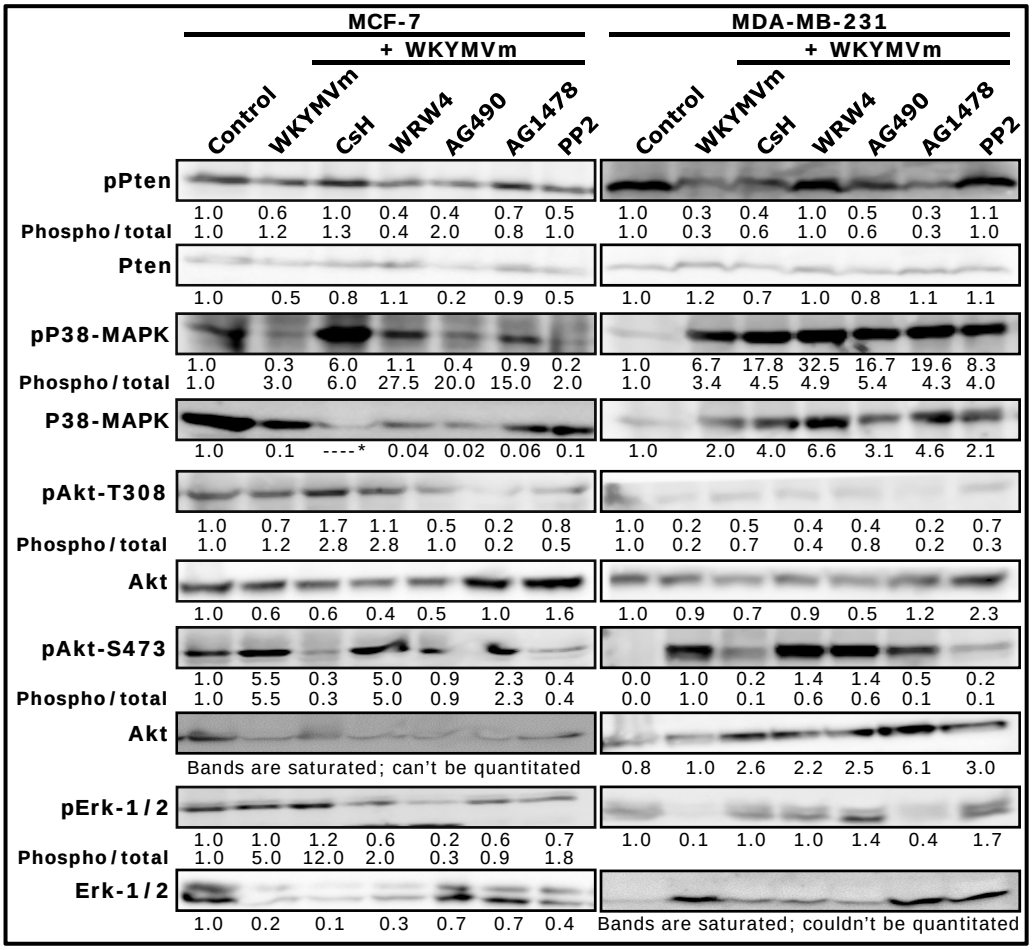

Fig-RB 23: WKYMVm Stimulation: Effect of WKYMVm was studied on various proteins in MCF-7 and MDA-MB-231 by Western blotting. Band density of the treatment group was compared to that of the solvent control to get fold change in expression. Fold change in expression of phospho protein was normalized with the fold change in expression of total protein to get absolute change in phospho protein. Each experiment was done in triplicate and representative blots are shown.

In MDA-MB-231 cell line, WKYMVm treatment caused decrease in the phosphorylation level of Erk-1/2 (Fig-RB 23). This decrease in Erk-1/2 phosphorylation upon WKYMVm treatment was inhibited in CsH, WRW4 and AG490 pre-treated MDA-MB-231 cell line, whereas slight increase in Erk-1/2 phosphorylation was observed in AG1478 pre-treated cell lines. AG490 pre-treated cells showed levels comparable to the basal levels, while PP2 pre-treated cells showed increase in the phosphorylation level of Ekr-1/2 upon WKYMVm treatment. These observations suggested that decrease in Erk-1/2 phosphorylation upon WKYMVm treatment in MDA-MB-231 cells was mediated by FPR1, FPR2, JAK2, EGFR and Src-kinase.

WKYMVm summary

MCF-7

Table-RB 11: Effect of WKYMVm on MCF-7

Signalling molecules	Effect of fMLP	Contributors to the effect	Negative regulators
EGFR-845	*No effect*	FPR1, FPR2, Src-kinase	------
STAT-3-Y705	*No effect*	FPR2, EGFR, Src-kinase	------
Rac	**Decrease**	------	------
RhoA	**Decrease**	FPR1*	JAK2, EGFR, Src-kinase
Cdc42	**Decrease**	------	------
Pten	*No effect*	FPR2	JAK2
p38-MAPK	**Increase**	Src-kinase	FPR1, FPR2, JAK2, EGFR
Akt-T308	*No effect*	EGFR, Src-kinase	FPR1, FPR2
Akt-S473	**Increase**	FPR1, JAK2, EGFR*, Src-kinase	------
Erk-1/2	**Increase**	EGFR, JAK2, FPR*, Src-kinase*	FPR1

Effect of WKYMVm treatment to MCF-7 is summarized in Table-RB 11 and Fig-RB 24A. As seen, WKYMVm activated FPR2 transactivated FPR1.

Though increase in EGFR phosphorylation was not observed, its contribution in activating other signalling molecules was evident. These transactivations ultimately led to activation of Ras-MAPK-Erk1-1/2 pathway, PI3K-Akt pathway, p38-MAPK pathway and inhibition of Ras-Rho-GTPase pathway. All activated pathways are known to play role in cell proliferation. Hence, FPR2 might be playing role in proliferation in MCF-7. The major difference between effect of WKYMVm and fMLP treatment to MCF-7 is activation of PI3K-Akt pathway and inhibition of Rho-GTPases pathway in WKYMVm treated MCF-7. Hence, it is proposed that by activating PI3K-Akt pathway WKYMVm might be contributing to higher proliferation and drug resistance in MCF-7 while inhibition of Rho-GTPase pathway contributed to reduced cell motility.

MDA-MB-231

WKYMVm treatment activated FPR2, which transactivated FPR1 and EGFR in MDA-MB-231 (Table-RB 12, Fig-RB 24B). This resulted into activation of PI3K-Akt pathway, Ras-Rho-GTPase pathway and p38-MAPK pathway while it led to inhibition of JAK-STAT pathway and Ras-MAPK-Erk-1/2 pathway. All activated pathways are known to play role in cell proliferation while PI3K-Akt and Ras-Rho-GTPases pathways are also involved in cell motility. Since JAK-STAT pathway is involved in apoptosis, inhibition of this pathway led to inhibition of apoptosis. Thus, FPR2 might be playing role in proliferation, motility and inhibiting apoptosis in MDA-MB-231.

Comparing to fMLP treatment to MDA-MB-231, WKYMVm treatment showed opposite effect on Ras-MAPK and PI3K-PDK-Akt pathway, where inhibition of

these was noted in WKYMVm treated MDA-MB-231. Activation of p38-MAPK was also seen in WKYMVm treated MDA-MB-231, unlike fMLP treatment. Hence, it is proposed that WKYMVm might induce less proliferation effect in MDA-MB-231 than fMLP.

Table-RB 12: Effect of WKYMVm on MDA-MB-231

Signalling molecules	Effect of fMLP	Contributors to the effect	Negative regulators
EGFR-845	**Increase**	EGFR, Src-kinase	FPR1
STAT-3-Y705	**Decrease**	FPR1, FPR2, JAK2	------
Rac	**Increase**	FPR2, JAK2*, EGFR, Src-kinase	------
RhoA	**Increase**	FPR1, FPR2, EGFR, Src-kinase	------
Cdc42	*No effect*	------	Src-kinase
Pten	**Decrease**	FPR2, Src-kinase	FPR1*, JAK2*
p38-MAPK	**Increase**	------	FPR1, FPR2, JAK2, EGFR, Src-kinase
Akt-T308	**Decrease**	FPR1, JAK2, FPR2	------
Akt-S473	**Increase**	FPR1, FPR2*, JAK2*, EGFR, Src-kinase	------
Erk-1/2	**Decrease**	FPR1, FPR2, EGFR*, JAK2, Src-kinase	------

Major differences in WKYMVm stimulated signalling in MCF-7 and MDA-MB-231 are activation of Rho-GTPase pathway and inhibition of JAK-STAT & Ras-MAPK-Erk-1/2 pathway in MDA-MB-231. Hence, it is proposed that activation of Rho-GTPase pathway might be contributing to higher metastasis, while inhibition of JAK-STAT might be contributing to decreased apoptosis in WKYMVm treated MDA-MB-231.

Stimulation with EGF

EGFR

As expected treatment of EGF showed activation of EGFR in both the cell lines studied (Fig-RB 25). In MCF-7, phosphorylation of EGFR was partially inhibited

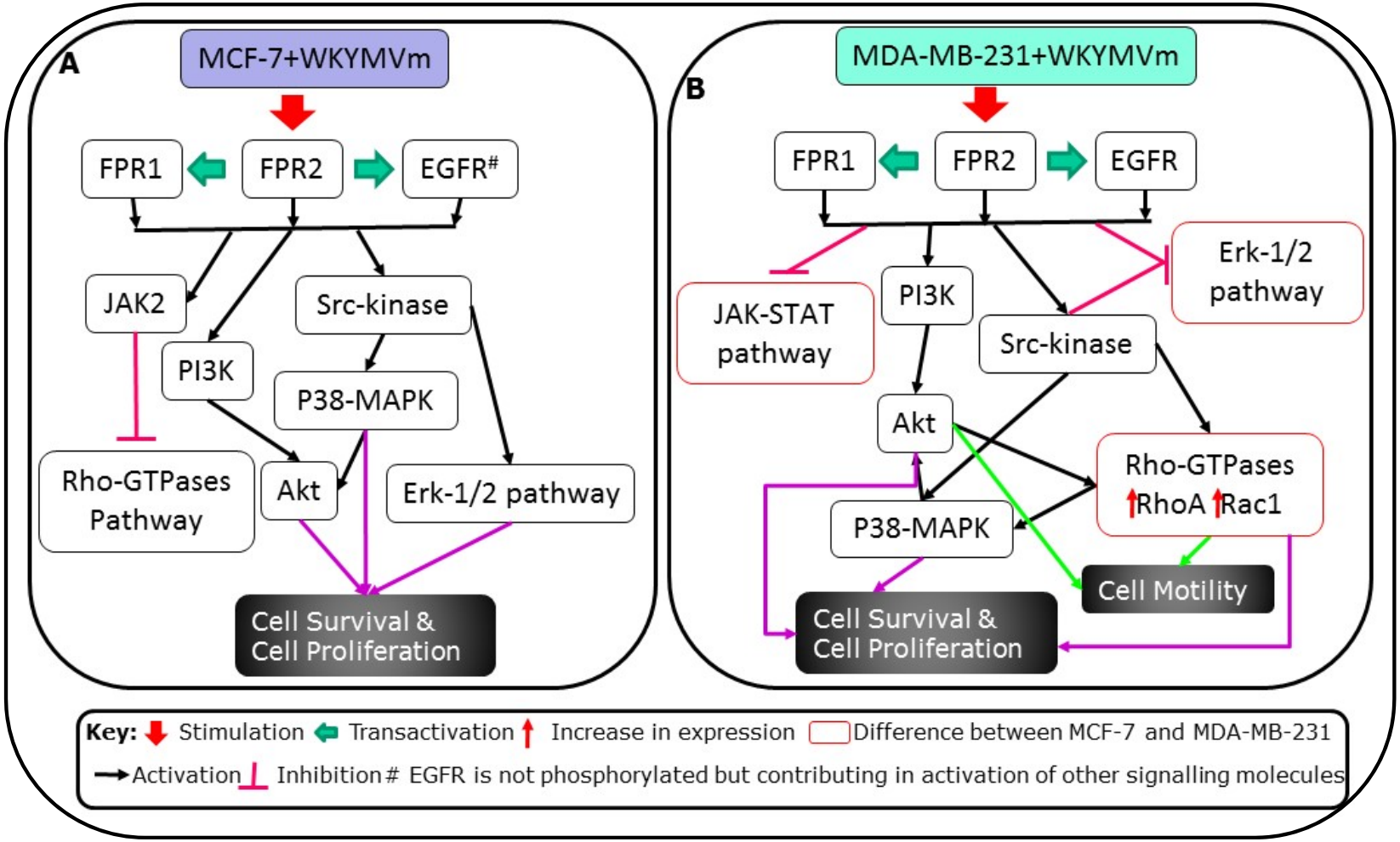

Fig-RB 24: Effect of WKYMVm treatment on signalling pathways in MCF-7 and MDA-MB-231 and probable resultant cellular events

by AG490, whereas complete inhibition of phosphorylation was seen in AG1478 and PP2 pre-treated cells. Further increase in EGFR phosphorylation was also seen in WRW4 pre-treated cells. These results suggested that increase in the phosphorylation of EGFR by EGF was mediated by the kinase activity of EGFR via Src-kinase and negatively regulated by FPR2. Furthermore, JAK2 also had a role in increase in EGFR phosphorylation.

In MDA-MB-231, phospho-EGFR level was further increase in the CsH, WRW4 and AG490 pre-treated cells (Fig-RB 25). Increase in the EGFR phosphorylation in CsH, WRW4 and AG490 pre-treated cells indicate that FPR1, FPR2and JAK2 negatively regulate the EGF mediated increase of EGFR phosphorylation. Partial inhibition of EGFR phosphorylation upon EGF treatment was observed in AG1478 and PP2 pre-treated cells. Although this decrease in the phosphorylation of EGFR was much less than EGF stimulation, it was still higher than the solvent control. It indicated involvement of EGFR per se and Src-kinase in EGFR phosphorylation. In addition, there was a possibility of involvement of the some other signalling pathway.

STAT3

EGF treatment had no effect on pSTAT3 levels in MCF-7 (Fig-RB 25). However, pre-treatment of cells with WRW4, AG490, AG1478 and PP2 showed increase in pSTAT3 levels. This observation showed that inhibition of FPR2, JAK2, EGFR and Src-kinase led to maintenance of pSTAT3 basal level even after EGF stimulation. EGF is a ligand for the EGFR and inhibition of EGFR kinase increased pSTAT3 level upon EGF stimulation. Hence, it could be postulated that activation of STAT3 upon EGF treatment in EGFR, FPR2 and JAK2 inhibited MCF-7 required some unknown signalling.

In MDA-MB-231, EGF treatment decreased pSTAT3 levels (Fig-RB 25). This decrease in pSTAT3 level was partially recovered in AG490 pre-treated cells, while increase in pSTAT3 level was observed in WRW4 and AG1478 pre-treated cells. FPR2 and EGFR led to dephosphorylation of STAT3 in MDA-MB-231.

Rac-1

EGF treatment led to decrease in expression of Rac-1 in MCF-7 (Fig-RB 25). The decrease in Rac-1 was inhibited in the cells pre-treated with CsH and AG490. Furthermore, Cells pre-treated with AG1478 and PP2, showed increase in the Rac-1 expression upon EGF stimulation. These results indicated that EGF caused decrease in Rac-1 expression by EGFR via cross talk with FPR1 and JAK2. EGFR and Src-kinase played major role in the EGF mediated decrease of Rac-1 because inhibition of these two could not only reverse the effect of EGF on Rac-1 but enhanced Rac-1 expression, in MCF-7.

In MDA-MB-231, treatment of EGF showed decrease in the expression of Rac-1 (Fig-RB 25). This decrease in Rac-1 upon EGF stimulation in MDA-MB-231 cell lines was partially inhibited in AG490 and AG1478 pre-treated cells while complete inhibition of EGF induced decrease in Rac-1 expression was inhibited in PP2 pre-treated cells. These observations indicated that EGF induced decrease in Rac-1 expression was mediated by EGFR, JAK2 and Src-kinase.

RhoA

EGF treatment to MCF-7 cells did not change expression of RhoA (Fig-RB 25). In addition, change in RhoA expression after EGF treatment was not observed in cells pre-treated with any of the inhibitors used.

In MDA-MB-231, treatment of EGF showed decrease in the expression of RhoA (Fig-RB 25). The lowered expression of RhoA in EGF stimulated in MDA-MB-231

was partially normalized in CsH, AG490, AG1478 and PP2 pre-treated cells. These observations suggested that the decrease in RhoA expression upon EGF treatment was mediated by FPR1, JAK2, EGFR and Src-kinase signalling.

Cdc42

EGF treatment led to decrease the expression of Cdc42 protein in MCF-7 (Fig-RB 25). Decrease in the Cdc42 upon EGF was partially inhibited by all the pre-treatments in the MCF-7. This suggested that the decrease in the Cdc42 upon EGF treatment was mediated by EGFR as well as FPR1, FPR2 and JAK2 via Src-kinase.

In MDA-MB-231, treatment of EGF led to decrease in Cdc42 expression (Fig-RB 25). This decrease in the Cdc42 expression, upon EGF stimulation, was inhibited in CsH, AG490 and PP2 pre-treated cells. These results suggested that decrease in the expression of Cdc42 upon EGF treatment in MDA-MB-231 was mediated by FPR1, JAK2 and Src-kinase signalling pathway.

PTEN

EGF treatment induced PTEN phosphorylation in both the HBCC (Fig-RB 26). In MCF-7, EGF induced increase in PTEN phosphorylation was inhibited in WRW4, AG490, AG1478 and PP2 pre-treated cells. These observations indicated that the increase in PTEN phosphorylation by EGF treatment was mediated by FPR2, JAK2, EGFR and Src-kinase.

In MDA-MB-231, further increase in PTEN phosphorylation upon EGF treatment was observed in CsH and WRW4 pre-treated cells, while the increase in PTEN phosphorylation was partially inhibited in AG490, AG1478 and PP2 pre-treated cells (Fig-RB 26). These observations suggested that increase in PTEN

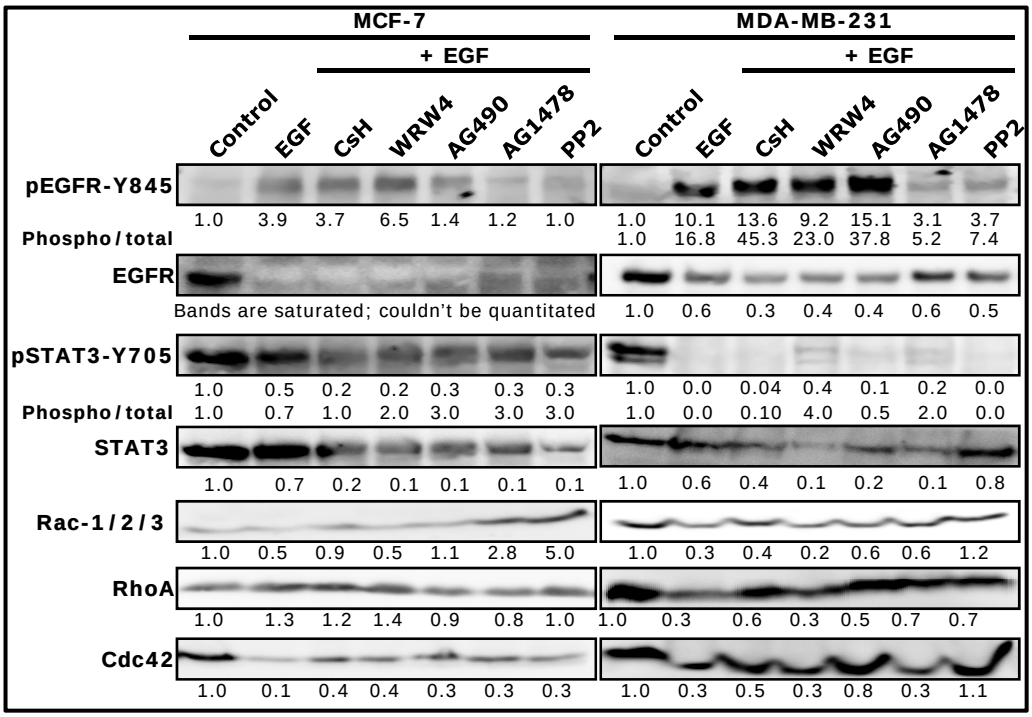

Fig-RB 25: EGF Stimulation: Effect of EGF was studied on various proteins in MCF-7 and MDA-MB-231 by Western blotting. Band density of the treatment group was compared to that of the solvent control to get fold change in expression. Fold change in expression of phospho protein was normalized with the fold change in expression of total protein to get absolute change in phospho protein. Each experiment was done in triplicate and representative blots are shown.

phosphorylation by EGF treatment was mediated via JAK2, EGFR and Src-kinase and EGF effect was negatively regulated by FPR1 and FPR2.

p38-MAPK

EGF stimulation led to the activation of p38-MAPK in both the cell lines (Fig-26 RB). In MCF-7, p38-MAPK phosphorylation was further increased upon EGF treatment in CsH, WRW4, AG490 and AG1478 pre-treated cells. It suggested that in MCF-7, activation of p38-MAPK followed the EGF stimulation might be mediated by some unknown signalling pathway, which was negatively regulated by FPR1, FPR2, JAK2 and EGFR per se.

In MDA-MB-231, increase in p38-MAPK phosphorylation upon EGF treatment was inhibited in the cells pre-treated with AG490 and therefore p38-MAPK phosphorylation level matched with that in the solvent control (Fig-RB 26). Further increase in p38-MAPK phosphorylation was seen in AG1478 pre-treated cell indicating presence of some feedback mechanism. Decrease in p38-MAPK phosphorylation than that in the solvent control, upon EGF stimulation was seen in CsH, WRW4 and PP2 pre-treated cells. Among these three, pre-treatment with WRW4 completely abolished phosphorylation. These observations suggested that EGF induced activation of p38-MAPK could be mediated through FPR1, FPR2 and Src-kinase and negatively regulated by EGFR. Among these receptors, activation of FPR1 and FPR2 was crucial for EGF induced p38-MAPK phosphorylation.

Akt

Akt-T308

EGF treatment increased phosphorylation of Akt at T308 (Fig-RB 26). Increase in pAkt-T308 upon EGF treatment was inhibited by the pre-treatment of cells with AG1478 and PP2, indicating the role of EGFR and Src-kinase in EGF stimulated

Akt phosphorylation at T308 in MCF-7. Increase in pAkt-T308 in cells pretreated with AG490 and stimulated with EGF indicate negative regulatory role of JAK2 in phosphorylation of Akt at T308.

At T308, EGF treatment caused decrease in phosphorylation of Akt in MDA-MB-231 (Fig-RB 26). This decrease in pAkt-T308 upon EGF treatment was inhibited in the cells pre-treated with AG490, while increase in the pAkt-T308 was observed in cells pre-treated with WRW4 and AG1478. These suggested that FPR2, JAK2 and EGFR were responsible for the decrease in pAkt-T308 upon EGF treatment.

Akt-S473

EGF treatment led to increase in phosphorylation of Akt at S473 in MCF-7 (Fig-RB 26). Increase in Akt phosphorylation at S473 by EGF treatment was further increased in the cells pre-treated with CsH while other pre-treatment did not show considerable effect. These results suggested that phosphorylation of Akt at S473 by EGF in MCF-7 involved some unknown mechanism, which was negatively regulated by FPR1.

In MDA-MB-231, EGF treatment stimulated phosphorylation of Akt only at S473. At S473, EGF induced Akt phosphorylation in MDA-MB-231 (Fig-RB 26). This phosphorylation was further increased with pre-treatment of cells with CsH, WRW4, AG490 and AG1478. These observations suggested that EGF induced phosphorylation of Akt at S473 was negatively regulated by FPR1, FPR2, JAK2, & EGFR.

The PTEN phosphorylation level did not show any inverse relation with the phosphorylation level of Akt in any EGF treatment group for MCF-7. Hence, PTEN activation failed to inhibit PI3K signalling in HBCC upon EGF treatment.

When changes in Akt phosphorylation levels upon EGF treatment were compared with the changes in phosphorylation levels of PTEN in EGF treated MDA-MB-231, it was found that PTEN phosphorylation levels showed inverse expression pattern with pAkt-T308. This inverse relationship between pAkt-308 level and PTEN phosphorylation level upon EGF treatment was disrupted in cells pre-treated with WRW4 and AG1478. This indicated that FPR2 and EGFR are essential for PTEN mediated inhibition of Akt activation in MDA-MB-231.

Erk-1/2

EGF led to the activation of the Erk-1/2 in both the cell lines (Fig-RB 26). In MCF-7, further increase in the Erk-1/2 phosphorylation was seen in CsH pre-treated cells, while partial inhibition of Erk-1/2 phosphorylation was observed in WRW4 and AG490 pre-treated cells. Complete abolition of Erk-1/2 phosphorylation upon fMLP stimulation was seen in AG1478 pre-treated cells. These observations showed that EGF treatment induced Erk-1/2 phosphorylation in MCF-7 cell lines, through EGFR in collaboration with FPR2 and JAK2. This EGF induced Erk-1/2 phosphorylation was negatively regulated by FPR1.

In MDA-MB-231, EGF induced Erk-1/2 phosphorylation was inhibited by AG1478 pre-treatment while increase in the Erk-1/2 phosphorylation was observed in PP2 pre-treated cells (Fig-RB 26). It indicated that EGF treatment induced the Erk-1/2 phosphorylation by the EGFR kinase signalling and this Ekr-1/2 phosphorylation was negatively regulated by Src-kinase.

EGF treatment increased Erk-1/2 phosphorylation in both the cell lines. In MCF-7, the increase was mediated by cross talk of FPR2, JAK2, and EGFR via Src-kinase and negatively regulated by FPR1, while in MDA-MB-231, the increase was mediated by EGFR and negatively regulated by Src-kinase.

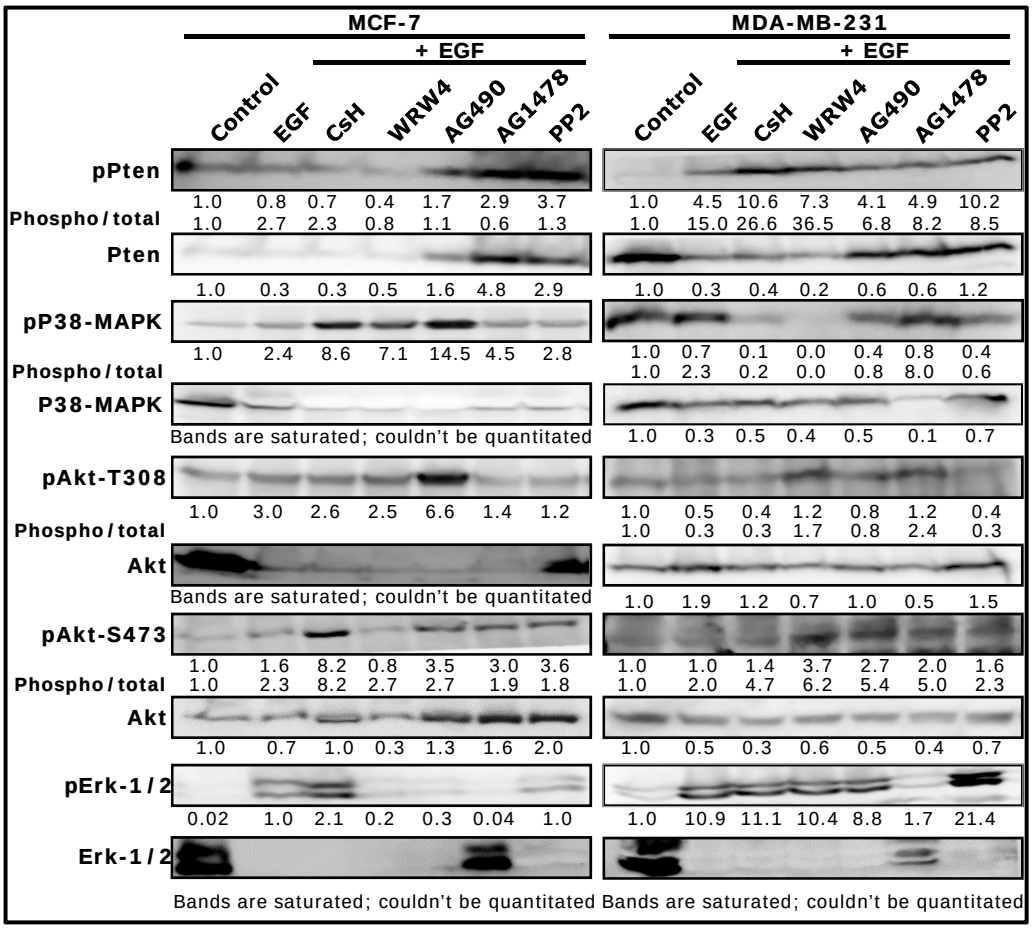

Fig-RB 26: EGF Stimulation: Effect of EGF was studied on various proteins in MCF-7 and MDA-MB-231 by Western blotting. Band density of the treatment group was compared to that of the solvent control to get fold change in expression. Fold change in expression of phospho protein was normalized with the fold change in expression of total protein to get absolute change in phospho protein. Each experiment was done in triplicate and representative blots are shown.

EGF summary

MCF-7

EGF treatment to MCF-7 led to activation of EGFR, which in turn transactivated FPR1 and FPR2 (Table-RB 13, Fig-RB 27A). These transactivated FPR further activated Ras-MAPK-Erk-1/2 pathway, PI3K-Akt pathway and p38-MAPK pathway, while inhibited Rho-GTPase pathway. All activated pathways are known to play role in cell proliferation. Thus, EGFR might be playing role only in proliferation of MCF-7.

Table-RB 13: Effect of EGF on MCF-7

Signalling molecules	Effect of fMLP	Contributors to the effect	Negative regulators
EGFR-845	**Increase**	EGFR, JAK2, Src-kinase	FPR2
STAT-3-Y705	*No effect*	------	FPR2, EGFR, JAK2, Src-kinase
Rac	**Decrease**	FPR1, EGFR, JAK2, Src-kinase	------
RhoA	*No effect*	------	------
Cdc42	**Decrease**	FPR1*, FPR2*, EGFR*, JAK2*, Src-kinase*	------
Pten	**Increase**	FPR2, JAK2, EGFR, Src-kinase	------
p38-MAPK	**Increase**	------	FPR1, FPR2, JAK2, EGFR
Akt-T308	**Increase**	EGFR, Src-kinase	JAK2
Akt-S473	**Increase**	------	FPR1
Erk-1/2	**Increase**	FPR2, JAK2, EGFR	FPR1

MDA-MB-231

Similar to MCF-7, EGF treatment activated EGFR, which transactivated FPR1 and FPR2 in MDA-MB-231 too (Fig-RB 27B, Table-RB 14). This resulted into activation of Ras-MAPK-Erk-1/2 and p38-MAPK pathway and deactivation Ras-Rho-GTPase, PI3K-Akt, and JAK-STAT pathway. All activated pathways are

known to play role in cell proliferation, while inhibition of JAK-STAT inhibits apoptosis. Thus, EGFR played role in only proliferation in MDA-MB-231.

Major differences in EGF stimulated signalling in MCF-7 and MDA-MB-231 are inhibition of PI3k-akt and JAK-STAT pathway in MDA-MB-231. Hence, it is proposed that PI3K-Akt pathway might be contributing to higher metastasis and drug resistance in EGF treated MCF-7.

Table-RB 14: Effect of EGF on MDA-MB-231

Signalling molecules	Effect of fMLP	Contributors to the effect	Negative regulators
EGFR-845	**Increase**	EGFR, Src-kinase	FPR1, FPR2, JAK2
STAT-3-Y705	**Decrease**	FPR2, EGFR, JAK2*	------
Rac	**Decrease**	JAK2, EGFR, Src-kinase	------
RhoA	**Decrease**	FPR1*, JAK2*, EGFR*, Src-kinase*	------
Cdc42	**Decrease**	FPR1*, JAK2, Src-kinase	------
Pten	**Increase**	JAK2*, EGFR*, Src-kinase*	FPR1, FPR2
p38-MAPK	**Increase**	FPR1, FPR2, JAK2, Src-kinase	EGFR
Akt-T308	**Decrease**	FPR2, JAK2, EGFR	------
Akt-S473	**Increase**	------	FPR1, FPR2, JAK2, EGFR
Erk-1/2	**Increase**	EGFR	Src-kinase

Stimulation with IL6

STAT3

In MCF-7, IL6 treatment led to increase in pSTAT3 level (Fig-RB 28), as expected. There was further increase in the pSTAT3 level upon IL6 treatment in AG1478 and PP2 pretreated cells. Increase in pSTAT3 upon IL6 treatment was partially inhibited by WRW4 and AG490 pre-treatment. These observations showed that, increase in pSTAT3 by IL6 was mediated by cross talk with FPR2

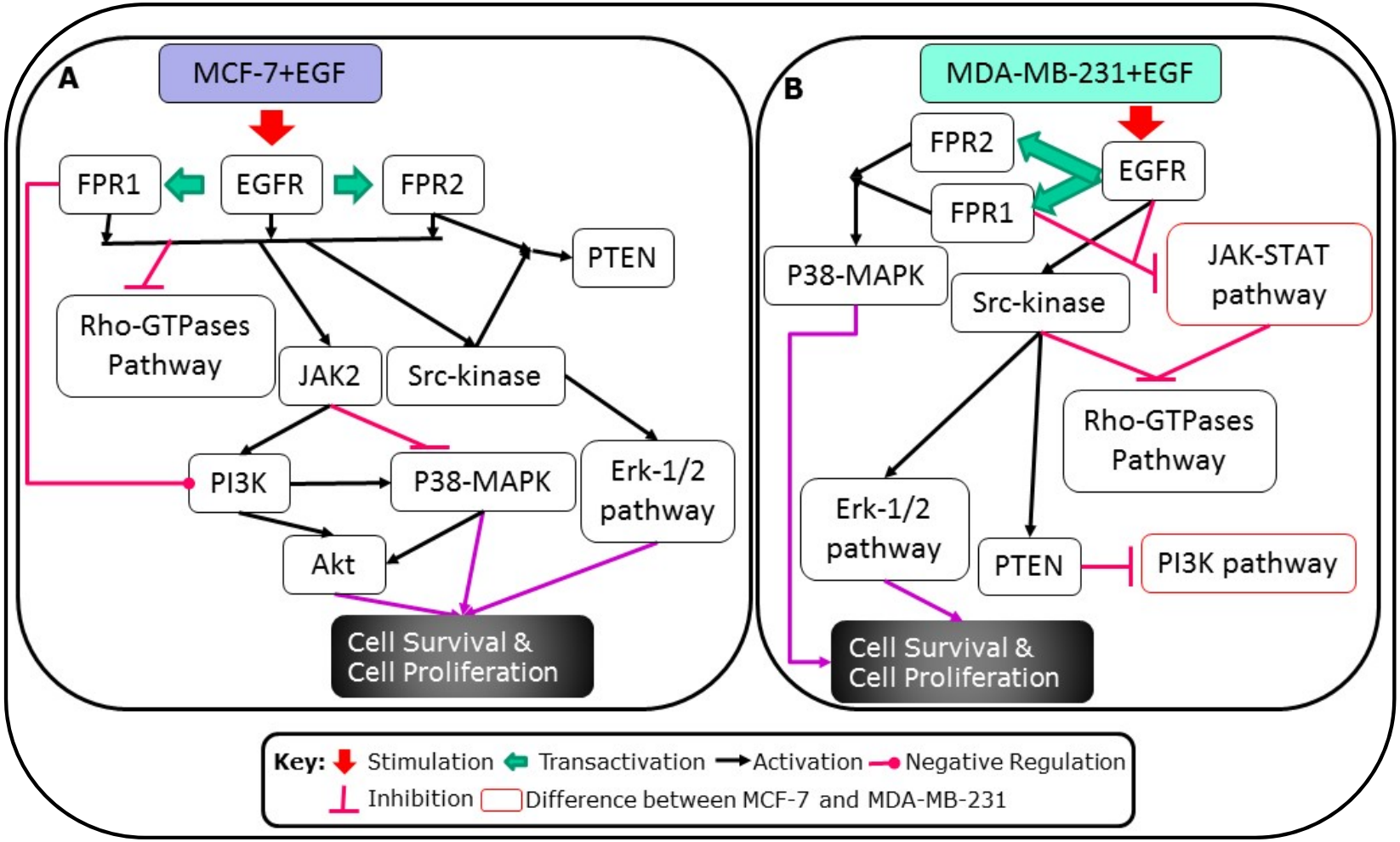

Fig-RB 27: Effect of EGF treatment on signalling pathways in MCF-7 and MDA-MB-231 and probable resultant cellular events

and induces JAK2 by some unknown pathway in MCF-7. EGFR and Src-kinase negatively regulate pSTAT3 upon IL6 stimulation. The protein in the CsH pre-treatment group had shown degradation in all the replicates.

In MDA-MB-231, IL6 led to the decrease in pSTAT3 (Fig-RB 28). The level of pSTAT3 was comparable to solvent control in CsH, WRW4, AG1478 and PP2 pre-treated cells, while AG490 pre-treated cells showed pSTAT3 level comparable to IL6 treated cells. This indicated that FPR1, FPR2, EGFR and Src-kinase were responsible for decrease in pSTAT3, upon IL6 treatment in MDA-MB-231, while JAK2 was not involved in it.

Generally, IL6 after binding to its receptor activates JAK-STAT signalling. However, IL6 treatment showed increase in pSTAT3 only in MCF-7 cell line, while MDA-MB-231 showed decrease in pSTAT3. This indicated a defect in the JAK-STAT signalling in triple negative MDA-MB-231 cell line. FPR2 played contrasting role in both the cell lines. In MCF-7, FPR2 and JAK2 cross talk helped in activation of STAT3 in MCF-7 upon IL6 treatment. While In MDA-MB-231, inhibition of FPR2 with FPR1 and EGFR restored the STAT3 phosphorylation via Src-kinase pathway.

Rac-1

IL6 treatment had no effect on Rac-1 protein expression in MCF-7 (Fig-RB 28). However, cells pre-treated with CsH and AG490 showed decrease in the expression of Rac-1, upon IL6 treatment. It showed that FPR1 and JAK2 helped in maintaining the basal level of Rac-1 expression in MCF-7, which otherwise was inhibited by IL6 through some unknown mechanism.

In MDA-MB-231 also, change in Rac-1 expression upon IL6 stimulation was not observed (Fig-RB 28). Nevertheless, increase in the expression of Rac-1 was

observed in CsH, WRW4, AG1478 and PP2 pre-treated cells upon IL6 stimulation. This observation showed that FPR1, FPR2, EGFR and Src-kinase inhibit IL6 mediated increase in Rac-1 expression in MDA-MB-231.

RhoA

IL6 treatment had no effect on RhoA protein expression in MCF-7 (Fig-RB 28). However, RhoA expression was decreased in CsH, WRW4, AG1478 and PP2 pre-treated, IL6 stimulated MCF-7 cells. This suggested that FPR1, FPR2, EGFR and Src-kinase, helped in maintaining the basal level of RhoA upon IL6 treatment in MCF-7 cells.

In MDA-MB-231, change in RhoA expression was not observed upon IL6 treatment (Fig-RB 28). However, unlike in MCF-7, increase in the expression of RhoA upon IL6 treatment, was observed in CsH, WRW4, AG490, AG1478 and PP2 pre-treated cells. This suggested that inhibition of FPR1, FPR2, JAK2, EGFR and Src-kinase increased expression of RhoA in IL6 stimulated MDA-MB-231 cell line. Thus, though FPR1, FPR2, EGFR and Src-kinase helped in maintaining basal level of RhoA in both the IL6 stimulated cell lines, the mechanism of action was opposite.

Cdc42

IL6 treatment had shown decrease in the Cdc42 protein expression in MCF-7 (Fig-RB 28). This decrease in Cdc42 was inhibited in cells pre-treated with AG490, AG1478 and PP2. This observation indicated that JAK2, EGFR and Src-kinase signalling were responsible for the decrease in the expression of Cdc42 in MCF-7 upon IL6 treatment.

PTEN

IL6 treatment induced PTEN phosphorylation in both HBCC cell lines (Fig-RB 28). In MCF-7, further increase in PTEN phosphorylation was observed in cells pre-treated with CsH and WRW4. The increase in PTEN phosphorylation upon IL6 treatment was inhibited in AG1478 pre-treated cells, while partial inhibition of PTEN phosphorylation was seen in AG490 and PP2 pre-treated cells. These observations indicated that the increase in PTEN phosphorylation in MCF-7 upon IL6 treatment was mediated by EGFR, JAK2 and Src-kinase, where JAK2 and Src-kinase had partial role. This increase in PTEN phosphorylation was negatively regulated by FPR1 and FPR2.

In MDA-MB-231, increase in PTEN phosphorylation upon IL6 treatment was partially inhibited in the cells pre-treated with the CsH, WRW4 and AG490, while level of PTEN phosphorylation comparable to solvent control was observed in AG1478 pre-treated cells (Fig-RB 28). Decrease in PTEN phosphorylation upon IL6 treatment was seen in PP2 pre-treated cells. This indicated that the increase in PTEN phosphorylation upon IL6 treatment in MDA-MB-231 was mediated by EGFR, FPR1, FPR2 and JAK2 where Src-kinase activity is indispensable for maintaining basal level.

p38-MAPK

IL6 treatment showed activation of p38-MAPK only in MDA-MB-231 (Fig-RB 28). In MCF-7, IL6 treatment caused decrease in p38-MAPK phosphorylation. This decrease in p38-MAPK phosphorylation was inhibited by AG1478 pre-treatment, whereas increase in the level of p38-MAPK phosphorylation was observed in CsH, WRW4 and AG490 pre-treated cells. It suggested that the decrease in p38-MAPK phosphorylation upon IL6 stimulation was mediated by EGFR. Moreover,

inhibition of FPR1, FPR2 and JAK2 led to the increase in p38-MAPK phosphorylation, upon IL6 treatment, suggesting their involvement in IL6 mediated decrease of p38-MAPK phosphorylation.

In MDA-MB-231, activation of p38-MAPK by IL6 was partially inhibited by the pre-treatment of CsH, WRW4 and AG490 while AG1478 pretreatment showed complete inhibition (Fig-RB 28). Moreover, further increase in p38-MAPK phosphorylation was seen in PP2 pre-treated cells. This indicated that activation of p38-MAPK by IL6 in MDA-MB-231 had involvement of FPR1, FPR2, JAK2 and EGFR signalling while Src-kinase negatively regulated the increase in p38-MAPK phosphorylation upon IL6 treatment.

Akt

Akt-T308

Treatment of IL6 did not induce phosphorylation of Akt at T308 (Fig-RB 28). However, pre-treatment of MCF-7 cells with CsH, AG490, AG1478 and PP2 yielded increase in pAkt-T308 by IL6. This observation showed that IL6 could induce Akt phosphorylation at T308 in MCF-7 by unknown signalling mechanism if FPR1, JAK2, EGFR and Src-kinase were inhibited.

In MDA-MB-231, though IL6 did not induce the phosphorylation at any of the sites, cells pre-treated with AG490 and PP2 showed increase in the Akt phosphorylation at T308 upon IL6 treatment (Fig-RB 28). It indicated that inhibition of JAK2 and Src-kinase played role in maintaining basal levels of pAkt-T308 in IL6 stimulated MDA-MB-231.

Akt-S473

Similar to T308, change in phosphorylation in Akt at S473 was not seen in MCF-7 upon IL6 treatment (Fig-RB 28). However, increase in the phosphorylation was

observed after IL6 treatment in CsH, WRW4, AG490 and AG1478 pre-treated MCF-7 cells. However, in PP2 pre-treated cells, decrease in the level of pAkt-S473 was seen after IL6 treatment. This indicated that IL6 could increase pAkt-S473 level in MCF-7 by signalling mechanism involving Src-kinase if FPR1, FPR2, JAK2 and EGFR were inhibited.

At S473 site of Akt, increase in the phosphorylation after IL6 treatment was not observed. But in cells pre-treated with CsH and AG490 increase in pAkt-S473 was seen (Fig-RB 28). Furthermore, decrease in the phosphorylation after IL6 treatment was observed in PP2 pre-treated cells. These observations showed that inhibition of FPR1 and JAK2 led to the increase in pAkt-S473, while inhibition of Src-kinase lead to decrease suggesting negative and positive regulatory role, respectively.

Akt phosphorylation pattern in IL6 treated MCF-7 and MDA-MB-231 cells was compared with PTEN phosphorylation pattern in IL6 treated MCF-7 cells to know the detailed mechanism of Akt phosphorylation. In both the cell lines increase in PTEN phosphorylation and absence of Akt phosphorylation on IL6 stimulation, suggested that increased PTEN might have inhibited PI3K-Akt pathway.

Erk-1/2

IL6 treatment activated Erk-1/2 in both the cell lines (Fig-RB 28) by increasing phosphorylation of Erk-1/2. In MCF-7, further increase in the Erk-1/2 phosphorylation was observed in WRW4 pre-treated cells while partial decrease in the phosphorylation was seen in CsH, AG490, AG1478 and PP2 pre-treated cells. These observations indicated that IL6 treatment induced the Erk-1/2 phosphorylation by FPR1, JAK2, EGFR and Src-kinase. FPR2 negatively regulated IL6 mediated increase in Erk-1/2 phosphorylation.

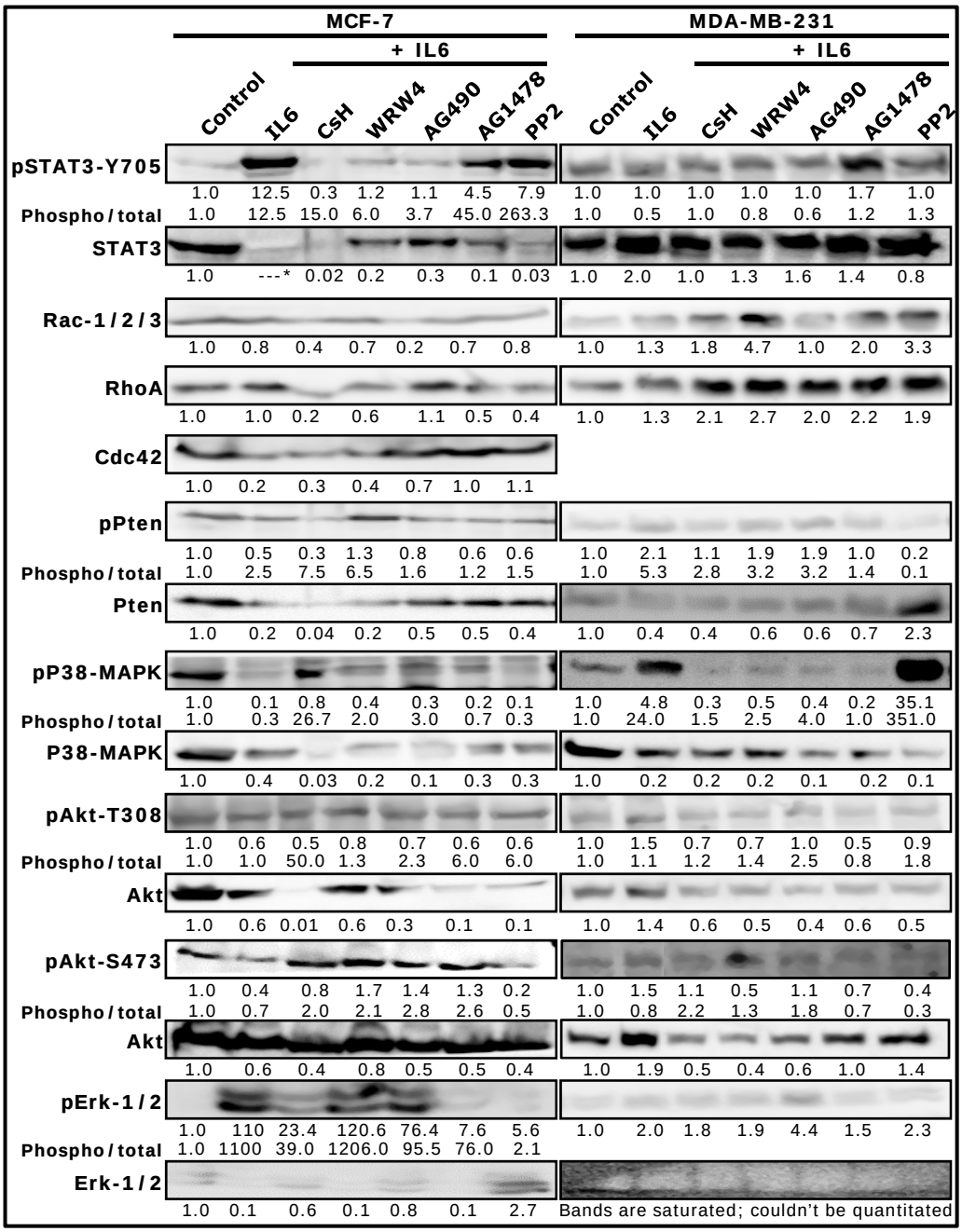

Fig-RB 28: IL6 Stimulation: Effect of IL6 was studied on various proteins in MCF-7 and MDA-MB-231 by Western blotting. Band density of the treatment group was compared to that of the solvent control to get fold change in expression. Fold change in expression of phospho protein was normalized with the fold change in expression of total protein to get absolute change in phospho protein. Each experiment was done in triplicate and representative blots are shown. *Bands are saturated; couldn't be quantitated

In MDA-MB-231, IL6 induced Erk-1/2 phosphorylation, which was further increased in the cells pre-treated with AG490 while partial inhibition of Erk-1/2 phosphorylation was seen AG1478 pre-treated cells (Fig-RB 28). This indicated that IL6 induced Erk-1/2 phosphorylation was partially mediated by EGFR and was negatively regulated by JAK2.

IL6 summary

MCF-7

IL6 treatment to MCF-7 activated FPR1, FPR2, EGFR, JAK2 and Src-kinase (Fig-RB 29A, Table-RB 15). This resulted into activation of Ras-MAPK-Erk-1/2 and JAK-STAT pathway while inhibition of Rho-GTPase, p38-MAPK & PI3K-Akt pathway. All activated pathways are known to play role in cell proliferation. Thus, IL6R might be playing role only in proliferation of MCF-7.

Table-RB 15: Effect of IL6 on MCF-7

Signalling molecules	Effect of fMLP	Contributors to the effect	Negative regulators
STAT-3-Y705	**Increase**	FPR2, JAK2	EGFR, Src-kinase
Rac	*No effect*	FPR1, JAK2	------
RhoA	*No effect*	FPR1, FPR2*, EGFR, Src-kinase	------
Cdc42	**Decrease**	JAK2*, EGFR, Src-kinase	------
Pten	**Increase**	JAK2*, EGFR, Src-kinase*	FPR1, FPR2
p38-MAPK	**Decrease**	FPR1, FPR2, JAK2, EGFR*	------
Akt-T308	*No effect*	------	FPR1, JAK2, EGFR, Src-kinase
Akt-S473	*No effect*	Src-kinase	FPR1, FPR2, JAK2, EGFR
Erk-1/2	**Increase**	FPR1*, JAK2*, EGFR*, Src-kinase	FPR2

MDA-MB-231

Similar to MCF-7, IL6 treatment to MDA-MB-231 activated FPR1, FPR2, EGFR, JAK2 and Src-kinase (Fig-RB 29B, Table-RB 16). This resulted into activation of Ras-MAPK-Ekr-1/2 pathway and p38-MAPK pathway and deactivation of JAK-STAT, PI3K-Akt and Rho-GTPase pathways. Both activated pathways are known to play role in cell proliferation. Hence, similar to MCF-7, IL6R might be playing role only in proliferation of MDA-MB-231. The major differences in IL6 stimulated signalling in MCF-7 and MDA-MB-231 are activation of p38-MAPK and deactivation of JAK-STAT pathways in MDA-MB-231. Hence, it is proposed that p38-MAPK might be contributing to higher cell proliferation in MDA-MB-231.

Table-RB 16: Effect of IL6 on MDA-MB-231

Signalling molecules	Effect of fMLP	Contributors to the effect	Negative regulators
STAT-3-Y705	**Decrease**	FPR1, FPR2, EGFR, Src-kinase	------
Rac	*No effect*	------	FPR1, FPR2, EGFR, Src-kinase
RhoA	*No effect*	------	FPR1, FPR2, JAK2, EGFR, Src-kinase
Pten	**Increase**	FPR1*, FPR2*, JAK2*, EGFR, Src-kinase	------
p38-MAPK	**Increase**	FPR1, FPR2, JAK2, EGFR,	Src-kinase
Akt-T308	*No effect*	------	JAK2, Src-kinase
Akt-S473	*No effect*	Src-kinase	FPR1, JAK2
Erk-1/2	**Increase**	EGFR*	JAK2

Above presented results had convincingly established the transactivation of EGFR by FPR1 and FPR2 and vice-versa in breast cancer. Above results, also presented evidence for the existence of signalling cross talk between FPR1,

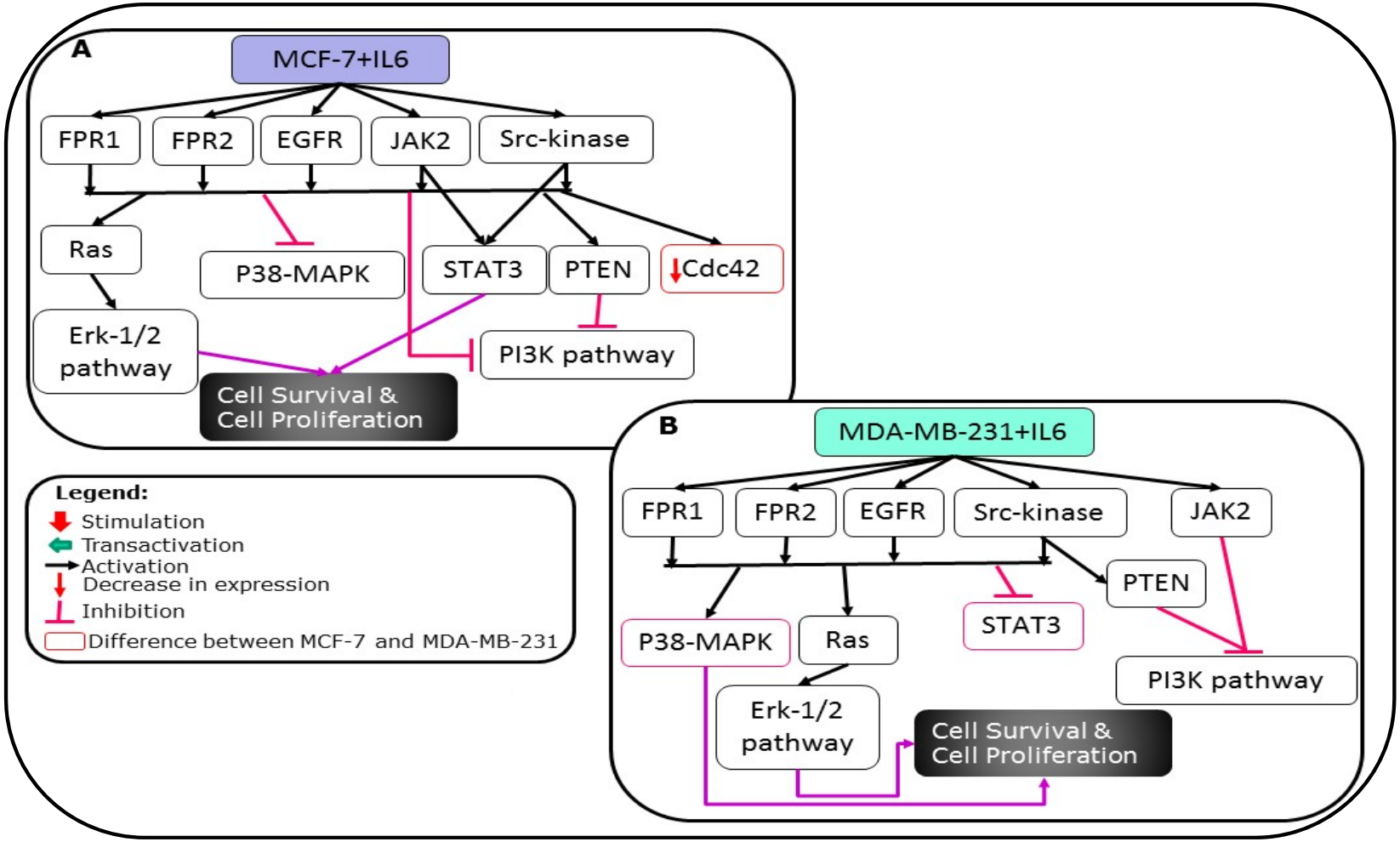

Fig-RB 29: Effect of EGF treatment on signalling pathways in MCF-7 and MDA-MB-231 and probable resultant cellular events

FPR2, EGFR and JAK-STAT. These receptors not only activate each other's downstream signalling, but also negatively regulate it. However, unlike glioblastoma, FPR1 and FPR2 did not activate STAT3, cross talk between FPR1, FPR2 and JAK-STAT was seen in the downstream signalling. It was evident from these results that in MCF-7, though FPR1 and FPR2 both played role in cell proliferation only FPR1 was playing role in cell motility. In MDA-MB-231, both FPR1 and FPR2 played role in cell proliferation and cell motility. Moreover, cell proliferation effect of EGF and IL6 was results of their respective signalling pathways with signalling pathways of FPR1 and FPR2.

Receptor signalling in cells do not act in an isolated fashion. Depending upon cell type and physiological environment, receptors showed trans-activation of other receptor and cross talk with other pathways. When a receptor gets activated as a result of another receptor's activation then this phenomenon is called as receptor trans-activation. When one or more components of the one signal transduction pathway activates another pathway, it is called cross talk. Our results demonstrated, transactivation of EGFR by FPR1 and FPR2 in breast cancer cell lines. These receptors regulated downstream signalling of each other. In addition, cross talk of these receptors with some unknown signalling pathway had also been suggested, which needs to be further investigated. Two HBCC were chosen for in depth study of receptor trans-activation and cross talk involving FPR1 and FPR2. Cells were treated with the specific inhibitor for FPR1, FPR2, EGFR, JAK2 and Src-kinase. After which each set of pretreated cells were sequentially stimulated with the specific ligands for FPR1, FPR2, EGFR and IL6. fMLP is a ligand for FPR1 and FPR2, where FPR is a high affinity receptor for fMLP while FPR2 is a low affinity receptor for fMLP[340]. Since FPR1 had higher

expression than FPR2 it was considered as a ligand for FPR1. WKYMVm, EGF and IL6 were used as specific ligands for FPR2, EGFR and cytokine receptors, respectively.

The presented results had convincingly established transactivation of EGFR by FPR1 and FPR2 and vice-versa in breast cancer. These receptors not only activate each other's downstream signalling, but sometime negatively regulate it too. EGFR is a transmembrane receptor tyrosine kinase that belongs to c-ErbB family[341]. It known to be over-expressed in various human malignancy[321]. Almost all subtypes of breast cancer over-express EGFR, but more frequent EGFR overexpression was seen in triple negative breast cancer and inflammatory breast cancer[342]. Overexpression of EGFR is linked to poor differentiation and poor clinical outcome[342]. Transactivation of EGFR by FPR1 was reported in human monocytes and glioblastoma cell lines, while FPR2 mediated EGFR transactivation was reported in human lung cells[58, 59, 343]. fMLP mediated transactivation of EGFR in glioblastoma was mediated by FPR1 via Src-kinase. In glioblastoma, fMLP stimulation increased EGFR phosphorylation only at Y992, while Y845 and Y1068 were unaffected[59]. In human monocytes fMLP stimulation led to the EGFR phosphorylation at Y1068 while other sites were not explored[58]. FPR2 mediated EGFR transactivation in Calu-6 cells, but specific phosphorylation position was not deduced as common phospho-tyrosine antibody was used[343]. EGFR transactivation by FPR2 in Calu-6 cells also required Src-kinase, which led to activation of STAT3[343]. In our results we also found that Src-kinase was required for transactivation of EGFR by FPR1 and FPR2.

However, unlike glioblastoma, FPR1 and FPR2 did not activate STAT3, although role of JAK2 was important for regulating FPR1, FPR2, EGFR and IL6R mediated

downstream signalling. The Janus kinase/signal transducers and activators of transcription (JAK/STAT) pathway is the principal signalling pathway utilized by various cytokine and growth factors[322]. STAT3 phosphorylation was the hallmark of JAK2-STAT3 signalling[322]. STAT3 is involved in cell differentiation, growth, cycle, survival and motility[344, 345]. Constitutively active STAT3 is found in more than 50% primary breast tumors, while higher level of STAT3 phosphorylation in stage-II breast cancer is associated with poor clinical response to neo-adjuvant therapy[346-358]. Inhibition of STAT3 in breast xenografts and cell lines led to increase in apoptosis, chemo sensitivity and decrease angiogenesis[350-353, 356, 359-361]. Our study showed that instead of activating STAT3, fMLP and WKYMVm helped in maintaining basal phosphorylation level of STAT3 in MCF-7, while in MDA-MB-231 these stimulants dephosphorylated STAT3. Activation of STAT3 by FPR1 and FPR2 has previously been reported in various human cells. In human monocytes, trans-activation of EGFR by FPR1 upon fMLP stimulation led to the activation of STAT3[58]. FPR mediated STAT3 phosphorylation upon fMLP stimulation was reported in U87MG –a glioblastoma cell line[60] and MKN28 – gastric tubular adenosarcoma cell line[362]. WKYMVm induced phosphorylation of STAT3 was reported in prostate epithelial cell line PNT1A and FPR2 transfecting RBL-2H3 cell line[363, 364]. In PNT1A, STAT3 phosphorylation by FPR2 required cMet and mediated by NADPH oxidase[364]. FPR2 expressing RBL-2H3 cell lines showed time and concentration dependent STAT3 phosphorylation at S727[31]. WKYMVm stimulation did not show phosphorylation of STAT3 at Y705. FPR1 expressing RBL-2H3 also showed STAT3-S727 phosphorylation upon WKYMVm showed transactivation of FPR1 by FPR2[31]. Another ligand of FPR2 –lipoxin-A4 also showed FPR2 mediated STAT3 phosphorylation in U937 cell lines[364]. Other ligand

for FPR2 –SAA failed to phosphorylate STAT3 in U937[364]. In contrast to these reports, STAT3 activation was not seen in fMLP and WKYMVm stimulated MCF-7. On the contrary, deactivation of STAT3 was seen in both fMLP and WKYMVm treated MDA-MB-231. There are many papers reporting signalling of FPR1 and FPR2, but cross talk of these two was never reported. To our knowledge, this would be the first experimental proof of existence of FPR1 and FPR2 cross talk. Cross talk between FPR1 & EGFR as well as FPR2 & EGFR was seen in fMLP stimulated and WKYMVm stimulated cells, respectively.

In MCF-7, FPR1 activation by fMLP led to the activation of JAK2, Ras-MAPK-Erk-1/2 and Ras-Rho GTPase pathway while in MDA-MB-231 it activated PI3K-Akt pathway, Ras-Rho-GTPase pathway and Ras-MAPK-Erk-1/2 pathway and deactivated of JAK-STAT pathway. The JAK/STAT signaling pathway stimulated by various cytokines and surface receptors. JAK2 is a member of the Janus family of non-receptor tyrosine kinases. V617F mutation of JAK2 which is common in myeloproliferative disorders, resulted into constitutively activation of its tyrosine kinase activity[365-368]. Very little information about presence and role of JAK2 in solid tumors is available. Recently upregulation of JAK2 was reported in gastric cancer[369]. In breast cancer, it was reported that JAK2-STAT3 signalling was required for the growth of $CD44^{+}/CD24^{-}$ stem cell like breast cancer cells. Activation of JAK2 signalling has been associated with cell survival, proliferation, tumor progression and increased angiogenesis[370].

The Ras-MAPK-Erk-1/2 is critical for normal physiological development as it coupled signals from surface receptors to transcription factors. In cancer, Erk-1/2 activity was higher in metastatic cells compared to non-metastatic cancer cells[371-374]. Increased Erk-1/2 activity was found in primary breast tumors as

compared to their adjacent normal breast tissues[371, 374]. This increased ERK activity was found to be associated with the enhanced nodal metastasis. Erk-1/2 stimulated release of MMPs. Therefore it has been implicated in progression and invasion of cancer[375]. It was also found to be associated with the cell survival, proliferation, autocrine transformation and drug resistance[376].

The PI3K-Akt pathway is highly conserved, multistep signalling pathway. Activation of PI3K-Akt pathway is initiated when a growth factor or ligand binds to the receptor tyrosine kinase (RTK) or GPCR[377]. PI3K pathway is frequently altered in cancer. Amplification of PIK3C, that encodes p110a catalytic subunit of PI3K, was found in various cancers[378, 379]. PI3K mutations were found to be responsible for resistance to anti-HER2 agents[380]. Furthermore, amplification of downstream Akt gene, especially Akt2, was seen in ovarian, pancreas, breast and stomach malignant tumors[381-383]. PI3K/Akt pathway played a major role in stimulation of proliferation and survival in cells overexpressing ErbB2[384]. Akt played an important role in cancer progression and cell survival[384]. Breast cancer cell lines with a constitutively activated PI3K/Akt pathway have been shown to be resistant to HER2 and EGFR-targeted therapies as well as to endocrine therapy[385]. Normally employed drugs in the treatment and management of breast cancer -trastuzumab, tamoxifen, paclitaxel, doxorubcin, etoposide rapidly activated Akt in breast cancer cell lines[385]. This increase in Akt activity helped these cancer cells to overcome the cell death induced by these drugs. Pharmacological or genetic inhibition of PI3K/Akt pathway increased sensitivity of cancer cells to these drugs. Breast cancer cells heavily depend on the Akt pathway as a survival factor to elude the effects of cytotoxic therapy. PTEN dephosphorylates PIP3 and acts as a negative regulator for PI3K[386]. PTEN is

frequently mutated in advanced stages of various malignancies. Loss of PTEN leads to permanent activation of PI3K/Akt pathway.

Small Rho-GTPases are involved in most of the steps of cancer initiation and progression. This includes unlimited proliferation potential, survival, tissue invasion, metastases and evasion from apoptosis. Mutations were rarely reported in small Rho-GTPases proteins in cancer but their expression and/or activity are frequently altered[387-389]. RhoA could stimulate transformation[390] and contribute in generation of epithelial polarity and junction assembly in normal epithelia[391]. However, it also affects epithelial disruption during tumour progression by regulating production of MMPs and induce cell invasion[392]. Rac1 knockout is embryonic lethal in mice[393] but conditional knockout mice have been extensively studied[394, 395]. It was reported that Rac1 function was required for K-Ras mediated proliferation and tumorigenicity[396]. Rac1 increased expression of cyclin D1 and thereby induced cell transformation[387, 390]. Rac1 mediated loss of adhesion and promoted migration[397-400]. Similar to RhoA, Rac1 could also regulate production of MMPs and thereby controls cancer cell invasion[392]. Apart from role in cell migration and invasion Cdc42 is the only Rho GTPases, which could affect cell cycle progression by regulating chromosome segregation during mitosis[391]. Cdc42 knockdown induced chromosome misalignment during cell division, which resulted into multinucleate cells. Cdc42 is involved in epithelial polarity as well as migratory polarity.

Thus, on fMLP stimulation, FPR1 seemed to play role in motility as well as proliferation of both the cell lines. However difference in the fMLP stimulated signalling in MCF-7 and MDA-MB-231 are activation of PI3K-Akt pathway and deactivation of JAK-STAT pathway in MDA-MB-231. This suggested that these

pathways might be involved in higher cellular proliferation and drug resistance of MDA-MB-231. On the other hand, transactivation of FPR1 and EGFR by FPR2 in WKYMVm treated MCF-7 led to the activation of similar pathway as in fMLP treated MCF-7, except activation of PI3K-Akt pathway and inhibition of Rho-GTPases pathway in WKYMVm treated cells. WKYMVm treatment to MDA-MB-231 also showed similar effect as fMLP treatment except inhibition of Ras-MAPK and activation of p38-MAPK. This suggested that WKYMVm treatment promotes higher proliferation and cell survival than fMLP treatment. But unlike fMLP, WKYMVm treatment induced motility only in MDA-MB-231 but not in MCF-7. Apart from transactivation of EGFR by FPR1 and FPR2, transactivation of FPR1 and FPR2 by EGFR was also found. In MCF-7, EGFR mediated increase in PTEN and Erk-1/2 involved cross talk with FPR2, while inhibition of Rho-GTPases by EGFR involved FPR1 cross talk. In MDA-MB-231 too, EGFR mediated inhibition of Rho-GTPases involved FPR1 cross talk. Cross talk with FPR1 and FPR2 were also involved in EGFR mediated activation of p38-MAPK, while inhibition of STAT3 and Akt was mediated by FPR2 cross talk. Similarly, in MCF-7, IL6R mediated activation of JAK-STAT pathway required FPR2 while activation of Erk-1/2 required cross talk with FPR1. In MCF-7 inhibition of p38 in MCF-7 by IL6R also required cross talk with FPR1 and FPR2. In MDA-MB-231, activation of PTEN and p38-MAPK and inhibition of STAT3 by IL6R required cross talk with FPR1 and FPR2. This is probably the first ever report of existence of any such involvement of FPR1 and FPR2 in EGFR and IL6R mediated signalling in breast cancer.

Effect of FPR1 and FPR2 agonist and antagonists on breast cancer cell line proliferation

FPR1 and FPR2 have been reported to promote cell proliferation in glioblastoma[59]. Since, FPR1 and FPR2 could transactivate EGFR and activated p38-MAPK, Akt, Erk-1/2, which has a role in cell proliferation, effect of FPR1 and FPR2 stimulation as well as inhibition was checked on cell proliferation in breast cancer.

Both MCF-7 and MDA-MB-231 were treated with FPR1 agonist fMLP and FPR2 agonist WKYMVm. Furthermore, these cell lines were also pre-treated with FPR1 antagonist, CsH and FPR2 antagonist, WRW4 followed by fMLP and WKYMVm stimulation, respectively. After treatment, cells were checked at 48 hrs for effect of these treatments on cell proliferation. Growth inhibition and proliferation only above 10% was considered as effect of treatment.

There were only two reports showing effect of fMLP on cell proliferation and one for WKYMVm, but none of them talked about effect of CsH and WRW. Huang et al showed that U87 cells treated with 1 µM fMLP showed 15-20% increase in cell growth after 48 hrs than that in the control. Khau et al have reported about 25% and 50% increase in growth of MCF-7 and MDA-MB-231, respectively, on treatment with 1 µM fMLP and 100 nM WKYMVm for 24 hrs. Unpublished data from our lab had showed increase in cell proliferation of HBCC upon 1 µM fMLP treatment. Though they have used 100 nM WKYMVm, it was found that WKYMVm functions effectively at 1 µM concentration[401]. Hence, MCF-7 and MDA-MB-231 were treated with 1µM fMLP and 1µM WKYMVm and cell growth was monitored after 48 hrs, which is a well established time point in drug discovery studies.

CsH & fMLP combination treatment was the only treatment group that displayed effect on growth of MCF-7 cell line (Fig-RB 30A; Table-17). 52% inhibition of growth was observed in MCF-7 after treatment with CsH followed by stimulation with fMLP. No other treatment group had shown any notable inhibitory effect on MCF-7 cell proliferation.

Table-RB 17: Effect of FPR1 and FPR2 agonists and antagonists on cell proliferation

		% Growth Inhibition			
		fMLP	CsH + fMLP	WKYMVm	WRW4 + WKYMVm
MCF-7	48 Hrs.	8.5 ± 0.5	51.5 ± 2.0	-3.5 ± 1.1	6.6 ± 1.0
MDA-MB-231	48 Hrs.	19.7 ± 3.2	12.2 ± 1.7	6.9 ± 1.1	14.7 ± 3.6

MDA-MB-231 showed ~20% growth inhibition by fMLP which was inhibited by the pre-treatment of CsH (Fig-RB 30B; Table-17). WKYMVm treatment did not show any significant change in growth of MDA-MB-231 but pre-treatment of cells with WRW4 results in 15% growth inhibition after WKYMVm treatment.

These results showed that stimulation of FPR1 and FPR2 did not affect proliferation in MCF-7 but inhibition of FPR1 was detrimental to cells. On the contrary, FPR1 though to a lesser extent, but significantly inhibited MDA-MB-231 cell growth. FPR2 stimulation did not contribute to MDA-MB-231 cell growth, but its inhibition had marginal inhibitory effect.

Results showed that FPR1 stimulation might not induce cell growth in MCF-7 but its inhibition severely hampered cell growth. In MDA-MB-231, FPR1 stimulation and inhibition marginally but significantly stimulated and inhibited the cell growth, respectively. FPR2 stimulation and inhibition did not show any effect on MCF-7 growth, but MDA-MB-231 cell growth was marginally inhibited by FPR2

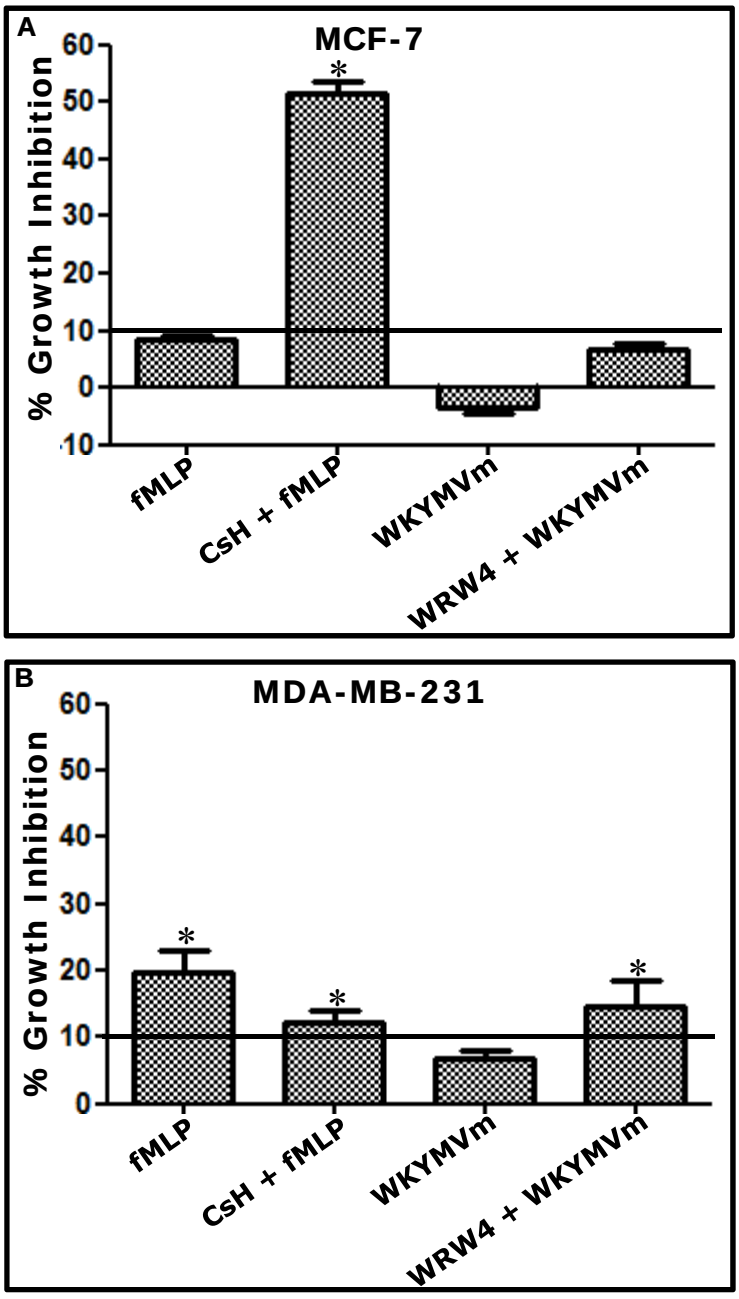

Fig-RB 30: Effect of FPR1 agonist & antagonist and FPR2 agonist & FPR2 antagonist on cell proliferation: Effect of FPR1 agonist –fMLP, FPR1 antagonist –CsH, FPR2 agonist –WKYMVm and FPR2 antagonist –WRW4 on cell proliferation of breast cancer cell lines MCF-7 (A) and MDA-MB-231 (B), after 48 hrs. Each experiment was done in triplicate. Data presented as average % growth inhibition ± SEM. * $p<0.05$ wrt to solvent control (Wilcoxon pair test).

inhibition. FPR1 and FPR2 have been reported to promote cell proliferation in glioblastoma[59]. In breast cancer, EGFR and other hormone receptors made the breast cancer cells highly proliferative. Since HBCC already had high rate of cell proliferation effect of fMLP on HBCC proliferation might not be observed. Furthermore, transactivation and cross talk in signalling pathways existed between EGFR and FPR1 &FPR2, due to which FPR1 and FPR2 might be already active in HBCC and hence, effect of their further stimulation with their ligand could not be seen. In contrast, inhibition of FPR1 or FPR2 also inhibited the signalling induced by cross talk. Hence downstream signalling was hampered which resulted in the inhibition of cell proliferation upon FPR1 or FPR2 inhibition in HBCC. Contrasting to our observations, Khau et al. had shown the increase in cell proliferation upon fMLP and WKYMVm stimulation in MCF-7 as well as MDA-MB-231[102]. In the experiment shown by Khau et al., cells were serum starved for 24 hrs before stimulation with fMLP and WKYMVm. Cell growth was monitored manually by counting the cells, using trypan blue dye exclusion method. In our experiments, we did not serum starved the cells because serum starvation did not represent the natural environment for cells. Furthermore, trypan blue dye exclusion method of cell counting is subjective method and prone for human errors, as the cells were manually counted. On other hand we had used highly sensitive automated CCK-8 method, which eliminate the human error for counting, hence the data is more reliable. Considering, the above facts our results are more realistic and reliable for understanding effect of fMLP and WKYMVm on HBCC growth and motility

Summary

CML

CML PMNL are defective in FPR mediated adhesion, transmigration, motility, chemotaxis, actin polymerization, phagocytosis and respiratory burst activities. Lowered FPR1 expression in CML PMNL might be responsible for these defective functions. CML cell lines showed decreased mFPR1, mFPR2, sFPR1, sFPR2 and sFPR3 expression than bcr-abl negative hematopoietic cell line – HL60, which suggested inverse relationship of these genes with bcr-abl expression. The receptors expressed by these cell lines were able to bind to the ligand and activate downstream signalling. CD marker analysis of the cell lines showed that expression of CD34 in CML cell lines was similar to co-expression of sFPR1 & sFPR2, sFPR1 & sFPR3 and sFPR1, sFPR2 & sFPR3, while pattern of expression of CD117 in CML cell lines was similar to that of sFPR1. This is indicative of probable role of FPR in cellular stemness. It was also found that in K562, expression of FPR2 and FPR3 genes might play role in imatinib resistance. Furthermore, when imatinib resistant cell lines were treated with combination of imatinib and FPR1 antagonist –CsH, it doubled the growth inhibitory effect of imatinib alone. FPR expression also showed an inverse relationship with bcr-abl mRNA expression. Thus, FPR expression was very well associated with the stemness and imatinib resistance in CML. Hence, it could be suggested that FPR might play role in imatinib resistance of stem like CML cells.

Breast Cancer

Role and significance of FPR in breast cancer was not reported. This could be first report which shed light on role of FPR in breast cancer. All the HBCC used in this study showed decreased FPR1 and increased FPR2 gene and protein expression than normal breast cell line. sFPR3 showed completely different pattern than that of mFPR3. All the cell lines, which had shown high mFPR3, showed low sFPR3 and vice-versa. The FPR1 and FPR2 expressed by these cell lines were able to bind the respective ligands. All the HBCC except T47D showed significantly higher ligand binding than that in normal breast cell line MCF-10A. It could be possible that the ligand binding affinity of cancerous cell lines might have increased because cancerous cells have become hypersensitive to extracellular signals, which promote cell proliferation and survival. After stimulation with 10^{-6} M fMLP, all the HBCC, except T47D showed significant changes in F-actin quantity. MDA-MB-231 and MDA-MB-468 showed significant increase in F-actin content after fMLP stimulation. LCM studies on MCF-7 cells showed that decrease in F-actin quantity was associated with the loss of epithelioid morphology of the cells and decrease in cell spreading, which could be the induction of epithelial-mesenchymal transition (EMT). Expression of stem cell marker genes nanog, nestin, oct-3/4 and sox2 was higher in HBCC than MCF-10. Cluster analysis indicated close association of FPR2 and FPR3 genes with oct-3/4, klf4, and nanog. Stimulation of HBCC with fMLP showed that FPR1induced expression of Oct-3/4, Nanog, and Sox-2 in HBCC. Western data analysis showed transactivation of EGFR by FPR1 and FPR2. It was also found that FPR1 might be playing role in motility as well as proliferation of MCF-7 and MDA-MB-231 while FPR2 might be playing role in proliferation in MCF-7 and

proliferation and motility in MDA-MB-231. Apart from transactivation of EGFR by FPR1 and FPR2, transactivation of FPR1 and FPR2 by EGFR was also seen. This is probably the first report of existence of any involvement of FPR1 and FPR2 signalling in EGFR and IL6R mediated signalling in breast cancer. FPR1 and FPR2 played role in activation and deactivation of many signalling molecules activated by EGFR and IL6R in MCF-7 and MDA-MB-231. Moreover, it was found that inhibition of FPR1 was detrimental to MCF-7 cells.

In short, HBCC showed differential expression of functional FPR, which displayed close association with expression of the stem cell marker gene. Stimulation of FPR increased stemness in HBCC. Transactivation of EGFR with FPR1 and FPR2 and vice-versa was also seen in MCF-7 and MDA-MB-231. Stimulation of FPR1 in MCF-7 and MDA-MB-231 led to activation of signalling pathways which are involved in cell proliferation and motility. Stimulation of FPR1 in MCF-7 also resulted into loss of epithelioid morphology of the cells, decrease in cell spreading, increase in long, thick, spike like cellular projections which could be the induction of epithelial-mesenchymal transition (EMT). Stimulation of FPR2 was also involved in cell proliferation in MCF-7 and MDA-MB-231, but in MDA-MB-231 it was also involved in cell motility. Inhibition of FPR1 was detrimental to growth of MCF-7 cells. Hence, it could be suggested that FPR might play role in oncogenesis of breast cells and could be used as a therapeutic target in breast cancer. Utility of FPR as biomarker for the breast cancer for prognosis is worth exploring.

Significant findings

CML

- Decrease in FPR1 expression in CML PMNL could be responsible for the defective behavior of CML PMNL.
- FPR might play role in imatinib resistance of stem like CML cells.

Breast Cancer

- FPR might play role in aggressiveness of HBCC.
- FPR might play role in increasing cellular stemness in HBCC.
- FPR transactivated EGFR in breast cancer cell lines.
- FPR might play role in cell proliferation, survival, and motility of breast cancer cells.
- FPR could be used as a therapeutic target in breast cancer and CML.
- Utility of FPR as biomarker needs to be explored using clinical samples.

Biological significance of FPR and future directions

Formyl peptide receptors are well known for their role as chemoattractant receptors in hematopoietic cells[340]. Their role in innate immunity has been well characterized[340]. In the last decade, expression of FPR in cells other than hematopoietic origin was reported. But their role in these cells was not well characterized. In CML, defective adhesion, transmigration, motility, chemotaxis, actin polymerization, phagocytosis and respiratory burst activities in CML PMNL were found to be associated with FPR expression. Studies in cell lines showed more complex role of FPR in CML. FPR expression showed an inverse relationship with bcr-abl mRNA expression. FPR expression was very well associated with the increased expression of stemness and imatinib resistance.

In breast cancer, above mentioned results clearly established the fact that all the three FPR homologues were functionally expressed by HBCC. Similar to their role in hematopoietic cells, these receptors were able to bind to the ligand and alter the F-actin levels in HBCC. In addition to this, stimulation of FPR by fMLP showed increase in expression of cellular pluripotency markers, which indicated that FPR could be involved in activities other than previously known. Furthermore, transactivation of EGFR by FPR1 and FPR2 indicated critical role of FPR in oncogenic transformation. Activation of MAPK pathway, Rho-GTPases and PI3K-Akt pathway by FPR via transactivation of EGFR and cross talk JAK

demonstrated that FPR could also be involved in cell proliferation, survival, drug resistance, metastasis, and tissue invasion.

Inhibition of cell proliferation by inhibition of FPR stimulation indicated that FPR could be used as a therapeutic target in both CML and breast cancer. Antiproliferative effect of FPR antagonist on imatinib resistant CML cell lines identifies it as a promising target for CML.

However, more in depth study is required to precisely define the role of FPR in CML and breast cancer pathogenesis. Events and signalling involved in antiproliferative effect on imatinib resistant cells and breast cancer metastasis upon FPR stimulation needs further studies. Imatinib resistance and breast cancer pathogenesis & metastasis are complex phenomena. FPR might not be the only factor regulating them however our observation showed that FPR could be an important player in these events and could be a candidate for developing novel therapeutics for CML and breast cancer.

Bibliography

1. Prossnitz ER, Ye RD. The N-formyl peptide receptor: a model for the study of chemoattractant receptor structure and function. *Pharmacol Ther*;74(1):73-102. 1997.
2. Le Y, Murphy PM, Wang JM. Formyl-peptide receptors revisited. *Trends Immunol*;23(11):541-548. 2002.
3. Bao L, Gerard NP, Eddy RL, Jr., Shows TB, Gerard C. Mapping of genes for the human C5a receptor (C5AR), human FMLP receptor (FPR), and two FMLP receptor homologue orphan receptors (FPRH1, FPRH2) to chromosome 19. *Genomics*;13(2):437-440. 1992.
4. Murphy PM, Ozcelik T, Kenney RT, Tiffany HL, McDermott D, Francke U. A structural homologue of the N-formyl peptide receptor. Characterization and chromosome mapping of a peptide chemoattractant receptor family. *J Biol Chem*;267(11):7637-7643. 1992.
5. Rabiet MJ, Huet E, Boulay F. Human mitochondria-derived N-formylated peptides are novel agonists equally active on FPR and FPRL1, while Listeria monocytogenes-derived peptides preferentially activate FPR. *Eur J Immunol*;35(8):2486-2495. 2005.
6. Migeotte I, Riboldi E, Franssen JD, et al. Identification and characterization of an endogenous chemotactic ligand specific for FPRL2. *J Exp Med*;201(1):83-93. 2005.
7. Prossnitz ER, Quehenberger O, Cochrane CG, Ye RD. Transmembrane signalling by the N-formyl peptide receptor in stably transfected fibroblasts. *Biochem Biophys Res Commun*;179(1):471-476. 1991.
8. Prossnitz ER, Quehenberger O, Cochrane CG, Ye RD. Signal transducing properties of the N-formyl peptide receptor expressed in undifferentiated HL60 cells. *J Immunol*;151(10):5704-5715. 1993.

9. He R, Nanamori M, Sang H, Yin H, Dinauer MC, Ye RD. Reconstitution of chemotactic peptide-induced nicotinamide adenine dinucleotide phosphate (reduced) oxidase activation in transgenic COS-phox cells. *J Immunol*;173(12):7462-7470. 2004.
10. Lavigne MC, Murphy PM, Leto TL, Gao JL. The N-formylpeptide receptor (FPR) and a second G(i)-coupled receptor mediate fMet-Leu-Phe-stimulated activation of NADPH oxidase in murine neutrophils. *Cell Immunol*;218(1-2):7-12. 2002.
11. Yang D, Chen Q, Le Y, Wang JM, Oppenheim JJ. Differential regulation of formyl peptide receptor-like 1 expression during the differentiation of monocytes to dendritic cells and macrophages. *J Immunol*;166(6):4092-4098. 2001.
12. Yang D, Chen Q, Gertz B, et al. Human dendritic cells express functional formyl peptide receptor-like-2 (FPRL2) throughout maturation. *J Leukoc Biol*;72(3):598-607. 2002.
13. Becker EL, Forouhar FA, Grunnet ML, et al. Broad immunocytochemical localization of the formylpeptide receptor in human organs, tissues, and cells. *Cell Tissue Res*;292(1):129-135. 1998.
14. Rotrosen D, Malech HL, Gallin JI. Formyl peptide leukocyte chemoattractant uptake and release by cultured human umbilical vein endothelial cells. *J Immunol*;139(9):3034-3040. 1987.
15. Adams MD, Dubnick M, Kerlavage AR, et al. Sequence identification of 2,375 human brain genes. *Nature*;355(6361):632-634. 1992.
16. Lacy M, Jones J, Whittemore SR, Haviland DL, Wetsel RA, Barnum SR. Expression of the receptors for the C5a anaphylatoxin, interleukin-8 and FMLP by human astrocytes and microglia. *J Neuroimmunol*;61(1):71-78. 1995.
17. Sozzani S, Sallusto F, Luini W, et al. Migration of dendritic cells in response to formyl peptides, C5a, and a distinct set of chemokines. *J Immunol*;155(7):3292-3295. 1995.

18. Rescher U, Danielczyk A, Markoff A, Gerke V. Functional activation of the formyl peptide receptor by a new endogenous ligand in human lung A549 cells. *J Immunol*;169(3):1500-1504. 2002.
19. VanCompernolle SE, Clark KL, Rummel KA, Todd SC. Expression and function of formyl peptide receptors on human fibroblast cells. *J Immunol*;171(4):2050-2056. 2003.
20. Kim MK, Min do S, Park YJ, Kim JH, Ryu SH, Bae YS. Expression and functional role of formyl peptide receptor in human bone marrow-derived mesenchymal stem cells. *FEBS Lett*;581(9):1917-1922. 2007.
21. McCoy R, Haviland DL, Molmenti EP, Ziambaras T, Wetsel RA, Perlmutter DH. N-formylpeptide and complement C5a receptors are expressed in liver cells and mediate hepatic acute phase gene regulation. *J Exp Med*;182(1):207-217. 1995.
22. Czapiga M, Gao JL, Kirk A, Lekstrom-Himes J. Human platelets exhibit chemotaxis using functional N-formyl peptide receptors. *Exp Hematol*;33(1):73-84. 2005.
23. Maxfield FR. Regulation of leukocyte locomotion by Ca2+. *Trends Cell Biol*;3(11):386-391. 1993.
24. Marks PW, Maxfield FR. Local and global changes in cytosolic free calcium in neutrophils during chemotaxis and phagocytosis. *Cell Calcium*;11(2-3):181-190. 1990.
25. McDonald PP, Bald A, Cassatella MA. Activation of the NF-kappaB pathway by inflammatory stimuli in human neutrophils. *Blood*;89(9):3421-3433. 1997.
26. Browning DD, Pan ZK, Prossnitz ER, Ye RD. Cell type- and developmental stage-specific activation of NF-kappaB by fMet-Leu-Phe in myeloid cells. *J Biol Chem*;272(12):7995-8001. 1997.
27. Lawrence T. The nuclear factor NF-kappaB pathway in inflammation. *Cold Spring Harb Perspect Biol*;1(6):a001651. 2009.
28. Newton K, Dixit VM. Signaling in innate immunity and inflammation. *Cold Spring Harb Perspect Biol*;4(3). 2012.

29. Yagi M, Kantarci A, Iwata T, et al. PDK1 regulates chemotaxis in human neutrophils. *J Dent Res*;88(12):1119-1124. 2009.

30. Rane MJ, Coxon PY, Powell DW, et al. p38 Kinase-dependent MAPKAPK-2 activation functions as 3-phosphoinositide-dependent kinase-2 for Akt in human neutrophils. *J Biol Chem*;276(5):3517-3523. 2001.

31. Ridley AJ. Rho family proteins: coordinating cell responses. *Trends Cell Biol*;11(12):471-477. 2001.

32. Moodie SA, Wolfman A. The 3Rs of life: Ras, Raf and growth regulation. *Trends Genet*;10(2):44-48. 1994.

33. Waetzig V, Herdegen T. Context-specific inhibition of JNKs: overcoming the dilemma of protection and damage. *Trends Pharmacol Sci*;26(9):455-461. 2005.

34. Shaulian E, Karin M. AP-1 as a regulator of cell life and death. *Nat Cell Biol*;4(5):E131-136. 2002.

35. Coulthard LR, White DE, Jones DL, McDermott MF, Burchill SA. p38(MAPK): stress responses from molecular mechanisms to therapeutics. *Trends Mol Med*;15(8):369-379. 2009.

36. Cuadrado A, Nebreda AR. Mechanisms and functions of p38 MAPK signalling. *Biochem J*;429(3):403-417. 2010.

37. Zu YL, Qi J, Gilchrist A, et al. p38 mitogen-activated protein kinase activation is required for human neutrophil function triggered by TNF-alpha or FMLP stimulation. *J Immunol*;160(4):1982-1989. 1998.

38. Takai Y, Sasaki T, Matozaki T. Small GTP-binding proteins. *Physiol Rev*;81(1):153-208. 2001.

39. Schmitz AA, Govek EE, Bottner B, Van Aelst L. Rho GTPases: signaling, migration, and invasion. *Exp Cell Res*;261(1):1-12. 2000.

40. Nobes CD, Hall A. Rho, rac, and cdc42 GTPases regulate the assembly of multimolecular focal complexes associated with actin stress fibers, lamellipodia, and filopodia. *Cell*;81(1):53-62. 1995.

41. Aspenstrom P, Fransson A, Saras J. Rho GTPases have diverse effects on the organization of the actin filament system. *Biochem J*;377(Pt 2):327-337. 2004.
42. Parri M, Chiarugi P. Rac and Rho GTPases in cancer cell motility control. *Cell Commun Signal*;8:23. 2010.
43. Spiering D, Hodgson L. Dynamics of the Rho-family small GTPases in actin regulation and motility. *Cell Adh Migr*;5(2):170-180. 2011.
44. Pollard TD, Blanchoin L, Mullins RD. Molecular mechanisms controlling actin filament dynamics in nonmuscle cells. *Annu Rev Biophys Biomol Struct*;29:545-576. 2000.
45. Govind S, Kozma R, Monfries C, Lim L, Ahmed S. Cdc42Hs facilitates cytoskeletal reorganization and neurite outgrowth by localizing the 58-kD insulin receptor substrate to filamentous actin. *J Cell Biol*;152(3):579-594. 2001.
46. Hall A. Rho GTPases and the actin cytoskeleton. *Science*;279(5350):509-514. 1998.
47. Fujiwara T, Mammoto A, Kim Y, Takai Y. Rho small G-protein-dependent binding of mDia to an Src homology 3 domain-containing IRSp53/BAIAP2. *Biochem Biophys Res Commun*;271(3):626-629. 2000.
48. Allen WE, Zicha D, Ridley AJ, Jones GE. A role for Cdc42 in macrophage chemotaxis. *J Cell Biol*;141(5):1147-1157. 1998.
49. Nobes CD, Hall A. Rho GTPases control polarity, protrusion, and adhesion during cell movement. *J Cell Biol*;144(6):1235-1244. 1999.
50. Bhola NE, Grandis JR. Crosstalk between G-protein-coupled receptors and epidermal growth factor receptor in cancer. *Front Biosci*;13:1857-1865. 2008.
51. Daub H, Wallasch C, Lankenau A, Herrlich A, Ullrich A. Signal characteristics of G protein-transactivated EGF receptor. *EMBO J*;16(23):7032-7044. 1997.
52. Kholodenko BN. MAP kinase cascade signaling and endocytic trafficking: a marriage of convenience? *Trends Cell Biol*;12(4):173-177. 2002.
53. Liebmann C. Regulation of MAP kinase activity by peptide receptor signalling pathway: paradigms of multiplicity. *Cell Signal*;13(11):777-785. 2001.

54. New DC, Wong YH. Molecular mechanisms mediating the G protein-coupled receptor regulation of cell cycle progression. *J Mol Signal*;2:2. 2007.
55. Herrlich A, Daub H, Knebel A, et al. Ligand-independent activation of platelet-derived growth factor receptor is a necessary intermediate in lysophosphatidic, acid-stimulated mitogenic activity in L cells. *Proc Natl Acad Sci U S A*;95(15):8985-8990. 1998.
56. Huang J, Chen K, Gong W, Dunlop NM, Wang JM. G-protein coupled chemoattractant receptors and cancer. *Front Biosci*;13:3352-3363. 2008.
57. Huang J, Chen K, Gong W, et al. Receptor "hijacking" by malignant glioma cells: a tactic for tumor progression. *Cancer Lett*;267(2):254-261. 2008.
58. El Zein N, D'Hondt S, Sariban E. Crosstalks between the receptors tyrosine kinase EGFR and TrkA and the GPCR, FPR, in human monocytes are essential for receptors-mediated cell activation. *Cell Signal*;22(10):1437-1447. 2010.
59. Huang J, Hu J, Bian X, et al. Transactivation of the epidermal growth factor receptor by formylpeptide receptor exacerbates the malignant behavior of human glioblastoma cells. *Cancer Res*;67(12):5906-5913. 2007.
60. Zhou Y, Bian X, Le Y, et al. Formylpeptide receptor FPR and the rapid growth of malignant human gliomas. *J Natl Cancer Inst*;97(11):823-835. 2005.
61. Xu CP, Zhang HR, Chen FL, et al. Human malignant glioma cells expressing functional formylpeptide receptor recruit endothelial progenitor cells for neovascularization. *Int Immunopharmacol*;10(12):1602-1607. 2010.
62. Chen DL, Ping YF, Yu SC, et al. Downregulating FPR restrains xenograft tumors by impairing the angiogenic potential and invasive capability of malignant glioma cells. *Biochem Biophys Res Commun*;381(3):448-452. 2009.
63. Hanahan D, Weinberg RA. The hallmarks of cancer. *Cell*;100(1):57-70. 2000.
64. Dufton N, Perretti M. Therapeutic anti-inflammatory potential of formyl-peptide receptor agonists. *Pharmacol Ther*;127(2):175-188. 2010.

65. Migeotte I, Communi D, Parmentier M. Formyl peptide receptors: a promiscuous subfamily of G protein-coupled receptors controlling immune responses. *Cytokine Growth Factor Rev*;17(6):501-519. 2006.

66. Huang J, Chen K, Huang J, et al. Regulation of the leucocyte chemoattractant receptor FPR in glioblastoma cells by cell differentiation. *Carcinogenesis*;30(2):348-355. 2009.

67. El Zein N, Badran B, Sariban E. VIP differentially activates beta2 integrins, CR1, and matrix metalloproteinase-9 in human monocytes through cAMP/PKA, EPAC, and PI-3K signaling pathways via VIP receptor type 1 and FPRL1. *J Leukoc Biol*;83(4):972-981. 2008.

68. Takafuji S, Ishida A, Miyakuni Y, Nakagawa T. Matrix metalloproteinase-9 release from human leukocytes. *J Investig Allergol Clin Immunol*;13(1):50-55. 2003.

69. Wiehler S, Cuvelier SL, Chakrabarti S, Patel KD. p38 MAP kinase regulates rapid matrix metalloproteinase-9 release from eosinophils. *Biochem Biophys Res Commun*;315(2):463-470. 2004.

70. Sawyers CL. Chronic Myeloid Leukemia. *New England Journal of Medicine*;340(17):1330-1340. 1999.

71. Goldman J. ABC of clinical haematology. Chronic myeloid leukaemia. *Bmj*;314(7081):657-660. 1997.

72. Calabretta B, Perrotti D. The biology of CML blast crisis. *Blood*;103(11):4010-4022. 2004.

73. Goldman JM. How I treat chronic myeloid leukemia in the imatinib era. *Blood*;110(8):2828-2837. 2007.

74. Fausel C. Targeted chronic myeloid leukemia therapy: seeking a cure. *J Manag Care Pharm*;13(8 Suppl A):8-12. 2007.

75. Hutchinson L. Human CML stem cells insensitive to imatinib even when BCR-ABL is inhibited. *Nat Rev Clin Oncol*;8(3):126. 2011.

76. Carulli G. The neutrophil granulocyte in chronic myeloid leukemia. *Haematologia (Budap)*;25(1):35-55. 1993.

77. Baker MA, Kanani A, Hindenburg A, Taub RN. Changes in the granulocyte membrane following chemotherapy for chronic myelogenous leukaemia. *Br J Haematol*;62(3):431-438. 1986.

78. Wysocki H, Wierusz-Wysocka B, Wykretowicz A. Possible prognostic value of plasma activity augmenting polymorphonuclear neutrophils (PMN) adherence estimations in untreated patients with chronic myeloid leukemia. *Leuk Res*;12(8):627-629. 1988.

79. Anklesaria PN, Advani SH, Bhisey AN. Studies on granulocyte functions in patients with chronic myeloid leukemia. *Tumori*;71(4):317-323. 1985.

80. Anklesaria PN, Advani SH, Bhisey AN. Defective chemotaxis and adherence in granulocytes from chronic myeloid leukemia (CML) patients. *Leuk Res*;9(5):641-648. 1985.

81. Bhisey AN, Rao SG, Advani SH, Ray V. Agglutination of granulocytes from chronic myeloid leukaemia by concanavalin A. *Acta Haematol*;63(4):211-216. 1980.

82. Kamble G, Advani SH, Bhisey AN. Impaired cell motility in chronic myeloid leukemic granulocytes related to altered cytoskeletal pattern. *Indian J Exp Biol*;44(3):193-202. 2006.

83. Naik NR, Advani SH, Bhisey AN. PMN cells from chronic myeloid leukemia (CML) patients show defective chemotaxis in remission. *Leuk Res*;13(11):959-965. 1989.

84. Naik NR, Advani SH, Bhisey AN. Fluid pinocytosis and esterase-oxidase in chronic myeloid leukemic granulocytes are differentially stimulated by chemotactic peptide. *Leuk Res*;16(4):395-401. 1992.

85. Naik NR, Bhisey AN, Advani SH. Flow cytometric studies on actin polymerization in PMN cells from chronic myeloid leukemia (CML) patients. *Leuk Res*;14(10):921-930. 1990.

86. Radhika V, Naik NR, Advani SH, Bhisey AN. Actin polymerization in response to different chemoattractants is reduced in granulocytes from chronic myeloid leukemia patients. *Cytometry*;42(6):379-386. 2000.

87. Radhika V, Thennarasu S, Naik NR, Kumar A, Advani SH, Bhisey AN. Granulocytes from chronic myeloid leukemia (CML) patients show differential response to different chemoattractants. *Am J Hematol*;52(3):155-164. 1996.

88. Tarachandani A, Advani SH, Bhisey AN. Chronic myeloid leukemia granulocytes have lower amounts of cytoplasmic actin. *Leuk Res*;17(10):833-838. 1993.

89. Tarachandani A, Advani SH, Bhisey AN. Chronic myeloid leukemia granulocytes exhibit reduced actin polymerization after chemotactic peptide stimulation. *Hematol Pathol*;9(1):27-35. 1995.

90. Eheman CR, Shaw KM, Ryerson AB, Miller JW, Ajani UA, White MC. The changing incidence of in situ and invasive ductal and lobular breast carcinomas: United States, 1999-2004. *Cancer Epidemiol Biomarkers Prev*;18(6):1763-1769. 2009.

91. Varga Z, Mallon E. Histology and immunophenotype of invasive lobular breast cancer. daily practice and pitfalls. *Breast Dis*;30:15-19. 2008.

92. Lehmann BD, Bauer JA, Chen X, et al. Identification of human triple-negative breast cancer subtypes and preclinical models for selection of targeted therapies. *J Clin Invest*;121(7):2750-2767. 2011.

93. Hu R, Dawood S, Holmes MD, et al. Androgen receptor expression and breast cancer survival in postmenopausal women. *Clin Cancer Res*;17(7):1867-1874. 2011.

94. Perou CM. Molecular Stratification of Triple-Negative Breast Cancers. *The Oncologist*;16(suppl 1):61-70. 2011.

95. Ignatiadis M, Sotiriou C. Luminal breast cancer: from biology to treatment. *Nat Rev Clin Oncol*;10(9):494-506. 2013.

96. Ades F, Zardavas D, Bozovic-Spasojevic I, et al. Luminal B breast cancer: molecular characterization, clinical management, and future perspectives. *J Clin Oncol*;32(25):2794-2803. 2014.

97. Prat A, Perou CM. Deconstructing the molecular portraits of breast cancer. *Mol Oncol*;5(1):5-23. 2011.
98. Ross JS. Multigene classifiers, prognostic factors, and predictors of breast cancer clinical outcome. *Adv Anat Pathol*;16(4):204-215. 2009.
99. Herschkowitz JI, Zhao W, Zhang M, et al. Comparative oncogenomics identifies breast tumors enriched in functional tumor-initiating cells. *Proceedings of the National Academy of Sciences*;109(8):2778-2783. 2012.
100. Marasco WA, Ward PA, Feltner DE, Varani J. Chemotactic factor binding by metastatic tumour cells: evidence for a formyl-peptide receptor on a non-myelogenous cell. *J Cell Sci*;73:121-134. 1985.
101. Rayner DC, Orr FW, Shiu RP. Binding of formyl peptides to Walker 256 carcinosarcoma cells and the chemotactic response of these cells. *Cancer Res*;45(5):2288-2293. 1985.
102. Khau T, Langenbach SY, Schuliga M, et al. Annexin-1 signals mitogen-stimulated breast tumor cell proliferation by activation of the formyl peptide receptors (FPRs) 1 and 2. *FASEB J*;25(2):483-496. 2011.
103. Collins SJ, Gallo RC, Gallagher RE. Continuous growth and differentiation of human myeloid leukaemic cells in suspension culture. *Nature*;270(5635):347-349. 1977.
104. Collins SJ, Ruscetti FW, Gallagher RE, Gallo RC. Normal functional characteristics of cultured human promyelocytic leukemia cells (HL-60) after induction of differentiation by dimethylsulfoxide. *J Exp Med*;149(4):969-974. 1979.
105. Lozzio CB, Lozzio BB. Human chronic myelogenous leukemia cell-line with positive Philadelphia chromosome. *Blood*;45(3):321-334. 1975.
106. Lozzio BB, Lozzio CB. Properties and usefulness of the original K-562 human myelogenous leukemia cell line. *Leuk Res*;3(6):363-370. 1979.
107. Kishi K. A new leukemia cell line with Philadelphia chromosome characterized as basophil precursors. *Leuk Res*;9(3):381-390. 1985.

108. Nakazawa M, Mitjavila MT, Debili N, et al. KU 812: a pluripotent human cell line with spontaneous erythroid terminal maturation. *Blood*;73(7):2003-2013. 1989.
109. Kubonishi I, Machida K, Sonobe H, Ohtsuki Y, Akagi T, Miyoshi I. Two new human myeloid cell lines derived from acute promyelocytic leukemia and chronic myelocytic leukemia. *Gann*;74(3):319-322. 1983.
110. Kubonishi I, Miyoshi I. Establishment of a Ph1 chromosome-positive cell line from chronic myelogenous leukemia in blast crisis. *Int J Cell Cloning*;1(2):105-117. 1983.
111. Miyoshi T, Nagai T, Ohmine K, et al. Relative importance of apoptosis and cell cycle blockage in the synergistic effect of combined R115777 and imatinib treatment in BCR/ABL-positive cell lines. *Biochem Pharmacol*;69(11):1585-1594. 2005.
112. Ohmine K, Nagai T, Tarumoto T, et al. Analysis of gene expression profiles in an imatinib-resistant cell line, KCL22/SR. *Stem Cells*;21(3):315-321. 2003.
113. Soule HD, Maloney TM, Wolman SR, et al. Isolation and characterization of a spontaneously immortalized human breast epithelial cell line, MCF-10. *Cancer Res*;50(18):6075-6086. 1990.
114. Soule HD, Vazguez J, Long A, Albert S, Brennan M. A human cell line from a pleural effusion derived from a breast carcinoma. *J Natl Cancer Inst*;51(5):1409-1416. 1973.
115. Lacroix M, Toillon RA, Leclercq G. p53 and breast cancer, an update. *Endocr Relat Cancer*;13(2):293-325. 2006.
116. Levenson AS, Jordan VC. MCF-7: the first hormone-responsive breast cancer cell line. *Cancer Res*;57(15):3071-3078. 1997.
117. Cailleau R, Olive M, Cruciger QV. Long-term human breast carcinoma cell lines of metastatic origin: preliminary characterization. *In Vitro*;14(11):911-915. 1978.
118. Keydar I, Chen L, Karby S, et al. Establishment and characterization of a cell line of human breast carcinoma origin. *Eur J Cancer*;15(5):659-670. 1979.
119. Patterson MK, Jr. Measurement of growth and viability of cells in culture. *Methods Enzymol*;58:141-152. 1979.

120. Cook JA, Mitchell JB. Viability measurements in mammalian cell systems. *Anal Biochem*;179(1):1-7. 1989.
121. Ishiyama M, Tominaga H, Shiga M, Sasamoto K, Ohkura Y, Ueno K. A combined assay of cell viability and in vitro cytotoxicity with a highly water-soluble tetrazolium salt, neutral red and crystal violet. *Biol Pharm Bull*;19(11):1518-1520. 1996.
122. Boyum A. Separation of blood leucocytes, granulocytes and lymphocytes. *Tissue Antigens*;4(4):269-274. 1974.
123. Chomczynski P. A reagent for the single-step simultaneous isolation of RNA, DNA and proteins from cell and tissue samples. *Biotechniques*;15(3):532-534, 536-537. 1993.
124. Wiame I, Remy S, Swennen R, Sagi L. Irreversible heat inactivation of DNase I without RNA degradation. *Biotechniques*;29(2):252-254, 256. 2000.
125. Livak KJ, Schmittgen TD. Analysis of relative gene expression data using real-time quantitative PCR and the 2(-Delta Delta C(T)) Method. *Methods*;25(4):402-408. 2001.
126. Laemmli UK. Cleavage of structural proteins during the assembly of the head of bacteriophage T4. *Nature*;227(5259):680-685. 1970.
127. Niedel JE, Kahane I, Cuatrecasas P. Receptor-mediated internalization of fluorescent chemotactic peptide by human neutrophils. *Science*;205(4413):1412-1414. 1979.
128. Sklar LA, Finney DA, Oades ZG, Jesaitis AJ, Painter RG, Cochrane CG. The dynamics of ligand-receptor interactions. Real-time analyses of association, dissociation, and internalization of an N-formyl peptide and its receptors on the human neutrophil. *J Biol Chem*;259(9):5661-5669. 1984.
129. Eisen MB, Spellman PT, Brown PO, Botstein D. Cluster analysis and display of genome-wide expression patterns. *Proc Natl Acad Sci U S A*;95(25):14863-14868. 1998.

130. Tamayo P, Slonim D, Mesirov J, et al. Interpreting patterns of gene expression with self-organizing maps: methods and application to hematopoietic differentiation. *Proc Natl Acad Sci U S A*;96(6):2907-2912. 1999.
131. Sharan R, Shamir R. CLICK: a clustering algorithm with applications to gene expression analysis. Proc Int Conf Intell Syst Mol Biol:16; 2000.
132. D'haeseleer P. How does gene expression clustering work? *Nature biotechnology*;23(12):1499-1501. 2005.
133. Panaro MA, Acquafredda A, Sisto M, Lisi S, Maffione AB, Mitolo V. Biological role of the N-formyl peptide receptors. *Immunopharmacol Immunotoxicol*;28(1):103-127. 2006.
134. Rabiet MJ, Huet E, Boulay F. The N-formyl peptide receptors and the anaphylatoxin C5a receptors: an overview. *Biochimie*;89(9):1089-1106. 2007.
135. Bufe B, Schumann T, Zufall F. Formyl peptide receptors from immune and vomeronasal system exhibit distinct agonist properties. *J Biol Chem*;287(40):33644-33655. 2012.
136. Liberles SD, Horowitz LF, Kuang D, et al. Formyl peptide receptors are candidate chemosensory receptors in the vomeronasal organ. *Proc Natl Acad Sci U S A*;106(24):9842-9847. 2009.
137. Riviere S, Challet L, Fluegge D, Spehr M, Rodriguez I. Formyl peptide receptor-like proteins are a novel family of vomeronasal chemosensors. *Nature*;459(7246):574-577. 2009.
138. Iribarren P, Zhou Y, Hu J, Le Y, Wang JM. Role of formyl peptide receptor-like 1 (FPRL1/FPR2) in mononuclear phagocyte responses in Alzheimer disease. *Immunol Res*;31(3):165-176. 2005.
139. Cui Y, Le Y, Yazawa H, Gong W, Wang JM. Potential role of the formyl peptide receptor-like 1 (FPRL1) in inflammatory aspects of Alzheimer's disease. *J Leukoc Biol*;72(4):628-635. 2002.

140. Liang TS, Wang JM, Murphy PM, Gao JL. Serum amyloid A is a chemotactic agonist at FPR2, a low-affinity N-formylpeptide receptor on mouse neutrophils. *Biochem Biophys Res Commun*;270(2):331-335. 2000.
141. Le Y, Gong W, Tiffany HL, et al. Amyloid (beta)42 activates a G-protein-coupled chemoattractant receptor, FPR-like-1. *J Neurosci*;21(2):RC123. 2001.
142. Phillipson M, Kubes P. The neutrophil in vascular inflammation. *Nat Med*;17(11):1381-1390. 2011.
143. Devosse T, Guillabert A, D'Haene N, et al. Formyl peptide receptor-like 2 is expressed and functional in plasmacytoid dendritic cells, tissue-specific macrophage subpopulations, and eosinophils. *J Immunol*;182(8):4974-4984. 2009.
144. Durstin M, Gao JL, Tiffany HL, McDermott D, Murphy PM. Differential expression of members of the N-formylpeptide receptor gene cluster in human phagocytes. *Biochem Biophys Res Commun*;201(1):174-179. 1994.
145. Colavita I, Esposito N, Martinelli R, et al. Gaining insights into the Bcr-Abl activity-independent mechanisms of resistance to imatinib mesylate in KCL22 cells: a comparative proteomic approach. *Biochim Biophys Acta*;1804(10):1974-1987. 2010.
146. Lim LH, Pervaiz S. Annexin 1: the new face of an old molecule. *FASEB J*;21(4):968-975. 2007.
147. Zhu F, Wang Y, Zeng S, Fu X, Wang L, Cao J. Involvement of annexin A1 in multidrug resistance of K562/ADR cells identified by the proteomic study. *OMICS*;13(6):467-476. 2009.
148. Esposito N, Colavita I, Quintarelli C, et al. SHP-1 expression accounts for resistance to imatinib treatment in Philadelphia chromosome-positive cells derived from patients with chronic myeloid leukemia. *Blood*;118(13):3634-3644. 2011.
149. Donato NJ, Wu JY, Stapley J, et al. BCR-ABL independence and LYN kinase overexpression in chronic myelogenous leukemia cells selected for resistance to STI571. *Blood*;101(2):690-698. 2003.

150. Donato NJ, Wu JY, Stapley J, et al. Imatinib mesylate resistance through BCR-ABL independence in chronic myelogenous leukemia. *Cancer Res*;64(2):672-677. 2004.
151. Ma L, Shan Y, Bai R, et al. A therapeutically targetable mechanism of BCR-ABL-independent imatinib resistance in chronic myeloid leukemia. *Sci Transl Med*;6(252):252ra121. 2014.
152. Lundberg E, Fagerberg L, Klevebring D, et al. Defining the transcriptome and proteome in three functionally different human cell lines. *Mol Syst Biol*;6:450. 2010.
153. Tian Q, Stepaniants SB, Mao M, et al. Integrated genomic and proteomic analyses of gene expression in Mammalian cells. *Mol Cell Proteomics*;3(10):960-969. 2004.
154. Vogel C, Abreu Rde S, Ko D, et al. Sequence signatures and mRNA concentration can explain two-thirds of protein abundance variation in a human cell line. *Mol Syst Biol*;6:400. 2010.
155. Schwanhausser B, Busse D, Li N, et al. Global quantification of mammalian gene expression control. *Nature*;473(7347):337-342. 2011.
156. Elliott SL, Taylor KM, Taylor DL, et al. Cytogenetic response to alpha-interferon is predicted in early chronic phase chronic myeloid leukemia by M-bcr breakpoint location. *Leukemia*;9(6):946-950. 1995.
157. Mills KI, MacKenzie ED, Birnie GD. The site of the breakpoint within the bcr is a prognostic factor in Philadelphia-positive CML patients. *Blood*;72(4):1237-1241. 1988.
158. Mills KI, Sproul AM, Leibowitz D, Burnett AK. Mapping of breakpoints, and relationship to BCR-ABL RNA expression, in Philadelphia-chromosome-positive chronic myeloid leukaemia patients with a breakpoint around exon 14 (b3) of the BCR gene. *Leukemia*;5(11):937-941. 1991.
159. Fioretos T, Nilsson PG, Aman P, et al. Clinical impact of breakpoint position within M-bcr in chronic myeloid leukemia. *Leukemia*;7(8):1225-1231. 1993.

160. Jaubert J, Martiat P, Dowding C, Ifrah N, Goldman JM. The position of the M-BCR breakpoint does not predict the duration of chronic phase or survival in chronic myeloid leukemia. *Br J Haematol*;74(1):30-35. 1990.

161. Morris SW, Daniel L, Ahmed CM, Elias A, Lebowitz P. Relationship of bcr breakpoint to chronic phase duration, survival, and blast crisis lineage in chronic myelogenous leukemia patients presenting in early chronic phase. *Blood*;75(10):2035-2041. 1990.

162. Rozman C, Urbano-Ispizua A, Cervantes F, et al. Analysis of the clinical relevance of the breakpoint location within M-BCR and the type of chimeric mRNA in chronic myelogenous leukemia. *Leukemia*;9(6):1104-1107. 1995.

163. Shepherd P, Suffolk R, Halsey J, Allan N. Analysis of molecular breakpoint and m-RNA transcripts in a prospective randomized trial of interferon in chronic myeloid leukaemia: no correlation with clinical features, cytogenetic response, duration of chronic phase, or survival. *Br J Haematol*;89(3):546-554. 1995.

164. Stein B, Dobrovic A. Relationship between M-BCR breakpoint position in blast crisis and length of chronic phase in chronic myeloid leukemia. *Blood*;79(11):3097-3098. 1992.

165. Melo JV. The diversity of BCR-ABL fusion proteins and their relationship to leukemia phenotype. *Blood*;88(7):2375-2384. 1996.

166. Ardern JC, Speak J, Hyde K, et al. Molecular analysis in chronic granulocytic leukaemia: location of breakpoints within M-BCR and relationship with presentation platelet counts. *Clinical & Laboratory Haematology*;15(4):253-258. 1993.

167. Inokuchi K, Futaki M, Yamada T, et al. The relationship between the site of breakpoints within the bcr gene and thrombopoiesis of Philadelphia-positive chronic myelocytic leukemia. *Leuk Res*;15(11):1067-1073. 1991.

168. Inokuchi K, Inoue T, Tojo A, et al. A possible correlation between the type of bcr-abl hybrid messenger RNA and platelet count in Philadelphia-positive chronic myelogenous leukemia. *Blood*;78(12):3125-3127. 1991.

169. Opalka B, Wandl UB, Kloke O, Beer U, Seeber S, Niederle N. No correlation between site of breakpoint in the BCR gene and platelet counts in Philadelphia chromosome-positive CML. *Leuk Res*;16(9):937-939. 1992.

170. Opalka B, Wandl UB, Stutenkemper R, Kloke O, Seeber S, Niederle N. No correlation between the type of bcr-abl hybrid messenger RNA and platelet counts in chronic myelogenous leukemia. *Blood*;80(7):1854-1855. 1992.

171. Lavallard VJ, Pradelli LA, Paul A, et al. Modulation of caspase-independent cell death leads to resensitization of imatinib mesylate-resistant cells. *Cancer Res*;69(7):3013-3020. 2009.

172. Lee SM, Bae JH, Kim MJ, et al. Bcr-Abl-independent imatinib-resistant K562 cells show aberrant protein acetylation and increased sensitivity to histone deacetylase inhibitors. *J Pharmacol Exp Ther*;322(3):1084-1092. 2007.

173. Karimiani EG, Marriage F, Merritt AJ, Burthem J, Byers RJ, Day PJ. Single-cell analysis of K562 cells: an imatinib-resistant subpopulation is adherent and has upregulated expression of BCR-ABL mRNA and protein. *Exp Hematol*;42(3):183-191 e185. 2014.

174. Stuart SA, Minami Y, Wang JY. The CML stem cell: evolution of the progenitor. *Cell Cycle*;8(9):1338-1343. 2009.

175. Corbin AS, Agarwal A, Loriaux M, Cortes J, Deininger MW, Druker BJ. Human chronic myeloid leukemia stem cells are insensitive to imatinib despite inhibition of BCR-ABL activity. *J Clin Invest*;121(1):396-409. 2011.

176. Jiang X, Zhao Y, Forrest D, Smith C, Eaves A, Eaves C. Stem cell biomarkers in chronic myeloid leukemia. *Dis Markers*;24(4-5):201-216. 2008.

177. Krause DS, Fackler MJ, Civin CI, May WS. CD34: structure, biology, and clinical utility. *Blood*;87(1):1-13. 1996.

178. Deaglio S, Mehta K, Malavasi F. Human CD38: a (r)evolutionary story of enzymes and receptors. *Leuk Res*;25(1):1-12. 2001.

179. Morita K, Saida M, Morioka N, Kitayama T, Akagawa Y, Dohi T. Cyclic ADP-ribose mediates formyl methionyl leucyl phenylalanine (fMLP)-induced intracellular Ca(2+) rise and migration of human neutrophils. *J Pharmacol Sci*;106(3):492-504. 2008.
180. Partida-Sanchez S, Cockayne DA, Monard S, et al. Cyclic ADP-ribose production by CD38 regulates intracellular calcium release, extracellular calcium influx and chemotaxis in neutrophils and is required for bacterial clearance in vivo. *Nat Med*;7(11):1209-1216. 2001.
181. Edling CE, Hallberg B. c-Kit--a hematopoietic cell essential receptor tyrosine kinase. *Int J Biochem Cell Biol*;39(11):1995-1998. 2007.
182. Gorczyca W. Flow Cytometry in Neoplastic Hematology: Morphologic-immunophenotypic Correlation: Taylor & Francis; 2006.
183. Fletcher MP, Gallin JI. Human neutrophils contain an intracellular pool of putative receptors for the chemoattractant N-formyl-methionyl-leucyl-phenylalanine. *Blood*;62(4):792-799. 1983.
184. Perez HD, Elfman F, Chenoweth D, Hooper C. Preparation and characterization of a derivative of wheat germ agglutinin which specifically inhibits polymorphonuclear leukocyte chemotaxis to the synthetic chemotactic peptide N-formyl-methionyl-leucyl-phenylalanine. *J Immunol*;136(5):1813-1819. 1986.
185. Perez HD, Elfman F, Lobo E, Sklar L, Chenoweth D, Hooper C. A derivative of wheat germ agglutinin specifically inhibits formyl-peptide-induced polymorphonuclear leukocyte chemotaxis by blocking re-expression (or recycling) of receptors. *J Immunol*;136(5):1803-1812. 1986.
186. Sklar LA, Jesaitis AJ, Painter RG, Cochrane CG. Ligand/receptor internalization: a spectroscopic analysis and a comparison of ligand binding, cellular response, and internalization by human neutrophils. *J Cell Biochem*;20(2):193-202. 1982.
187. Van Epps DE, Simpson S, Bender J, Chenoweth D. Regulation of C5a and formyl peptide receptor expression on human polymorphonuclear leukocytes. *The Journal of Immunology*;144(3):1062-1068. 1990.

188. Sengelov H, Boulay F, Kjeldsen L, Borregaard N. Subcellular localization and translocation of the receptor for N-formylmethionyl-leucyl-phenylalanine in human neutrophils. *Biochem J*;299 (Pt 2):473-479. 1994.
189. O'Flaherty JT, Rossi AG, Jacobson DP, Redman JF. Roles of Ca2+ in human neutrophil responses to receptor agonists. *Biochem J*;277 (Pt 3):705-711. 1991.
190. Bootman MD, Berridge MJ. The elemental principles of calcium signaling. *Cell*;83(5):675-678. 1995.
191. Pettit EJ, Hallett MB. Two distinct Ca2+ storage and release sites in human neutrophils. *J Leukoc Biol*;63(2):225-232. 1998.
192. Al-Mohanna FA, Pettit EJ, Hallett MB. Does actin polymerization status modulate Ca2+ storage in human neutrophils? Release and coalescence of Ca2+ stores by cytochalasins. *Exp Cell Res*;234(2):379-387. 1997.
193. Perianin A, Synderman R. Analysis of calcium homeostasis in activated human polymorphonuclear leukocytes. Evidence for two distinct mechanisms for lowering cytosolic calcium. *J Biol Chem*;264(2):1005-1009. 1989.
194. Revankar CM, Advani SH, Naik NR. Altered Ca2+ homeostasis in polymorphonuclear leukocytes from chronic myeloid leukaemia patients. *Mol Cancer*;5:65. 2006.
195. Montero M, Garcia-Sancho J, Alvarez J. Activation by chemotactic peptide of a receptor-operated Ca2+ entry pathway in differentiated HL60 cells. *J Biol Chem*;269(47):29451-29456. 1994.
196. Cowen DS, Lazarus HM, Shurin SB, Stoll SE, Dubyak GR. Extracellular adenosine triphosphate activates calcium mobilization in human phagocytic leukocytes and neutrophil/monocyte progenitor cells. *J Clin Invest*;83(5):1651-1660. 1989.
197. Howard TH, Meyer WH. Chemotactic peptide modulation of actin assembly and locomotion in neutrophils. *J Cell Biol*;98(4):1265-1271. 1984.
198. Boxer LA, Hedley-Whyte ET, Stossel TP. Neutrophil action dysfunction and abnormal neutrophil behavior. *N Engl J Med*;291(21):1093-1099. 1974.

199. Wallace PJ, Packman CH, Wersto RP, Lichtman MA. The effects of sulfhydryl inhibitors and cytochalasin on the cytoplasmic and cytoskeletal actin of human neutrophils. *J Cell Physiol*;132(2):325-330. 1987.

200. Howard TH, Wang D. Calcium ionophore, phorbol ester, and chemotactic peptide-induced cytoskeleton reorganization in human neutrophils. *J Clin Invest*;79(5):1359-1364. 1987.

201. Sha'afi RI, Shefcyk J, Yassin R, et al. Is a rise in intracellular concentration of free calcium necessary or sufficient for stimulated cytoskeletal-associated actin? *J Cell Biol*;102(4):1459-1463. 1986.

202. Norgauer J, Just I, Aktories K, Sklar LA. Influence of botulinum C2 toxin on F-actin and N-formyl peptide receptor dynamics in human neutrophils. *J Cell Biol*;109(3):1133-1140. 1989.

203. Wallace PJ, Wersto RP, Packman CH, Lichtman MA. Chemotactic peptide-induced changes in neutrophil actin conformation. *J Cell Biol*;99(3):1060-1065. 1984.

204. Yassin R, Shefcyk J, White JR, et al. Effects of chemotactic factors and other agents on the amounts of actin and a 65,000-mol-wt protein associated with the cytoskeleton of rabbit and human neutrophils. *J Cell Biol*;101(1):182-188. 1985.

205. Fechheimer M, Zigmond SH. Changes in cytoskeletal proteins of polymorphonuclear leukocytes induced by chemotactic peptides. *Cell Motility*;3(4):349-361. 1983.

206. Omann GM, Allen RA, Bokoch GM, Painter RG, Traynor AE, Sklar LA. Signal transduction and cytoskeletal activation in the neutrophil. *Physiol Rev*;67(1):285-322. 1987.

207. Downey GP, Chan CK, Grinstein S. Actin assembly in electropermeabilized neutrophils: role of G-proteins. *Biochem Biophys Res Commun*;164(2):700-705. 1989.

208. Hsu LS, Becker EL. Volume decrease of glycerinated polymorphoneclear leukocytes induced by ATP and Ca-2. *Exp Cell Res*;91(2):469-473. 1975.

209. Boxer LA, Stossel TP. Interactions of actin, myosin, and an actin-binding protein of chronic myelogenous leukemia leukocytes. *J Clin Invest*;57(4):964-976. 1976.

210. Nagata K, Sagara J, Ichikawa Y. A New Protein Factor Inhibiting Actin-Polymerization in Leukemic Myeloblasts. *Cell Structure and Function*;7(1):1-7. 1982.

211. Nagata K, Sagara J, Ichikawa Y. Changes in actin-related gelation of crude cell extracts during differentiation of myeloid leukemia cells. *Cell Struct Funct*;8(2):171-183. 1983.

212. Hilmo A, Howard TH. F-actin content of neonate and adult neutrophils. *Blood*;69(3):945-949. 1987.

213. Marinovich M, Guizzetti M, Grazi E, Trombetta G, Galli CL. F-actin levels but not actin polymerization are affected by triphenyltin in HL-60 cells. *Environ Toxicol Pharmacol*;1(1):13-20. 1996.

214. Cui YD, Inanami O, Yamamori T, Niwa K, Nagahata H, Kuwabara M. FMLP-induced formation of F-actin in HL60 cells is dependent on PI3-K but not on intracellular Ca2+, PKC, ERK or p38 MAPK. *Inflamm Res*;49(12):684-691. 2000.

215. Meyer WH, Howard TH. Actin polymerization and its relationship to locomotion and chemokinetic response in maturing human promyelocytic leukemia cells. *Blood*;70(2):363-367. 1987.

216. Rao KM, Currie MS, Ruff JC, Cohen HJ. Lack of correlation between induction of chemotactic peptide receptors and stimulus-induced actin polymerization in HL-60 cells treated with dibutyryl cyclic adenosine monophosphate or retinoic acid. *Cancer Res*;48(23):6721-6726. 1988.

217. Rix U, Hantschel O, Durnberger G, et al. Chemical proteomic profiles of the BCR-ABL inhibitors imatinib, nilotinib, and dasatinib reveal novel kinase and nonkinase targets. *Blood*;110(12):4055-4063. 2007.

218. Stenfeldt AL, Karlsson J, Wenneras C, Bylund J, Fu H, Dahlgren C. Cyclosporin H, Boc-MLF and Boc-FLFLF are antagonists that preferentially inhibit activity triggered through the formyl peptide receptor. *Inflammation*;30(6):224-229. 2007.

219. Yang D, Chen Q, Stoll S, Chen X, Howard OM, Oppenheim JJ. Differential regulation of responsiveness to fMLP and C5a upon dendritic cell maturation: correlation with receptor expression. *J Immunol*;165(5):2694-2702. 2000.

220. Tiffany HL, Lavigne MC, Cui YH, et al. Amyloid-beta induces chemotaxis and oxidant stress by acting at formylpeptide receptor 2, a G protein-coupled receptor expressed in phagocytes and brain. *J Biol Chem*;276(26):23645-23652. 2001.

221. Ries LAG, Melbert D, Krapcho M, et al. SEER cancer statistics review, 1975-2005. Bethesda, MD: U.S. National Institutes of Health, National Cancer Institute; 2008.

222. Research ICoM. Female Breast (ICD-10:C50). In: ICMR ed. Consolidated Report of Hospital Based Cancer Registries 2007-2011. Baglore, India: NCDIR-NCRP (Indian Council of Medical Research); 2013.

223. Bartek J, Iggo R, Gannon J, Lane DP. Genetic and immunochemical analysis of mutant p53 in human breast cancer cell lines. *Oncogene*;5(6):893-899. 1990.

224. Nigro JM, Baker SJ, Preisinger AC, et al. Mutations in the p53 gene occur in diverse human tumour types. *Nature*;342(6250):705-708. 1989.

225. Shao G, Julian MW, Bao S, et al. Formyl peptide receptor ligands promote wound closure in lung epithelial cells. *Am J Respir Cell Mol Biol*;44(3):264-269. 2011.

226. Keitoku M, Kohzuki M, Katoh H, et al. FMLP actions and its binding sites in isolated human coronary arteries. *J Mol Cell Cardiol*;29(3):881-894. 1997.

227. Chen K, Liu M, Liu Y, et al. Formylpeptide receptor-2 contributes to colonic epithelial homeostasis, inflammation, and tumorigenesis. *J Clin Invest*;123(4):1694-1704. 2013.

228. Schneider EH, Weaver JD, Gaur SS, et al. The leukocyte chemotactic receptor FPR1 is functionally expressed on human lens epithelial cells. *J Biol Chem*;287(48):40779-40792. 2012.

229. Biondi C, Pavan B, Ferretti ME, Corradini FG, Neri LM, Vesce F. Formyl-methionyl-leucyl-phenylalanine induces prostaglandin E2 release from human amnion-derived

WISH cells by phospholipase C-mediated [Ca+]i rise. *Biol Reprod*;64(3):865-870. 2001.

230. Le Y, Hu J, Gong W, et al. Expression of functional formyl peptide receptors by human astrocytoma cell lines. *J Neuroimmunol*;111(1-2):102-108. 2000.
231. Babbin BA, Lee WY, Parkos CA, et al. Annexin I regulates SKCO-15 cell invasion by signaling through formyl peptide receptors. *J Biol Chem*;281(28):19588-19599. 2006.
232. Coffelt SB, Marini FC, Watson K, et al. The pro-inflammatory peptide LL-37 promotes ovarian tumor progression through recruitment of multipotent mesenchymal stromal cells. *Proc Natl Acad Sci U S A*;106(10):3806-3811. 2009.
233. Coffelt SB, Tomchuck SL, Zwezdaryk KJ, Danka ES, Scandurro AB. Leucine leucine-37 uses formyl peptide receptor-like 1 to activate signal transduction pathways, stimulate oncogenic gene expression, and enhance the invasiveness of ovarian cancer cells. *Mol Cancer Res*;7(6):907-915. 2009.
234. Prevete N, Liotti F, Visciano C, Marone G, Melillo RM, de Paulis A. The formyl peptide receptor 1 exerts a tumor suppressor function in human gastric cancer by inhibiting angiogenesis. *Oncogene*. 2014.
235. Chakravarti N, Peddareddigari VG, Warneke CL, et al. Differential expression of the G-protein-coupled formyl Peptide receptor in melanoma associates with aggressive phenotype. *Am J Dermatopathol*;35(2):184-190. 2013.
236. Varani J, Wass J, Piontek G, Ward PA. Chemotactic factor-induced adherence of tumor cells. *Cell Biol Int Rep*;5(5):525-530. 1981.
237. Wass JA, Varani J, Piontek GE, Ward PA, Orr FW. Responses of normal and malignant cells to collagen, collagen-derived peptides and the C5-related tumor cell chemotactic peptide. *Cell Differ*;10(6):329-332. 1981.
238. Lam WC, Delikatny EJ, Orr FW, Wass J, Varani J, Ward PA. The chemotactic response of tumor cells. A model for cancer metastasis. *Am J Pathol*;104(1):69-76. 1981.

239. Varani J. Chemotaxis of metastatic tumor cells. *Cancer Metastasis Rev*;1(1):17-28. 1982.

240. Orr FW, Varani J, Delikatny J, Jain N, Ward PA. Comparison of the chemotactic responsiveness of two fibrosarcoma subpopulations of differing malignancy. *Am J Pathol*;102(2):160-167. 1981.

241. Orr FW, Lam WC, Delikatny EJ, Mokashi S, Varani J. Localization of intravenously injected tumor cells in the rat mesentery after intraperitoneal administration of chemotactic stimuli. *Invasion Metastasis*;1(4):239-247. 1981.

242. Huang J, Chen K, Chen J, et al. The G-protein-coupled formylpeptide receptor FPR confers a more invasive phenotype on human glioblastoma cells. *Br J Cancer*;102(6):1052-1060. 2010.

243. Cheng TY, Wu MS, Lin JT, et al. Annexin A1 is associated with gastric cancer survival and promotes gastric cancer cell invasiveness through the formyl peptide receptor/extracellular signal-regulated kinase/integrin beta-1-binding protein 1 pathway. *Cancer*;118(23):5757-5767. 2012.

244. Viswanathan A, Painter RG, Lanson NA, Jr., Wang G. Functional expression of N-formyl peptide receptors in human bone marrow-derived mesenchymal stem cells. *Stem Cells*;25(5):1263-1269. 2007.

245. Shin MK, Jang YH, Yoo HJ, et al. N-formyl-methionyl-leucyl-phenylalanine (fMLP) promotes osteoblast differentiation via the N-formyl peptide receptor 1-mediated signaling pathway in human mesenchymal stem cells from bone marrow. *J Biol Chem*;286(19):17133-17143. 2011.

246. Roussos ET, Condeelis JS, Patsialou A. Chemotaxis in cancer. *Nat Rev Cancer*;11(8):573-587. 2011.

247. Al-Hajj M, Wicha MS, Benito-Hernandez A, Morrison SJ, Clarke MF. Prospective identification of tumorigenic breast cancer cells. *Proc Natl Acad Sci U S A*;100(7):3983-3988. 2003.

248. Mani SA, Guo W, Liao MJ, et al. The epithelial-mesenchymal transition generates cells with properties of stem cells. *Cell*;133(4):704-715. 2008.
249. Marotta LL, Almendro V, Marusyk A, et al. The JAK2/STAT3 signaling pathway is required for growth of CD44(+)CD24(-) stem cell-like breast cancer cells in human tumors. *J Clin Invest*;121(7):2723-2735. 2011.
250. Honeth G, Bendahl PO, Ringner M, et al. The CD44+/CD24- phenotype is enriched in basal-like breast tumors. *Breast Cancer Res*;10(3):R53. 2008.
251. Meyer MJ, Fleming JM, Lin AF, Hussnain SA, Ginsburg E, Vonderhaar BK. CD44posCD49fhiCD133/2hi defines xenograft-initiating cells in estrogen receptor-negative breast cancer. *Cancer Res*;70(11):4624-4633. 2010.
252. Sheridan C, Kishimoto H, Fuchs RK, et al. CD44+/CD24- breast cancer cells exhibit enhanced invasive properties: an early step necessary for metastasis. *Breast Cancer Res*;8(5):R59. 2006.
253. Mylona E, Giannopoulou I, Fasomytakis E, et al. The clinicopathologic and prognostic significance of CD44+/CD24(-/low) and CD44-/CD24+ tumor cells in invasive breast carcinomas. *Hum Pathol*;39(7):1096-1102. 2008.
254. Ricardo S, Vieira AF, Gerhard R, et al. Breast cancer stem cell markers CD44, CD24 and ALDH1: expression distribution within intrinsic molecular subtype. *J Clin Pathol*;64(11):937-946. 2011.
255. Croker AK, Goodale D, Chu J, et al. High aldehyde dehydrogenase and expression of cancer stem cell markers selects for breast cancer cells with enhanced malignant and metastatic ability. *J Cell Mol Med*;13(8B):2236-2252. 2009.
256. Meyer MJ, Fleming JM, Ali MA, Pesesky MW, Ginsburg E, Vonderhaar BK. Dynamic regulation of CD24 and the invasive, CD44posCD24neg phenotype in breast cancer cell lines. *Breast Cancer Res*;11(6):R82. 2009.
257. Shi MF, Jiao J, Lu WG, et al. Identification of cancer stem cell-like cells from human epithelial ovarian carcinoma cell line. *Cell Mol Life Sci*;67(22):3915-3925. 2010.

258. Bourguignon LY. CD44-mediated oncogenic signaling and cytoskeleton activation during mammary tumor progression. *J Mammary Gland Biol Neoplasia*;6(3):287-297. 2001.

259. Hill A, McFarlane S, Mulligan K, et al. Cortactin underpins CD44-promoted invasion and adhesion of breast cancer cells to bone marrow endothelial cells. *Oncogene*;25(45):6079-6091. 2006.

260. Lopez JI, Camenisch TD, Stevens MV, Sands BJ, McDonald J, Schroeder JA. CD44 attenuates metastatic invasion during breast cancer progression. *Cancer Res*;65(15):6755-6763. 2005.

261. Baumann P, Cremers N, Kroese F, et al. CD24 expression causes the acquisition of multiple cellular properties associated with tumor growth and metastasis. *Cancer Res*;65(23):10783-10793. 2005.

262. Schabath H, Runz S, Joumaa S, Altevogt P. CD24 affects CXCR4 function in pre-B lymphocytes and breast carcinoma cells. *J Cell Sci*;119(Pt 2):314-325. 2006.

263. Aoi T, Yae K, Nakagawa M, et al. Generation of pluripotent stem cells from adult mouse liver and stomach cells. *Science*;321(5889):699-702. 2008.

264. Takahashi K, Yamanaka S. Induction of pluripotent stem cells from mouse embryonic and adult fibroblast cultures by defined factors. *Cell*;126(4):663-676. 2006.

265. Welstead GG, Brambrink T, Jaenisch R. Generating iPS cells from MEFS through forced expression of Sox-2, Oct-4, c-Myc, and Klf4. *J Vis Exp*;(14). 2008.

266. Silva J, Barrandon O, Nichols J, Kawaguchi J, Theunissen TW, Smith A. Promotion of reprogramming to ground state pluripotency by signal inhibition. *PLoS Biol*;6(10):e253. 2008.

267. Wade M, Wahl GM. c-Myc, genome instability, and tumorigenesis: the devil is in the details. *Curr Top Microbiol Immunol*;302:169-203. 2006.

268. Schmidt EV. The role of c-myc in cellular growth control. *Oncogene*;18(19):2988-2996. 1999.

269. D'Cruz CM, Gunther EJ, Boxer RB, et al. c-MYC induces mammary tumorigenesis by means of a preferred pathway involving spontaneous Kras2 mutations. *Nat Med*;7(2):235-239. 2001.
270. Ying S, Walden A. Function of KLF4 in Stem Cell Biology. In: Bhartiya DD, Lenka N, eds. Pluripotent Stem Cells: InTech:317-343; 2013.
271. Evans PM, Liu C. Roles of Krupel-like factor 4 in normal homeostasis, cancer and stem cells. *Acta Biochim Biophys Sin (Shanghai)*;40(7):554-564. 2008.
272. Mitsui K, Tokuzawa Y, Itoh H, et al. The homeoprotein Nanog is required for maintenance of pluripotency in mouse epiblast and ES cells. *Cell*;113(5):631-642. 2003.
273. Zhang X, Stojkovic P, Przyborski S, et al. Derivation of human embryonic stem cells from developing and arrested embryos. *Stem Cells*;24(12):2669-2676. 2006.
274. Cregan MD, Fan Y, Appelbee A, et al. Identification of nestin-positive putative mammary stem cells in human breastmilk. *Cell Tissue Res*;329(1):129-136. 2007.
275. Hoffman RM. The potential of nestin-expressing hair follicle stem cells in regenerative medicine. *Expert Opin Biol Ther*;7(3):289-291. 2007.
276. Park D, Xiang AP, Mao FF, et al. Nestin is required for the proper self-renewal of neural stem cells. *Stem Cells*;28(12):2162-2171. 2010.
277. Fillmore C, Kuperwasser C. Human breast cancer stem cell markers CD44 and CD24: enriching for cells with functional properties in mice or in man? *Breast Cancer Res*;9(3):303. 2007.
278. Wang D, Lu P, Zhang H, et al. Oct-4 and Nanog promote the epithelial-mesenchymal transition of breast cancer stem cells and are associated with poor prognosis in breast cancer patients. *Oncotarget*;5(21):10803-10815. 2014.
279. Lu X, Mazur SJ, Lin T, Appella E, Xu Y. The pluripotency factor nanog promotes breast cancer tumorigenesis and metastasis. *Oncogene*;33(20):2655-2664. 2014.

280. Almstrup K, Hoei-Hansen CE, Wirkner U, et al. Embryonic stem cell-like features of testicular carcinoma in situ revealed by genome-wide gene expression profiling. *Cancer Res*;64(14):4736-4743. 2004.
281. Chiou SH, Wang ML, Chou YT, et al. Coexpression of Oct4 and Nanog enhances malignancy in lung adenocarcinoma by inducing cancer stem cell-like properties and epithelial-mesenchymal transdifferentiation. *Cancer Res*;70(24):10433-10444. 2010.
282. Ezeh UI, Turek PJ, Reijo RA, Clark AT. Human embryonic stem cell genes OCT4, NANOG, STELLAR, and GDF3 are expressed in both seminoma and breast carcinoma. *Cancer*;104(10):2255-2265. 2005.
283. Gibbs CP, Kukekov VG, Reith JD, et al. Stem-like cells in bone sarcomas: implications for tumorigenesis. *Neoplasia*;7(11):967-976. 2005.
284. Hart AH, Hartley L, Parker K, et al. The pluripotency homeobox gene NANOG is expressed in human germ cell tumors. *Cancer*;104(10):2092-2098. 2005.
285. Nagata T, Shimada Y, Sekine S, et al. Prognostic significance of NANOG and KLF4 for breast cancer. *Breast Cancer*;21(1):96-101. 2014.
286. Jeter CR, Liu B, Liu X, et al. NANOG promotes cancer stem cell characteristics and prostate cancer resistance to androgen deprivation. *Oncogene*;30(36):3833-3845. 2011.
287. Lengerke C, Fehm T, Kurth R, et al. Expression of the embryonic stem cell marker SOX2 in early-stage breast carcinoma. *BMC Cancer*;11:42. 2011.
288. Leis O, Eguiara A, Lopez-Arribillaga E, et al. Sox2 expression in breast tumours and activation in breast cancer stem cells. *Oncogene*;31(11):1354-1365. 2012.
289. Rodriguez-Pinilla SM, Sarrio D, Moreno-Bueno G, et al. Sox2: a possible driver of the basal-like phenotype in sporadic breast cancer. *Mod Pathol*;20(4):474-481. 2007.
290. Simoes BM, Piva M, Iriondo O, et al. Effects of estrogen on the proportion of stem cells in the breast. *Breast Cancer Res Treat*;129(1):23-35. 2011.

291. Brzozowska A, Sodolski T, Duma D, Mazurkiewicz T, Mazurkiewicz M. Evaluation of prognostic parameters of E-cadherin status in breast cancer treatment. *Ann Agric Environ Med*;19(3):541-546. 2012.

292. Kim HS, Moon HG, Han W, et al. COX2 overexpression is a prognostic marker for Stage III breast cancer. *Breast Cancer Res Treat*;132(1):51-59. 2012.

293. Miglietta A, Toselli M, Ravarino N, et al. COX-2 expression in human breast carcinomas: correlation with clinicopathological features and prognostic molecular markers. *Expert Opin Ther Targets*;14(7):655-664. 2010.

294. Neto JC, Ikoma MM, Carvalho KC, et al. MGMT and PTEN as potential prognostic markers in breast cancer. *Exp Mol Pathol*;92(1):20-26. 2012.

295. Younis LK, El Sakka H, Haque I. The Prognostic Value of E-cadherin Expression in Breast Cancer. *Int J Health Sci (Qassim)*;1(1):43-51. 2007.

296. Lee HJ, Park MK, Lee EJ, Lee CH. Resolvin D1 inhibits TGF-beta1-induced epithelial mesenchymal transition of A549 lung cancer cells via lipoxin A4 receptor/formyl peptide receptor 2 and GPR32. *Int J Biochem Cell Biol*;45(12):2801-2807. 2013.

297. Li Y, Cai L, Wang H, et al. Pleiotropic regulation of macrophage polarization and tumorigenesis by formyl peptide receptor-2. *Oncogene*;30(36):3887-3899. 2011.

298. Chiang N, Arita M, Serhan CN. Anti-inflammatory circuitry: lipoxin, aspirin-triggered lipoxins and their receptor ALX. *Prostaglandins Leukot Essent Fatty Acids*;73(3-4):163-177. 2005.

299. van Roy F, Berx G. The cell-cell adhesion molecule E-cadherin. *Cellular and Molecular Life Sciences*;65(23):3756-3788. 2008.

300. Takeichi M. Cadherins: A Molecular Family Important in Selective Cell-Cell Adhesion. *Annual Review of Biochemistry*;59(1):237-252. 1990.

301. Takeichi M. Cadherins in cancer: implications for invasion and metastasis. *Current Opinion in Cell Biology*;5(5):806-811. 1993.

302. Maeda M, Johnson KR, Wheelock MJ. Cadherin switching: essential for behavioral but not morphological changes during an epithelium-to-mesenchyme transition. *J Cell Sci*;118(Pt 5):873-887. 2005.
303. Harris RE, Casto BC, Harris ZM. Cyclooxygenase-2 and the inflammogenesis of breast cancer. *World J Clin Oncol*;5(4):677-692. 2014.
304. Virchow R. Reizung und Reizbarkeit. *Virchows Archiv*;14(1):1-63. 1858.
305. Balkwill F, Mantovani A. Inflammation and cancer: back to Virchow? *Lancet*;357(9255):539-545. 2001.
306. Coussens LM, Werb Z. Inflammation and cancer. *Nature*;420(6917):860-867. 2002.
307. Philip M, Rowley DA, Schreiber H. Inflammation as a tumor promoter in cancer induction. *Semin Cancer Biol*;14(6):433-439. 2004.
308. Lee HY, Kim SD, Shim JW, et al. Serum amyloid A induces CCL2 production via formyl peptide receptor-like 1-mediated signaling in human monocytes. *J Immunol*;181(6):4332-4339. 2008.
309. Sansal I, Sellers WR. The biology and clinical relevance of the PTEN tumor suppressor pathway. *J Clin Oncol*;22(14):2954-2963. 2004.
310. Heit B, Robbins SM, Downey CM, et al. PTEN functions to 'prioritize' chemotactic cues and prevent 'distraction' in migrating neutrophils. *Nat Immunol*;9(7):743-752. 2008.
311. Chalhoub N, Baker SJ. PTEN and the PI3-kinase pathway in cancer. *Annu Rev Pathol*;4:127-150. 2009.
312. Sobolewski C, Cerella C, Dicato M, Ghibelli L, Diederich M. The role of cyclooxygenase-2 in cell proliferation and cell death in human malignancies. *Int J Cell Biol*. 2010.
313. Wenzel-Seifert K, Grünbaum L, Seifert R. Differential inhibition of human neutrophil activation by cyclosporins A, D, and H. Cyclosporin H is a potent and effective inhibitor of formyl peptide-induced superoxide formation. *The Journal of Immunology*;147(6):1940-1946. 1991.

314. Bae Y-S, Lee HY, Jo EJ, et al. Identification of Peptides That Antagonize Formyl Peptide Receptor-Like 1-Mediated Signaling. *The Journal of Immunology*;173(1):607-614. 2004.
315. De Vos J, Jourdan M, Tarte K, Jasmin C, Klein B. JAK2 tyrosine kinase inhibitor tyrphostin AG490 downregulates the mitogen-activated protein kinase (MAPK) and signal transducer and activator of transcription (STAT) pathways and induces apoptosis in myeloma cells. *Br J Haematol*;109(4):823-828. 2000.
316. Levitzki A, Gazit A. Tyrosine kinase inhibition: an approach to drug development. *Science*;267(5205):1782-1788. 1995.
317. Hanke JH, Gardner JP, Dow RL, et al. Discovery of a novel, potent, and Src family-selective tyrosine kinase inhibitor. Study of Lck- and FynT-dependent T cell activation. *J Biol Chem*;271(2):695-701. 1996.
318. Oda K, Matsuoka Y, Funahashi A, Kitano H. A comprehensive pathway map of epidermal growth factor receptor signaling. *Mol Syst Biol*;1:2005 0010. 2005.
319. Downward J, Parker P, Waterfield MD. Autophosphorylation sites on the epidermal growth factor receptor. *Nature*;311(5985):483-485. 1984.
320. Nicholson RI, Gee JM, Harper ME. EGFR and cancer prognosis. *Eur J Cancer*;37 Suppl 4:S9-15. 2001.
321. Normanno N, De Luca A, Bianco C, et al. Epidermal growth factor receptor (EGFR) signaling in cancer. *Gene*;366(1):2-16. 2006.
322. Rawlings JS, Rosler KM, Harrison DA. The JAK/STAT signaling pathway. *J Cell Sci*;117(Pt 8):1281-1283. 2004.
323. Yu H, Kortylewski M, Pardoll D. Crosstalk between cancer and immune cells: role of STAT3 in the tumour microenvironment. *Nat Rev Immunol*;7(1):41-51. 2007.
324. Jarnicki A, Putoczki T, Ernst M. Stat3: linking inflammation to epithelial cancer - more than a "gut" feeling? *Cell Div*;5:14. 2010.

325. Selvatici R, Falzarano S, Mollica A, Spisani S. Signal transduction pathways triggered by selective formylpeptide analogues in human neutrophils. *Eur J Pharmacol*;534(1-3):1-11. 2006.

326. Cattaneo F, Parisi M, Ammendola R. Distinct Signaling Cascades Elicited by Different Formyl Peptide Receptor 2 (FPR2) Agonists. *International Journal of Molecular Sciences*;14(4):7193-7230. 2013.

327. Lo HW, Hsu SC, Hung MC. EGFR signaling pathway in breast cancers: from traditional signal transduction to direct nuclear translocalization. *Breast Cancer Res Treat*;95(3):211-218. 2006.

328. Etienne-Manneville S, Hall A. Rho GTPases in cell biology. *Nature*;420(6916):629-635. 2002.

329. Huang S, Chen LY, Zuraw BL, Ye RD, Pan ZK. Chemoattractant-stimulated NF-kappaB activation is dependent on the low molecular weight GTPase RhoA. *J Biol Chem*;276(44):40977-40981. 2001.

330. Pandey A, Podtelejnikov AV, Blagoev B, Bustelo XR, Mann M, Lodish HF. Analysis of receptor signaling pathways by mass spectrometry: identification of vav-2 as a substrate of the epidermal and platelet-derived growth factor receptors. *Proc Natl Acad Sci U S A*;97(1):179-184. 2000.

331. Pelletier S, Duhamel F, Coulombe P, Popoff MR, Meloche S. Rho family GTPases are required for activation of Jak/STAT signaling by G protein-coupled receptors. *Mol Cell Biol*;23(4):1316-1333. 2003.

332. Fayard E, Tintignac LA, Baudry A, Hemmings BA. Protein kinase B/Akt at a glance. *J Cell Sci*;118(Pt 24):5675-5678. 2005.

333. Mahajan K, Mahajan NP. PI3K-independent AKT activation in cancers: a treasure trove for novel therapeutics. *J Cell Physiol*;227(9):3178-3184. 2012.

334. Chen Q, Powell DW, Rane MJ, et al. Akt phosphorylates p47phox and mediates respiratory burst activity in human neutrophils. *J Immunol*;170(10):5302-5308. 2003.

335. Tokunaga E, Kimura Y, Mashino K, et al. Activation of PI3K/Akt signaling and hormone resistance in breast cancer. *Breast Cancer*;13(2):137-144. 2006.

336. Tokunaga E, Kataoka A, Kimura Y, et al. The association between Akt activation and resistance to hormone therapy in metastatic breast cancer. *Eur J Cancer*;42(5):629-635. 2006.

337. Aznar S, Lacal JC. Rho signals to cell growth and apoptosis. *Cancer Lett*;165(1):1-10. 2001.

338. Coxon PY, Rane MJ, Uriarte S, et al. MAPK-activated protein kinase-2 participates in p38 MAPK-dependent and ERK-dependent functions in human neutrophils. *Cell Signal*;15(11):993-1001. 2003.

339. Roskoski R, Jr. ERK1/2 MAP kinases: structure, function, and regulation. *Pharmacol Res*;66(2):105-143. 2012.

340. Ye RD, Boulay F, Wang JM, et al. International Union of Basic and Clinical Pharmacology. LXXIII. Nomenclature for the formyl peptide receptor (FPR) family. *Pharmacol Rev*;61(2):119-161. 2009.

341. Herbst RS. Review of epidermal growth factor receptor biology. *Int J Radiat Oncol Biol Phys*;59(2 Suppl):21-26. 2004.

342. Masuda H, Zhang D, Bartholomeusz C, Doihara H, Hortobagyi GN, Ueno NT. Role of epidermal growth factor receptor in breast cancer. *Breast Cancer Res Treat*;136(2):331-345. 2012.

343. Cattaneo F, Iaccio A, Guerra G, Montagnani S, Ammendola R. NADPH-oxidase-dependent reactive oxygen species mediate EGFR transactivation by FPRL1 in WKYMVm-stimulated human lung cancer cells. *Free Radic Biol Med*;51(6):1126-1136. 2011.

344. Clevenger CV. Roles and regulation of stat family transcription factors in human breast cancer. *Am J Pathol*;165(5):1449-1460. 2004.

345. Yu H, Jove R. The STATs of cancer--new molecular targets come of age. *Nat Rev Cancer*;4(2):97-105. 2004.

346. Cotarla I, Ren S, Zhang Y, Gehan E, Singh B, Furth PA. Stat5a is tyrosine phosphorylated and nuclear localized in a high proportion of human breast cancers. *Int J Cancer*;108(5):665-671. 2004.

347. Dechow TN, Pedranzini L, Leitch A, et al. Requirement of matrix metalloproteinase-9 for the transformation of human mammary epithelial cells by Stat3-C. *Proc Natl Acad Sci U S A*;101(29):10602-10607. 2004.

348. Diaz N, Minton S, Cox C, et al. Activation of stat3 in primary tumors from high-risk breast cancer patients is associated with elevated levels of activated SRC and survivin expression. *Clin Cancer Res*;12(1):20-28. 2006.

349. Dolled-Filhart M, Camp RL, Kowalski DP, Smith BL, Rimm DL. Tissue microarray analysis of signal transducers and activators of transcription 3 (Stat3) and phospho-Stat3 (Tyr705) in node-negative breast cancer shows nuclear localization is associated with a better prognosis. *Clin Cancer Res*;9(2):594-600. 2003.

350. Garcia R, Bowman TL, Niu G, et al. Constitutive activation of Stat3 by the Src and JAK tyrosine kinases participates in growth regulation of human breast carcinoma cells. *Oncogene*;20(20):2499-2513. 2001.

351. Garcia R, Yu CL, Hudnall A, et al. Constitutive activation of Stat3 in fibroblasts transformed by diverse oncoproteins and in breast carcinoma cells. *Cell Growth Differ*;8(12):1267-1276. 1997.

352. Gritsko T, Williams A, Turkson J, et al. Persistent activation of stat3 signaling induces survivin gene expression and confers resistance to apoptosis in human breast cancer cells. *Clin Cancer Res*;12(1):11-19. 2006.

353. Leslie K, Lang C, Devgan G, et al. Cyclin D1 is transcriptionally regulated by and required for transformation by activated signal transducer and activator of transcription 3. *Cancer Res*;66(5):2544-2552. 2006.

354. Li L, Shaw PE. Autocrine-mediated activation of STAT3 correlates with cell proliferation in breast carcinoma lines. *J Biol Chem*;277(20):17397-17405. 2002.

355. Lo HW, Hsu SC, Ali-Seyed M, et al. Nuclear interaction of EGFR and STAT3 in the activation of the iNOS/NO pathway. *Cancer Cell*;7(6):575-589. 2005.

356. Turkson J, Kim JS, Zhang S, et al. Novel peptidomimetic inhibitors of signal transducer and activator of transcription 3 dimerization and biological activity. *Mol Cancer Ther*;3(3):261-269. 2004.

357. Vultur A, Cao J, Arulanandam R, et al. Cell-to-cell adhesion modulates Stat3 activity in normal and breast carcinoma cells. *Oncogene*;23(15):2600-2616. 2004.

358. Watson CJ, Miller WR. Elevated levels of members of the STAT family of transcription factors in breast carcinoma nuclear extracts. *Br J Cancer*;71(4):840-844. 1995.

359. Alvarez JV, Febbo PG, Ramaswamy S, Loda M, Richardson A, Frank DA. Identification of a genetic signature of activated signal transducer and activator of transcription 3 in human tumors. *Cancer Res*;65(12):5054-5062. 2005.

360. Selander KS, Li L, Watson L, et al. Inhibition of gp130 signaling in breast cancer blocks constitutive activation of Stat3 and inhibits in vivo malignancy. *Cancer Res*;64(19):6924-6933. 2004.

361. Kotha A, Sekharam M, Cilenti L, et al. Resveratrol inhibits Src and Stat3 signaling and induces the apoptosis of malignant cells containing activated Stat3 protein. *Mol Cancer Ther*;5(3):621-629. 2006.

362. de Paulis A, Prevete N, Rossi FW, et al. Helicobacter pylori Hp(2-20) promotes migration and proliferation of gastric epithelial cells by interacting with formyl peptide receptors in vitro and accelerates gastric mucosal healing in vivo. *J Immunol*;183(6):3761-3769. 2009.

363. Jo EJ, Lee HY, Kim JI, et al. Activation of formyl peptide receptor-like 1 by WKYMVm induces serine phosphorylation of STAT3, which inhibits its tyrosine phosphorylation and nuclear translocation induced by hydrogen peroxide. *Life Sci*;75(18):2217-2232. 2004.

364. Cattaneo F, Parisi M, Ammendola R. WKYMVm-induced cross-talk between FPR2 and HGF receptor in human prostate epithelial cell line PNT1A. *FEBS Lett*;587(10):1536-1542. 2013.

365. Baxter EJ, Scott LM, Campbell PJ, et al. Acquired mutation of the tyrosine kinase JAK2 in human myeloproliferative disorders. *Lancet*;365(9464):1054-1061. 2005.

366. James C, Ugo V, Le Couedic JP, et al. A unique clonal JAK2 mutation leading to constitutive signalling causes polycythaemia vera. *Nature*;434(7037):1144-1148. 2005.

367. Kralovics R, Passamonti F, Buser AS, et al. A gain-of-function mutation of JAK2 in myeloproliferative disorders. *N Engl J Med*;352(17):1779-1790. 2005.

368. Levine RL, Wadleigh M, Cools J, et al. Activating mutation in the tyrosine kinase JAK2 in polycythemia vera, essential thrombocythemia, and myeloid metaplasia with myelofibrosis. *Cancer Cell*;7(4):387-397. 2005.

369. Ding L, Xu Y, Zhang W, et al. MiR-375 frequently downregulated in gastric cancer inhibits cell proliferation by targeting JAK2. *Cell Res*;20(7):784-793. 2010.

370. Yu H, Lee H, Herrmann A, Buettner R, Jove R. Revisiting STAT3 signalling in cancer: new and unexpected biological functions. *Nat Rev Cancer*;14(11):736-746. 2014.

371. Adeyinka A, Nui Y, Cherlet T, Snell L, Watson PH, Murphy LC. Activated mitogen-activated protein kinase expression during human breast tumorigenesis and breast cancer progression. *Clin Cancer Res*;8(6):1747-1753. 2002.

372. Coutts AS, Murphy LC. Elevated mitogen-activated protein kinase activity in estrogen-nonresponsive human breast cancer cells. *Cancer Res*;58(18):4071-4074. 1998.

373. Krueger JS, Keshamouni VG, Atanaskova N, Reddy KB. Temporal and quantitative regulation of mitogen-activated protein kinase (MAPK) modulates cell motility and invasion. *Oncogene*;20(31):4209-4218. 2001.

374. Sivaraman VS, Wang H, Nuovo GJ, Malbon CC. Hyperexpression of mitogen-activated protein kinase in human breast cancer. *J Clin Invest*;99(7):1478-1483. 1997.

375. McCawley LJ, Li S, Wattenberg EV, Hudson LG. Sustained activation of the mitogen-activated protein kinase pathway. A mechanism underlying receptor tyrosine kinase specificity for matrix metalloproteinase-9 induction and cell migration. *J Biol Chem*;274(7):4347-4353. 1999.

376. Dhillon AS, Hagan S, Rath O, Kolch W. MAP kinase signalling pathways in cancer. *Oncogene*;26(22):3279-3290. 2007.

377. Hemmings BA, Restuccia DF. PI3K-PKB/Akt pathway. *Cold Spring Harb Perspect Biol*;4(9):a011189. 2012.

378. Ma YY, Wei SJ, Lin YC, et al. PIK3CA as an oncogene in cervical cancer. *Oncogene*;19(23):2739-2744. 2000.

379. Shayesteh L, Lu Y, Kuo WL, et al. PIK3CA is implicated as an oncogene in ovarian cancer. *Nat Genet*;21(1):99-102. 1999.

380. Berns K, Horlings HM, Hennessy BT, et al. A functional genetic approach identifies the PI3K pathway as a major determinant of trastuzumab resistance in breast cancer. *Cancer Cell*;12(4):395-402. 2007.

381. Bellacosa A, de Feo D, Godwin AK, et al. Molecular alterations of the AKT2 oncogene in ovarian and breast carcinomas. *Int J Cancer*;64(4):280-285. 1995.

382. Cheng JQ, Ruggeri B, Klein WM, et al. Amplification of AKT2 in human pancreatic cells and inhibition of AKT2 expression and tumorigenicity by antisense RNA. *Proc Natl Acad Sci U S A*;93(8):3636-3641. 1996.

383. Ruggeri BA, Huang L, Wood M, Cheng JQ, Testa JR. Amplification and overexpression of the AKT2 oncogene in a subset of human pancreatic ductal adenocarcinomas. *Mol Carcinog*;21(2):81-86. 1998.

384. Nicholson KM, Anderson NG. The protein kinase B/Akt signalling pathway in human malignancy. *Cell Signal*;14(5):381-395. 2002.

385. Clark AS, West K, Streicher S, Dennis PA. Constitutive and inducible Akt activity promotes resistance to chemotherapy, trastuzumab, or tamoxifen in breast cancer cells. *Mol Cancer Ther*;1(9):707-717. 2002.

386. Fresno Vara JA, Casado E, de Castro J, Cejas P, Belda-Iniesta C, Gonzalez-Baron M. PI3K/Akt signalling pathway and cancer. *Cancer Treat Rev*;30(2):193-204. 2004.

387. Benitah SA, Valeron PF, van Aelst L, Marshall CJ, Lacal JC. Rho GTPases in human cancer: an unresolved link to upstream and downstream transcriptional regulation. *Biochim Biophys Acta*;1705(2):121-132. 2004.

388. Gomez del Pulgar T, Benitah SA, Valeron PF, Espina C, Lacal JC. Rho GTPase expression in tumourigenesis: evidence for a significant link. *Bioessays*;27(6):602-613. 2005.

389. Gouw LG, Reading NS, Jenson SD, Lim MS, Elenitoba-Johnson KS. Expression of the Rho-family GTPase gene RHOF in lymphocyte subsets and malignant lymphomas. *Br J Haematol*;129(4):531-533. 2005.

390. Jaffe AB, Hall A. Rho GTPases: biochemistry and biology. *Annu Rev Cell Dev Biol*;21:247-269. 2005.

391. Braga VM, Yap AS. The challenges of abundance: epithelial junctions and small GTPase signalling. *Curr Opin Cell Biol*;17(5):466-474. 2005.

392. Lozano E, Betson M, Braga VM. Tumor progression: Small GTPases and loss of cell-cell adhesion. *Bioessays*;25(5):452-463. 2003.

393. Sugihara K, Nakatsuji N, Nakamura K, et al. Rac1 is required for the formation of three germ layers during gastrulation. *Oncogene*;17(26):3427-3433. 1998.

394. Benninger Y, Thurnherr T, Pereira JA, et al. Essential and distinct roles for cdc42 and rac1 in the regulation of Schwann cell biology during peripheral nervous system development. *J Cell Biol*;177(6):1051-1061. 2007.

395. Walmsley MJ, Ooi SK, Reynolds LF, et al. Critical roles for Rac1 and Rac2 GTPases in B cell development and signaling. *Science*;302(5644):459-462. 2003.

396. Kissil JL, Walmsley MJ, Hanlon L, et al. Requirement for Rac1 in a K-ras induced lung cancer in the mouse. *Cancer Res*;67(17):8089-8094. 2007.

397. Engers R, Springer E, Michiels F, Collard JG, Gabbert HE. Rac affects invasion of human renal cell carcinomas by up-regulating tissue inhibitor of metalloproteinases (TIMP)-1 and TIMP-2 expression. *J Biol Chem*;276(45):41889-41897. 2001.

398. Espina C, Cespedes MV, Garcia-Cabezas MA, et al. A critical role for Rac1 in tumor progression of human colorectal adenocarcinoma cells. *Am J Pathol*;172(1):156-166. 2008.

399. Mertens AE, Rygiel TP, Olivo C, van der Kammen R, Collard JG. The Rac activator Tiam1 controls tight junction biogenesis in keratinocytes through binding to and activation of the Par polarity complex. *J Cell Biol*;170(7):1029-1037. 2005.

400. Sander EE, van Delft S, ten Klooster JP, et al. Matrix-dependent Tiam1/Rac signaling in epithelial cells promotes either cell-cell adhesion or cell migration and is regulated by phosphatidylinositol 3-kinase. *J Cell Biol*;143(5):1385-1398. 1998.

401. Bae YS, Park JC, He R, et al. Differential signaling of formyl peptide receptor-like 1 by Trp-Lys-Tyr-Met-Val-Met-CONH2 or lipoxin A4 in human neutrophils. *Mol Pharmacol*;64(3):721-730. 2003.

Annexes

Annexure-I

Table-1: Chemicals

Name of Reagent	Company	Catalogue No.
Acetic acid glacial AR	Merck	100063.2511
Acrylamide	Sigma-Aldrich	A8887
AG1478	Calbiochem	658548
AG490	Calbiochem	658401
Ammonium per Sulphate	Sigma-Aldrich	A-3678-100g
Bench Mark prestained Protein Ladder	Invitrogen	10748-010
Bis-acrylamide	Sigma-Aldrich	66669-100g
Boric Acid	Sisco Research Laboratories	244112
Bromophenol blue	Sigma-Aldrich	B-8026-5g
Calcium carbonate,	Sisco Research Laboratories	349181
Calcium chloride	Sisco Research Laboratories	349152
Chloroform	SD fine Chem Limited	20077
Chloroform AR	SD fine Chem Limited	20077
Complete Tablet proteases inhibitors	Roche, Germany	1697498
Cyclosporin H 5mg	AXXORA	LKT-C9614-M005
Dasatinib	ChemieTek	CT-DS001
DEPC	Sigma-Aldrich	D 5758
D-Glucose,	Merck	108337
Disodium hydrogen phosphate	Sisco Research Laboratories	1944143
DMSO	Sigma-Aldrich	D8418
6X DNA Loading Dye	MBI Fermentas	R0611
EDTA	Sigma-Aldrich	E5134-500G
Ethidium bromide	Sigma-Aldrich	E8751
Fast Green,	Sigma-Aldrich	F7258-25G
Formaldehyde	Merck	104003
Formic Acid,	Merck	100264
Gelatin Ultrapure grade; Porcine skin	USB	70086

Glycerol,	Sisco Research Laboratories	72438
Glycine	Sigma-Aldrich	G8898
Guanidine Hydrochloride	Sigma-Aldrich	G4505
HCl	Merck	1.00317.2500
Hepes,	Sigma-Aldrich	H3537-500ML
Histopaque-1077	Sigma-Aldrich	10771-500Ml
Hybond P	Amersham	RPN 303F
Imatinib	ChemieTek	CT-IM001
Isoamyl alcohol,	Sisco Research Laboratories	92945
2-Mercaptoethanol	Sigma-Aldrich	M-6250
Methanol	Merck	106009
Methanol AR	Sisco Research Laboratories	132977
MgCl2	Sisco Research Laboratories	1349117
MgSO4	Sisco Research Laboratories	1349115
Milk powder Non-fat skimmed	Sagar	
Mowiol 4-88	Calbiochem	475904
N-Formyl-Met-Leu-Phe	Sigma-Aldrich	F3506
Nilotinib	ChemieTek	CT-NL001
N-t-BOC-MET-LEU-PHE	MP biomedicals	215279925
Nuclease free water	Qiagen	129115
Paraformaldehyde	Sigma-Aldrich	P6148
Phenol Red	Sigma-Aldrich	P4758-50G
Phenol TE saturated	Sigma-Aldrich	77607-250ML
Polyoxyethylene Sorbitan Monolaurate Tween 20	Sigma-Aldrich	P9416-100ML
Potassium permanganate,	Sisco Research Laboratories	1649287
Potassium Chloride,	Sisco Research Laboratories	1644133
Potassium Dichromate,	Sisco Research Laboratories	1649166
potassium dihydrogen phosphate	Sisco Research Laboratories	1647250
Potassium Hydroxide,	Sisco Research Laboratories	164941
Potassium Sodium Tartrate,	Sisco Research Laboratories	1949136
PP2	Calbiochem	529573
2-propanol	Merck	17813

SDS	Sigma-Aldrich	L3771-1KG
Sodium Acetate Anhydrous for molecular biology	Sisco Research Laboratories	1944117
Sodium Bicarbonate,	Sisco Research Laboratories	1944142
Sodium Chloride,	Sisco Research Laboratories	1949134
Sodium Citrate,	Sisco Research Laboratories	1949110
Sodium deoxycholate	Sigma-Aldrich	30970-100GM
Sodium Fluoride,	Sigma-Aldrich	S-7920
Sodium Hydroxide,	Sisco Research Laboratories	194882
Sodium Hypochlorite	Merck	105614
Sodium orthovanadate	Sigma-Aldrich	S6508
Sodium phosphate monobasic dihydrate extrapure AR	Sisco Research Laboratories	1949145
Sodium Pyruvate	Sigma-Aldrich	P 5280
Sodium Pyruvate	Sigma-Aldrich	S8636-100ml
Sucrose	Sisco Research Laboratories	1944115
TEMED	Sigma-Aldrich	T9281-25ML.
Triton X 100	Sigma-Aldrich	T-9284-100ML
Trizma,	Sigma-Aldrich	T 6066
TRIzol	Invitrogen	15596026
Urea,	Sisco Research Laboratories	214321
WKYMVm	Tocris Biosciences	1800
WRW4	Tocris Biosciences	2262
Xylene Cyanole,	Sigma-Aldrich	X4126 10G

Table-2: Bio-chemicals

Name of Reagent	Company	Catalogue No.
Agar	HiMedia	M337
Agarose	Invitrogen	15510-019
Antibiotic anti mycotic liquid (100x)	Invitrogen	15240062
BSA	HiMedia	RM 3115
DMEM	Invitrogen	11965-118
DNA ladder 1 Kb	Invitrogen	15615-024
DNA ladder 100bp	Invitrogen	15628-019
DNase I, RNase Free	New England Biolabs	M0302S
F-10 Nutrient Mixture (Ham)	Invitrogen	11550-043
Fetal Bovine Serum	Biological Industries	04-121-1A
GeneRuler™ 100 bp Plus DNA Ladder	MBI Fermentas	SM0321
Giemsa Stain	HiMedia	S011-100ml
Goat serum	Invitrogen	16210-064
Goat Serum	Sigma-Aldrich	G6767
IL6 Rec Hu Interleukin 6	Calbiochem	RCYT-213BSL
IMDM with phenol red	Invitrogen	12440-061
L- Glutamine	Sigma-Aldrich	G7513-20ml
Lysophosphatidylcholine from egg yolk	Sigma-Aldrich	L4129
MEGM SingleQuot Kit Suppl. & Growth Factors	Lonza	CC-3150
RNase H	MBI Fermentas	EN0201
Roswell Park Memorial Institute 1640 (RPMI-1640)	Invitrogen	21870-092
Trypsin	Sigma-Aldrich	T4799-25G

Table-3: Kits

Name of Reagent	Company	Catalogue No.
cDNA synthesis Kit	MBI Fermentas	K1632
Cell Counting Kit-8	Dojindo	CK04-20
Fluo-4 NW Calcium Assay Kit	Invitrogen	F36206
MESA green QPCR master mix	Eurogentech	room temperature-SY2X-03
Precision Red™ Advanced Protein Assay	Cytoskeleton	ADV02
RNeasy Minikit	Qiagen	74104
StemLight™ Pluripotency Antibody Kit	Cell Signaling	9656
SuperSignal ELISA Femto Maximum Sensitivity Substrate	Thermo Scientific	37074

Table-4: Plastic wares

Name of Reagent	Company	Catalogue No.
10 ml pipette	NUNC	159633
15 ml Centrifuge tube PP	BD FALCON	352096
167 Filter Units - 1000 ml Capacity, MF75™ Series	Nalgene	167-0045
5 ml pipette	NUNC	159625
50 ml Centrifuge tube PP	BD FALCON	352070
ABI PRISM® Optical Adhesive Covers.	Applied Biosystems	4311971
EASY FLASK 25 FIT NUNCLON	NUNC	156367
Micro centrifuge tubes 0.6 ml	Axygen	MCT-060-C
Micro centrifuge tubes 1.7 ml	Axygen	MCT-175-C
Micro centrifuge tubes 2ml	Axygen	MCT-200-C
MicroAMp Fast optical 96-well Reaction plate with barcode	Applied Biosystems	4346906
Multiwell Plates 24 well	NUNC	142475
Multiwell Plates 6 well	NUNC	140675
Multiwell Plates 96 well	NUNC	167008-57
NUNC cryo tubes	NUNC	368632
RNAse Free tips	Axygen	TF-200 R-S
RNAse Free tips	Axygen	TF-1000-RS

Table-5: Primary antibodies

Name	Company	Catalogue No.	Origin
Akt	Cell Signaling Technology	9272	Rabbit
Beta-Catenin	Santa cruz Biotechnology, Inc	SC7963	Mouse
CD-117-PE	BD biosciences	340529	Mouse
CD24-FITC	BD biosciences	555427	Mouse
CD34-PE	BD biosciences	555822	Mouse
CD-38-PE-Cy5	BD biosciences	555461	Mouse
CD44-PE	BD biosciences	550989	Mouse
Cdc42	Santa cruz Biotechnology, Inc	SC-8401	Mouse
CDH-1	Cell Signaling Technology	3195	Rabbit
EGFR	Cell Signaling Technology	2232	Rabbit
Erk 1/2	Cell Signaling Technology	4695	Rabbit
FPR	Inhouse	N.A.	Rabbit
p38 MAPK	Cell Signaling Technology	9212	Rabbit
Phospho-Akt ser-473	Cell Signaling Technology	4051	Mouse
Phospho-Akt Thr-308	Cell Signaling Technology	4056	Rabbit
Phospho-EGFR-tyr-845	Cell Signaling Technology	2231	Rabbit
phospho-EGFR-tyr-992	Cell Signaling Technology	2235	Rabbit
phospho-Erk 1/2	Cell Signaling Technology	9101	Rabbit
Phospho-p38 MAPK (Thr180/Tyr182)	Cell Signaling Technology	4631	Rabbit
Phospho-PTEN (Ser380/Thr382/383)	Cell Signaling Technology	9554S	Rabbit
phospho-STAT-3 (Tyr-705)	Cell Signaling Technology	9145	Rabbit

PTEN Antibody	Cell Signaling Technology	9552S	Rabbit
Rac1/2/3	Cell Signaling Technology	2465	Rabbit
RhoA	Santa cruz Biotechnology, Inc	SC-418	Mouse
Sox2-PE	BD biosciences	560291	Mouse
STAT-3	Cell Signaling Technology	9139	Mouse

Table-6: Secondary antibodies

Name	Company	Catalogue No.	Origin
Alexa Fluor 568 Goat Anti-mouse IgG (H+L)	Molecular Probes	A-11001	Goat
Alexa Fluor 488 Goat Anti-rabbit IgG	Molecular Probes	A-11004	Goat
Goat anti-rabbit IgG-HRP:	Santa cruz Biotechnology, Inc	sc-2301	Goat
Goat anti-mouse IgG-HRP	Santa cruz Biotechnology, Inc	sc-2302	Goat

Table-7: Fluorescent probes

Name	Company	Catalogue No.
4´,6-diamidino-2-phenylindole, dilactate (DAPI)	Molecular probes	D3571
Alexa Fluor® 488 phalloidin	Molecular Probes	A12379
formyl-Nle-Leu-Phe-Nle-Tyr-Lys, fluroescein derivative	Molecular Probe	F1314
TRITC-Phalloidin	Sigma-Aldrich	P1951

Table-8: Primer Sequences

Primers sequences, specific to *Homo sapiens* were designed with the help of online softwares (Primer-3 and Primer-Blast) and were obtained from Sigma-Aldrich, USA.

Gene name	Primer strand	Sequence (5'->3')	Start	Stop	Product size (bp)
Actin	Forward	CCAACCGCGAGAAGATGA	425	442	97
	Reverse	CCAGAGGCGTACAGGGATAG	521	502	
b2a2	Forward	CGGGAGCAGCAGAAGAAGTG	175	194	131
	Reverse	AGGGCTTCTTCCTTATTGATGGT	305	283	
b3a2	Forward	GTCCACTCAGCCACTGGATT	340	359	88
	Reverse	CTTCACTCAGACCCTGAGGC	427	408	
CDH1	Forward	GCCGAGAGCTACACGTTCAC	224	243	117
	Reverse	GTCGAGGGAAAAATAGGCTG	340	321	
COX2	Forward	ATTGCCCGACTCCCTTGGGTGT	568	589	196
	Reverse	CCGTTGGTGAAAGCTGGCCCT	763	743	
FPR1	Forward	TATTGCCACCAAGATCCACA	764	783	104
	Reverse	GATATGGGGACCAGCAGAGA	867	848	
FPR2	Forward	TACCATGCTGACAGCCAGAG	728	747	90
	Reverse	GCAATGAGCCCATAGCAGAT	817	798	
FPR3	Forward	ATTGCTCTGGACCGCTGTAT	539	558	103
	Reverse	TGAAAATCCAGAGTCCCGTC	641	622	
GAPDH	Forward	ACACCCACTCCTCCACCTTT	968	987	60
	Reverse	TGACAAAGTGGTCGTTGAGG	1027	1008	
HPRT1	Forward	TGACACTGGCAAAACAATGCA	578	598	94
	Reverse	GGTCCTTTTCACCAGCAAGCT	671	651	
Klf4	Forward	GGGAGAAGACACTGCGTCA	683	701	88
	Reverse	GGAAGCACTGGGGGAAGT	770	753	
cMyc	Forward	GCTGCTTAGACGCTGGATTT	514	533	114
	Reverse	CACCGAGTCGTAGTCGAGGT	627	608	
Nanog	Forward	TGATTTGTGGGCCTGAAGAA	296	315	60
	Reverse	GAGGCATCTCAGCAGAAGACA	355	335	
Nestin	Forward	GCATGGAACCTGGAGAATTT	2822	2841	176
	Reverse	ACCGTATCTTCCCACCTCTG	2997	2978	
Oct4/3	Forward	GTGGAGGAAGCTGACAACAA	1008	1027	97
	Reverse	GGTTCTCGATACTGGTTCGC	1104	1085	
Pten	Forward	TGAAGGCGTATACAGGAACAAT	1157	1178	110
	Reverse	CGGTGTCATAATGTCTTTCAGC	1266	1245	
Sox2	Forward	GCGAACCATCTCTGTGGTCT	2082	2101	145
	Reverse	GGAAAGTTGGGATCGAACAA	2226	2207	

Annexure-II

While studying gene expression in clinical samples, to compare normal samples with CML samples, absolute quantitation method using standard curve analysis was used. However, for comparing expression of different gene within the same sample $\Delta\Delta$Ct method was used. Absolute quantities obtained for a gene were normalized by the quantity of actin. These normalized quantities for normal and CML samples were compared for a given gene. To compare different genes within the same sample, ratio of normalized quantities of the genes needs to be calculated. This double division method is mathematically rejected, because PCR amplification is exponential. This method would have been correct if PCR amplification is liner. Livak et al[125] proposed $\Delta\Delta$Ct method, which incorporated the exponential nature of PCR amplification. Hence, $\Delta\Delta$Ct method was used to calculate the fold change of one gene with respect to another gene in a given sample.

Annexure-II

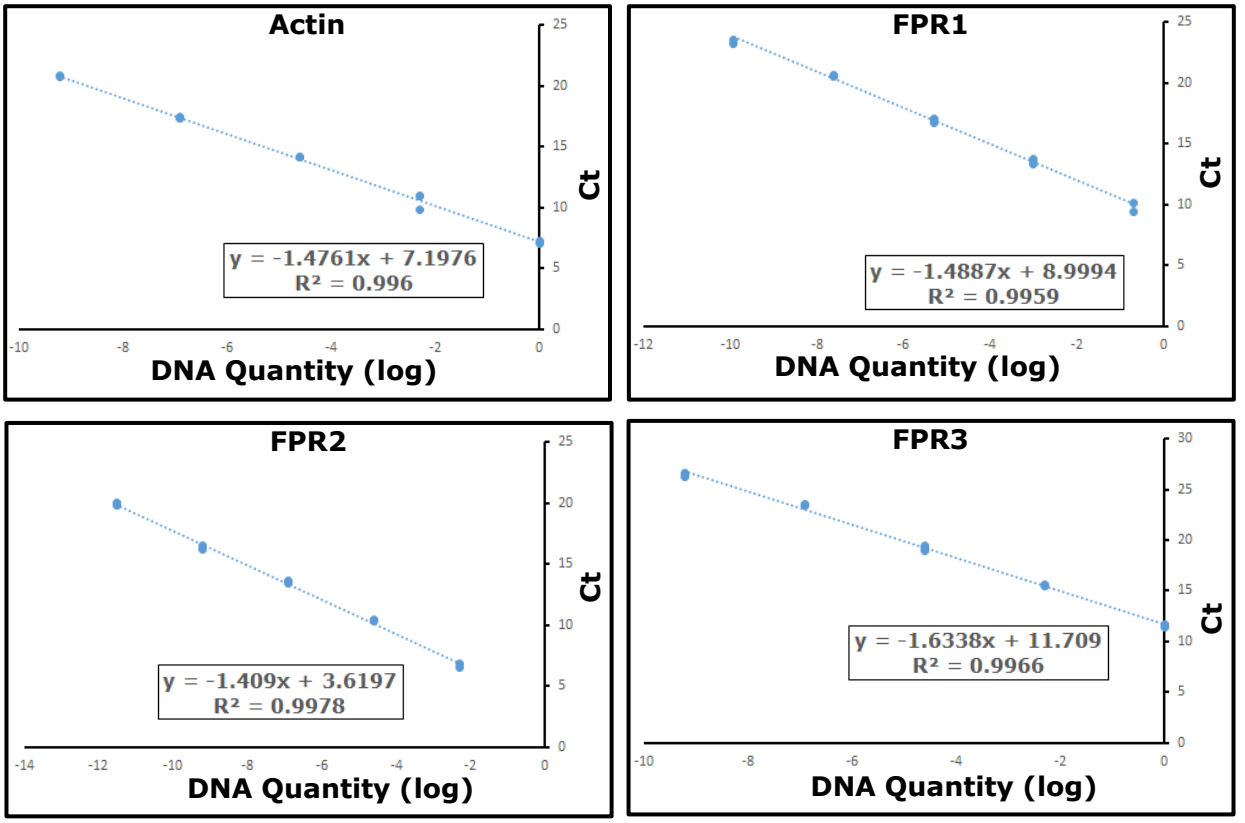

Fig-1: Standard Curve for Various Genes: Absolute gene expression by standard curve analysis was quantitated for clinical samples by QPCR. Plasmid containing known quantity of gene of interest was serially diluted and QPCR reactions were run along with cDNA prepared from clinical samples. Standard curve for log DNA quantity vs Ct value was drawn. By using this curve, quantity of gene of interest was calculated in clinical samples. Representative standard curves for each gene are presented as indicated.